Investigation into the Efficacy of the Anti-CD20 Monoclonal Antibody Ofatumumab in Chronic Lymphocytic Leukaemia

Odette Middleton
BSc, MSc

Submitted in fulfilment of the requirements for the
Degree of Doctor of Philosophy

School of Medicine
College of MVLS
University of Glasgow

Submitted: September 2015

Summary

Chronic lymphocytic leukaemia (CLL) is the most common leukaemia of the Western world, and unfortunately despite advances in chemotherapeutic agents CLL remains incurable to date. CLL is a highly heterogeneous disease. CLL patients exhibiting progressive disease often become refractory to standard first line therapies, underpinning the need for novel drugs. An emerging field is targeted monoclonal antibody (MAb) development. Rituximab (RTX) a chimeric anti-CD20 MAb is registered as a first line therapy in combination with fludarabine and cyclophosphamide. A next generation type I, human IgG1 anti-CD20 MAb, ofatumumab (OFA), binds to a novel epitope of CD20 resulting in higher potency of complement dependent cytotoxicity (CDC) induction. OFA has recently been given FDA approval for treatment in combination with chlorambucil for previously untreated CLL patients when fludarabine based regimes are not appropriate. OFA is also licensed as a single agent for the treatment of CLL patients refractory to both fludarbine and anti-CD52 MAb alemtuzumab.

This research was conducted to establish what factors within CLL biology may influence RTX or OFA efficacy, in order to highlight the improved activity of OFA in comparison to RTX for the treatment of CLL. The ability of OFA to elicit a CDC response is an important part of its efficacy. Within this study we have demonstrated that OFA activity is limited in the treatment of CLL by several different factors including; complement levels, CD20 expression, microenvironmental stimulation and CLL genetic mutations.

Our study identified that a large proportion, 37.5%, of CLL patients harbour complement deficiencies within their sera, this then led to a significant amount of complement exhaustion with successive OFA treatments, abrogating CDC induction. The detection of excessive complement exhaustion potentially has a clinical impact on the administration of anti-CD20 MAbs.

CD20 expression levels also impact upon CDC induction by OFA, CD20 expression levels display a positive linear correlation with the percentage of CDC induction. Importantly OFA is superior in the induction of CDC in CLL patients with low CD20 expression levels in comparison to RTX. It is well established that CLL

patients have lower CD20 expression compared to other B cell malignancies, which is an important factor for anti-CD20 MAb efficacy as CDC induction is critically dependent on the expression levels of the target antigen on the surface of the cell.

Recurrent mutations within *NOTCH1* (NOTCH1^{MUT}) have recently been identified as a poor prognostic marker within CLL. Emerging data suggests this mutation confers resistance against anti-CD20 MAbs, possibly through a down-regulation of CD20. We demonstrate that NOTCH1^{MUT} CLL cells do display reduced expression levels of CD20, however this alone did not appear to contribute to all the reduced susceptibility towards anti-CD20 MAb activity. Preliminary gene expression data in combination with Ca^{2+} flux analysis suggest that NOTCH1^{MUT} CLL cells have deregulated Ca^{2+} signalling which highlights the role of CD20 as a store-operated Ca^{2+} channel, and provides another mechanism for their resistance.

Microenvironmental stimulation also impacts upon CLL cell response to RTX and OFA. Mimicking CLL cell interaction with their microenvironmental niche, caused an increase in CDC induction within different CLL cytogenetic subsets, independently to changes in CD20 expression. This is important as the interaction of CLL cells with other components of the microenvironment cause an up-regulation of anti-apoptotic proteins aiding CLL survival and promoting drug resistance.

In conclusion this study highlights the increased efficacy of OFA as a chemotherapeutic agent in the treatment of CLL in comparison to RTX. Collectively these results also demonstrate that a change within the dosing schedule of OFA and complement supplementation using an exogenous source such as fresh frozen plasma could diminish some of the limitations in CDC induction, and potentially lead to enhanced clinical efficacy.

Table of Contents

List of Tables

List of Figures

Acknowledgements

I am incredibly grateful to both my supervisors Dr Alison Michie and Dr Helen Wheadon for their continuous support and understanding throughout this research project. I am indebted to them for all the knowledge, guidance, patience and kindness they have shown me over the past 4 years, providing me with valuable skills for my future and making my time under their supervision very enjoyable. I am thankful to the members of the Michie research group Dr Ailsa Holroyd and Karen Dunn for their help and Dr Emilio Cosimo for his guidance and insight. I'm grateful to Jennifer Cassels, Heather Morrison and Dr Anuradha Tarafdar for their advice, support and most importantly friendship. A special thank you to Professor Tessa Holyoake and her research group as well as Professor Mhairi Copland's, Dr. Helen Wheadon's and Dr Karen Keeshan's research groups, for their advice and help whilst I carried out my research. I am especially grateful to everyone in the POG for humouring me every few weeks when I ran out of normal healthy serum and needed blood donations. I greatly appreciate all the help the clinical diagnostic immunology laboratory at Gartnavel General Hospital provided by tirelessly carrying out C3c and C4 analysis on serum samples. I'm thankful to Professor Anna Schuh and the Oxford Molecular Diagnostics Centre for providing a fantastic sequencing service. I am grateful to Dr Alison M^{C}Caig, Dr Mike Leach and Dr Susan Rhodes for their help with obtaining CLL patient samples. A special thank you goes to all the CLL patients who donated blood samples, allowing this research to be carried out. Importantly I would like to thank the University of Glasgow, the friends of Paul O'Gorman and GlaxoSmithKline for funding this project. Finally I also need to thank my family and friends for their endless encouragement and support, as well as my partner George for his continuous love and understanding.

Author's Declaration

This work represents original work carried out by the author and has not been submitted in any form to any other University.

Odette Middleton

September 2015

Definitions/Abbreviations

Abs	Antibodies
ADCC	Antibody-dependent cellular cytotoxicity
AID	Activation-induced cytidine deaminase
AMS	Age matched serum
APRIL	A proliferation inducing ligand
ATM	Ataxia telangiectasia mutated
BAFF	B cell activating factor
BCL10	B cell lymphoma/leukaemia 10
Bcl-2	B cell CLL/lymphoma 2
BCMA	B cell maturation
BCR	B cell receptor
BIM	B cell CLL/lymphoma 2 interacting mediator
BIRC3	Baculoviral IAP repeat containing protein 3
BLNK	B-cell linker protein
BM	Bone marrow
Bp	Base pairs
Btk	Bruton's tyrosine kinase
C1INK	C1 inhibitor
Ca^{2+}	Calcium
CAR	Chimeric antigen receptors
CCL3	Chemokine (C-C motif) ligand
CD154	CD40 ligand
CD16	FcγRIII
CD46	Membrane co-factor of proteolysis
CD55	Decay-accelerating factor

CD59	Protectin
CDC	Complement dependent cytotoxicity
CFSE	Carboxyfluorescein diacetate succinimidyl ester
CHOP	Cyclophosphamide, doxorubicin, vincristine and prednisone
CLL	Chronic lymphocytic leukaemia
CLP	Common lymphoid progenitor
CR	Complete remission
CSL	Centromere Binding Factor 1, Suppressor of Hairless and Lag-1
CSR	Class switching recombination
CTLA-4	Cytotoxic T lymphocyte associated antigen 4
CXCL12	Cell-derived factor 1
D	Diversity
DAG	Diacylglycerol
DAPK1	Death associated protein kinase 1
DLL1	Delta-like ligand 1
DMSO	Dimethylsulphoxide
DOS	Delta and OSM-11
DSL	Delta, Serrate and Lag-2
EBF	Early B-cell factor
EGF	Epidermal growth factor
ER	Endoplasmic reticulum
ERK	Extracellular signal-regulated kinase
FBS	Fetal bovine serum
FC	Fludarabine and cyclophosphamide
FCR	Fludarabine, cyclophosphamide and rituximab
FDC	Follicular dendritic cells

FFP	Fresh frozen plasma
FISH	Fluorescent *in situ* hybridisation ()
GA101	Obinutuzumab
GC	Germinal centres
GEPs	Gene expression profiling
GPI	Glycosylphosphatidylinositol
GSK-3β	Glycogen synthase kinase -3 beta
HBSS	Hanks Buffered Saline Solution
HCD122	Lucatumumab
HCDR3	Heavy chain complementarity-determining region
HD	Heterodimerisation domain
HDAC	Histone deacetylases
HES	Hairy enhancer of split
HLA-G	Human leukocyte antigen G
HMGB1	High mobility group box-1
HRP	Horseradish-peroxidase
HSCs	Haemopoietic stem cells
ICN	Intracellular Notch1
Ig	Immunoglobulin
IGH	Immunoglobulin heavy chain
IGL	Immunoglobulin light chain
IKK	Inhibitor of kappa B kinase
IL	Interleukin
IL-1R	Interleukin-1 receptor
IL-4R	Interleukin-4 receptor
Iono	Ionomycin

IP_3	Inositol-1,4,5-triphosphate
IRS-1	Insulin receptor substrate-1
ITAMs	Immunoreceptor tyrosine activation motifs
J	Joining
JNK	C-Jun NH2 terminal kinase
LDT	Lymphocyte doubling time
LNRs	Lin-Notch repeats
MAb	Monoclonal antibody
MAC	Membrane attack complex
MALT1 1	Mucosa associated lymphoid tissue lymphoma translocation protein
MAML	Mastermind-like protein
MAPK	Mitogen-activated protein kinases
MBL	Monoclonal B cell lymphocytosis
MCL-1	Myeloid cell leukaemia 1
MFI	Mean fluorescent intensity
MHC II	Major histocompatibility complex class II
MPPs	Multipotent progenitor cells
MRD	Minimal residual disease
MYD88	Myeloid differentiation primary response 88
NARP	Notch-related ankyrin repeat protein
NDC	No drug control
NFAT	Nuclear factor of activated T cells
NF-κB	Nuclear factor kappa B
NHS	Normal healthy serum
NK	Natural killer
NLC	Nurse like cells

NLS	Nuclear localisation signals
NOTCH1^{MUT}	*NOTCH1* mutations
OFA	Ofatumumab
ORR	Overall response rates
OS	Overall survival
PCR	Polymerase chain reaction
PD1	Programmed cell death 1
PEST	Pro-Glu-Ser-Thr
PFS	Progression free survival
PH	Pleckstrin-homology
PI	Propidium iodide
PI3K	Phosphatidylinositol 3 kinase
PIP_2	Phosphatidylinositol-4,5-biphosphate
PIP_3	Phosphatidylinositol-3,4,5-triphosphate
PKC	Protein kinase C
PVDF	Immun-Blot polyvinyliden difluoride
RAG	Recombination activating genes
RAGE	Receptor for advanced glycation end-products
Rb	Retinoblastoma
RG73S6	Anti-CD44 humanised MAb
RID	Radial immunodiffusion
ROS	Reactive oxygen species
RT	Room temperature
RTX	Rituximab
SCF	Stem-cell factor
SD	Standard deviation

SDS	Sodium Dodecyl Sulphate
SDS-PAGE	Sodium Dodecyl Sulphate – Polyacrylamide gel electrophoresis
SEM	Standard error of mean
SF3B1	Splicing factor 3b subunit
SH2	Src homology
SHM	Somatic hypermutation ()
SLE	Systemic lupus erythematosus
SLL	Small cell lymphoma
SNBTS	Scottish National Blood Transfusion Service
SNP	Single nucleotide polymorphism
STAT3	Signal transducer and activator of transcription 3
Syk	Spleen tyrosine kinase
TACI interactor	Transmembrane activator calcium modulator and cyclophilin ligand
TAD	Transactivation domain
T-ALL	T cell acute lymphoblastic leukaemia
TCF/LEF	T cell factor / lymphoid enhancer factor
TCL1	T cell leukaemia/lymphoma 1
TD	Transmembrane domain
TdT	Terminal deoxynucleotidyl transferase
TL9	Toll like receptor 9
TLR	Toll-like receptor
TNF	Tumour necrosis factor
TNF-R	Tumour necrosis factor -receptor
TRAFs	Tumour necrosis factor –receptor associated factors
V	Variable
VCAM-1	Vascular cell adhesion molecule 1

VEGF	Vascular endothelial growth factor
VLA-4	Very late activation 4 receptor
VPA	Valporic acid
vWF	Willebrand Factor
WAC	WaC3CD5^{+}
ZAP-70	Zeta-chain-associated protein kinase 70 kDa

1 Introduction

The body's ability to mount an effective immune response is fundamental for our health and wellbeing. The first line of defence when fighting invading pathogens is innate immunity, the second is the adaptive immune system. Innate immunity is fast acting and relatively nonspecific compared to adaptive immunity. Innate immunity clears target pathogens through several different pathways including phagocytosis, inducing apoptosis and complement activation. In contrast the adaptive immune system consists of two responses; cell-mediated immunity in which the effector cells are T lymphocytes (T cells) and humoral immunity mediated by B lymphocytes (B cells). Adaptive immunity displays extensive specificity, adaptability and memory against foreign molecules. Despite the body's rigorous control mechanisms, numerous immune disorders and malignancies have been identified. My research focused on chronic lymphocytic leukaemia (CLL) a malignancy of B cells and monoclonal antibody (MAb) immunotherapy. MAbs harness the body's innate immune system to efficiently clear cancerous cells, described in more detail in section 1.4.

1.1 B cell development

All blood cells are derived from multipotent haemopoietic stem cells (HSCs); B cells develop from HSCs located within the bone marrow (BM). Stromal cells located within the BM guide the developing HSC to differentiate into a B cell through cell to cell contact and the release of cytokines and chemokines. A schematic of the maturation of HSCs into B cells is shown in Figure 1.1[1].

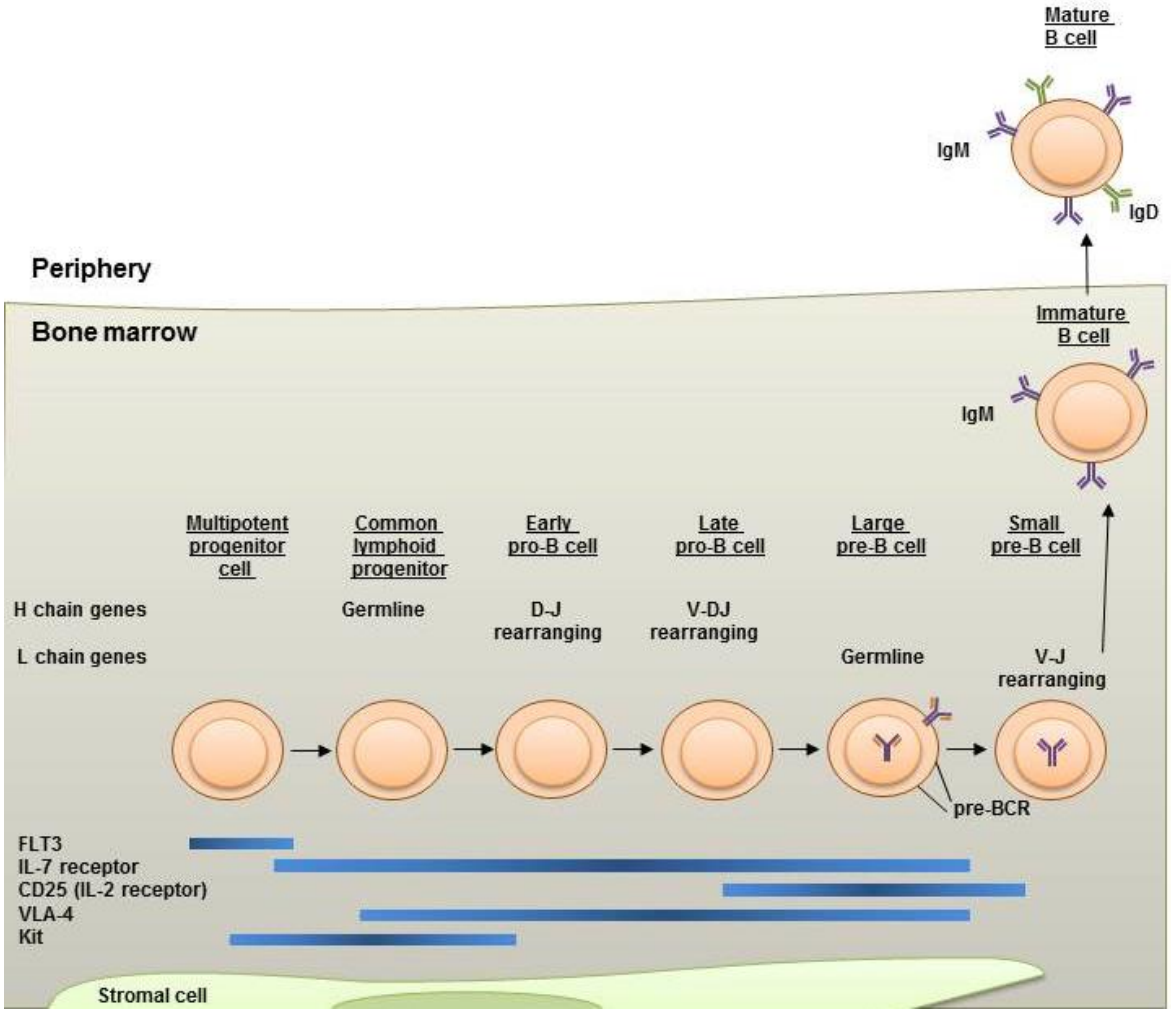

Figure 1.1 B cell development.
Modified from Murphy. K., 2012.

HSCs committed to the lymphoid lineage become multipotent progenitor cells (MPPs) which express FLT3, a tyrosine kinase receptor, this then interacts with FLT3 ligand present on BM stromal cells. Activation of the FLT3 pathway is fundamental for MPPs to transform into the common lymphoid progenitor (CLP) along with the initiation of the transcription factor PU.1[1,2]. In mice this is also characterised by the expression of IL-7 receptor on CLP cells, with IL-7 being

secreted by stromal cells, although how fundamental IL-7 receptors are for human B cell development and growth is still to be established[3]. Other components that stimulate the HSC to B cell commitment include the expression of stem-cell factor (SCF). SCF is a cytokine secreted by BM stromal cells which associates with the receptor tyrosine kinase c-Kit on precursor cells. The chemokine stromal cell-derived factor 1 (CXCL12) is constitutively secreted from BM stromal cells in order to retain the B-cell precursors within the BM microenvironment[1,2]. The transition to the pro-B cell stage from CLP is specified by the activation of the transcription factors E2A and early B-cell factor (EBF). Transcription factors PU.1 and Ikaros are essential for the initiation of E2A expression. Sequentially, E2A then induces EBF expression, which then act in tandem to initiate the expression of proteins associated with differentiation into the pro-B cell[4].

Further development of the B cell is characterised by rearrangements of the B cell receptor (BCR), which occurs in a step wise fashion as the B cell differentiates from the early pro-B cell into the mature B cell. The BCR comprises of two identical heavy chains and two identical light chains which form the surface immunoglobulin (Ig), shown in Figure 1.2. Gene rearrangement of the BCR is a highly controlled operation with several check points to prevent self-activation and deregulation of the immune system. The first rearrangement occurs in the diversity (D_H) locus of the immunoglobulin heavy chain (*IGH*) gene, whereby the D segment joins to the joining (J_H) segment. The germline arrangements of the *IGH* and light chain (*IGL*) loci are shown in Figure 1.2, and are derived from an extensive repertoire of the different gene segments[1]. E2A and EBF activity is critical for D to J_H joining to occur, as these transcription factors mediate the expression of proteins required for gene rearrangement; recombination activating genes 1 and 2 (RAG-1 and RAG-2)[1]. PAX5 is also a fundamental transcription factor in B cell development, without PAX5 expression developing B cells fail to fully commit to the B cell lineage and to develop past the pro-B cell stage. PAX5 expression targets both CD19, the B cell co-receptor component, and also B-cell linker protein (BLNK) which is required for signalling from the mature B cell BCR[1,4]. D-J_H rearrangements mark the transition into the pro-B cell stage. At the late pro-B cell stage only one allele of the variable heavy chain (V_H) gene segment will rearrange to join the DJ_H sequence. RAG-1 and

RAG-2 form a complex with several different enzymes, mostly ubiquitous DNA modifying proteins, which form the V(D)J recombinase. RAG-1 and RAG-2 mediate the endonucleolytic cleavage of the target DNA introducing double strand breaks and DNA repair mechanisms bring the desired segments together. The diversity of BCR-antigen recognition is further enhanced at the pro-B cell stage by the enzyme terminal deoxynucleotidyl transferase (TdT), which inserts non-template nucleotides in between the rearranged gene segments[1].

When V-DJ_H rearrangement is successful, a full length μ heavy chain is produced and the cell is now termed a pre-B cell. A large proportion of developing B cells are lost at this stage due to unsuccessful rearrangements of the μ heavy chain. The immune system requires strict control mechanisms to prevent the production of ineffective inert and self-reactive B cells. Before the pro-B cell develops further, the functionality of the recently produced heavy chain needs to be checked. E2A and EBF in the pro-B cell signal the production of two surrogate light chains, λ5 and VpreB, which pair with the heavy chain to become the pre-B cell receptor[1]. Invariant proteins Igα (CD79a) and Igβ (CD79b) are also important in the formation of the pre-B cell receptor as well as the fully functioning BCR until the death of the B cell or it becomes a fully differentiated plasma cell. Igα and Igβ span the cell membrane and through interaction with the pre-BCR or BCR are able to transduce intracellular signals through the kinase activity of the immunoreceptor tyrosine activation motifs (ITAMs) in their cytoplasmic tails[1]. Upon successful rearrangement of the heavy chain and correct pairing with the two surrogate light chain molecules the pre-BCR will cluster on the surface of the cell. Subsequent intracellular signalling then inhibits RAG-1 and RAG-2 expression, thus preventing further rearrangement of the heavy chain genes. The cells are now susceptible to the activity of IL-7, leading to cell proliferation and development into the large pre-B cell[1]. Large pre-B cells go through several rounds of cell divisions to produce resting small pre-B cells. Once again the expression of RAG proteins is initiated, but this time it is to induce the rearrangement of light chain genes. There are two forms of the light chains (κ and λ) but only one will be expressed in conjunction with the heavy chain. Light chains lack the D segment and therefore rearrangement between V and J occurs. Successful rearrangement of the light chain produces an intact IgM molecule on the surface of the now immature B cell. Surface IgM then

associates with Igα and Igβ to form the BCR[1]. At this stage it is important for the B cell to be tested to prevent auto reactivity.

Self-reactive B cells are prevented from entering the circulating compartment by either; undergoing apoptosis, developing a new receptor by receptor editing, undergoing a permanent state of anergy against antigens or become immunologically ignorant[1]. This ensures that surviving B cells are tolerant to self-antigens. B cells that pass this check point become mature B cells that express surface IgD as well as IgM, mature B cells then egress from the BM and migrate towards peripheral lymphoid tissues.

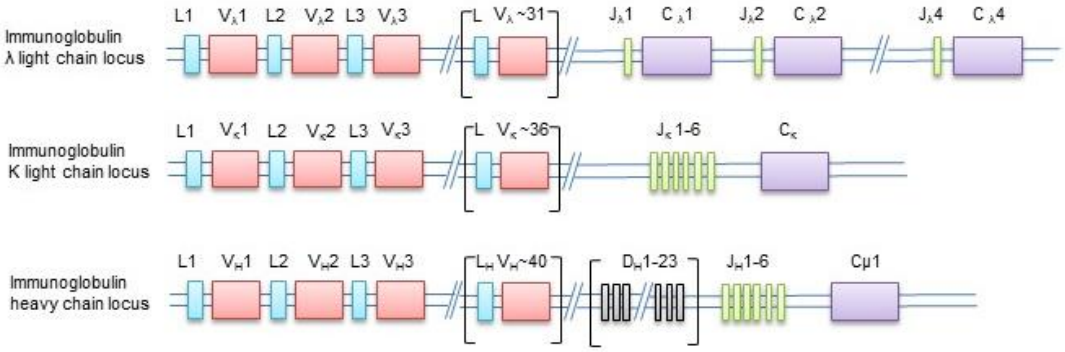

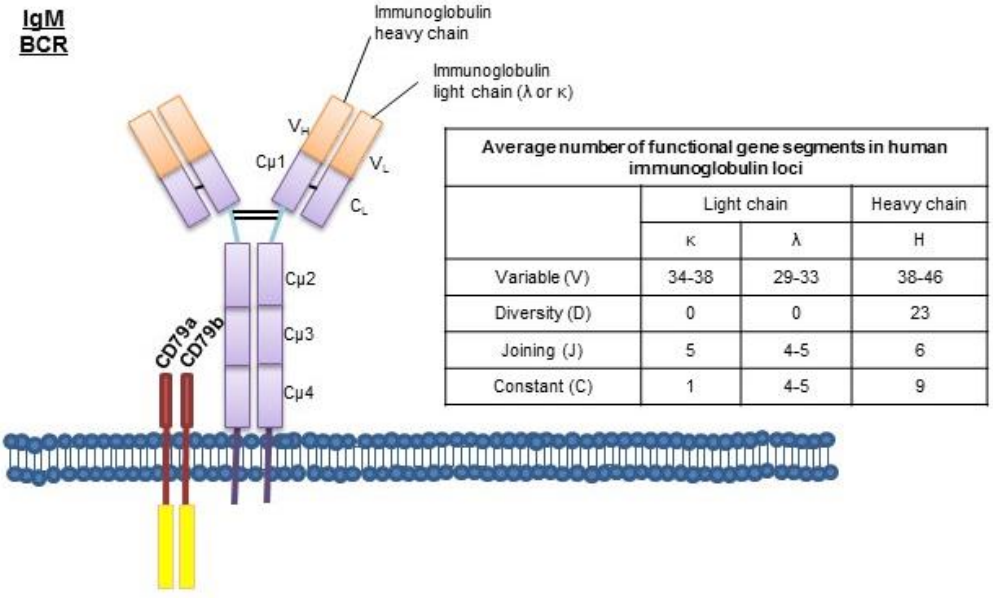

Average number of functional gene segments in human immunoglobulin loci

	Light chain		Heavy chain
	κ	λ	H
Variable (V)	34-38	29-33	38-46
Diversity (D)	0	0	23
Joining (J)	5	4-5	6
Constant (C)	1	4-5	9

Figure 1.2 Germline arrangements of the immunoglobulin heavy and light chain loci and BCR structure.

Modified from Murphy. K., 2012

1.1.1 B cell immune response

The humoral immune response is characterised by the secretion of antibodies from plasma cells, which are terminally differentiated B cells. The humoral immune response is activated when the BCR comes into contact with an antigen. The antigen is then internalised and degraded. Antigen peptides are processed and transverse to the B cell surface and bind to the major histocompatibility complex class II (MHC II); this is then recognised by activated $CD4^+$ T cells (helper T cells). The helper T cell provides activating signals to the B cells to proliferate and differentiate into antibody producing plasma cells. Helper T cells express CD40 ligand (CD154) which interacts with CD40 expressed on the B cell, this binding helps stimulate the B cell to proliferate, undergo Ig class switching and somatic hypermutation (SHM)[1,5-7]. Helper T cells also produce cytokines to aid B cell proliferation and differentiation. In some instances it is possible for some antigens, such as bacterial polysaccharides to induce antibody production from B cells in a T cell independent manner; these antigens are termed B cell mitogens and can induce proliferation of B cells[1]. However in the majority of cases B cell/helper T cell interaction is required. B cells and T cells inhabit different areas of the peripheral lymphoid tissues; B cells are located within the primary lymphoid follicles and T cells in the T-cell areas. B cells that have encountered antigen move along a CCR7 chemokine gradient within the primary lymphoid follicles towards the T-cell area. T cells also migrate towards CCR7 ligand being highly expressed by dendritic and stromal cells at the T cell/B cell boundary. Expression of CXCR5 is then induced in T cells and they start to proliferate[1,7]. At this point T cells can differentiate into either effector cells or follicular helper T cells (T_{FH} cell); T_{FH} cells recognise peptides displayed on the MHC II of B cells, and in doing so activate the B cell. Once associated, the B and T cells then migrate back to the primary lymphoid follicle where they proliferate and form a germinal centres (GC), termed secondary lymphoid follicles.

1.1.1 Germinal centre reaction

B cells comprise the majority of GC, with antigen-specific T_{FH} cells making up 10% of the population[1]. The surrounding area of a GC is comprised of resting B cells, called the mantle zone. The production of the GC is important for long term defence against invading pathogens, such as if the infection becomes

chronic or if the host becomes re-infected. B cells enter the GC as it enables them to undergo crucial modifications such as SHM and class switching of surface Ig to provide a more tailored immune response. The GC can be distinguished by two different zones, the light zone and the dark zone (Figure 1.3)[8].

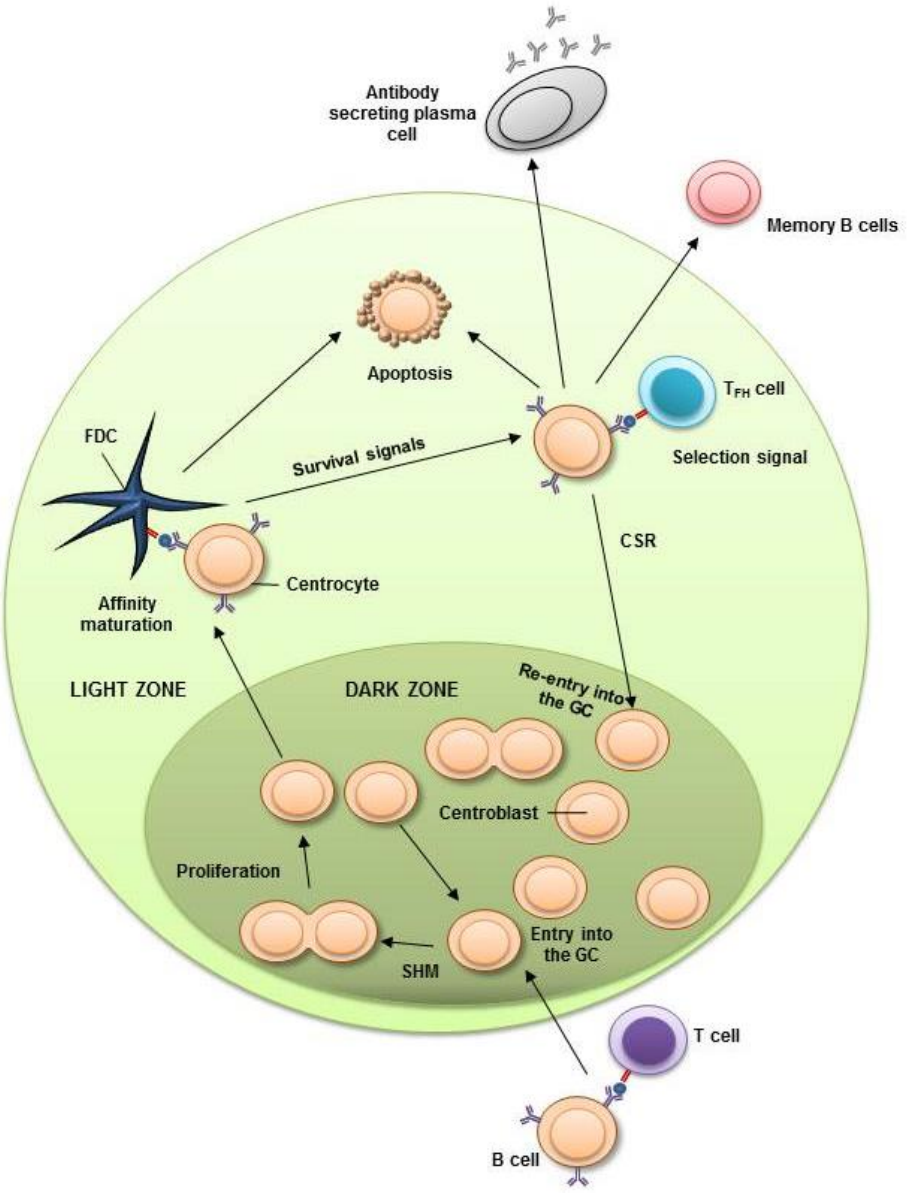

Figure 1.3 Germinal centre reaction.

Modified from Heesters. B., *et.al.* 2014.

The dark zone of the GC contains densely packed rapidly proliferating B cells termed centroblasts, which express the chemokine receptors CXCR4 and CXCR5, but low levels of IgD. Within the dark zone, stromal cells express CXCL12, a ligand for CXCR4[9,10]. As with the BM, CXCL12 expression retains the centroblast within the dark zone. To produce B cells with a higher affinity to invading

pathogen, surface Ig undergoes SHM of the V gene region. SHM results in the inclusion of individual point mutations within the Ig, subsequently several B cell clones which have very subtly different affinities towards the target antigen are produced[11]. Approximately 1 per 10^3 base pairs (bp) are changed each time the cell divides, this mutation rate is much higher than the rest of the genome. The B cell is able to target just the V region for increase mutation rate by the enzyme activation-induced cytidine deaminase (AID). AID catalyses the deaminating of cytidine residues directly on DNA. It is thought that the inclusion of somatic mutations into the DNA is through the error prone repair mechanisms after AID has damaged the DNA, although the full extent of AID activity is not fully elucidated[1,8,10,12]. Most of the mutations generated will produce a different amino acid within the antigen binding site of the Ig which will result in altered binding affinity towards the target antigen. The majority of the mutations generated will lower the binding affinity to the antigen. Only B cells that have increased affinity receive pro-survival signals and the rest are removed by apoptosis. Eventually the rates of division of the centroblast subside and they enter the growth phase, halting the expression of CXCR4 and increasing Ig levels. After this transformation the centroblasts are termed centrocytes, which transverse into the light zone and are held there by follicular dendritic cells (FDC) producing CXCL13; a ligand for CXCR5. The affinity of the BCR is tested on the FDC bearing the target antigen, if binding is successful then CXCR4 is re-expressed and the B cell travels back into the dark zone to undergo successive rounds of SHM, termed affinity maturation[8,10-13]. Activated B cells within the GC can also undergo class switching recombination (CSR) of the Ig, the heavy chain V region associates with a different C exon of any isotype through non-homologous end joining caused by AID[11]. There are five different classes of Ig; IgA, IgD, IgE, IgG and IgM, each type has a very specific and immunologically unique function. Therefore it is important for B cells to express the most appropriate Ig for the particular immune response. CD40/CD154 interaction of T_{FH} cells associated with a B cell provides important B cell survival signals and also signals T_{FH} cells to release cytokines to help guide B cells to undergo CSR from IgM into the desired Ig[12]. Centrocytes within the GC display a genetic profile of having high expression levels of pro-apoptotic genes such as B cell CLL/lymphoma 2 (Bcl-2) interacting mediator of cell death (BIM) and low levels of the anti-apoptotic genes Bcl-2 and Bcl-X_L. It is thought that interaction with

BCR and antigen along with CD40-CD154 interaction on T cells is required to induce elevated expression levels of Bcl-2 and Bcl-X_L to aid survival[10]. Eventually some B cells will leave the GC and develop into either an antibody producing plasma cells or a memory B cells. Differentiation into a plasma B cell is associated with the down-regulation of PAX5 and Bcl6. Bcl6 is considered to be a master regulator of centroblasts and is critical for the generation and maintenance of the GC reaction[10].

1.1.2 BCR signalling

The BCR can become activated via two different pathways; antigen dependent signalling or the lesser understood ligand-independent (termed tonic signalling). Signalling through the BCR can result in B cell survival, migration, proliferation and the induction of apoptosis (Figure 1.4)[14-16].

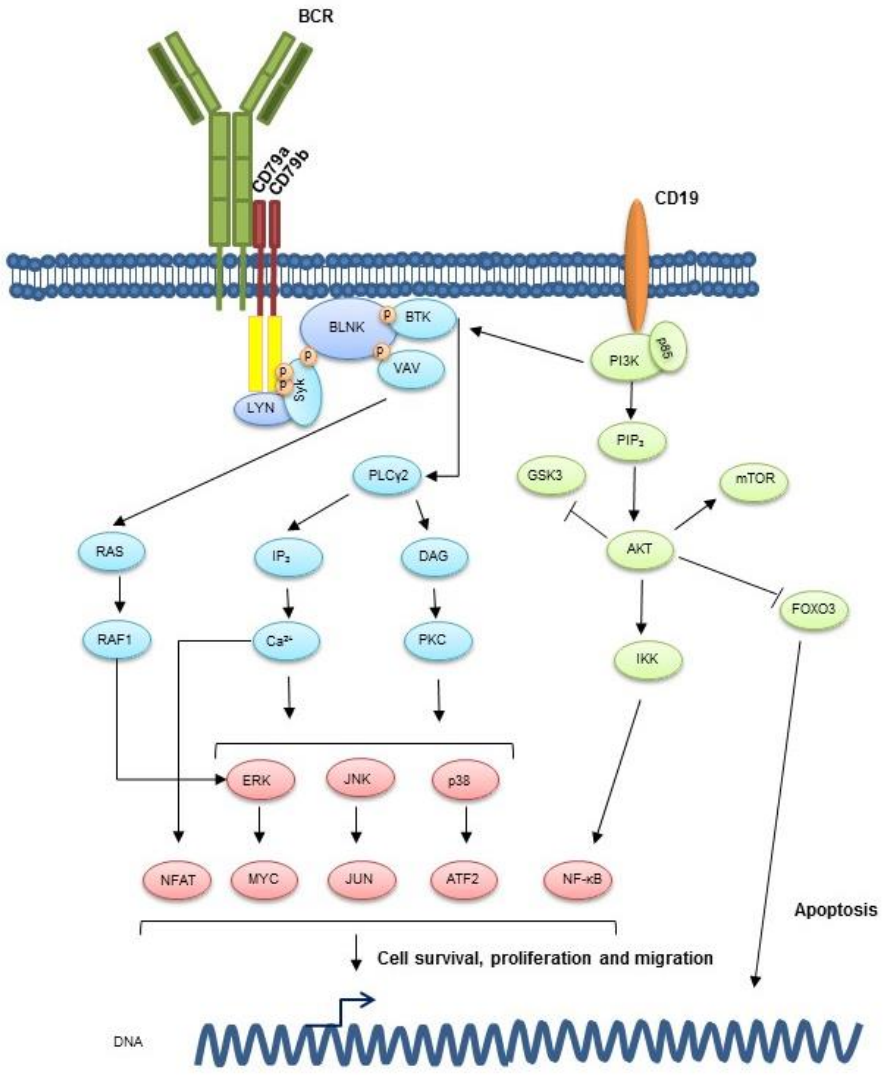

Figure 1.4 BCR signalling pathway.

Modified from Choi. M. Y., *et.al.* 2012.

As previously described the BCR is associated with two heterodimers that are able to transduce an intracellular signal; CD79a and CD79b (Figure 1.2). BCR signalling is activated when a bound antigen causes BCR aggregation, tyrosine residues within CD79a and CD79b then become phosphorylated by the Src family of tyrosine kinases Lyn, Fyn and Blk[17]. Phosphorylation of ITAM generates docking sites for proteins with Src homology (SH2) domains, such as spleen tyrosine kinase (Syk). The signal transduction of the BCR can be amplified if a B-cell co-receptor such as CD19, also clusters with the aggregated BCRs[18]. CD19 also contains tyrosine residues that can be phosphorylated by Lyn and subsequently activated. This activation leads to the phosphorylation of phosphatidylinositol 3 kinase (PI3K) at the SH2 containing p85 subunit. PI3K in turn phosphorylates phosphatidylinositol-4,5-biphosphate (PIP_2) to become phosphatidylinositol-3,4,5-triphosphate (PIP_3)[17,19]. PIP_3 production results in the recruitment of Bruton's tyrosine kinase (Btk). The adapter protein BLNK can be phosphorylated by Syk and Btk. BLNK has the ability to act as a scaffold for the activation of several different pathways. PLCγ2 docks on BLNK via its SH2 domain, PLCγ2 also contains a pleckstrin-homology (PH) domain which interacts with PI3K generated PIP_3[17]. The interaction of PLCγ2 with PIP_3 results in the cleavage of PIP_2 into diacylglycerol (DAG) and inositol-1,4,5-triphosphate (IP_3) which both individually lead to the activation of different cellular responses. DAG mediates the activation of protein kinase C (PKC)[20]. PKC then stimulates the mitogen-activated protein kinases (MAPK). MAPKs are serine-threonine protein kinases which include c-Jun NH2 terminal kinase (JNK), extracellular signal-regulated kinase (ERK) and p38[16,21]. Each of these kinases then phosphorylate and activate particular transcription factors; c-Jun and ATF-2 are activated by JNK, Elk-1 and Myc are activated by ERK and ATF-2 and MAX by p38. IP_3 on the other hand associates with IP_3 receptors on the surface of the endoplasmic reticulum (ER) resulting in a cytoplasmic flux of calcium (Ca^{2+}) from intracellular Ca^{2+} stores within the ER lumen. An increase in cytosolic Ca^{2+} levels results in a further cascade of Ca^{2+} release from store-operated calcium channels. Ca^{2+}-calmodulin complexes activate the transcription factor nuclear factor of activated T cells (NFAT)[17,20,22]. Classical PKCs (α, ßI/II and γ) become activated in the presence of Ca^{2+} and DAG. PKCß causes the activation of the pro-survival nuclear factor (NF)-κB pathway. Active PKCß in turn activates CARD11. CARD11 then recruits B cell lymphoma/leukaemia 10 (BCL10) and mucosa associated

lymphoid tissue lymphoma translocation protein 1 (MALT1), to form a complex termed CBM. CBM initiates inhibitor of κB kinase (IKK) which results in the activation of NF-κB[14,15]. The ERK and MAPK signalling pathway can be further propagated through the activation of the Rho family of GTPases signalling pathway, RAS/RAF1 signalling. RAS/RAF1 signalling becomes activated by Vav, a guanine exchange factor, which binds to BLNK resulting in tyrosine phosphorylation and activation[23]. Signalling through the BCR results in the propagation of a complex network of signalling pathways which finely tunes the B cell to survive, migrate, divide or undergo apoptosis (Figure 1.4).

1.2 Chronic lymphocytic leukaemia

CLL is characterised by an unregulated clonal expansion of a B cell population with a distinct immunophenotype. This immunophenotype distinguishes CLL from other B cell malignancies. CLL cells express the T cell antigen CD5, B cell surface antigens CD19 and CD23, and have surface IgM^{low} and $FMC7^{-}$ [24]. CLL is the most common leukaemia of the Western world, with a median age at diagnosis of 72 years, however approximately 10% of CLL patients are diagnosed before 55 years. More males are affected by CLL than females (1.7:1 ratio). CLL is typically diagnosed when 5,000 circulating B cells/μl are present in the peripheral blood for 3 months or longer[25].

There is a vast amount of heterogeneity in CLL; at the onset of disease it is very difficult to predict the clinical course. Some CLL patients may succumb to disease within a very short time course and require extensive treatment whilst others may never require medical treatment[26,27]. Historically CLL was thought to be a disease of accumulating B cells resistant to apoptosis. The investigation by Messmer *et al*. using deuterated water labelling, was pivotal for understanding CLL biology as they observed that *in vivo,* CLL cells are more dynamic than originally thought. They identified that there was significant death and proliferation of CLL cells, with 0.1 to over 1 % cell 'birth rates' of the entire clonal population per day, with higher proliferation rates corresponding to a more progressive disease[28].

1.2.1 Clinical staging

There are two different staging methods used for CLL, proposed by Rai and Binet. Both staging systems have different classifications categories, which CLL patients fall into, based upon results of both physical examination and standard laboratory tests[29,30]. The Rai system;

- Stage 0: Lymphocytosis and no enlargement of the LN, spleen or liver, and blood cell and platelet counts within a normal range.

- Stage I: Lymphocytosis with enlarged LN and blood cell and platelet counts within a normal range.

- Stage II: Lymphocytosis with enlarged spleen +/- enlarged LN. Blood cell and platelet counts within a normal range.

- Stage III: Lymphocytosis with anaemia +/- enlarged LN, spleen or liver. Platelet counts within a normal range.

- Stage IV: Lymphocytosis with thrombocytopenia +/- anaemia. LN, spleen or liver enlarged.

The Rai staging system is split into low, intermediate and high risk to determine appropriate treatment strategies. Low risk are those CLL patients with stage 0, intermediate risk are those at stage I&II and high risk patients are those with stage III&IV disease.

The Binet system however includes the number of areas affected by CLL, such as the LNs (1 cm in diameter or larger) or an enlarged organ. Areas of the body investigated are the head and neck, axillae, groin, palpable spleen and palpable liver[31]. The Binet system;

- Stage A includes up to two of the areas described above being affected and haemaglobin (Hb) levels ≥ 10 g/dL and platelets ≥ 100 x 10^9/L.

- Stage B is defined by at least three or more areas being affected and Hb ≥ 10 g/dL and platelets ≥ 100 x 10^9/L.

- Stage C is defined as patients with Hb levels less than 10 g/dL and/or platelet counts less than 100 x 10^9/L.

The different staging systems can be used to predict survival times for CLL patients; low risk or stage A confers 10 year survival, intermediate/stage B confers 5-7 year survival and high risk/stage C confers reduced survival to 2-3.5 years for CLL patients within this group[25,32]. Although clinical staging provides a good indicator for when treatment will be required, it does not always provide an accurate system for predicting disease progression or explaining the large degree of heterogeneity observed within CLL.

1.2.2 Prognostic markers

Prognostic markers are very valuable tools to help predict the clinical course the disease will follow and the time to first treatment. Extensive research into the heterogeneity in CLL has led to a comprehensive list of different prognostic markers, described below.

1.2.2.1 Lymphocyte doubling time

Lymphocyte doubling time (LDT) is an important indicator during early diagnosis; it can help predict the activity of the disease and time until first treatment is required. LDT is typically best used when lymphocyte counts are above 30,000 cells/μl. LDT of 6 months, or more than a 50% increase in lymphocyte counts within 2 months, is an indicator of active disease requiring treatment as outlined by the International Workshop on Chronic Lymphocytic Leukemia (IWCLL) [32-34].

1.2.2.2 Serum markers

There are three main serum markers that correspond with CLL prognosis; $ß_2$ microglobulin, serum thymidine kinase and soluble CD23. $ß_2$ microglobulin is an extracellular protein which is non-covalently bound to the α chain of MHC class I proteins. Elevated $ß_2$ microglobulin levels are associated with poor prognosis, high tumour burden, bulky disease and displays a correlation with CD38 and zeta-chain-associated protein kinase 70 kDa (ZAP-70) expression levels[35]. Serum thymidine kinase expression is present in dividing cells and therefore provides a valuable marker for proliferating and rapidly progressing disease[36]. Soluble CD23 is a low affinity receptor of IgE and expression correlates with diffuse BM infiltration, reduced survival and short LDT[34,36].

1.2.2.3 *IGHV* mutational status

CLL patients typically fall into two distinct prognostic groups depending on the mutational status of their *IGHV* gene. As described earlier, during B cell development in the GC *IGV* genes undergo SHM to expand the Ig repertoire. It has been identified that approximately 40% of CLL cases have unmutated and 60% have mutated *IGHV* gene segments[24]. Patients with less than 2% variance between *IGHV* and germline sequence are classified as being unmutated. CLL

cells with mutated *IGHV* tend to be relatively anergic with weak B cell signalling and are associated with cytogenetic abnormalities trisomy 12 and 13q14 del[37,38]. Unmutated *IGHV* on the other hand correlates with a more aggressive clinical course, with shorter remission times and progression free survival (PFS), a higher association with the acquisition of high risk cytogenetic abnormalities and shorter survival times irrespective of the disease stage[38-40]. An investigation of Binet stage A CLL patients found that median survival times for unmutated patients was 95 months compared to 293 months for patients with mutated *IGHV*[39]. Interestingly the use of the specific variable region encoded by *VH3-21* gene segment is associated with a more aggressive disease irrespective of mutational status[41,42]. The costly and laborious nature involved in identifying *IGHV* mutational status of CLL patient cells led to the search for more easily identifiable surrogate markers, of which CD38 and ZAP-70 were identified[43-45].

1.2.2.4 ZAP-70

ZAP-70 is a receptor associated protein tyrosine kinase, typically found in T cells and natural killer (NK) cells, and not in normal healthy mature B cells[46]. However ZAP-70 expression has been identified in CLL patients, with a strong correlation between expression and unmutated *IGHV*. Irrespective of mutational status, ZAP-70 expression is an independent poor prognostic marker resulting in reduced PFS and overall survival (OS), and a valuable indicator of time to first treatment[34]. ZAP-70 expression like mutational status remains constant over time, and is a good tool for predicting mutational status[47]. ZAP-70 expression can be established through flow cytometry and immunohistochemistry, and the correspondence with correct determination of mutational status has been shown to be between 77-95%[34]. In one study ZAP-70 expression of 5.54 fold or higher expression in unmutated CLL displayed 93% accuracy at correctly establishing the mutation status[48]. ZAP-70 augments the activity of BCR signalling. Upon BCR ligation, BCR signalling is enhanced in the presence of ZAP-70 resulting in an activating and proliferative response[46].

1.2.2.5 CD38

CD38 is a transmembrane glycoprotein that has also been shown to be an independent poor prognostic marker[44]. Elevated CD38 expression has been

associated with advanced disease stage, high risk cytogenetic aberrations and reduced PFS and OS[49]. CD38 has cyclic adenosine diphosphate-ribose activity and can act as both a receptor and an enzyme. Like ZAP-70, CD38 is also thought to augment BCR signalling. The use of CD38 as a surrogate marker for mutational status is controversial as the association is not an absolute; it is also thought that CD38 expression levels vary during the course of the disease in contrast to mutational status[50,51]. Experiments with deuterium labelling have shown that high expression level of CD38 is associated with high proliferation rates, suggesting a more active disease[52].

1.2.3 Genetic influence and CLL

Unlike other haematological malignancies there is no defining chromosomal abnormality that results in increased susceptibility to CLL. Indeed, familial CLL cases are rare and defined as having one affected relative[53]. Approximately 5% of CLL cases report family history of CLL[54,55]. Although there have been several conflicting reports it appears that familial CLL displays no adverse prognosis with little molecular differences between familial and sporadic CLL[56]. Monoclonal B cell lymphocytosis (MBL) has been suggested to precede the development of disease in the majority of CLL cases. MBL is characterised by an indolent expansion of monoclonal B cells within the peripheral blood at a concentration lower than 5,000 cells[57]. In some cases MBL cells display typical CLL surface protein phenotype, and can demonstrate similar chromosomal abnormalities[58]. 13% of relatives of CLL patients present with MBL compared to approximately 3-5% with no family history of CLL. The increased frequency indicates that there is some heritability towards the susceptibility of developing B cell clones[59,60].

1.2.3.1 Epigenetic alterations

Epigenetic alterations can result in the activation or silencing of gene transcription without changing the DNA sequence. Epigenetic changes can be transmitted to daughter cells and when occurring in germline cells alterations in gene expression can be passed onto the following generation[56]. The epigenetic silencing of death associated protein kinase 1 *(DAPK1)* through the methylation of the promoter sequence has been frequently identified in both familial and sporadic CLL cases[61]. In a case study of a large family affected by CLL they

identified *DAPK1* as predisposing factor to the development of CLL, with family members having a single nucleotide polymorphism (SNP) within the promoter sequence aiding the binding of the transcriptional regulator HOXB7 effectively silencing the gene[61]. *DAPK1* is thought to mediate the induction of either apoptosis or autophagy following cellular stress.

1.2.3.2 Cytogenetic abnormalities

Several cytogenetic abnormalities have been frequently identified in CLL patients, which subsequently have an impact on PFS, OS and response to treatment. Fluorescent *in situ* hybridisation (FISH) is a valuable tool for identifying cytogenetic aberrations, which have been identified in approximately 80% of CLL patients. The functional impact the different cytogenetic abnormalities have upon CLL patient survival and treatment free survival from the date of diagnosis is shown in Figure 1.5[62,63]. CLL patients with a normal karyotype with no mutations detected by FISH typically have a median survival of 111 months (Figure 1.5)[63,64].

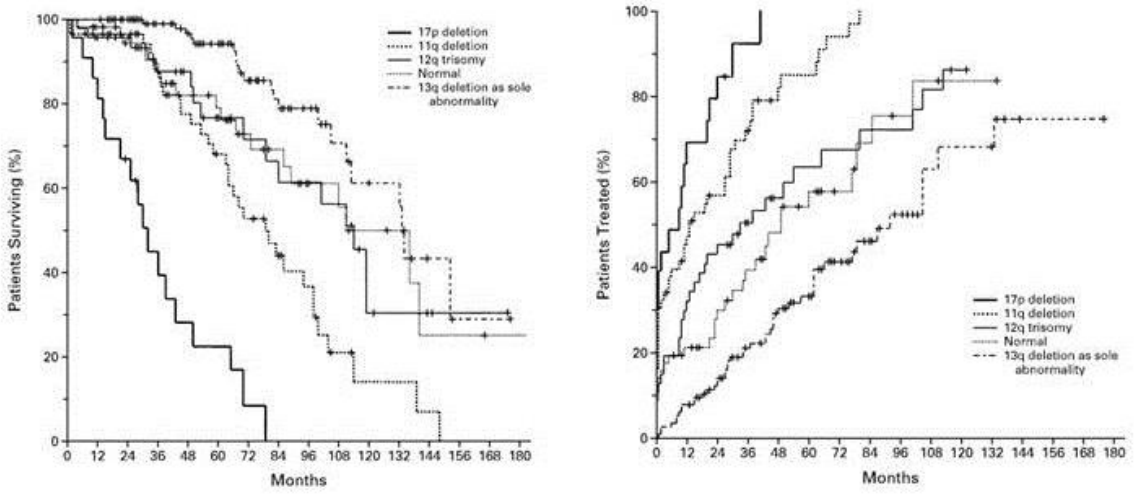

Figure 1.5 Impact of the different cytogenetic abnormalities within CLL upon the probability of survival and disease progression.
Reproduced with permission from (Döhner. M.D., *et.al.* 2000), Copyright Massachusetts Medical Society.[63]

6q21 del

Deletions of chromosome 6q21 are observed at low frequencies within CLL (3-6%), although they have not currently been determined to present a functional

impact on CLL patient survival, 6q del are associated with intermediate risk [65,66]. Patients with 6q del present with atypical CLL morphology, high white cell counts, progressive disease and high CD38 expression[65].

Del 13q14

The most commonly identified cytogenetic abnormality is the deletion of the band 13q14, observed in approximately 55-60% of CLL cases[62]. 13q14 del is the most favourable cytogenetic karyotype due to its association with slowly progressing disease with median survival of 133 months[67]. 13q14 del encompasses two microRNAs; miR15a and miR16-1, which negatively regulate the expression of the anti-apoptotic protein Bcl-2[68,69]. Deletion of these two microRNAs in mice leads to the development of a clonal B-lymphoproliferative disorder similar to CLL[70].

Trisomy 12

Trisomy of chromosome 12 is observed in approximately 7-20% of CLL cases, with median survival time of 114 months, similar to that of CLL patients with normal karyotype[34]. The full pathogenesis of trisomy 12 has not been fully elucidated, there appears to be little increase in reported incidences with advanced disease stage or the transition to refractory disease[71]. This suggests that trisomy 12 provides little clonal advantage[72]. One suggested association is between the expression of trisomy 12 and CD49d a subunit of the late activation 4 receptor (VLA-4), which is important for the migration of CLL cells towards secondary organs[73].

11q22-q23 del

Detection of 11q23 deletion is a poor prognostic indicator observed in 18% of CLL cases. 11q del is associated with a shortened median survival of 79 months, younger age at diagnosis and more advanced disease stage[34]. 11q del patients are also more likely to suffer from extensive peripheral, abdominal and mediastinal lymphadenopathy[74]. The pathogenic nature of 11q23 del acts through the deletion of the gene ataxia telangiectasia mutated (*ATM*) encoded within this region. ATM protein is a crucial component of the DNA damage

response pathway[75,76]. ATM becomes activated in the presence of undesirable double strand breaks caused by either an endogenous event or DNA damaging agent. ATM can then halt the cell at either G1/S or G2/M phase by preventing cyclin dependent kinase (Cdk) activity. Depending on the damage caused by the DNA break, ATM can either induce apoptosis or directly help repair the break. Monoallelic deletion of 11q23 results in poor prognostic and biallelic inactivity of the remaining *ATM* results in a more severe clinical outcome[77,78]. Mutations of *ATM* are observed in approximately 12% of CLL patients and 33% of 11q23 del patients. [77,79,80]

17p13 del

The cytogenetic aberration associated with the poorest clinical outcome is deletion of 17p13, and 17p del is observed in 16% of CLL patients[34]. CLL patients with 17p13 del have a median survival of 32 months, with rapid disease progression. Early treatment strategies are required and 17p del typically display poor response to treatment[62,81]. The aggressive nature of 17p13 del is associated with this region harbouring the tumour suppressor *TP53* gene locus. Monoallelic deletion of 17p13 is commonly associated with an inactivating mutation of the remaining allele, observed in over 80% of cases[82]. *TP53* gene encodes for p53. p53 is commonly referred to as the guardian of the genome and is crucial for preventing the replication of cells that contain DNA damage. p53 regulates the transition of dividing cells from G1 to S phase and can activate apoptosis if DNA damage is detected[83]. CLL patients with 17p del have limited treatment strategies compared to other cytogenetic karyotypes. Many chemotherapeutic agents, such as alkylating and purine analogues, mediate CLL cell death through the induction of DNA damage and subsequently p53 driven apoptosis[84]. In 17p del patients that are fit enough, allogenic stem-cell transplantation is a recommended treatment strategy[85]. Alemtuzumab an anti-CD52 MAb is also used when allogenic stem cell transplantation is not appropriate[86]. The incidence of 17p del increases dramatically in cases of relapsed and refractory CLL, observed in approximately 45% of cases, demonstrating clonal evolution of poor prognostic cytogenetic aberrations[87]. CLL treatment strategies are discussed in more detail in section 1.4.

1.2.3.3 Newly identified recurrent mutations

Recent advances in sequencing technology have led to more readily available whole genome and whole exome sequencing of CLL cell DNA[88,89], and the ability to conduct targeted deep sequencing. NFκB pathway is constitutively active in CLL and recent deep sequencing data of this pathway revealed frequent mutations encompassing IκBε[90]. IκBε mutations were identified in 7% of CLL patients, of these mutations approximately 60% were caused by an identical 4bp frameshift deletion resulting in truncated protein[90]. IκBε mutations were also predominantly associated with poor prognostic CLL patients with inferior outcome[90]. From whole genome analysis other novel mutations were also identified, with some demonstrating an impact on CLL prognosis. The numerous recurrent gene mutations found included; *NOTCH1, XPO1, MYD88, KLHL6, SF3B1, ZMYM3, MAPK1, FBXW7*, *DDX3X* and *BIRC3*. *ZMYM3* is located on the X chromosome, the encoded protein forms part of a histone deacetylase (HDAC) multi-protein complex that epigenetically silences gene transcription[91]. *DDX3X* is also located on the X chromosome, and mutations in CLL demonstrate a predominance towards males being afflicted[92]. *DDX3X* mutations in CLL result in a truncated protein[92]. *DDX3X* is a dead-box RNA helicase associated with RNA splicing, RNA transport and translation initiation. *DDX3X* also interacts directly with *XPO1*[91]. *XPO1* is a nuclear exporter which transports over 200 proteins, including p53 and NF-κB, from the nucleus to cytoplasm. *XPO1* mutations although not fully understood, are thought to be oncogenic and display an association with unmutated *IGHV* CLL[91,93]. *KLHL6* is involved in GC formation during B cell maturation and SHM in CLL displays an association with mutated *IGHV* CLL[88]. *FBXW7* is an ubiquitin ligase that targets several oncogenes such as c-Myc, myeloid cell leukaemia 1 (MCL-1) and Notch1 for degradation[91]. *FBXW7* mutations in CLL are thought to abrogate function resulting in an alternative mechanism for uncontrolled Notch1 activation[94,95]. MAPK1 kinase forms an integral part of many intracellular pathways such as proliferation, development, transcription regulation and differentiation. Mutations within *MAPK1* in CLL are thought to encompass the kinase domain[91].

NOTCH1, SF3B1, MYD88 and *BIRC3* have been the most extensively studied genes to date, due to their higher functional impact, association with prognostic outcome, high frequency of occurrence and their association with

chemotherapeutic resistance, and will be discussed in more detail below. Of the four genes *MYD88* is the only recurrent gene mutation associated with improved prognostics[88,89,94].

NOTCH1

NOTCH1 mutations (NOTCH1^{MUT}) have been recently identified as an independent poor prognostic marker for CLL patients, present in approximately 10-12% of CLL cases[96]. The majority of mutations, greater than 80%, are generated from a 2 base pair frameshift deletion c.7544_7545delCT[88,97-99]. In CLL a mutated Notch1 results in constitutively active truncated protein lacking the C-terminal PEST domain. NOTCH1^{MUT}, as well as being an independent poor prognostic marker, displays an association with high expression of CD38 and ZAP-70, increased incidence with advancing disease, trisomy 12 karyotype and unmutated *IGHV*[97,100]. The rate of incidence increases to 13-20% in CLL patients with progressive disease with increased chance of relapse. For NOTCH1^{MUT} CLL patients, the time to first treatment is approximately 4.8 months from diagnosis[101,102]. Patients with NOTCH1^{MUT} are observed to have a 21-45% OS to 10 years compared to wild-type at 56-66% OS to 10 yrs[103,104]. NOTCH1^{MUT} also demonstrate a propensity for being associated with Richter's transformation. The rate of incidence of Richter's transformation is 10% for CLL patients 5 years after diagnosis[105]. Richter's transformation is a very aggressive disease which is lethal in almost all incidences; the disease is generally resistant to chemotherapy and displays rapid disease kinetics[106,107]. The most common mutation observed in Richter's transformation is *TP53* mutations, however in 30% of cases NOTCH1^{MUT} are observed almost exclusively in the presence of oncogenic activation of *c-MYC*[97].

A retrospective study of the CLL8 trial identified which patients within the trial had NOTCH1^{MUT}, and then determined how this predicted their response to fludarabine in combination with cyclophosphamide (FC) vs FC with rituximab (RTX) treatment. From these data it was determined that there was no advantage to combining RTX with FC treatment[108]. 17p del CLL patients displayed at least marginal improvement with the addition of RTX to FC treatment. At ASH 2013, research was presented from a trial investigating the effect of chlorambucil with or without ofatumumab (OFA) on PFS. They observed

an improvement in PFS with chlorambucil plus OFA in NOTCH1^{MUT} patients up until 18 months, but after this the affect was lost and PFS becomes the same as chlorambucil alone for these patients[109]. This suggests therefore that NOTCH1^{MUT} CLL cells have obtained resistance to type I anti-CD20 MAbs.

SF3B1

Mutations of splicing factor 3b subunit (*SF3B1*) have been observed in 3-10% of newly diagnosed CLL cases rising to 20% in relapsed refractory CLL patients[89,91,110]. Mutations are typically missense mutations limited to five codon hotspots (codons 662, 666, 700, 704 and 742) within the Heat domain[89,91,110]. These mutations are thought to modify the function of the protein instead of abrogating activity[111]. SF3B1 is a core component of the spliceosome machinery involved in the removal of introns from precursor mRNA. *SF3B1* mutations are also an independent poor prognostic marker associated with an aggressive disease with the malignant *SF3B1* clone expanding as the disease progresses[112]. *SF3B1* mutations display an association with 11q del mutations, genomic instability and dysregulated epigenetic modification. OS to 10 years reduces from 60-77% in unmutated to 10-48% in *SF3B1* mutated CLL cases with the time to first treatment being 2.4 months[89,91,103,110].

BIRC3

Mutations within baculoviral IAP repeat containing protein 3 (*BIRC3)* result in an aggressive disease which is extensively observed within CLL patients relapsed refractory to fludarabine whom are p53 wild-type[113]. The rate of incidence rises from 5% in freshly diagnosed CLL cases to 25% in those that are relapsed refractory, with OS being 3.5 years[113]. In most cases mutations are either frameshift deletions/insertions or nonsense substitutions[104]. Mutations result in truncation of the C-terminal ring domain disrupting the function of the protein[114]. *BIRC3* is a negative regulator of non-canonical NF-κB signalling. Mutations in *BIRC3* usually result in abolishing the E3 ubiquitin ligase activity of the protein. Therefore the protein can no longer degrade its target MAP3KI4 serine threonine kinase, the principle activator of the non-canonical NF-κB pathway[115].

MYD88

Myeloid differentiation primary response 88 (*MYD88*) has a very low observation rate in CLL, affecting approximately 3% of cases[88]. *MYD88* mutations are typically associated with younger age at diagnosis, 83% ≤ 50 yrs. *MYD88* mutations are also associated with low expression levels of CD38 and ZAP-70, and a mutated *IGHV* phenotype. *MYD88* mutations present a favourable prognostic outcome with 100% OS to 10 years compared to 62% wild-type cases[116]. Most mutations occur as a result of a SNP within exon 5, L265P[91,94]. MYD88 has a crucial role in B cell homeostasis and functions as the adaptor protein of interleukin-1 receptor (IL-1R)/ toll-like receptor (TLR) innate immune response[117]. Active TLR leads to the phosphorylation of MYD88 which in turn recruits IL-1R and other downstream proteins like TRAF6, resulting in NF-κB signalling[116]. CLL cells with *MYD88* mutations display overexpression of several genes within the NF-κB pathway, which atypically confers improved prognosis.

1.2.4 Origin of the CLL cell

Determining the cell of origin in CLL remains a highly complex problem which is yet to be solved. New advances and breakthroughs in immunogenetics and gene expression profiling (GEPs) has resulted in a shift in the hypothesis as to the nature of CLL development. Part of the complexity in determining the cell of origin is due to the immunophenotype observed with CLL; $CD5^+$, $CD19^+$, $CD23^+$ and low IgM which is not identifiable in any normal B cell subset[107]. With the identification of two different subsets of CLL, unmutated or mutated *IGHV*, it was proposed that there was a two cell origin model for CLL. However GEP data has demonstrated that unmutated and mutated CLL cells share large amount of GEP homology with few genes displaying differential expression[118]. This suggests that unmutated and mutated *IGHV* CLL cells are derived from the same antigen experienced progenitor cell. This lead to the hypothesis that CLL cell types are derived from marginal zone B cells. Marginal zone B cells surround the GC and typically have IgM^{high} IgD^{low} expression, and are associated with responding to bacterial polysaccharides in a T cell-independent fashion[119]. Marginal zone B cells have been demonstrated to be antigen experienced through clonal expansion and can display either mutated or unmutated *IGHV*[120,121].

Further evidence to suggest CLL cells are derived from antigen experienced cells is the observation that there is a skew in BCR use, approximately 30% of unmutated *IGHV* CLL patients express one of >150 grouped stereotyped BCR subsets[122,123]. Therefore it is thought that antigenic stimulation is involved in the processes of CLL pathogenesis. Unmutated *IGHV* CLL cases exhibit high degrees of homology of heavy chain complementarity-determining region (*HCDR3*), which often codes for identical *IGHV, IGHD* and *IGHJ* gene segments. This same bias is observed in stereotyped light chains with *KCDR3* and *LCDR3* displaying similar protein structure[56,124-126]. This bias in BCR expression suggests that common antigens are recognised by CLL cells and are a propagating factor in the development of the disease. Such level of similarity of BCR between CLL patients is striking, the probability of finding the same extent of similarities between the BCRs in two different individuals would be expected to be one in over a million cases[56]. Unmutated *IGV* marginal zone B cells are the first line of defence within the humoral immune response; they are also polyreactive and autoreactive Igs[119]. Unmutated *IGV* protect against invading microbes and catabolic debris such as non-muscle myosin heavy chain IIA, the latter of which has been proposed to be a propagating factor in CLL development[56,127]. However aside from expressing IgM and IgD like CLL cells, marginal zone B cells display a surface phenotype dissimilar to CLL cells as they are; $CD5^-$,$CD23^-$ and $CD22^+$.[119] It has been proposed that these surface proteins become switched on, upon activation of CLL cells[128]. However this has not been unanimously agreed and so marginal zone B cells have not definitively been identified as the CLL cell of origin.

$CD5^+$ B cells have been identified in mice that also display stereotyped BCR use, termed B-1 cells[129]. B-1 cells display both unmutated and mutated *IGV* genes, and are polyreactive receptors, which can bind autoantigens from endogenous or exogenous proteins[130]. A population of $CD5^+$ B cells in humans has been identified; however there were several conflicting factors in determining if they are the CLL cell of origin[131]. It was thought human $CD5^+$ B cells are non polyreactive, do not mature or proliferate upon stimulation with T-cell type II independent antigens and displayed no stereotypy[132]. However recent research opposes this opinion; they demonstrate a statistically significant number of stereotyped BCRs in $CD5^+$ B cells[133,134]. GEP data identified the $CD5^+$ B cell

population as baring a closer resemblance to CLL cells when compared to marginal zone B cells. They also identified a population of $CD5^+$ $CD27^+$ B cells which displayed SHM, potentially representing the mutated CLL patient subset[133,134].

Another recent study showed HSCs of CLL patients are already primed to generate clonal B cells. Furthermore they identified a bias in *IGHV* genes independent of the original CLL clone in a xenograft mouse model, with the bias reflecting that seen in human CLL, indicating the importance of BCR signalling in clonal selection[135]. However the lymphoid expansions present in the mice were unrelated to the original patient, suggesting that the genetic lesions occurred *de novo*. These new findings need to be corroborated, but they add to the complexity of identifying the true progenitor cell of CLL[107].

1.3 CLL and the microenvironment

The clinical efficacy of chemotherapeutic agents are limited in CLL by the pro-survival and pro-proliferative signals received within the BM and LN. The dependency of CLL cells on microenvironmental stimulation is also observed *in vitro*, isolated CLL cells undergo spontaneous apoptosis unless rescued through co-culture with BM derived stromal cells[136]. CLL is no longer considered an indolent disease, with 1-2% of the entire clone being born per day[28]. CLL cells proliferate within pseudofollicles, located within the BM and LN[137]. Malignant CLL cells have been shown to modify the microenvironment to aid in their survival and proliferation[138,139]. The interaction of CLL cells with the other components of this niche, such as stromal cells, T cells and soluble factors, can also promote drug resistance[137,138,140]. A schematic overview of the interaction of CLL cells within the tissue microenvironment is shown in Figure 1.6.

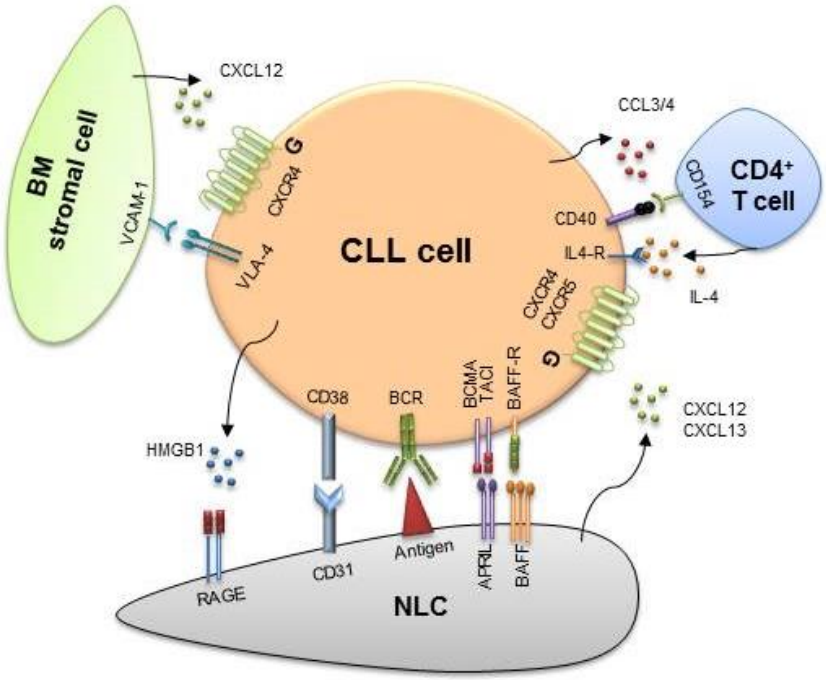

Figure 1.6 Microenvironmental interaction of CLL cells within lymphoid organs.
Modified from Ten Hacken. E., *et.al.* 2014.

1.3.1 Stromal cells

BM stromal cells provide important interaction with CLL cells to aid their survival. VLA-4 an integrin on the surface of CLL cells interacts with vascular cell adhesion molecule 1 (VCAM-1) expressed on the surface of endothelial cells, BM stromal cells, and extracellular matrix molecular fibronectin[136]. VLA-4 stimulation results in the up-regulation of the Bcl-2 family of anti-apoptotic proteins; MCL-1 and T cell leukaemia/lymphoma 1 (TCL1)[141,142]. As described earlier CXCL12 is highly expressed by BM stromal cells. CXCL12 interacts with the chemokine receptor CXCR4 on CLL cells, providing an important chemokine gradient critical for the migration and homing of CLL cells towards the lymphoid organs. Migration of CLL cells is observed *in vitro* by the spontaneous migration of CLL cells below the stromal layer within culture, termed pseudoemperipoiesis, in a CXCR4 dependent fashion[143]. There is also some suggestion that BM stromal cells can lead to the down-regulation of CD20 on CLL cells[144].

1.3.2 Nurse-like cells

Nurse like cells (NLC), are located within the secondary lymphoid organs, including LNs of CLL patients[145]. The differentiation of NLC from peripheral blood mononuclear cells is still under investigation. However it has been established that *in vitro* CLL cells express the nuclear protein high mobility group box-1 (HMGB1) which when released by CLL cells results in NLC differentiation through the activation of the receptor for advanced glycation end-products (RAGE)- TLR9 pathway[146]. NLC are also able to activate BCR signalling and secrete CXCL12 and CXCL13 to attract circulating CLL cells to enter the tissue microenvironment[145,147]. NLC express tumour necrosis factor (TNF) family members; B cell activating factor (BAFF) and proliferation inducing ligand (APRIL)[148]. BAFF and APRIL activate B cell maturation (BCMA), transmembrane activator and calcium modulator and cyclophilin ligand interactor (TACI) and BAFF receptor which together aid the survival and proliferation of CLL cells[148]. CD31 expression on NLC interacts with CD38 from CLL cells to provide further pro-survival signals[52]. Chemokine receptors CXCR4 and CXCR5 are expressed at high levels on CLL cells; making them highly adept at sensing and following the chemokine gradient produced by the release of CXCL12 and CXCL13 by NLC[143]. Aside from migration, CXCR4 and CXCR5 stimulation activates the pro-survival pathways ERK1/2 and signal transducer and activator of transcription 3 (STAT3) signalling, which has been shown to prolong CLL cell survival *in vitro*[149,150]. Deuterium labelling of CLL cells has also provided insight into $CXCR4^+$ CLL cells, which have an increased rate of lymphoid organ infiltration and subsequently inferior outcome for the patient[151]. VLA-4 along with CD38 has been shown to provide a poor prognostic association for CLL patients, with higher expression linked with enhanced migration towards CXCL12[152,153]. Chemokine (C-C motif) ligand (CCL3) and CCL4 are secreted by CLL cells upon BCR stimulation and NLC co-culture *in vitro*[154]. Secretion of CCL3 and CCL4 attracts monocytes and T cells to the tissue microenvironment. Higher levels of CCL3 and CCL4 expression is associated with $CD38^+$ VLA-4^+ CLL cells[155]. Within normal B cells CCL3 and CCL4 expression is regulated by Bcl-6 transcriptional repression[156]. The plasma levels of CCL3 provide an independent poor prognostic marker for CLL patients, with reduced time to first treatment[157].

1.3.3 T cells

As previously described, the association of B cells and T cells within the GC provide important signals to aid B cell survival. Interaction of CD154 on $CD4^+$ T cells with CD40 on the surface of B cells is critical during antigen presentation. CD40 signalling is also important for CLL cells, as CD40 ligation promotes CLL survival[158]. In conjunction with CD40 stimulation, release of the pro-inflammatory cytokine interleukin-4 (IL-4) by $CD4^+$ T cells also propagates pro-survival signals[159,160]. CLL disease also impacts upon the ability of T cells to function fully. The number of circulating oligoclonal $CD4^+$ and $CD8^+$ T cells is increased in CLL[161]. However their activity is de-regulated; they are unable to form functional immune synapses, have reduced T-cell motility mediated by Rho GTPase and have higher levels of exhaustion markers such as programmed cell death 1 (PD1)[162-165]. γδT cells, part of the innate immune system which respond to microbial pathogens, display reduced cytotoxicity activity within CLL patients[166]. T cells from CLL patients also express high levels of inhibitory receptor cytotoxic T lymphocyte associated antigen 4 (CTLA-4), resulting in impaired function[167].

1.3.3.1 CD40 signalling

CD40 is a transmembrane glycoprotein receptor from the TNF-receptor (TNF-R) superfamily[168]. CD40 signalling through CD154 binding is important during antigen presentation for T cell-dependent B cell activation. CD154 is expressed on $CD4^+$ T cells, monocytes and dendritic cells. CLL cells use CD40 signalling to mediate survival and proliferation[169,170]. CD40 displays no intrinsic catalytic activity, therefore TNF-R associated factors (TRAFs) act as adaptors for signalling. Upon CD154 engagement of CD40, CD40 clusters within lipid rafts to propagate intracellular signals[168]. TRAF adaptors when bound to CD40, couple CD40 with PI3K, PLCγ, MAPK-ERK, stress related protein kinase p38, JNK and NF-κB[171]. NF-κB activation results in the activation of Bcl-2 anti-apoptotic proteins Bcl-X_L, Bfl-1, A1 and MCL-1 and subsequently enhanced cell survival[168]. Typically Bcl-2 and Bcl-X_L expression results in G_o/G_1 cell-cycle arrest, however CD40 signalling is able to bypass this in order to stimulate proliferation [172]. CD40 stimulation enhances the drive to proliferate in CLL cells through down-regulation of the cell cycle inhibitory protein cyclin dependent kinase $p27^{Kip-1}$

whilst enhancing the activation of cyclin dependent kinases Cdk4 and Cdk6[173]. Cdk4 and Cdk6 are both essential for G_1 progression, they phosphorylate retinoblastoma (Rb) protein leading to the activation of E2F transcription factors[168].

Approximately 30% of CLL cases display expression of CD154 suggesting autocrine and paracrine signalling is present within CLL[174]. Noxa is a member of the Bcl-2 family, but unlike the other proteins described, the expression of Noxa is associated with the induction of apoptosis in a caspase dependent fashion. Consequently with CD40 stimulation there is a reduction in *NOXA* gene expression both within the LN and following *in vitro* stimulation[175]. PLCγ2 activation by CD40 signalling leads to the assembly of IP_3. IP_3 associates with IP_3 receptors on the surface of the ER causing cytoplasmic flux of Ca^{2+} from intracellular Ca^{2+} stores within the ER lumen. Elevated cytosolic Ca^{2+} levels result in a further cascade of Ca^{2+} release from store-operated calcium channels[17]. In an *in vitro* study investigating the efficacy of RTX against CLL cells stimulated through CD40 there was an increase in cytosolic Ca^{2+} levels when CD20 was bound by RTX, this caused an increase in reactive oxygen species (ROS) which enhanced the ability of RTX mediated direct cell death[176]. The use of a cross-linking antibody was required as RTX is not a potent inducer of direct cell death, with activity associated with complement dependent cytotoxicity (CDC) and antibody-dependent cellular cytotoxicity (ADCC) induction. The increase in direct cell death when stimulated with CD40 was not observed for alemtuzumab suggesting this is particular to anti-CD20 MAbs. It is not clear whether it is the role of CD20 as a store operated Ca^{2+} channel that causes this rise in cytosolic Ca^{2+} with RTX binding or whether CD20 couples with another Ca^{2+} channel. Importantly based on mRNA expression levels, the induction of direct cell death was not caused by typical apoptosis and therefore was p53 independent[176].

1.3.3.2 IL-4 signalling

T cells secrete several different cytokines which can promote different cellular responses within B cells such as proliferation - IL-2 and TNFα, and survival - IFNα, IFNγ, IL-2 and IL-4.[177] Within normal B cells binding of IL-4 to the IL-4 receptor (IL-4R) on B cells results in the tyrosine phosphorylation and activation of Jak kinases Jak1/2/3[178]. Activation of Jak subsequently phosphorylates and

activates IL-4Rα. IL-4Rα then functions as a docking site for further signalling molecules such as insulin receptor substrate-1 (IRS-1) and IRS-2[178]. IRS1/2 become phosphorylated after recruitment onto IL-4Rα, which in turn results in the association with the p85 subunit of PI3K. This interaction causes a conformational change within PI3K resulting in the activation of its catalytic ability, resulting in downstream activation of PKC and Akt kinase[179,180]. Activation of these signalling pathways results in increased proliferation and CLL survival. PI3K aids in CLL cell viability by protecting against apoptosis by up-regulating anti-apoptotic proteins from the Bcl-2 family[181].

IL-4Rα also contains three tyrosine binding sites at residues 575, 603 and 631 for the docking of STAT6. STAT6 consequently becomes activated by Jak resulting in disengagement[182]. STAT6 then homodimerises and translocates to the nuclease where it binds to the promoters of certain genes either alone or in concert with other transcription factors. Other transcription factors include c-Jun, SP-1, c/EBPα and NF-κB which results in aiding cell survival and cellular differentiation[183]. IL-4 signalling within CLL is thought to be induced by both autocrine and paracrine signalling. PHA-activated CD2 purified T cells from the peripheral blood of CLL patients demonstrated increased secretion of IL-4 into culture when compared against those from normal individuals. CLL cells isolated from patients with early stage of disease also displayed elevated cytoplasmic levels of IL-4, *in vitro* they had IL-4 mRNA expression and demonstrated IL-4 secretion following culture[184-187].

1.3.4 Tailored CLL microenvironment

Aside from the factors already mentioned, NK cells, like T cells, display impaired cytotoxicity in CLL patients. Expression of the plasma molecule human leukocyte antigen G (HLA-G) within CLL patients results in the induction of NK cell apoptosis and impairs their cytotoxic ability[188]. NK cell cytotoxic response is described in more detail in section 1.4.4.6. CLL cells also release microvesicles which activate Akt within BM stromal cells, consequently leading to the production of vascular endothelial growth factor (VEGF) and enhancing CLL cell survival[189]. Microenvironmental stimulation clearly demonstrates a huge obstacle in the treatment of CLL. Chlorambucil and fludarabine *in vitro* demonstrate reduced efficacy at inducing apoptosis in CLL cells when co-cultured with BM

stromal cells[141,190]. The BM and LN microenvironment provides support to CLL cells that have escaped chemotherapy strategies propagating the appearance of minimal residual disease (MRD) within CLL[191]. Finding therapeutic agents effective against CLL cells hiding within the tissue microenvironment is crucial for the future treatment and management of CLL.

BCR signalling within the tissue microenvironment is a key component to the survival and drug resistance observed within CLL[139]. Unmutated *IGHV* CLL cells are more responsive to BCR stimulation compared to mutated *IGHV*, which is enhanced by higher expression of ZAP-70 and CD38[46,192]. The signalling protein Lyn is also over expressed resulting in enhanced survival[193]. There is evidence to suggest both autonomous and antigen-dependent BCR signalling play important roles in the pathogenesis of CLL. The BCR signalling pathway was described in section 1.1.4. Dysregulation of tonic BCR signalling within CLL is observed by the hyperactivity of BCR signalling components Lyn, Syk, Btk, and PI3K[138]. Stereotyped BCRs within CLL highlight the importance of antigen stimulation in the pathogenesis of CLL. As previously stated unmutated *IGHV* CLL cells are polyreactive, possibly to catabolic debris, such as; non-muscle myosin heavy chain IIA, single stranded and double stranded DNA and lipopolysaccharides[138,194]. BCR from mutated CLL patients respond to yeast, fungi and ß-glucans stimulation[194]. One stereotyped BCR subset from unmutated CLL cells, IGHV1-69 recognises HIV-1, Hepatitis C, viral antigens and commensal bacteria[195]. CLL cells also demonstrate autonomous signalling within some BCRs, with self-recognition of epitopes within the HCDR3 region of the BCR[196]. Unlike other malignancies like diffuse large B cell lymphoma, there are currently no activating mutations identified within the BCR of CLL patients to explain the reliance on BCR signalling[197]. This implies that both autonomous and antigen stimulation are important in receptor signalling and CLL cell survival and propagation. Inhibitors that target the BCR signalling pathway in CLL are currently in development to combat microenvironmental stimulation. Promising therapeutic agents are described in section 1.4.1.2.

1.3.5 Notch signalling

Oncogenic transformation of Notch signalling has been identified in several different cancer types; lungs, head and neck as well as in the haematological

malignancies, T cell acute lymphoblastic leukaemia (T-ALL), Hodgkin's lymphoma and more recently CLL[198]. Advances in genome wide sequencing technologies has provided an insight into the role of Notch1 in CLL. The importance of Notch signalling within lymphocyte development has been well characterised[199]. $NOTCH1^{MUT}$ have been identified in approximately 12% of CLL patients and are an independent poor prognostic marker[96]. Notch signalling has been shown to suppress p53 and Jnk function, as well as the pro-apoptotic proteins Bax, Bim and Noxa[200-202]. Canonical and non-canonical Notch signalling also leads to elevated activation of PI3K/Akt and NF-κB signalling whilst also causing an increase in the anti-apoptotic proteins Bcl-2 and Bcl-X_L[200,201,203].

1.3.5.1 Notch receptors and ligands

The Notch receptor was first identified in 1917 by Thomas Hunt Morgan, after the identification of a strain of Drosophila with notched wing phenotype[198]. Within mammals there are four members of the Notch family (Notch1-4). Notch receptors are cleaved within the Golgi by furin-like convertase (S1 cleavage) after which they transverse to the cellular membrane and as non-covalently linked heterodimers act as single pass type I transmembrane receptors[204]. Distinguishing features between the receptors include the number of epidermal growth factor (EGF)-like repeats - Notch1 and Notch2 both have 36 repeats whereas Notch3 has 34 and Notch4 has 29[205]. The EGF-repeats of the receptor become fucosylated by *o*-fucosyltransferase at specific serine threonine residues[205-207]. Notch receptors can also undergo post-translational modifications at the *o*-fucose moiety sites by Fringe family 1,3, *N*-acetylglucosaminyltransferases addition of N-acetylglucosamine. EGF-like repeats and post-translational modifications impact upon the binding affinity of the Notch ligand[208,209]. There are five known canonical Notch signalling ligands; Delta-like ligand 1 (DLL1), DLL3 and DLL4 and Jagged 1 and 2. Notch ligands are also transmembrane proteins with large EGF-like repeats, and all, except DLL3, have a Delta, Serrate and Lag-2 (DSL) domain associated with receptor binding[210]. DLL3 acts as an inhibitory ligand[211]. Figure 1.7 provides a schematic representation of the Notch1 protein domains and Notch1 ligands Jagged 1 and DLL1. As the receptor and ligand are both membrane bound, Notch signalling is relatively short ranged and requires close cell to cell contact.

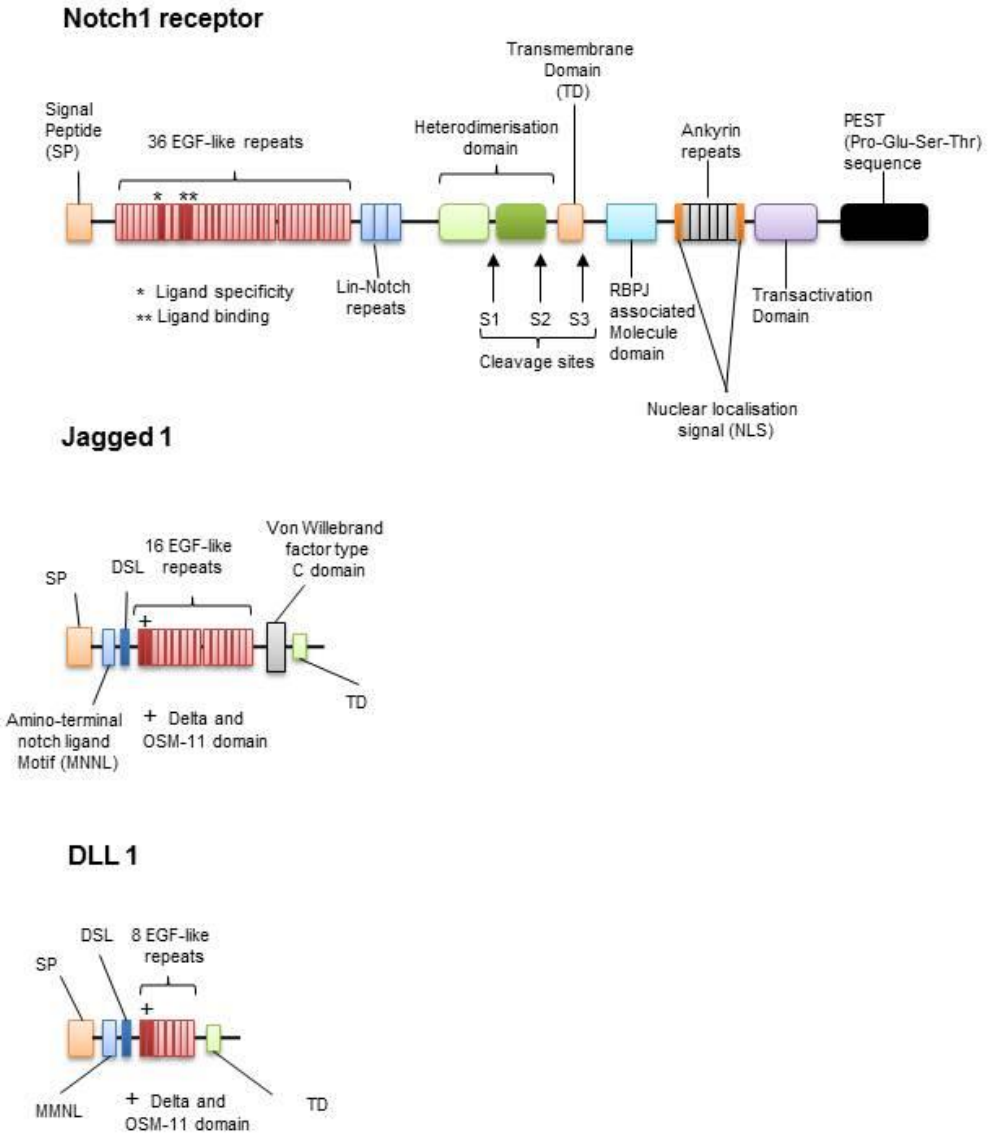

Figure 1.7 Notch1 receptor and ligand domains.

Modified from Andersson. E.R., *et.al.* 2014[211].

The extracellular portion of the Notch1 receptor contains a signal peptide followed by 36 EGF-like repeats, EGF-like repeat 8 is associated with ligand specificity and repeats 11&12 are essential for ligand binding. EGF-repeats are followed by three Lin-Notch repeats (LNRs). The first two cleavage sites (S1&S2) are located within the heterodimerisation domain (HD), the third (S3) is located after the transmembrane domain (TD). After cleavage ICN is released. ICN contains RBPJ associated molecule domain followed by ankyrin repeats which are both important for protein-protein interactions. Nuclear localisation signals (NLS) are important for translocation to the nucleus whereby the transactivation domain (TAD) activates downstream events. At the C terminal the Pro-Glu-Ser-Thr (PEST) domain is important for ICN degradation. Notch1 ligands Jagged1 and DLL1 both contain amino-terminal Notch ligand motif, followed by DSL domain and two atypical EGF-like repeats termed Delta and OSM-11 (DOS). Jagged family ligands tend to have 15-16 EGF-like repeats whilst DLL family have approximately 6-8. Jagged family ligands also contain cysteine rich von Willebrand Factor (vWF) type C domain. Both ligands have TD and short C terminal fragments approximately 125 -155 amino acids in length[211].

1.3.5.2 Canonical Notch1 signalling

Canonical Notch1 signalling is activated when the receptor comes into contact with a Notch ligand on the signalling cell. This then activates S2 cleavage by ADAM10 metalloprotease, which in turn provides the substrate for S3 cleavage by γ secretase complex. The γ secretase complex consists of presenilin/APH1, PEN2 and Nicastrin. Nicastrin is responsible for identifying the amino terminus of the cleaved Notch1 receptor for further cleavage[210,212]. After both rounds of cleavage, the truncated Notch1 is then able to translocate to the nucleus and is termed intracellular Notch1 (ICN). ICN then associates with the DNA binding protein CSL (Centromere Binding Factor 1, Suppressor of Hairless, Lag-1), which is also known as RBP-J_k[198,213,214]. In the absence of ICN, CSL acts as a transcriptional repressor and associates with other co-repressors such as SMRT/NCOR, SHAPP and HDACs to enable epigenetic gene silencing. In active Notch signalling, ICN displaces the bound co-repressors so that mastermind-like protein (MAML) and HDACs such as p300 can take their place and form a transcriptional complex. The transcriptional complex produced in normal tissues is relatively short lived and gene expression is tissue specific, however key Notch1 target genes include hairy enhancer of split (*HES*) a transcriptional repressor, Notch-related ankyrin repeat protein (*NARP*), *c-MYC* and *DELTEX*[203,214]. Once target genes have been transcribed, ICN becomes marked for ubiquitination by the E3 ligase FBXW7[215]. In order for FBXW7, an F box protein, to mark ICN for proteasome degradation, the degron sequence within the carboxyl terminus of the PEST domain needs to be phosphorylated at a core threonine residue[95]. Cdk8 has been identified as being able to phosphorylate ICN and mark the protein for FBXW7 degradation[216]. The most frequent $NOTCH1^{MUT}$ identified in CLL cells is a 2 base pair frameshift deletion c.7544_7545delCT, observed in approximately 80% of $NOTCH1^{MUT}$ cases, which results in a truncated protein lacking the PEST domain. Therefore ICN is no longer recognised for ubiquitination leading to an accumulation of active ICN within the nucleus, causing deregulated activation of various different cellular pathways involved in cell cycle and cell survival such as NF-κB1 and c-Myc[210,217]. A representation of normal Notch1 and $NOTCH1^{MUT}$ signalling in CLL is shown in Figure 1.8.

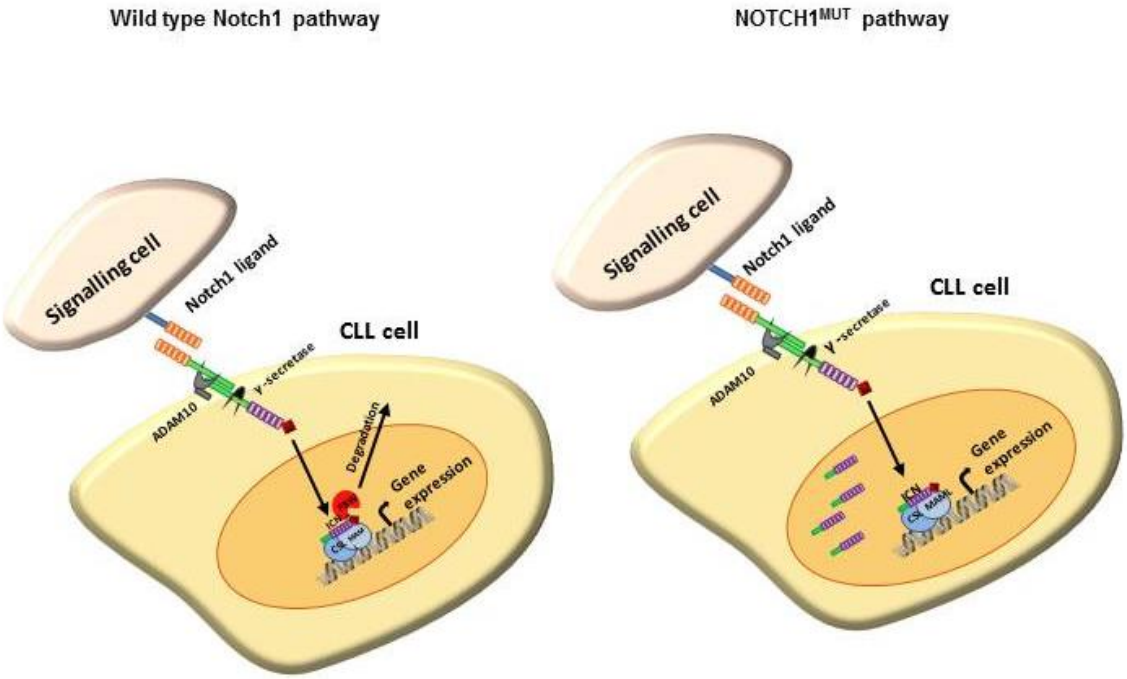

Figure 1.8 Wild type and NOTCH1^{MUT} pathway

1.3.5.3 Non-canonical Notch signalling.

Non-canonical Notch signalling, which acts in a CSL independent fashion, is not as well understood and the ligands not as well defined as canonical signalling. The most studied non-canonical pathway is Notch regulation of Wnt/ß catenin signalling[218-220]. Wnt/ß catenin signalling is associated with embryonic development and homeostatic self-renewal within cells. Like Notch, dysregulated Wnt/ß catenin signalling has been identified in several different cancer types from colorectal cancer to tumourigenesis within the skin, breast and BM[221,222]. Notch controls Wnt/ß catenin signalling by binding to un-phosphorylated active ß catenin thus negatively regulating ß catenin activity. Notch sequesters ß catenin without the need for ligand dependent membrane Notch cleavage and glycogen synthase kinase -3ß (GSK-3ß)[218,223]. GSK-3ß activity is associated with the ß catenin destruction complex. In the presence of Wnt, ß catenin becomes de-phosphorylated causing activation of the protein. Active ß catenin joins the co-activator transcription factor T cell factor / lymphoid enhancer factor (TCF/LEF) to promote cell cycle and has been shown to aid CLL cell survival[224,225].

1.3.5.4 Notch signalling, microenvironmental stimulation and resistance to treatment

BM stromal cells express Notch1 ligands Jagged-1 and DLL1, which activate Notch1 signalling[226,227]. Enhanced Notch1 signalling is observed within the LN of CLL patients *in vivo* and with BM stromal cell co-culture *in vitro*. Notch1 mutations within CLL patients were also more frequently observed within the LN compared to circulating cells within the peripheral blood. *SF3B1* mutations displayed no such bias towards location within the tissue microenvironment[228]. CLL cells have also been found to express both DLL1 and Jagged-1, which within the close CLL to CLL cell contact of the LN and BM could provide enhanced activation of Notch1 signalling[229]. NF-κB levels are also elevated in CLL cells within the LN and BM microenvironment leading to increased CLL cell survival and chemotherapy resistance[101,200]. NF-κB signalling is able to induce Jagged-1 expression on B cells during activation, resulting in Notch signalling and in turn further elevated NF-κB levels[230]. Elevated expression of MCL-1 has been identified in CLL as being an important protein in increased drug and apoptotic resistance of CLL cells within the LN. Notch1 signalling increases and sustains MCL-1 expression[200]. Further tumourigenesis activity of Notch1 signalling in CLL is observed by its association with glycolytic switch. Glycolytic switch causes the cell to switch from producing energy from mitochondrial respiration to gaining energy from glycolysis. Glycolytic switch is associated with growth advantage and chemoresistance of CLL cells[231]. BM stromal cells promoted a glycolytic switch in CLL cells *in vitro*, which was found to be dependent on Notch1 and its target gene c-Myc expression. Co-culture of CLL cells with BM stromal cells has been associated with increased chemoresistance to fludarabine, cyclophosphamide, bendamustine, prednisone and hydrocortisone *in vitro*. Antibodies against Notch1, Notch2 and Notch4 reverted this chemoresistance effect after 3 days of the inhibitors in co-culture[232]. This highlights the role of Notch1 mutations within CLL cells, suggesting that these cells rely heavily on stromal contact for enhanced malignancy and leads to the production of drug resistant clones of $NOTCH1^{MUT}$ within the LN. $NOTCH1^{MUT}$ within the LN of CLL patients could lead to ineffective CLL cell clearance by standard chemotherapy strategies resulting in the appearance of MRD and relapse following the expansion of the malignant $NOTCH1^{MUT}$ cell clone. Further to this $NOTCH1^{MUT}$ related chemoresistance, clinical trials of both RTX and OFA identified

resistance of NOTCH1^{MUT} CLL cells to anti-CD20 MAbs[108,109]. One study has found that NOTCH1^{MUT} CLL cells have lower expression levels of CD20, observed in 87 NOTCH1^{MUT} CLL patients from a total cohort of 692 CLL patients. ICN displaces HDACs from the CSL transcriptional complex, leaving the now free HDAC to bind to the promoter of CD20 epigenetically silencing transcription[233]. OFA is a potent inducer of CDC, however CDC induction is critically dependent on the concentration of the target antigen on the surface of the cell. Therefore low expression levels of CD20 within NOTCH1^{MUT} CLL cells could lead to the observed OFA resistance.

1.3.6 Cell cycle pathway

Typical cell cycle progression is restricted in normal cells, only in the presence of mitogen signals will the cell undergo proliferation. Proliferation occurs in four stages, an initial growth phase G_1, followed by DNA synthesis during (S phase), cells then enter a second growth phase where they prepare for mitosis (G_2) and following G_2 cells undergo mitosis (M phase), shown in Figure 1.9. Cells primed for proliferation enter the early growth phase (G_1), if there is no stimulation to undergo proliferation then the cell exits the cycle and becomes a quiescent cell in G_0 phase[83]. Proliferation is dependent on the tight regulation of interactions between Cdks with their positive regulators Cyclins and negative regulators Cdk inhibitors. When mitogenic signals are present, they are detected by D-type Cyclins (Cyclin D1-D3). Cyclin D proteins bind and activate Cdk4 and Cdk6, which occurs during G_1 phase for the initiation of DNA synthesis[234]. The Cyclin D-Cdk4/6 complexes lead to the partial inactivation of the negative regulators Rb, p107 and p130. The partial inactivation allows Cyclins E1&2 to be released, which then bind and activate Cdk2[234]. This newly formed complex is essential for G_1/S transition and results in the phosphorylation and complete inactivation of Rb, p107 and p130. Inactivation of Rb, p107 and p130 leads to the release of E2F which promotes the synthesis of proteins required for S phase[235]. Cyclin E expression is limited to early stages of DNA synthesis. G_1/S check point is tightly controlled by complicated interplay between serine/threonine Cdks and Cdk inhibitors. Cdk2 expression is particularly important in determining whether there is DNA damage before progressing further. Under normal circumstances, in the presence of DNA damage the cell will either undergo DNA repair or apoptosis[236]. After passing the G_1/S checkpoint the cell enters the S phase where

DNA is replicated, following this the cell enters G_2[83]. Cdk2 activation by Cyclin A2 is important at the later stages of DNA replication within the S phase to drive cells towards M phase. Following DNA replication, the cell enters G_2 where the replicated DNA is checked[83]. After passing all the checkpoints the cell enters M phase. During M phase the nuclear membrane breaks down and compact duplicated chromosomes separate, with sister chromatids migrating to opposite poles of the cell. Once the chromosomes are separated, the nuclear membrane re-forms and two daughter cells are produced[83].

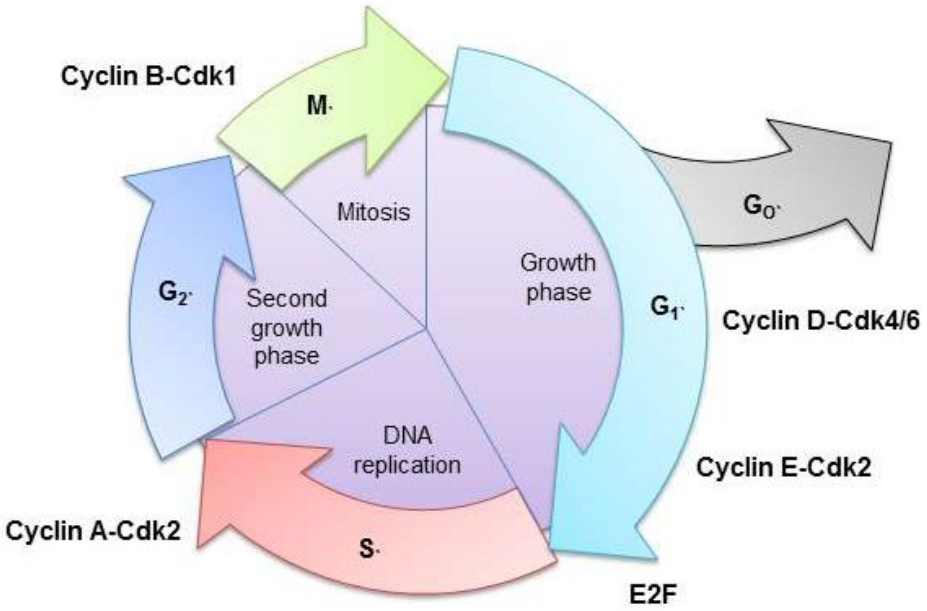

Figure 1.9 Cell cycle progression, identifying the key Cyclin-Cdk complexes.

1.3.6.1 CLL and cell cycle

Cell cycle progression is a tightly controlled process and dysregulation can result in uncontrolled proliferation and the generation of genetic mutations. Outside of the tissue microenvironment CLL cells are typically in the G_0/G_1 phase of the cell cycle[237,238]. CLL cells have been shown to overexpress Cyclin D2 and the inhibitor $p27^{Kip-1}$, which are regulators during the early phases of cell cycle progression. Elevated expression of the Cdk inhibitor $p27^{Kip-1}$ is associated with a poorer outcome for CLL patients[239]. Progression through G_1 is dependent on Cyclins D1/2/3, Cdk4 and Cdk6 resulting in the phosphorylation of Rb. In normal B cells it appears that Cyclin D3, Cdk6 and $p27^{Kip-1}$ are the most important

regulators of G_1 progression *in vitro* following anti-IgM and CD40 stimulation[240]. Cyclin D1 is not typically present in either resting or active B cells and Cyclin D2 is only very moderately regulated in active B cells. Mitogenic stimulation of CLL cells *in vitro* with CpG-ODN and IL-2 largely up-regulated Cyclin D2 and Cyclin D3 and stimulation favoured Cdk4 as opposed to Cdk6. Despite having higher expression in circulating cells, $p27^{Kip-1}$ was more readily down-regulated upon proliferation stimuli then B cells[238]. This highlights the finding that CLL cells are primed towards proliferation. Notch signalling has also been shown to influence proliferation in different cancers. Within pancreatic cells down-regulation of Notch1 results in growth inhibition with an increase in cells within G_0/G_1, associated with an increase in the Cdk inhibitors $p21^{WAF1/CIP1}$ and $p27^{Kip1}$ [241]. Within small cell lung cancer Notch signalling has been associated with cell cycle block at G_0/G_1 again due to $p21^{WAF1/CIP1}$ and $p27^{Kip1}$ expression [242]. T-ALL, like CLL, display activating mutations of Notch1, with Notch1 activation causing a decrease in $p27^{Kip-1}$ inhibition for increased passage into G_1/S phase[243]. The influence of Notch on apoptosis has been the main focus of research within CLL as opposed to cell cycle progression. Interestingly one study identified over expression of several genes involved in cell cycle progression within $NOTCH1^{MUT}$ CLL patients[244]. $NOTCH1^{MUT}$ within CLL have favoured association with trisomy 12 karyotype, and the cell cycle genes identified in this study as being over expressed were those located on chromosome 12. Although the study does not state which genes were elevated, cell cycle genes Cdk2 and Cdk4 are both located on chromosome 12[245].

Notch1 signalling within CLL demonstrates a pathway that deserves further investigation to determine its role in the pathogenesis of CLL and the appearance of MRD within CLL patients.

1.4 CLL treatments

While some CLL patients never require medical treatment, for the majority of patients diagnosed < 60 years treatment is required. Despite recent advances in chemotherapeutic agents CLL remains incurable to date.

1.4.1 Single agents

Alkylating agents such as chlorambucil were previously considered the 'Gold standard' for treatment of CLL especially in those with reduced fitness, due to its relatively low levels of toxicity. Alkylating agents add alkyl groups onto DNA bases, DNA breaks are then caused by DNA repair enzymes. Alkylating agents can also generate DNA crosslinks which prevent DNA from being transcribed and replicated. The presence of DNA breaks then activates p53 mediated apoptosis[246]. Treatment of patients with chlorambucil alone demonstrates relatively low levels of complete remission (CR), with the most promising responses observed using combination therapy[247]. Purine analogues include fludarabine, pentostatin and cladribine. Purine analogues cause inhibition of both DNA synthesis and DNA repair mechanisms causing an accumulation of DNA breaks within the cell. Accumulation of DNA breaks results in p53 driven apoptosis and activation of poly (ADP-ribose) polymerase causing necrosis[248]. The most extensively used and assessed purine analogue is fludarbine which displays superior overall response rates (ORR), CR 7-40% more remission than CHOP (cyclophosphamide, doxorubicin, vincristine, prednisone), but does not improve OS as a single agent[249,250]. Bendamustine is an alkylating agent that has similar properties to both alkylating agents and purine analogues. Bendamustine can drive both p53 dependent and independent apoptosis and also cause inhibition of mitotic check point genes[251]. Bendamustine displays good responses but at a cost of increased toxicity. Bendamustine ORR and median PFS was 67% and 22 months respectively, which was an improvement upon the responses observed with chlormabucil[252].

1.4.1.1 MAbs

MAbs against the cell surface protein CD20 have been used extensively in the treatment of CLL and their production, function and efficacy will be discussed in more detail in the following sections. RTX a chimeric MAb against CD20 is used comprehensively for the treatment of CD20 positive non-Hodgkin lymphomas[253]. CLL expression level of CD20 is low in comparison to other B cell malignancies. RTX is licenced as first line therapy for the treatment of CLL when used in combination with fludarabine and cyclophosphamide. RTX produces limited

responses as a single agent and displays highest efficacy when used in combination therapy.

OFA is the next generation of MAb from RTX and binds to a novel epitope on CD20. The novel binding site results in increased binding affinity, prolonged dissociation rates and enhanced CDC[254,255]. OFA has currently been licensed for the treatment of CLL patients as a single agent in those refractory to both fludarabine and alemtuzumab (double refractory CLL patients), displaying ORR of 51% within these patients[256,257]. OFA has recently been given approval for treatment of previously untreated CLL patients when in combination with either chlorambucil or bendamustine.

Obinutuzumab (GA101) is a humanised glycoengineered type II anti-CD20 MAb, which induces high levels of apoptosis with increased induction of ADCC, but reduced levels of CDC. Phase II of the GAUGUIN trial using 1,000 mg GA101 for 20 CLL patients demonstrated ORR of 30% with 10.7 months PFS[258,259].

The other main MAb target for the treatment of CLL is CD52, with MAb alemtuzumab. CD52 expression is not limited to the B cell lineage and is found on the surface of thymocytes, T cells, B cells and monocytes. Alemtuzumab is a recombinant fully humanised MAb. Alemtuzumab is an effective second-line treatment strategy for CLL patients that have become refractory to fludarabine or have poor prognostic genetics like 17p del or *TP53* mutations. Compared with chlorambucil, alemtuzumab displayed superior OR, CR, PFS and 42% reduction in the risk of disease progression[86,260,261].

Other MAbs have been assessed for their efficacy such as anti-CD19 and anti-CD23 MAbs, but they displayed limited efficacy in pilot clinical trials[262]. Anti-CD40 MAb lucatumumab (HCD122), which blocks the CD40 receptor disrupting microenvironmental signals and mediates ADCC, has also undergone a phase I clinical trial. Unfortunately despite acceptable tolerability of the drug there was minimal effect as a single agent within 26 relapsed CLL patients, however further research is required to determine if lucatumumab may prove beneficial when in combination with other therapies[263]. Early analysis of an anti-CD44 humanised MAb (RG73S6) has shown promising results. RG73S6 displayed CLL only cytotoxicity and was able to induce caspase-dependent apoptosis in ZAP-70

positive CLL patients. When 1 mg/kg RG73S6 was used to treat mice engrafted with human CLL cells there was complete clearance of leukaemic cells, suggesting a novel immunotherapy option[264].

1.4.1.2 BCR targeting

As previously described BCR signalling is important in CLL cell survival and therefore provides a promising target for the eradication of CLL, a schematic diagram of the currently used BCR inhibitors and MAb targets is shown in Figure 1.10. Several different small molecule BCR inhibitors are currently being assessed and are showing great promise. Fostamatinib, a Syk inhibitor, is able to induce apoptosis through disrupting BCR signalling. A Phase I/II clinical trial demonstrated ORR of 54% in 6 out of 11 CLL patients and 6.4 months PFS[265,266]. Idelalisib (CAL101, GS101) is a specific inhibitor of the PI3Kδ, and *in vitro* displays effective activity against CLL cells interacting with the tissue microenvironment. A phase I idelalisib clinical trial of 54 patients with relapsed refractory CLL demonstrated an ORR of 72% and median PFS of 15.8 months[267,268]. Other new inhibitors include ibrutinib, a BTK inhibitor, which induces apoptosis *in vitro*. Ibrutinib has been given FDA approval for the treatment of relapsed or refractory CLL patients and has shown clinical promise with estimated PFS of 90% and ORR of 42.6% at 12 months[269,270].

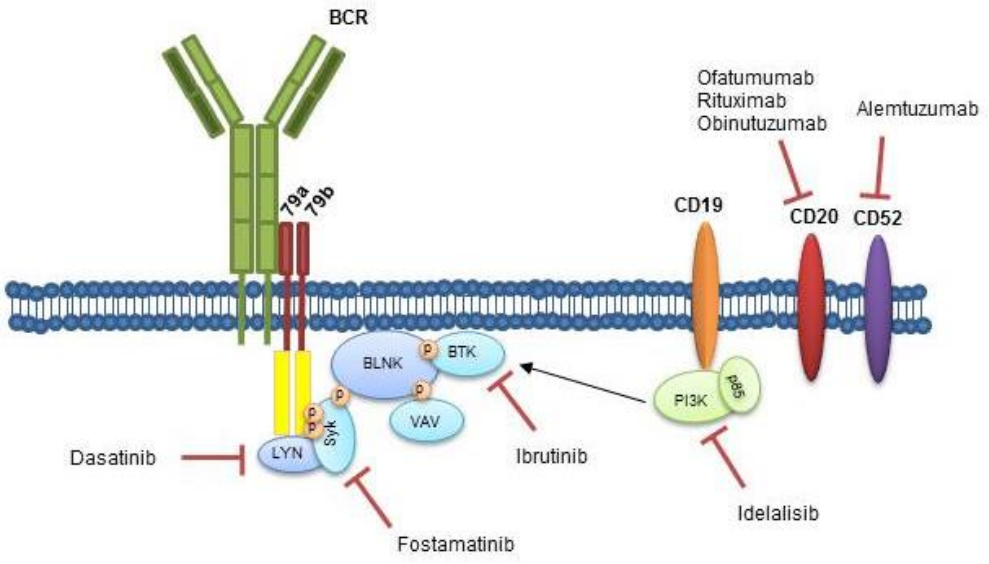

Figure 1.10 BCR inhibitors and MAb targets.

Other single agents include inhibitors of the key regulators of apoptosis in CLL cells- the Bcl-2 family, inhibitors of which include; AT-101 and ABT-199 the latter of which has shown good clinical promise[25]. Immunomodulatory agents include lenalidomide which has antiangiogenic properties, and has shown encouraging clinical results[271]. Harnessing T cell mediated cytotoxicity is also currently under development for the treatment of CLL. T cells can be genetically engineered to express chimeric antigen receptors (CAR) which are produced from an antigen recognition domain made into a single chimeric protein with the intracellular domain of CD3-zeta or FcγRI protein from T cells[272]. For the treatment of CLL CAR against CD19 are currently being investigated with early reports demonstrating high potency[273].

1.4.2 Combination therapy

Current first line therapy for CLL involves the administration of purine analogue fludarabine in combination with the alkylating agent cyclophosphamide (FC) for patients determined fit enough to withstand this regime. The UK phase III CLL4 trial identified vast improvement in CR with FC, 38%, compared to fludarabine single agent use, 7-15%[274]. They also observed improvements in ORR and PFS, and although a higher frequency of neutropenias was identified there was no significantly higher risk of severe infection[275]. The addition of RTX to FC (FCR) further increased the potency of the chemoimmunotherapy treatment. The CLL8 trial investigated FC vs FCR in 817 CLL patients and identified ORR increased from 85.4% to 92.8% with the addition of RTX, CR went from 22.9% to 44.5% ($p<0.001$) and PFS went from 62.3% to 76.6% [25,276]. FCR combination therapy represents a benchmark comparator to determine the effectiveness of new combination therapies. Other combination therapies include FCR plus alemtuzumab which went to phase II clinical trial and appeared promising for high risk CLL patients[277]. Bendamustine has been combined with RTX and assessed in 81 relapsed CLL patients producing a median of 14.7 months event free survival[278]. When compared against FCR the results were relatively comparable, although CR rates were lower there were fewer neutropenias observed. Other combinations tested include purine analogue cladribine with RTX and alemtuzumab with RTX[25]. OFA has also been combined with chlorambucil and displayed significantly improved PFS of 22.4 months vs 13.1 months and higher ORR[279]. Small molecule inhibitors are also being tested for

additive and synergistic activity. Idelalisib in combination with OFA has gone to phase I clinical trial. Idelalisib on its own within 21 relapsed refractory CLL patients demonstrated 72% ORR and PFS of 15.8 months[268]. When in combination with OFA ORR was 76% and PFS 17.8 months in 21 relapsed refractory patients[137].

Although most patients exhibit an initial response to therapy nearly all relapse, due to the re-emergence of MRD, and many become refractory to fludarabine based regimes[280-282]. This group of CLL patients represents a small subset that have very poor prognosis, are difficult to treat with no clear standard therapy, with a median survival time of 8 months, underpinning the need for novel drugs[283].

1.4.3 MAb treatments

MAbs exert anti-tumour activity by harnessing the body's own natural immune response especially ADCC involving the recruitment of NK cells to cause phagocytosis and CDC requiring the activation of the classical complement pathway, and/or apoptosis[284].

1.4.3.1 CD20

CD20, a B-cell marker, is a non-glycosylated phosphoprotein member of the MS4A family of proteins. This 33-37 kDa protein, is a tetraspan membrane bound protein. The extracellular portion of CD20 is marginal, 44 amino acids in length, and is the docking site for anti-CD20 MAbs binding, shown in Figure 1.11[254,285-288]. CD20 expression becomes activated at the pre-B cell stage of development and remains consistent until terminal differentiation into a plasma cell. The biological activity of CD20 is not fully elucidated, however it is thought to act as an ion channel and a store operated Ca^{2+} channel[289,290]. Although CD20 knockout mice lacked any obvious phenotype[289], CD20 is also thought to function as a modulator of cell growth, differentiation and initiate intracellular signals. Binding of different MAbs to CD20 have identified differential responses in cell cycle progression, one MAb enhanced progression from G_0 to G_1 phase, whereas the other inhibited progression from G_1 to S/G_2 stages[291]. Binding of MAbs can also induce the activation of tyrosine and serine/threonine protein kinases non-covalently associated with CD20, which in turn leads to the activation of PLCγ[291].

As previously described PLCγ activation can lead to several different cellular responses such as survival, proliferation and migration. Hyper cross-linking of MAb bound to CD20 with a secondary Ab results in the mobilisation of Ca^{2+} from intracellular stores[176]. Although the function of CD20 is not fully understood it clearly has dynamic cellular activity and remains an ideal specific therapeutic target for B cell malignancies.

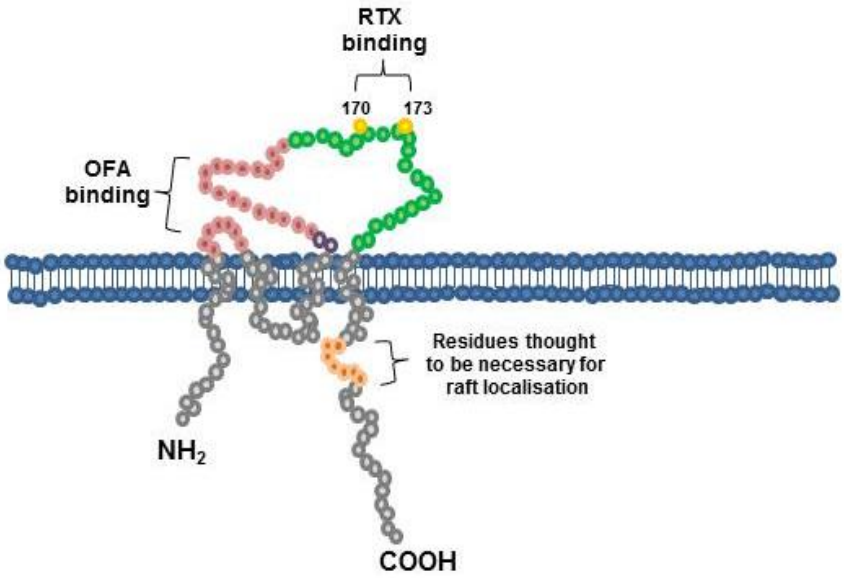

Figure 1.11 CD20 structure with RTX and OFA binding sites.
Modified from Ruuls. S.R., *et.al.* 2008[287]

1.4.3.2 MAb production

MAbs can be produced in several different ways; the suffix of the MAb name indicates the production type. MAbs ending in ~ximab, such as RTX have been produced from splicing the antigen binding variable region of a mouse antibody with the constant Fc region of a human IgG. MAbs ending with ~ zumab, such as alemtuzumab, are humanised with murine hypervariable regions spliced into a human antibody. A suffix of ~mumab, such as OFA are fully humanised[1].

RTX was produced from the parent murine anti-CD20 MAb 2B8[292]. Light and heavy chain V regions were amplified using polymerase chain reaction (PCR) and then cloned into cDNA expression vector with human IgG1 heavy and κ-light chain C regions. High levels of C2BB (RTX) were then produced in hamster ovary cells. Activity was checked in human B cell lines and binding affinity, approximately 8.0 nM, to CD20 was similar to that observed with 2B8[292,293]. OFA

on the other hand was generated by human Ig transgenic mice being transfected with non- Ig secreting (NS/O) CD20 transfected cells using prime-boost strategy[255,294]. Hybridomas are a cell line used to produce a singular type of Ig protein. Hybridomas producing IgG1 MAbs from successfully immunised mice were isolated and the binding affinity to CD20 established. From this method three different MAbs were produced 2F2 (OFA), 7D8 and 11B8[255]. The superior binding and induction of CDC when compared to RTX lead to OFA being chosen for clinical practice.

1.4.4 MAb activity

1.4.4.1 Type 1 & 2

Anti-CD20 MAbs fit into two categories, type I, which includes both RTX and OFA and type II, which includes GA101[262]. Type I MAbs are potent inducers of CDC but are less able to trigger programmed cell death, while type II MAbs are less competent at inducing CDC but are able to initiate direct cell death. However there are no differences in their ability to recruit NK cells for ADCC. These two types of MAbs are distinguished from each other by the ability to rearrange CD20 into 'microdomains' or 'lipid rafts'[285,295,296]. Type I MAbs, when bound to CD20, are able to effectively reorganise the plasma membrane into detergent insoluble lipid rafts whereas type II MAbs are not. The ability to induce lipid rafts is thought to aid type I MAbs to activate CDC, as the translocation of the CD20/anti-CD20 MAb complex provides an effective docking site for the globular head of C1q onto the Fc region of the CD20 Mab[254,255,285]. It is unclear what the differences are in binding of anti-CD20 MAbs that leads to such dramatically different functions[255]. The immune responses activated by type I MAbs are shown in Figure 1.12.

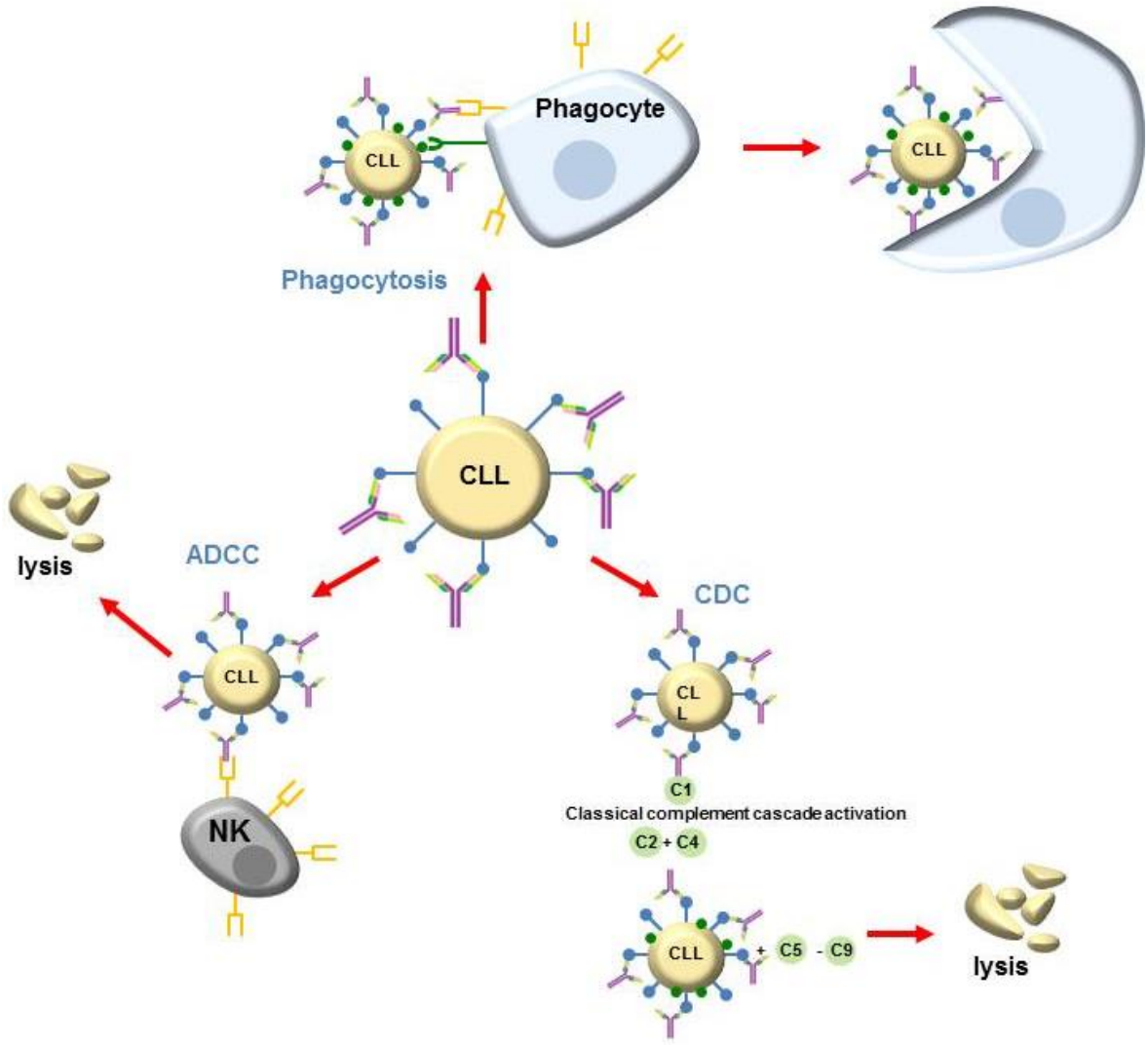

Figure 1.12 Innate immune responses activated by type I anti-CD20 MAbs.

MAb binds to its target antigen activating three possible pathways to cause tumour lysis. CDC is activated when bound MAb is recognised by complement C1 activating the classical complement cascade resulting in the formation of membrane attack complex (MAC) and lysis. ADCC becomes activated when the Fc portion of the MAb is recognised by NK cells which activate targeted cell death. The Fc portion of the MAb can also be recognised by phagocytic cells, their ability to engulf the target cell is further enhanced by complement opsonisation on the surface of the cell.

1.4.4.2 CDC

The complement system is a fundamental part of the body's innate immunity, providing a fast acting antimicrobial defence mechanism. Complement was first discovered in 1980 by Jules Bordet, whereby the activity was identified as 'complementing' Ab activity by helping to opsonise the surface of the bacteria to mediate the killing of the invading pathogen. This pathway was termed the classical complement cascade. Since then two other complement activating pathways have been identified, alternative and lectin pathway[1]. The classical pathway is activated by antibody binding. Complement proteases are synthesised

as inactive pro-enzymes (zymogens), which become enzymatically active after proteolytic cleavage[297,298]. To activate the complement cascade either IgM or IgG MAb bound to an antigen on the surface of the target/cancer cell is then recognised by the complement component C1. The classical cascade becomes activated when C1 binds to an antigen on the surface of the target cell. C1 is comprised of three segments; C1q recognition segment, C1r and C1s serine proteases. C1q contains six globular heads that recognise the bound MAb (Figure 1.13)[1,284]. When two or more of the globular heads bind to the MAb, a conformational change occurs within the C1 complex, resulting in C1r becoming autocatalytic, activating C1s serine protease function[299].

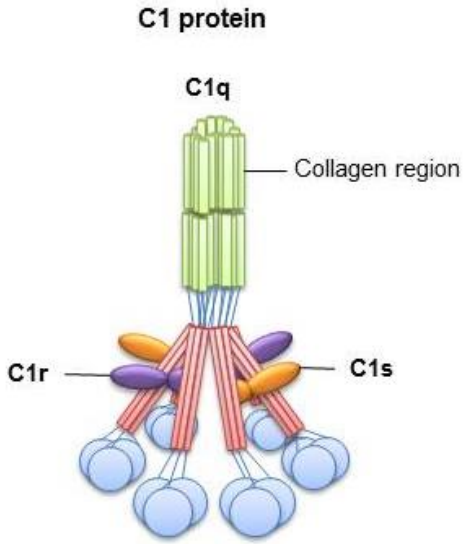

Figure 1.13 Schematic of C1 structure.
Modified from Murphy. K., 2012.

A catalytic cascade follows, of complement components being cleaved into active forms to eventually produce the membrane attack complex (MAC), which perforates the cell membrane creating a pore. C1s activates complement component C4 cleaving it into two components C4a, a peptide mediator of inflammation, and C4b which binds C2 so that C1s can then cleave C2 into two. C2a in combination with C4b forms the active C3 convertase complex, while C2b acts as a precursor of vasoactive C2 kinin[300]. Complement activation is confined to the target cell on which the MAb is bound, therefore it is crucial that MAb epitopes are located as close to the cellular membrane. C4b opsonises the target cell; if C4b does not efficiently form a covalent bond with carbohydrates on the surface of the target cell then the thioester bond within C4b is irreversibly

cleaved resulting in an inactive complement component. C3 convertase, covalently bound to the cell surface, then cleaves a large volume of C3 to generate C3b proteins[1,301]. C3a is also produced during C3 cleavage which is associated with inflammation induction. C3 cleavage is the critical step in the complement cascade and like C4b, C3b also forms a covalent bond with the surface of the target cell. Once again if the exposed thioester bond takes too long to attach then it also becomes inactive by hydrolysis. Large amounts of C3b opsonise the surface of the target cell. C3b opsonisation apart from being important for CDC can also signal the target cell to be engulfed by a phagocyte, described in section 1.4.3.4. Alternatively C3b can join C4b-C2a, to generate C5 convertase, resulting in the release of subunits C5a and C5b. C5a release is highly inflammatory[284,302]. C5b is the first complement component to start the formation of the MAC (Figure 1.14).

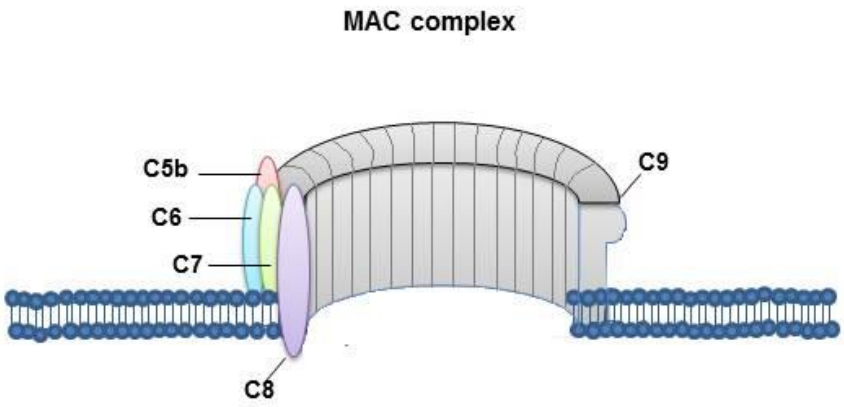

Figure 1.14 MAC complex.
Modified from Murphy. K., 2012.

C5b anchors the remaining MAC complement components to the cell membrane and initiates the assembly. C5b binds to one unit of C6, which in turn binds one C7 protein. This complex of C5b-C6-C7 then results in a conformational change in C7 allowing the hydrophobic site on C7 to become exposed so that it can be inserted into the lipid bilayer of the cell membrane. C8 and C9 complement components also contain hydrophobic domains allowing them to also transverse the lipid bilayer. C8 binds adjacent to the C5b-C6-C7 complex and once C9 also starts to bind then C8 activates the polymerisation of between 10-16 C9 molecules to form a pore within the lipid bilayer of the cell[1,303]. The channel that is generated is approximately 100Å in diameter with the external part being

hydrophobic and the internal hydrophilic[1,304]. The channel allows passage of solutes and water out of the target cell destroying homeostasis and inducing cellular lysis. Naturally the body has strict control mechanisms to prevent uncontrolled activation of the complement cascade.

1.4.4.3 Regulation of complement activation

Understandably strict control is required to prevent excessive complement activation. As several of the subunits are opsonins and act as pro-inflammatory molecules, uncontrolled activation can cause unnecessary damage to surrounding tissues[305]. Complement activation can be controlled at several different points within the CDC pathway. The activity of C1 is controlled by C1 inhibitor (C1INK), which is a plasma serine protease inhibitor, which binds to C1r:C1s causing its dissociation from C1q. Therefore C1INK provides a limited timeframe in which C1s is able to cleave C2 and C4[1,306]. Plasma serine protease factor I works in conjunction with the co-factor membrane co-factor of proteolysis (MCP; CD46) acting together to cleave C3b/C4b into an inactive form. Plasma serine protease factor I also acts with complement receptor 1, to binds to C4b displacing C2a[1,306]. C4b is then cleaved and inactivated by factor I. Decay-accelerating factor (DAF; CD55) also competes for C4b binding, again causing C2a to be displaced so that C3 convertase can no longer be formed. DAF is associated with the plasma membrane of the cell through its glycosylphosphatidylinositol (GPI) tail[307]. Protectin (CD59) is also anchored to the membrane in this way. CD59 stops the MAC forming at the final stage by inhibiting the binding of C9 polymers. Therefore effective MAbs have to be able to overcome these complement inhibitory proteins[308,309]. The most critical factor for RTX activity is expression levels of CD20, although complement inhibitory protein expression in CLL has been studied their full effect upon MAb therapy remains ambiguous. Inhibitors of both CD55 and CD59 have been shown by some to aid the activity of RTX but have limited effect on OFA induced CDC[310-314].

1.4.4.4 CDC and CLL

CDC induction is critically dependent on the distance between MAb binding and the plasma membrane, with closer binding associated with more efficient coating of active complement components onto the target cell[315]. The novel

epitope binding site of OFA brings the complex closer to the surface of the cell (Figure 1.11) making it more potent at inducing CDC then RTX[254,255]. This is of particular importance in CLL, as CD20 expression levels, are relatively low compared to other B-cell lymphomas. CD20 expression levels will then predict the response to MAbs[310,311]. One study estimated that on 14 CLL patient samples there were between 1,500-70,000 CD20 molecules per cell, compared to 100,000 - 250,000 molecules per cell observed on normal B cells, demonstrating the vast down-regulation of CD20 in CLL[262,310]. OFA also demonstrates superior binding affinity to CD20 and C1q, with longer dissociation rates, increasing its activity in comparison to RTX[316]. In addition, recent studies demonstrate that CLL cells can evade RTX, through sequestration of CD20-RTX complexes by phagocytic cells, resulting in trogocytosis[317]. This enables CD20 depleted lymphocytes to remain in circulation, no longer responsive to RTX treatment[318-320]. These findings highlight the importance of generating a MAb capable of effectively inducing CDC.

1.4.4.5 Complement deficiencies

Complement deficiencies are generally quite rare; and have been linked with approximately 2% of primary immunodeficiency disorders[321]. C2 is the most commonly identified deficiency with a prevalence of 1/20,000 within Western countries[300]. Deficiencies within the classical complement cascade (C1, C2 and C4) have been well documented in their exacerbation of the pathogenesis of the autoimmune disorder systemic lupus erythematosus (SLE)[322]. Deficiencies within the classical cascade result in: impaired ability to clear circulating immune complexes and reduced clearance of apoptotic cells; increased tolerance to autoantigens, and dysregulation of cytokines. Individuals with impaired activity of the classical cascade and C3 are susceptible to infections with encapsulated bacteria due to ineffective clearance after Ab binding[1]. C2 deficiencies have been linked with recurrent *Streptococcus pneumonia* infections causing septicaemia or meningitis[300,323]. Deficiencies within the MAC result in increased susceptibility to the species *Neisseria meningitidis*[324]. Early reports in the 1980's indicated that CLL patients harbour deficiencies in classical complement components C1 and C4 resulting in defective immune complex clearance. Deficiencies in classical complement components have also been linked to CLL patients being more susceptible to infections with *S. pneumonia*, and exhibiting a propensity to develop autoimmune syndromes[325-328]. Research has indicated

that complement is rapidly exhausted *in vivo* following the administration of both RTX and OFA independently[319,329]. Therefore the limited pool of available complement components and the potential for CLL patients to harbour complement deficiencies has important consequences for the efficacy of type I anti-CD20 MAbs.

1.4.4.6 ADCC

Target cells bound with Ab can also be destroyed by NK cells. NK cells contain prominent intracellular granules. NK cells have a limited repertoire of recognition sites for identifying invading pathogens and their action is generally carried out without the aid of Abs. However Abs can signal a cell for degradation by NK cells through the NK receptor FcγRIII (CD16), which recognises both IgG1 and IgG3 antibody subclasses. Once associated with a bound Ab, NK cells release toxic cytoplasmic granules containing perforin and granzymes onto the surface of their target. Exocytosis causes the granules to be incorporated into the target cell resulting in cell death[1,330].

1.4.4.7 Phagocytosis

Bound MAb can also cause the cell to be destroyed by phagocytosis. The Fc portion of the antibody is recognised by phagocytic cells. Phagocytic cells include; monocytic and myelocytic lineages, in particular macrophages and neutrophils. The Fcγ receptor engages the antibody on the surface of the target cell. Phagocytosis activity can also be synergised by complement opsonisation which interacts with the complement receptor CR1 on the effector cell. Through successive binding with the receptors on the effector cell the target cell gradually becomes engulfed. Once enclosed the target cell is sequestered into an acidified vesicle, the phagolysosome. Lysosomes are then released into the vesicle effectively destroying the target[1,331,332].

1.4.4.8 Direct cell death

Although Type I MAbs are poor inducers of direct cell death, there is some evidence to support their ability to do so. There is some controversy over how clinically relevant the ability of type I to induce programme cell death is, as several studies demonstrate that cross-linking with a secondary reagent is

required to initiate the pathway[176,333]. It has been proposed that type I and type II anti-CD20 MAbs induce cell death via two different pathways. It is thought that type I MAbs when in a lipid raft as a CD20: anti-CD20 Mab complex also aggregate with the BCR, and type 1 anti-CD20 MABs then commandeer the Ca^{2+} flux pathway to trigger apoptosis[334,335]. Type II anti-CD20 MAbs can cause programmed cell death through the induction of the autophagy pathway. Autophagy results in the cytoplasmic material including organelles being enveloped by vesicles which are targets for recycling and destruction[262,336]. One of the benefits of using type II MAbs is through the avoidance of using the classical apoptotic pathway, as several proteins within the apoptotic pathway are deregulated in poor prognosis CLL.

1.4.5 Rationale for investigating OFA efficacy in CLL

RTX is currently used as first line therapy in the treatment of CLL in combination with FC. OFA has recently been given approval for the treatment of CLL patients in combination with chlorambucil for previously untreated CLL patients, when fludarabine based therapy is not suitable, and as a single agent for CLL patients that are double refractory. RTX as a single agent displays poor improvement in PFS and OS[274]. OFA on the other hand displays superior PFS and OS as a single agent and may therefore display a greater benefit for CLL patients if given approval as a first line therapy for all CLL patients[337]. The ability of OFA to produce a CDC response is important for its efficacy. We wanted to establish the limiting factors of OFA treatment in CLL. The exact role CDC induction plays in the efficacy of anti-CD20 MAbs remains controversial with some paying more emphasis towards the induction of ADCC and phagocytosis. However recent studies have identified that complement exhaustion has been observed *in vivo*, highlighting that CDC is an important pathway for the eradication of CLL cells[319,329]. Therefore we further investigated the prevalence and consequences complement deficiencies may or may not have upon the ability of CLL cells to elicit a CDC response. Complement is extremely important, enhancing the immune system ability to eradicate encapsulated bacteria. Therefore MAbs that cause large amount of complement exhaustion could result in CLL patients having an even more compromised immune system with greater risk of morbidity and mortality due to infection[338].

The recent identification of recurrent NOTCH1^{MUT} has given rise to the observation that dysregulation of different genetic pathways within CLL cells may impact upon the efficacy of anti-CD20 MAbs. As described a retrospective investigation of the CLL8 trial identified that there was no observable benefit of adding RTX to FC within NOTCH1^{MUT} CLL patients[108]. This was also highlighted in a clinical trial investigating the effect of chlorambucil and OFA in NOTCH1^{MUT} CLL patients. Unlike RTX there was an initial benefit of adding OFA to chlormabucil treatment but this only lasted 18 months[109]. Therefore it is important to further characterise the impact *NOTCH1* and other genetic changes may have on anti-CD20 MAb efficacy.

The microenvironment plays a critical role in the pathogenesis and drug resistance capabilities of CLL cells. Others have established that there is an increase in anti-CD20 MAb induced direct cell death when CLL cells are stimulated through CD40[176]. This was observed in both type I and type II anti-CD20 MAbs, despite type I MAbs being poor inducers of programmed cell death. Therefore investigating the effect of CD40 stimulation has upon CDC maybe more clinically relevant for type I anti-CD20 MAbs. The Notch1 pathway becomes up-regulated within the tissue microenvironment[227]. Therefore it is also important to determine NOTCH1^{MUT} CLL cells response to anti-CD20 MAbs when stimulated by IL-4 and stromal cells expressing CD154. When simulating the tissue microenvironment we aimed to determine whether CLL cells deregulate CD20 expression level and/or complement inhibitory proteins. It was also our aim to determine if CLL cells that survive OFA induced CDC activity displayed distinct gene signatures compared with untreated cells. If deregulation of certain pathways is apparent at the gene expression level this may provide a possible therapeutic avenue for enhancing the activity of anti-CD20 MAbs, providing more effective clearance of CLL cells.

1.5 Aims

1. Establish the prevalence of complement deficiencies within our CLL patient cohort.

2. Determine the functional consequences of complement deficiencies and exhaustion upon anti-CD20 MAb induced CDC.

3. Define ADCC and CDC induction in our CLL patient cohort between RTX and OFA. Establish if there are any statistically significant trends between CD20, CD55 and CD59 and the induction of OFA CDC.

4. Establish the impact mimicking microenvironmental signals *in vitro* has on our different CLL cytogenetic subsets and their ability to undergo anti-CD20 MAb induced CDC.

5. Characterise gene expression profiles in CLL cells that evade OFA induced CDC.

6. Further define the efficacy of anti-CD20 MAbs upon $NOTCH1^{MUT}$ CLL cells in comparison to cytogenetically normal CLL cells.

7. Delineate the mechanism surrounding $NOTCH1^{MUT}$ CLL cell resistance to anti-CD20 MAbs.

2 Materials and Methods

The names and addresses of the suppliers of the reagents and materials used for this study are shown in Table 2.1.

2.1 Serum collection and assessment

Ethical approval for this study was obtained from the West of Scotland Research Ethics Committee, NHS Greater Glasgow and Clyde (United Kingdom). Peripheral blood samples were obtained following informed consent, from patients with a confirmed diagnosis of CLL (mean age 67.9 ± 6.78 years, range 48–88 years and percentage male 57.9%), the clinical parameters of CLL serum used in this study are shown in Table 2.2. Peripheral blood samples were also collected from healthy volunteers to isolate normal healthy serum (NHS; age range 25–50 years old) and age matched serum (AMS; mean age 64.8 ± 12.91 years, range 47–84 years and percentage male 41.7%). Serum was separated from blood cells using serum clot activator, followed by centrifugation at 3000*g* for 10 min. Sera was immediately snap frozen on dry ice and stored at -80^{o}C. Pooled NHS was prepared by isolating and mixing sera from 10 different healthy volunteers, prior to freezing.

2.1.1 Complement assessment

C1 and C2 levels in sera were determined by radial immunodiffusion (RID) (The Binding Site Group Ltd., Birmingham, UK) following the manufacturer's protocol using the RID reference table provided. In order to use the RID reference table, the precipitin ring needs to develop to completion, for C1 this is at least 96 hr and for C2 at least 120 hr. C3c and C4 were determined by immunonephelometry in the clinical diagnostic immunology laboratory (Gartnavel General Hospital, NHS Greater Glasgow and Clyde). The activity of the classical complement cascade in serum was determined using a total haemolytic complement kit, CH100 assay (The Binding Site Group Ltd.) following the manufacturer's instructions.

2.2 CLL samples and normal B cells

2.2.1 CLL cells

CLL cells were isolated from peripheral blood using RosetteSep™ human B cell enrichment cocktail (StemCell Technologies, Vancouver, Canada) following the manufacturer's instructions. The clinical parameters of CLL patient cells used in this study are shown in Table 2.3. CLL cell purity was determined by flow cytometry using anti-CD19, -CD5 and -CD23 antibodies (Abs) and samples collected were >95% $CD19^+/CD5^+$. Of the CLL cells collected $2x10^7$ cells were pelleted for RNA extraction, described in section 2.9.1, and stored long-term at -80°C. The remainder CLL cells were resuspended in freezing media (90% fetal bovine serum (FBS; Invitrogen Ltd., Paisley, UK) and 10% dimethylsulphoxide (DMSO; Sigma Aldrich, Dorset, UK). $1\text{-}10x10^7$ CLL cells in 1 ml of freezing solution were then aliquoted into cryovials (Greiner Bio-One, Ltd., Gloucestershire, UK) for rate controlled freezing at around 1°C per hour in a -80°C freezer overnight. Frozen cells were then transferred into the vapour phase of a liquid nitrogen freezer for long term storage.

2.2.2 Normal B cells

Normal B lymphocytes used for gene expression analysis were isolated from buffy coat samples obtained from healthy individuals provided by the Scottish National Blood Transfusion Service (SNBTS), with approval from the SNBTS ethics committee. Standard virology screening was performed on the blood samples, which were received within 24 hrs of being collected. B cells were isolated by MACS human CD19 MicroBeads following the manufacturer's protocol (Militenyi Biotec, Surrey, UK), B cell purity was >80% assessed by FACS staining ($CD19^+/CD20^+$). Buffy coat B cells were washed once in PBS and then pelleted for RNA extraction as described in section 2.9.1. B cells used for assessment of surface protein expression were obtained from peripheral blood samples from 10 healthy volunteers, lymphocytes and mononuclear cells were isolated using density separation medium Histopaque®-1077 (Sigma Aldrich, Dorset, UK), following the manufacturer's protocol.

2.3 Cell culture

Cell culture was conducted under sterile conditions using a laminar air flow hood. All consumables used were purchased from either Fisher Scientific (Loughborough, U.K) or Greiner Bio-One Ltd unless otherwise stated.

2.3.1 Thawing primary CLL cells

CLL cells were thawed by warming the cryovial at 37°C in a water bath, cells were then gently transferred to the bottom of a sterile tube. 10 ml DAMP solution (DNAse 10000 units/L (Stemcell Technologies), $MgCl_2$ 2.5 mM, trisodium citrate 16 mM (both Sigma Aldrich), 1% Human Serum Albumin (SNBTS) in PBS) was added drop wise to the cells with gentle agitation over 10 min and then centrifuged at 300*g* for 5 min. Supernatant was discarded, CLL cells were resuspended in complete medium-RPMI-1640 containing 10% FBS, 50 U/mL penicillin, 50 mg/mL streptomycin and 2 mM L-glutamine (Invitrogen Ltd.), followed by centrifugation at 300*g* for 5 min. Supernatant was discarded and CLL cells were then re-suspended in complete medium at a concentration between 5-10 x 10^6 cells/ml, CLL cells were then transferred to tissue culture plates/flasks and cultured in a humidified incubator at 37 °C and 5% (v/v) CO_2.

2.3.2 B cells from healthy volunteers

Lymphocytes and mononuclear cells from healthy volunteers were cultured in 10 ml complete medium in a T75 tissue culture flask and incubated at 37 °C and 5% (v/v) CO_2 for 18 hr to enable the monocytes to adhere. Thereafter the non-adherent lymphocytes were removed gently so as not to dislodge the adherent cells. B cells were then isolated from the suspension by FACS, described in section 2.6.1, for assessment of surface protein expression.

2.3.3 Cell line cells

2.3.3.1 CLL cell lines

The HG3 cell line was used throughout this study. HG3 cells were originally produced from a Rai stage II individual with a deletion of 13q on both chromosomes[339]. Another CLL cell line WaC3CD5$^+$ (WAC), was also used for CDC

optimisation of anti-CD20 MAbs OFA and RTX. WAC cells are characterised as being from a Rai stage I individual with deletions of both 13q and 17p[340]. CLL cell line cells were cultured in complete medium at a density of approximately 5 x 10^5 cells/ml and cultured in a humidified incubator at 37 °C with 5% (v/v) CO_2.

2.3.3.2 Ramos cells

Ramos cells are derived from a patient with Burkitt's lymphoma, and were used for the optimisation of ADCC assay, described section 2.4.2[341]. Ramos cells were cultured in complete medium at a density of approximately 1 x 10^6 cells/ml and cultured in a humidified incubator at 37 °C with 5% (v/v) CO_2.

2.3.3.3 Stromal cell lines

Mouse fibroblast L cells (NTL) and NTL cells transfected with CD154 (NTL/CD154) were used in co-culture experiments to simulate the CLL microenvironment and support CLL cell survival and proliferation as previously described[140,342]. NTL and NTL/CD154 cells were cultured in complete media, and cultured in a humidified incubator at 37 °C with 5% (v/v) CO_2. When CLL cells were co-cultured on NTL/CD154 cells, complete media was supplemented with 10 ng/ml IL-4 (Peprotech EC Ltd., London, UK) and referred to as NTL/CD154+IL-4.

2.4 MAb treatment and assessment of cell death

2.4.1 CDC

CLL cell lines were split 1:2 with complete medium 24 hr prior to assessing CDC levels. Primary CLL cells were defrosted 18 hr before assessment of CDC. Unless otherwise stated 2.5 x 10^6 cells/ml were pelleted by centrifuging for 5 min, 300*g* at room temperature (RT), and then resuspended in CDC buffer - Hanks Buffered Saline Solution (HBSS; PAA Laboratories, Buckinghamshire, UK), 10 mM Hepes, 1 mM sodium pyruvate and 10 μg/ml Gentamicin (Invitrogen Ltd.). OFA (GlaxoSmithKline, Brentford, UK) and RTX (Roche, West Sussex, UK) were diluted in CDC buffer and added to cells at 20 μg/ml, for 30 min at RT. Untreated control cells were treated equivalently except no MAb was added to the CDC buffer. CLL cells were then pelleted and the supernatant removed. Thawed human serum was diluted in CDC buffer (1:1) and added to cells and mixed

gently. CLL cells were then incubated with sera for 2 hr at 37^{o}C. Following MAb/sera treatment, CLL cells were washed in CDC buffer, harvested and stained with 1 μg/ml propidium iodide (PI) (BD Biosciences, Oxford, UK) to assess the levels of CDC, as described in section 2.6.2.

2.4.1.1 Supplementing CLL sera

For CLL patient sera supplementation assays, purified human complement components C2 and/or C4 (Complement Technology, Inc, Texas, USA) or NHS were added at the concentrations indicated and CDC performed.

2.4.2 Assessment of ADCC

The induction of ADCC was determined by using an ADCC Reporter Bioassay Kit provided by Promega (Southampton, UK) and following the manufactures protocol. Primary CLL cells were defrosted as described, and cultured for 18 hr at a concentration of 1.25 x 10^6 CLL cells/ml in complete media. Cell lines were split 1:2 with complete medium 24 hr prior to use. The effector: target cell ratio used was 6:1. OFA and RTX were prepared at a range of concentrations from 1 ng/ml to 100 μg/ml. Luciferase luminescence was measured at 1500 ms on a Spectramax M5 plate reader (MDS Analytical Technologies, Berkshire, UK) and analysed with SoftMax Pro 5.2 software (MDS Analytical Technologies).

2.5 Microenvironmental stimulation

To assess how microenvironmental stimulation affected the susceptibility of CLL cells to anti-CD20 MAb activity, CLL cells were cultured normally or with stromal cells. CLL cells were cultured using three different systems; no stromal cells (plastic), NTL or NTL/CD154+IL-4. NTL and NTL/CD154+IL-4 cells were plated at a ratio of 25:1 for CLL: stromal cells. NTL and NTL/CD154 were plated into 6 well plates to allow the stromal cells to adhere to the surface 4 hr prior to the start of experiment.

2.5.1 Assessment of CDC and surface protein expression

After thawing, CLL cells were plated into a 6 well plate at a density of 4 x 10^6 cells/well in complete medium using the three different culture systems, plastic, NTL and NTL/CD154+IL-4. For each of the different systems, cells were incubated with either no MAb (untreated) or 20 µg/ml of either RTX or OFA in a humidified incubator at 37^{o}C with 5% (v/v) CO_2. CLL cells were collected at time points; 24, 48 and 72 hr. For CLL cells cultured on stromal cells, CLL cells were gently washed from the well, taking care not to disturb the stromal layer. CLL cells cultured with either RTX or OFA then underwent CDC as previously described in section 2.4.1, omitting the incubation with OFA or RTX step. Untreated CLL cells (cultured without MAb), 2.5 x 10^5 cells were used for assessment of surface protein expression as described in section 2.6.1. The remaining untreated CLL cells underwent CDC as previously described, with some of the cells remaining untreated (control) and the cells treated with MAb named as control + MAb (either OFA or RTX) in the results section.

2.5.2 Characterisation of CLL cells escaping OFA CDC

To determine differentially expressed genes involved in CLL cells resistant to OFA induced CDC, Fluidigm (Fluidigm Ldt, London, UK) gene profiling was performed. The experimental design is shown in Figure 2.1. CLL cells were cultured in a 6 well plate at a density of 4 x 10^6 cells/well in complete medium with NTL/CD154+IL-4 cells and cultured in a humidified incubator at 37 ^{o}C with 5% (v/v) CO_2. After 24 hr of co-culture 20 µg/ml OFA was added to half of the CLL cells plated. After 24 hr incubation with OFA, CLL cells were removed from co-culture and pelleted by centrifuging for 5 min, 300*g* at RT. The supernatant was removed and cells were washed once in CDC buffer. After washing, CLL cells were pelleted and the supernatant removed. Half of the CLL cells from the OFA treated or untreated wells were then incubated for 2 hr at 37 ^{o}C with 50% NHS diluted in CDC buffer at a concentration of 2.5x10^6 cells/ml (CDC assay see section 2.4.1). At the same time CLL cells not undergoing CDC were incubated with complete medium at 37 ^{o}C for 2 hr. After incubation 2.5 x 10^5 cells were used to check the level of CDC by PI staining described in section 2.6.2. The remainder of cells were washed once in CDC buffer, once in complete medium and then re-cultured with NTL/CD154+IL-4 in a humidified incubator at 37 ^{o}C

with 5% (v/v) CO_2 for an additional 24 hr. CLL cells were then gently washed from the NTL/CD154+IL-4 stromal layer and placed into a fresh 6 well plate to allow any stromal cells that may also have been removed to re-attach to the surface of the well. After 2 hr when NTL/CD154+IL-4 cells had adhered to the plate, CLL cells were removed, pelleted and washed twice with PBS, prior to RNA extraction for gene expression analysis, described in detail in section 2.9.1.

2.5.3 Characterisation of the molecular response of CLL cells when stimulated with and without OFA on plastic and CD154/IL-4

Thawed CLL cells were cultured as described either on plastic or with NTL/CD154+IL-4 in 6 well plates at a density of 4 x 10^6 cells/well, in the presence or absence of 20 µg/ml OFA for 48 hr. The cells cultured on NTL/CD154+IL-4 were then re-plated as described in 2.5.2 to remove any remaining NTL/CD154+IL-4 cells. CLL cells were then harvested, pelleted, and washed once in ice-cold PBS. CLL cell lysates were then prepared for either RNA extraction (section 2.6.1) or protein extraction (section 2.10.1).

2.6 Flow cytometry

2.6.1 Assessment of surface antigen expression

Normal B cells and CLL cells in the CDC, ADCC and co-culture with plastic, NTL and NTL/CD154+IL-4 experiments were all assessed for the expression levels of CD19, CD20, CD52, CD55 and CD59, using FACS Abs shown in Table 2.4. In brief, 2.5 x 10^5 cells were pelleted, washed once with PBS and centrifuged at 300*g* for 5 min at RT. The supernatant was then removed and cells were gently re-suspended in 200 µl PBS containing a mix of all five antibodies at 1/100 dilution. Staining of CD19 alone was also performed as an additional control in the experiments where CLL cells were assessed by PI staining following co-culture with NTL or NTL/CD154+IL-4. For this 5 x 10^5 cells were re-suspended in 200 µl PBS containing anti-CD19 Ab (1/100 dilution). Once Abs were added, cells were incubated on ice for 30 min in the dark. Cells were then washed once in PBS and re-suspended in 100 µl PBS for FACS analysis. FACS analysis was performed using a FACSCantoII flow cytometer (BD Biosciences), data was acquired using BD

FACSDiva (BD Biosciences) software and analysed using FlowJo (Tree Star Inc, Ashland, USA) software.

2.6.2 PI staining

PI staining was used for the assessment of cell death following induction of CDC. 5 x 10^5 CLL cells were washed with 2 ml CDC buffer, and centrifuged for 5 min, 300*g* at RT. CDC buffer was then removed and the cells re-suspended in 100 µl 1 µg/ml PI in CDC buffer. Immediately following PI staining the percentage of CDC was determined by acquiring the number of PI positive and PI negative cells within the PE fluorochrome channel using a FACSCanto II flow cytometer (BD Biosciences). PI^- cells were considered viable, as indicated in Figure 2.2. If CLL cells were co-cultured on NTL or NTL/CD154+IL-4 then CD19 staining was performed first as described in section 2.6.1, 30 min prior to PI being added, and only $CD19^+$ PI^+ cells were then used to determine the percentage of CDC.

2.7 Genomic DNA extraction

For the identification of $NOTCH1^{MUT}$ from our CLL cell bank, 1-5 x 10^6 cells were pelleted and re-suspended in 200 µl PBS. DNA was isolated using DNeasy Kit (Qiagen, West Sussex, UK) following the manufacturer's protocol, DNA was then dissolved in AE buffer (10 mM Tris-Cl, 0.5 mM EDTA pH9) supplied by Qiagen. DNA concentration was determined on a spectrophotometer (Nanodrop ND1000 Spectrophotometer; Labtech International Ltd, East Sussex, UK), using 2 µl of the sample at 260 nm. DNA samples were stored at -20 °C.

2.7.1 ARMS PCR

ARMS PCR was used to identify the presence of the c.7544_6545delCT mutation of the NOTCH1 PEST domain. The PCR reaction was performed using 25 ng DNA and 1 U Go Taq (Promega) with 1 mM $MgCl_2$, 0.4 mM dNTP and primers (Eurofins MWG Operon,London, UK) as indicated in Table 2.5, in a 30 µl reaction, following a previously described protocol[98]. Cycling conditions were as follows; initial denaturing step of 95 °C for 3 min and then 30 cycle of; 95 °C for 30 sec, 57 °C for 40 sec and 72 °C for 40 sec. Products were resolved on a 1% agarose gel by electrophoresis using TBE buffer containing 10 µg/ml of Ethidium Bromide

(EtBr), visualisation was performed under Ultra Violet (UV) illumination of the Molecular Imager® ChemiDoc^{TM} XRS system (BioRad, West Sussex, UK).

2.8 Sequencing (Oxford University)

ARMS positive NOTCH1^{MUT} CLL samples (n=8) and NOTCH1^{WT} CLL samples (n=13) were sent to Oxford University for sequencing. DNA concentrations were measured by Oxford BRC Molecular Diagnostic Laboratory using Qubit® 2.0 Fluorometer and Qubit® assays (Invitrogen), two samples failed this quality control. The 19/21 samples were sequenced on the Miseq (Illumina, Inc., Essex, UK) using a 300 cycle MiSeq Reagent Kit v2. Library preparation was performed using TruSeq Custom Amplicon Kit (Illumina, Inc) v 1.5. The kit was designed to target >400 amplicons across 24 genes, including *NOTCH1* 2-bp frameshift deletion (ΔCT7544-7545, P2515fs). The cluster density was 1000/kmm2. Total yield was around 5.6 G and total % >= Q30 was 91.5. Four CLL samples (CLL041, CLL044, CLL068, and CLL101) showed very low percentage of Reads Identified across all amplicons and failed. Data analysis was performed on Illumina MiSeq Reporter Software version 2.4 or an earlier version, applying two different variant callers: GATK and somatic caller for low variant allele frequency (VAF) (Illumina, Inc). The annotation and filtering was performed using Variant Studio tool ((Illumina, Inc). The filter includes: filtering out all VAFs with read depth > 20, quality > 99, and filter in all consequences (Missense, framshift, Stop gain and loss and splice site). VAF present in > 5% of 1000 genome database was filtered out. An additional filter was then applied to filter out all VAF > 5% and which were then visually inspected by IGV viewer in order to remove false mutations. This analysis detected 53 mutations in total from the 15 CLL patients screened (described in more detail in Chapter 6; Figure 6.1). A simplified flow chart of the mutation screening process is shown in Figure 2.3.

2.9 Gene expression analysis

2.9.1 RNA extraction

Total RNA was isolated using the RNeasy Mini Kit (Qiagen) following the manufacturer's protocol, and RNA was re-suspended in RNase free H_2O. RNA

concentration was determined on a Nanodrop spectrophotometer, using 2 µl of the sample at 260 nm and remaining sample stored at -80°C.

2.9.2 Reverse transcription of RNA

RNA (450 ng) was used for cDNA synthesis using SuperScript III Reverse Transcriptase (Invitrogen) following the manufacturer's protocol. SuperScript III, involves a two-step programme. The first step involves incubating RNA, 50-250 ng random primers and 0.5mM dNTP mix made up to 13 µl in total using RNase free H_2O, at 65°C for 5 min then 1 min on ice. The remaining reagents (1x First-Strand Buffer, 0 5 mM DTT, 40 U of RNaseOUT™ and 200 of U SuperScript™ III RT) were then added, totalling a reaction mix of 20 µl. The second step reaction then involved incubating the samples at 25°C for 5 min, 50°C for 60 min, the reaction was then inactivated by heating at 70°C for 15 min.

2.9.3 Fluidigm analysis

Prior to quantification of gene expression levels by Fluidigm analysis, cDNA templates were pre-amplified for chosen genes using Qiagen® Multiplex PCR Plus kit following the manufacturer's protocol. Pre-amp cycling conditions involved an initial PCR activation step for 5 min at 95°C, then 14 cycles of; 30 sec at 95°C, 90 sec at 60°C and 90 sec at 72°C, the reaction was then finished with a final extension of 10 min at 68°C. Unincorporated primers were removed using Exonuclease I (New England BioLabs, Hertfordshire, UK), following the manufacturer's protocol. Exonuclease I thermal cycling conditions were 30 min at 37°C (digestion step), then 15 min at 80°C (enzyme inactivation step). Gene expression levels were determined by 48:48 Dynamic Array BioMark™ (Fluidigm, London, UK), following the manufacturer's defined protocols for either primer or probe based assays, depending on which was being analysed. Cycling conditions for primers involved 60 sec hot start at 95°C and then 30 cycles of; 5 sec at 96°C and 20 sec at 60°C, followed by a melting curve step for 3 sec at 60°C. Cycling conditions for probes were as follows, 120 sec at 50°C, hot start for 600 sec at 95°C, then 40 PCR cycles of; 15 sec at 95°C then 60 sec at 60°C. Relative gene expressions were analysed by the $\Delta\Delta C_t$ method using an average of six housekeeping genes (UBE2D2, B2M, ENOX2, GN2B1, TYW1 and CYC1) for primers and four housekeeping genes for probes (B2M, UBE2D2, GUSB and TBP) as a

reference control and an assigned calibrator. Primers were purchased from Eurofins MWG Operon (Germany) shown in Table 2.6, housekeeping genes in Table 2.7, and probes from Invitrogen shown in Table 2.8. PCR buffers were purchased from Applied Biosystems (Warrington, UK). Heat maps were produced using PermutMatrix software (ATGC, France) using Pearson distance for dissimilarity and Complete linkage for hierarchical clustering[343].

2.10 Western Blotting

CLL cells (1 x 10^7 cells) pelleted from the 48 hr co-culture experiment (section 2.5.3), were washed in ice-cold PBS and re-suspended in 50 µl lysis buffer (20 mM Tris pH7.5, 137 mM NaCl, 10% glycerol, 1% NP40) containing protease inhibitor cocktail (Roche) and phosphatase inhibitor cocktail (Roche) on ice for 30 min. Lysates were then centrifuged at 12 000*g* for 30 min at 4 °C and the supernatant transferred to a fresh eppendorf (Eppendorf, Cambridge, UK).

2.10.1 Protein quantification

Protein lysates were quantified using Quickstart Bradford Dye Reagent (BioRad), following the manufacturer's protocol, standard curve was prepared using BSA protein (BioRad), at concentrations ranging from 0 to 20 µg/ml. Absorbance was read at 595 nM on a Spectramax M5 plate reader and analysed with SoftMax Pro 5.2 software.

2.10.2 Sample preparation

Protein lysates (15-20 µg) were made up to a final volume of 12 µl in solubilisation buffer and 3 µl of Sample buffer (5x; 10% (w/v) Sodium Dodecyl Sulphate (SDS) (Sigma-Aldrich), Milli Q ultrapure water, 200 mM Tris-HCl pH6.8, 50% (v/v) glycerol, Bromophenol blue and 5% (v/v) 2-mercaptoethanol (50 µl/ml) reducing agent (Sigma-Aldrich) was added. Samples were then boiled for 5 min at 95°C. Samples were stored long-term at -80°C, before being thawed on ice and then boiled for 1 min at 95°C prior to Sodium Dodecyl Sulphate – Polyacrylamide gel electrophoresis (SDS-PAGE).

2.10.3 SDS-PAGE

Samples were then resolved by SDS-PAGE, 7.5% gels were used to separate proteins larger than 50 kDa and 10% gels for proteins smaller than 50 kDa (Table 2.8). Cell lysates were fractioned by SDS-PAGE in 1 x Running buffer (25 mM Trizma base (Sigma-Aldrich), 192 mM Glycine (Sigma-Aldrich) and 0.1% (w/v) SDS) at 80 V for 30 min and 180 V for 45 min. Separated proteins were then transferred onto Immun-Blot polyvinyliden difluoride (PVDF) membrane (BioRad) using a semi-dry transfer method. PVDF was immersed in 100% methanol for 1 min, before being saturated in 1 x semi-dry transfer buffer (39 mM Glycine, 48 mM Tris-base, 0.04% (w/v) SDS). Four 1.0 mm Whatman paper strips were placed below the PVDF membrane, the gel was then added on top of the membrane followed by four more paper strips, the stack was then compressed to remove any air bubbles. Proteins were transferred onto the membrane at 40 mA/gel for 60 min. Blots were washed with 1 x TBST (20 mM Tris HCl pH 7.4, 150 mM NaCl, 0.01% Tween 20 (Sigma-Aldrich)), blocked in TBST containing either 5% BSA or 5% milk for 1 hr at RT. Following block the blots were incubated with primary antibody overnight at 4^{o}C as outlined in Table 2.10. Blots were then washed four times with TBST and incubated with horseradish-peroxidase (HRP)-labelled secondary antibodies for 1 hr at RT. Secondary antibody was then washed four times with TBST, followed by two washes with TBS and then blots were developed using Bio-Rad ECL and developed on a SRX-101A Medical Film Processor (Konica Minolta Medical Graphic, Inc., Banbury, UK).

2.10.4 Membrane re-probing

PVDF membranes were stripped if multiple proteins of similar molecular weights were being viewed. Blots were incubated in stripping solution (10% (w/v) SDS, 62.5 mM Tris-HCl pH7.4, 108 mM 2-Mercaptoethanol) for 30 min at 65^{o}C, with vigorous shaking every 10 min. After stripping the blots were washed with TBST and then blocked with the appropriate blocking solution and incubated with primary antibody as previously described.

2.11 Calcium Signalling

Fluo-4 AM cell permeant (Invitrogen) was used as a calcium indicator. Fluo-4 stock solution was prepared at 5 mM in DMSO. Calcium buffer was prepared by 1 x HBSS (Invitrogen), 10 mM Hepes and 0.2 % BSA. CLL cells (2-3 x 10^6 cells) were cultured overnight in complete medium on plastic, after which cells were pelleted by centrifuging for 5 min, 300*g* at RT and re-suspended in RPMI media with 0.5% BSA and cultured on plastic for a further 2 hr. CLL cells were pelleted by centrifuging as previously described, washed once with calcium buffer and re-suspended in 9 ml calcium buffer with 2 µM fluo-4. Cells were protected from light and incubated at 37^{o}C for 45 min. Cells were then washed twice with calcium buffer and then re-suspended in 9 ml calcium buffer, 2.6 ml of cell suspension was treated with 20 µg/ml of either OFA or RTX for 15 min at 37^{o}C and then pelleted and re-suspended in 2.6 ml calcium buffer. Cells in suspension were left to incubate at 37^{o}C for 30 min to allow complete de-esterification of intracellular AM esters. Calcium signalling was measured on the FACSCantoII flow cytometer for 2 min. Stimulation with the addition of 10 µg/ml F(ab')$_2$ (Jackson ImmunoResearch Laboratories Inc., Suffolk, UK), 10 µg/ml IgM (BDBiosciences), 500 nM Ionomycin (Iono; Sigma-Aldrich), OFA (20 µg/ml) and RTX (20 µg/ml) was carried out by adding the reagent directly to the CLL cell suspension immediately prior to measuring fluo-4 signal.

2.12 Statistical analysis and Software

All statistical analysis was performed using GraphPad Prism 4 software (GraphPad Software Inc., CA, USA), P values were determined by students paired or unpaired *t*-test as indicated. Mean ± standard error of mean (SEM) or mean ± standard deviation (SD) are shown as indicated. Flow cytometry data were acquired using FACSDiva software (BD Biosciences) and analysed using FlowJo (Tree Star Inc., Ashland, OR) software.

Table 2.1 List of suppliers

Company	Address
Applied Biosystems	Lingley House, 120 Birchwood Boulevard, Warrington, WA3 7QH, UK
ATGC	South of France bioinformatics platform
BD Biosciences	The Danby Building, Edmund Halley Road, Oxford, OX4 4DQ, UK
The Binding Site Group Ltd.	8 Calthorpe Road, Edgbaston, Birmingham, B15 1QT, UK.
BioRad	Maxted Rd, Hemmel Hempstead, West Sussex, HP2 7DX, UK
Bioscience Lifescience Ltd.	10 Orchard Place, Nottingham Business Park, Nottingham, NG8 6PX, UK
Cell Signaling Technology c/o New England Biolabs	75-77 Knowl Piece, Wilbury Way, Hitchin, Herts SG4 0TY, UK
Complement Technology, Inc.	4801 Troup Hwy, Suite 701, Tyler, Texas, 75703, USA
Eppendorf UK Ltd.	Endurance House, Vision Park, Histon, Cambridge, CB24 9ZR
Eurofins MWG Operon	Westway Estate 28-32 Brunel Road, Acton, London, W3 7XR, UK
Fisher Scientific UK	Bishop Meadow Road, Loughborough, Leicestershire, LE1 5RG, UK
Fluidigm UK Ltd	90 Fetter Lane, London, EC4A 1EQ, UK
GlaxoSmithKline (GSK)	GSK House, 980 Great West Rd, Brentford, Middlesex, TW8 9GS, UK
GraphPad Software, Inc.	7825 Fay Avenue, Suite 230 La Jolla, CA 92037 USA
Greiner Bio-One Ltd.	Unit 5, Stroudwater Business Park, Gloucestershire, GL10 3SX, UK
Illumina, Inc.	Chesterfield Research Park, Essex, CB10 1XL, UK
Invitrogen, Paisley, UK Ltd. Part of Life Technologies	3 Foundation Drive, Paisley, UK
Jackson ImmunoResearch, Laboratories, Inc.	UK distributor; Stratech Scientific Limited**,**
Konica Minolta, Inc.	Konica Minolta Medical & Graphic Imaging Europe B.V. Barford Road, Banbury, OX15 4FF, UK
Labtech International Ltd.	Acorn House, The Broyle, Ringmer, East Sussex, BN8 5NN, UK
Merk Chemicals Ltd.	Boulevard Industrial Park, Padge Road, Beeston, Nottingham, NG9 2JR, UK
Millipore (U.K.) Limited	Suite 3 & 5, Croxley Green Buisiness Pakr, Watford, WD18 8YH, UK.
Miltenyi Biotec Ltd.	Almac House, Church Lane, Bisley, Surrey, GU24 9DR, UK
PAA Laboratories (now part of GE Healthcare Life Sciences)	Amersham Place, Little Chalfont, Buckinghamshire,HP7 9NA, UK
Peprotech EC Ltd.	Peprotech House, 29 Margavine Road, London, W6 8LL, UK
Promega UK	Delta House, Southampton Science Park, Southampton, SO16 7NS, UK
Qiagen	Fleming Way, Crawley, West Sussex, RH10 9NQ, UK
R&D Systems	19 Barton Lane, Abingdon Science Park, Abingdon, OX14 3NB, UK
Roche	Roche, West Sussex, Charles Avenue, Burgess Hill, RH15 9RY, UK

Company	Address
Sigma-Aldrich	The Old Brickyard, New Rd, Gillingham, Dorset, SP8 4XT, UK
Stemcell Technologies	40 Rues des Berges, Miniparc Polytec, Bâtiment Sirocco, 38000 Genoble, France
Stratech Scientific Limited	Oaks Drive, Newmarket, Suffolk, CB8 7SY, UK
Tree Star, Inc.	340 A Street #101 Ashland, OR97520, USA
Whatman plc	Springfield Mill, James Whatman Way, Maidstone, Kent, ME14 2LE, UK

Table 2.2 Summary of the CLL patient clinical parameters for the CLL serum samples

[a] Previously undergone treatment but not within three months prior to sample collection

[b] Received RTX immunotherapy. Patients (except CLL 105) have not been previously exposed to RTX and received at least 5 cycles of FCR. CLL105 had previously received FCR, and received R-CHOP, with RTX given as a split dose over two days. Absolute lymphocyte count prior to treatment ranged from 44.5 – 430 and was reduced to 0.9 – 29.1 prior to the second cycle of RTX.

[c] ZAP-70 analysis was conducted by immunohistochemistry in the regional haematology laboratory.

Bolding indicates subnormal levels of complement component, or complement activity as appropriate.

CLL sample ID	Treatment[a]	RIT treatment[b]	Sex	Stage	Zap-70 status[c]	Cytogenetics	C1q (g/L) NR: 0.119-0.24	C2 (g/L) NR: 0.018 – 0.035	C3 (g/L) NR: 0.88-1.82	C4 (g/L) NR: 0.16-0.45	CH100 units NR: 80-100 U	Exhaustion (%)
5	N		M	A	Neg	13q del	0.1428	0.0425	1.34	0.290	92	-1.12
8	N		F	A	Neg	11q del	0.1194	0.0190	1.15	0.181	100	**52.58**
11	N		M	A	Neg	13q del & Tr 12	0.1950	0.0379	1.19	0.283	100	7.5
16	Y		F	A	Pos	Normal	**0.1097**	0.0311	1.27	0.427	85	27.09
18	Y		F	B	Pos	11q del	**0.0839**	**0.0131**	**0.46**	**0.061**	**70**	-
26	Y		M	A	Pos	13q del	-	-	**0.44**	**0.052**	**60**	**54.12**
28	N		F	A	Pos	17p del	0.1260	0.0299	1.10	0.205	94	9.3
29	Y		M	C	Pos	Normal	0.1310	**0.0104**	1.13	0.238	86	**68.84**
32	N		F	C	Pos	Normal	-	0.0311	0.88	0.200	98	**41.48**
35	N		M	A	Pos	11q	-	-	**0.86**	**0.131**	100	-
41	N		M	A	Neg	Normal	-	-	1.51	0.305	100	28.54
42	Y		F	B	Pos	Normal	0.1760	**0.0131**	**0.87**	**0.070**	**78**	**77.14**
44	N		F	A	Neg	Normal	-	-	**0.86**	**0.040**	**0**	-
50	Y		M	C	Pos	Normal	0.1950	0.0227	1.20	0.221	93	0.44
52	Y		F	B	Neg	11q del	**0.1003**	0.0282	1.04	0.324	100	14.67
53	N		F	A			0.1227	0.0237	1.39	0.191	100	**51.5**
54	N		F	A	Neg	Normal	0.1950	**0.0165**	1.55	0.326	89	**35**
57	N		M	C	Pos	Normal	**0.1161**	0.0347	1.15	0.316	100	**31.57**
67	N		M	A	Pos	Normal	0.1326	0.0305	1.15	0.370	100	8.29
68	Y		F	C	Pos	Normal	0.1785	0.0360	0.94	0.255	100	28.8
69	Y		M	A	Pos	Normal	0.1515	**0.0109**	1.27	0.246	100	-
70	N		F	C	Neg	Normal	-	-	1.25	0.478	100	**54.01**
72	N		F	A	Pos	Normal	0.1445	0.0379	1.17	0.330	100	23.36
73	Y		F	A	Pos	Normal	0.2845	**0.0091**	1.02	0.236	100	**38.84**
74	Y		F	A	Neg		0.1604	0.0288	1.15	0.209	92	**32.6**
76	N		F	A	Pos	6q del	0.1725	0.0305	0.94	0.302	100	-
79	Y		M	C	Pos	17p del	-	-	0.90	0.188	100	**58.3**
81	Y		M	C	Pos	Normal	-	0.0373	0.95	0.194	92	-4.12
82	Y		F	B	Pos		0.1950	0.0341	1.45	0.395	100	7.8
83	Y		M	B	Pos	Normal	-	-	0.98	**0.122**	85	**66.34**
84	Y		M	B	Neg	11q del	0.1532	0.0392	0.91	0.425	92	-
85	Y		F	A		11q del	0.1480	0.0341	1.21	**0.159**	100	17.04

CLL sample ID	Treatment[a]	RIT treatment[b]	Sex	Stage	Zap-70 status[c]	Cytogenetics	C1q (g/L) NR: 0.119-0.24	C2 (g/L) NR: 0.018 – 0.035	C3 (g/L) NR: 0.88-1.82	C4 (g/L) NR: 0.16-0.45	CH100 units NR;80-100 U	Exhaustion (%)
86	N	Y	F	A	Pos	11q del	0.1194	0.0341	1.18	0.338	100	9.1
87	N		M	C	Neg	Normal	0.1394	0.0254	1.02	0.187	-	**42.74**
91	Y		M	C	Pos	11q del	0.1533	0.0493	1.57	0.264	93	27.5
92	Y		M	C	Pos	11q del	0.1935	0.0452	1.17	0.363	100	3.4
93	Y		M	C	Pos	17p del	0.1990	**0.0109**	0.88	**0.092**	**22**	**60.94**
94	N		M	B	Pos	11q del	0.1326	0.0360	1.04	0.356	**25**	8.18
96	Y		M		Pos	11q del	0.1550	0.0265	1.21	0.214	100	**30.55**
97	Y		M	C			0.1360	0.0305	1.39	0.382	100	9.1
98	N		M	B	Neg	17p del	**0.0911**	0.0254	1.33	0.402	100	**50**
101	Y		M	C			0.1604	0.0271	1.58	0.517	100	14.65
102	Y		F	C	Pos	11q del	0.1326	0.0299	1.42	0.376	100	15.15
104	N		M				0.1428	0.0360	1.01	0.284	100	6.8
105	Y	Y	M	C	Pos	Normal	0.1394	0.0425	0.95	0.173	**62**	9.9
106	N	Y	M	B	Pos	Normal	0.1245	**0.0150**	1.19	**0.153**	100	**72.9**
107	Y		F	C	Neg	Normal	0.1515	0.0323	1.25	**0.152**	100	-
108	Y	Y	F	C	Pos		-	0.0341	1.22	0.300	100	8.4
109			M			17p del	0.1310	**0.0032**	**0.87**	**0.111**	**58**	**43**
111	Y		M	C		11q del	0.2025	0.0367	1.06	0.299	**76**	1.8
112	N		M				0.1990	0.0221	1.09	0.323	94	13.2
113	Y		F	C		17p del	0.1280	0.0360	1.14	0.173	**50**	12.5
114	Y		M	B	Pos	Normal	0.1550	0.0385	1.01	0.276	100	0.8
115	Y		M	C	Pos		**0.1150**	0.0242	1.07	**0.118**	100	14.8
117			M				0.1550	**0.0179**	1.15	0.274	100	**70.6**
118			M				0.1725	0.0398	1.19	0.225	100	-0.1
119	N		F			17p del	0.2800	0.0392	1.28	0.231	100	-3
120	Y		M	C	Pos	Normal	-	0.0265	1.13	0.187	100	**34.9**
121	N	Y	M	C	Pos	Normal	**0.0762**	0.0354	1.24	**0.069**	**42**	**47.6**
123							0.1480	0.0282	**0.84**	0.195	94	
124	Y	Y	M	B	Pos	Normal	0.1638	0.0329	1.52	0.278	100	
127	Y		M			17p del		0.0626	1.81	0.414		-1.3
129							0.2800	0.0418	1.31	0.248	**69.5**	
131							**0.0529**	0.0360	1.36	0.166	92	

Table 2.3 Summary of the CLL patient clinical parameters of CLL cell samples
[a] Previously undergone treatment but not within three months prior to sample collection
[b] ZAP-70 analysis was conducted by immunohistochemistry in the regional haematology laboratory

CLL sample ID	Treatment[a]	Sex	Stage	Zap-70 status[b]	Cytogenetics
14	Y	M	C	Pos	17p del
23	N	F	A		NOTCH1^{MUT}
28	N	F	A	Pos	17p del
41	N	M	A	Neg	Normal
42	Y	F	B	Pos	Normal
44	N	F	A	Neg	Normal
51	N	M	A+C	Neg	Normal
54	N	F	A	Neg	Normal
57	N	M	C	Pos	Normal
65	Y	F	C	Neg	Partial NOTCH1^{MUT}
67	N	M	A	Pos	NOTCH1^{MUT}
68	Y	F	C	Pos	NOTCH1^{MUT}
69	Y	M	A	Pos	Normal
70	N	F	C	Neg	Normal
73	Y	F	A	Pos	NOTCH1^{MUT}
78	Y	M		Pos	17p del
81	Y	M	C	Pos	Normal
84	Y	M	B	Neg	11q del
86	N	F	A	Pos	11q del
90	N	F	B	Pos	Normal
91	Y	M	C	Pos	11q del
92	Y	M	C	Pos	11q del
93	Y	M	C	Pos	17p del
94	N	M	B	Pos	11q del
95	Y	M			
101	Y	M	C		NOTCH1^{MUT}
104	N	M	A	Neg	Normal
105	Y	M	C	Pos	Normal
106	N	M	B	Pos	Normal
107	Y	F	C	Neg	Partial NOTCH1^{MUT}
108	Y	F	C	Pos	NOTCH1^{MUT}
109		M			17p del
112	N	M			
113	Y	F	C		17p del
114	Y	M	B	Pos	Normal
121	N	M	C		Normal
122	M				17p del/ partial NOTCH1^{MUT}
124	Y	M	B	Pos	Normal
125	N	M	C	Low	Normal
126	N	M	B	Pos	Normal
130 (Oxford Sample)					NOTCH1^{MUT}
133	N	F	C	Neg	NOTCH1^{MUT}
162 (Oxford Sample)					NOTCH1^{MUT}
190 (Oxford Sample)					NOTCH1^{MUT}

Table 2.4 FACS antibodies

Antibody name	Clone	Fluorochrome	Manufacturer's reference
CD5	UCHT2	PE	BD 555353
CD19	SJ25C1	APC-Cy7	BD 555791
CD20	L27	V450	BD 561164
CD23	M-L233	APC	BD 558690
CD45	2D1	APC-Cy7	BD 557833
CD52	HI186	PE	Bio-legend 316006
CD55	JS11	APC	Bio-legend 311312
CD59	p282 (H19)	FITC	Bio-legend 304706

Table 2.5 ARMS DNA primer sequences and concentrations

Primer	Sequence	Concentration (μM)
Forward control	GTGACCGCACGGGACTT	0.1
Forward mutation	TCCTCACCCCGTCCCGA	0.4
Reverse	AAGGCTTGGGAAAGGAAGC	0.5

Table 2.6 cDNA primer sequences and product size

Gene	Forward sequence	Reverse sequence	Product size (bp)
HES1	CCAAAGACAGCATCTGAGC	TTCTCCAGCTTGGAATGCC	149
HES3	ACGCATCAATGTGTCACTGG	GCTTCTCATGTACTTCACG	125
HES5	CATCCTGGAGATGGCTGTC	GAGCGTCAGGAACTGCAC	136
HES6	AAGCTGGAGAACGCCGAAGT	CGTGCATGCACTGGATGTAG	138
HEY1	CCGTGGATCACCTGAAAATGC	GGCATCTAGTCCTTCAATGATGC	149
HEY2	GAAGATGCTCCAGGCTACAGG	CCTTCCACTGAGCTTAGGTACC	126
TLE1	TAACCTCCTCAATGCTTGGC	AGACTGTAGCCTTCTTGTCC	140
TLE4	ACTTGGTGGTTGACGTTTCC	ATAGAGGCTGGACTAATCGG	130
DELTEX	AATCCCGAGGATGTGGTTCG	GTAGCCTGATGCTGTGACCA	102
CDKN1A	GTGGACCTGGAGACTCTCAG	CCTCTTGGAGAAGATCAGCCG	92
RUNX3	GGCAATGACGAGAACTACTC	GTTGGTGAACACAGTGATGG	144
C-FMS	CAAGTTCATTCAGAGCCAGG	CTGGGATGACTTTCTGCACT	101
FBXW7	CCTTCTCTGGAGAGAGAAATGC	CTGTCTGATGTATGCACTTTTCC	121
NUMB	CCAAACCAGTGACAGTGGTGGC	CCCAAGGGTTGGTTTCACGC	141
MAML	GCAACAGCAGTTCCTTCAGAGG	GTGAACTGTCCAACCTGCTGTG	141
LFNG	GCCACAAGGAGATGACGTT	GAGCAGTTTGTGATGACCACG	88
MFNG	CTGGTACAGTTCTGGTTTGC	ATGTGTCCATGAAACGGGAGC	106
ADAM19	GTTTACACAACAGACCAAGAAGC	CTTGTGTTTGGTGGCGTCC	142
C-JUN	CTTGAAAGCTCAGAACTCGGAG	CTGCGTTAGCATGAGTTGGC	121
VEGF	AGAAGGAGGAGGGCAGAATCA	AGGGTACTCCTGGAAGATGTCC	109
DKK3	GCATCATCGACGAGGACTGT	GTCTCCACAGCACTCACTGT	122
DLL1	GCCTGGATGTGATGAGCAGC	ACAGCCTGGATAGCGGATACAC	109
STAT3	CCTAGATCGGCTAGAAAACTGG	GGGTCCCCTTTGTAGGAAAC	114
NFKB1	AGATGATCCATATTTGGGAAGGC	TTGCTCTAATATTTGAAGGTATGGGC	142
JAG1	TGGGATTCCAGTAATGACACCG	GTAGTCATCACAGGTCACGC	156
JAG2	CAAAAACCTGATTGGCGGCT	CACACACTGGTACCCGTTCA	142
ADAM17	CTTCTACAGATACATGGGCAGAG	CTCTATCTGTATTCCATAGCCTTTAA	139
ADAM10	ATGGCAAAGATGATAAAGAATTATGCC	AATCGTTGCAAGGGGATCC	147
FURIN	CCACATGACTACTCCGCAGAT	TACGAGGGTGAACTTGGTCAG	150
PSEN	GGTGGTTCTGTATAAATACAGGTGC	AACAGTAATGTAGTCCACAGCAA	145
CCND1	CAGAAGGAGATTGTGCCATCC	GAAGCGGTCCAGGTAGTTCA	120
TP53	TTCTTGCATTCTGGGACAGCC	GGGGGTGTGGAATCAACCC	119
MYC	GACTCTGAGGAGGAACAAGA	TTGGCAGCAGGATAGTCCTT	218
NOTCH1	TCCACTGTGAGAACAACACGC	ACTCATTGACATCGTGCTGGC	141
NOTCH2	GCAAAGTGTATCGATCACCCGA	TGCAGGTGTAGGAATCAATACCATC	148
NOTCH3	TACTGGTAGCCACTGTGAGCAG	CAGTTATCACCATTGTAGCCAGG	129
NOTCH4	TTCCACTGTCCTCCTGCCAGAA	TGGCACAGGCTGCCTTGGAATC	142
DLL3	CACTCAACAACCTAAGGACGCAG	GAGCGTAGATGGAAGGAGCAGA	126
DLL4	TCGCTCATCATCGAAGCTTGG	CAGTTCTGACCCACAGCTAGG	119

Table 2.7 cDNA primer sequences for housekeeping genes and product size

Gene	Forward sequence	Reverse sequence	Product size (bp)
B2M	TTGTCTTTCAGCAAGGACTGG	ATCCGGCATCTTCAAACCTCC	172
CYC1	ACTGCGGGAAGGTCTCTACTT	GGGTGCCATCGTCAAACTCTA	101
ENOX2	GAGCTGGAGGGAACCTGATTT	CACTGGCACTACCAAACTGCA	182
GNB2L1	TCCATACCTTGACCAGCTTG	GCAGATTGTCTCTGGATCTC	179
TYW1	ATTGTCATCAAGACGCAGGGC	GTTGCGAATCCCTTCGCTGTT	167
UBE2D2	CCATGGCTCTGAAGAGAATCC	GATAGGGACTGTCATTTGGCC	302

Table 2.8 cDNA gene expression probes

Gene	ID	Gene	ID
APC	Hs00181051_m1	HDAC4	Hs00195814_m1
AXIN1	Hs00394718_m1	HDAC5	Hs00608366_m1
AXIN2	Hs00610344_m1	JUN	Hs99999141_s1
B2M	Hs00984230_m1	JUNB	Hs00357891_s1
BAD	Hs00188930_m1	LEF1	Hs00212390_m1
BCL2	Hs00608023_m1	LYN	Hs00176719_m1
BCL9L	Hs00699441_m1	MAML2	Hs00287205_m1
CCL4	Hs99999148_m1	MAPK8IP2	Hs00183753_m1
CCND1	Hs00765553_m1	MAX	Hs00231142_m1
CCND3	Hs00236949_m1	MCL1	Hs01050896_m1
CCNE1	Hs01026536_m1	MMP7	Hs01042796_m1
CCNE2	Hs00180319_m1	MMP9	Hs00957555_m1
CD247	Hs00167901_m1	NCAM1	Hs00941830_m1
CD38	Hs01120071_m1	NFATC1	Hs00542678_m1
CD44	Hs00153304_m1	NFATC3	Hs00190046_m1
CDC25C	Hs00156411_m1	NFATC4	Hs00190037_m1
CDK1	Hs00364293_m1	NOXA	Hs00736699_m1
CDK2	Hs01548894_m1	PECAM1	Hs00169777_m1
CDKN1B	Hs01597588_m1	PRDM1	Hs00153357_m1
CDKN2A	Hs99999189_m1	PRKCa	Hs00176973_m1
DAPK1	Hs00234480_m1	PRKCb	Hs00176998_m1
DELTEX1	Hs01092201_m1	PRKCd	Hs01090047_m1
DV1	Hs00182896_m1	PRKCe	Hs00178455_m1
E2F1	Hs00153451_m1	PRKCz	Hs00177051_m1
E2F2	Hs00231667_m1	ROR1	Hs00178178_m1
E2F3	Hs00605457_m1	ROR2	Hs00171695_m1
FASLG	Hs00181225_m1	RRAD	Hs00188163_m1
FOS	Hs00170630_m1	SYK	Hs00374292_m1
FOXO3	Hs00818121_m1	TBP	Hs00427620_m1
GATA3	Hs00231122_m1	TP73	Hs01056231_m1
GLI1	Hs01110766_m1	VEGFA	Hs00900055_m1
GUSB	Hs99999908_m1	UBE2D2	Hs00366152_m1

Table 2.9 SDS-PAGE Running and stacking gel preparation

Gel (%)	5.5	7.5	10
Gel type	Stacking	Running	Running
30% bis-Acrylamide	5.5%	7.5%	10 %
Milli Q Ultrapure water	667 µl/ml	373 µl/ml)	290 µl/ml
1M Tris-HCl pH 8.8	-	373 mM	373 mM
1M Tris-HCl ph 6.8	139 mM	-	
10% (w/v) SDS	0.17%	0.17%	0.17%
10% (w/v) Ammonium Persulphate	0.06%	0.07%	0.07%
Temed	2.2 µl/ml	1.3 µl/ml	1.3 µl/ml

Table 2.10 Western blot antibodies

Antibody name	Reactive Species	Dilution	Block	Manufacturer's reference
ADAM10, C-terminus	Rabbit	1:1000	5 % Milk	Millipore AB19026
Akt (pan) (C67E7)	Rabbit	1:1000	5 % BSA	Cell Signaling 4691
Phospho-Akt (Ser473)(D9E)	Rabbit	1:1000	5 % BSA	Cell Signaling 4060
Cyclin E1 (HE12)	Mouse	1:1000	5 % Milk	Cell Signaling 4129
Cyclin E2	Rabbit	1:1000	5 % BSA	Cell signaling 4132
GAPDH (D16H11)	Rabbit	1:1000	5 % Milk	Cell Signaling 5174
GSK-3β (27C10)	Rabbit	1:1000	5 % BSA	Cell Signaling 9315
Phospho-GSK-3β (Ser9)	Rabbit	1:1000	5 % BSA	Cell Signaling 9336
Notch1 (A-8)	Mouse	1:500	5 % BSA	Santa Cruz Biotechnology, sc-376403
Notch2 (D67C8)	Rabbit	1:1000	5 % BSA	Cell Signaling 4530
Notch3 (D11B8)	Rabbit	1:1000	5 % Milk	Cell Signaling 5276
Notch4 (L5C5)	Mouse	1:1000	5 % Milk	Cell Signaling 2423
Anti-rabbit IgG (H+L) – HRP conjugated	Goat	1:10000	5 % BSA	Cell Signalling 7074
Anti-mouse IgG (H+L) – HRP conjugated	Horse	1:10000	5 % BSA	Cell Signalling 7076

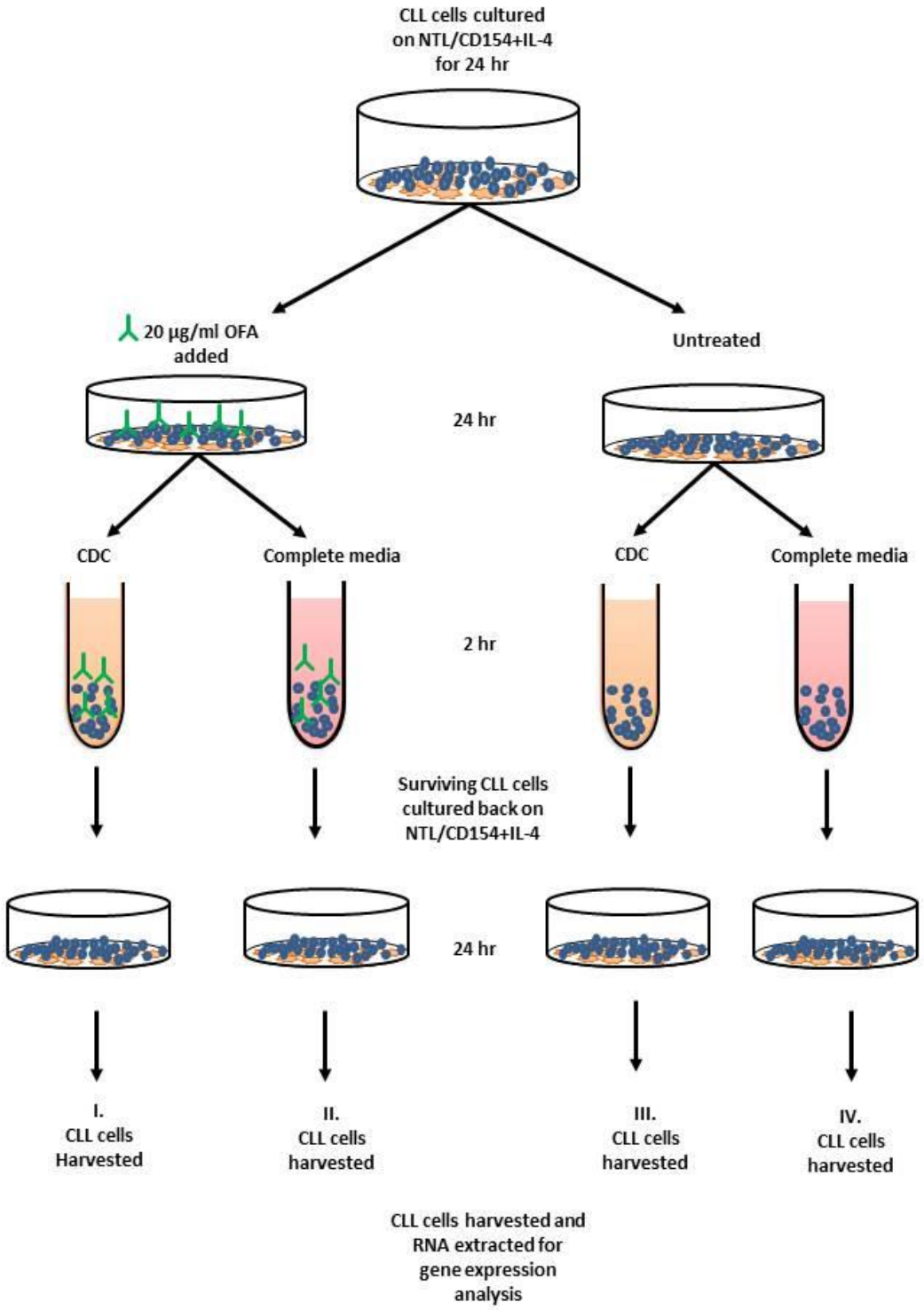

Figure 2.1 Experimental outline for molecular characterisation of CLL cells escaping OFA induced CDC

CLL cells were cultured on NTL/CD154+IL-4 for 24 hr, cells were then either left untreated or 20 µg/ml OFA was added for a further 24 hr. CLL cells were then collected and half underwent CDC and the remaining half incubated with complete medium. The surviving CLL cells were then co-cultured with NTL/CD154+IL-4 for a further 24 hr. After co-culture the CLL cells were separated from the stromal layer and gene expression analysis performed as described in section 2.9.

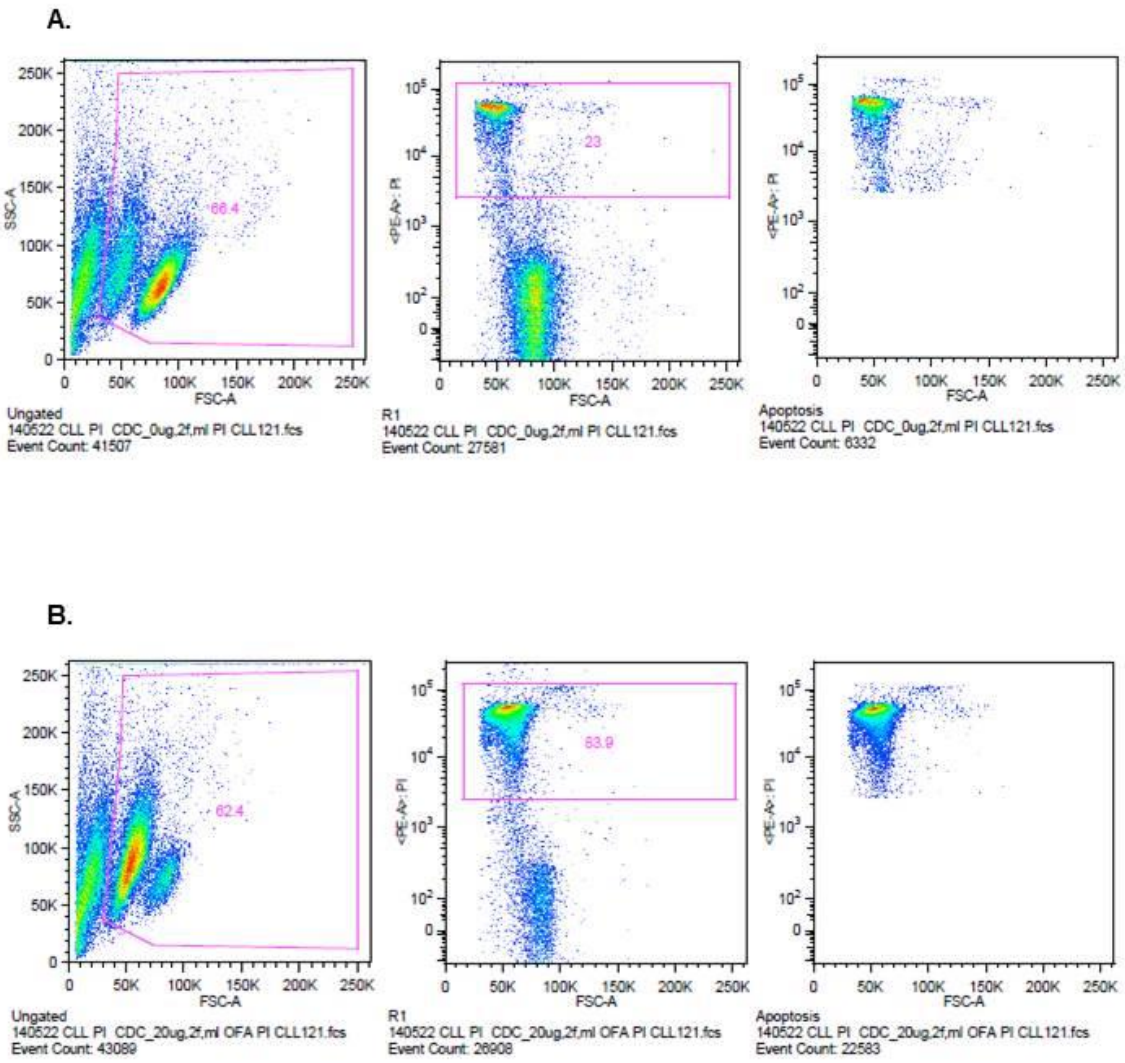

Figure 2.2 Cell death assessed by PI staining

CLL cells were stained with PI as described in section 2.6.2, and the gating is shown above. Debris was at first gated out and then the percentage of dead cells determined by the number of cells positive for PI staining. A. CLL sample (121) untreated. B. CLL sample (121) treated with 20 µg/ml OFA.

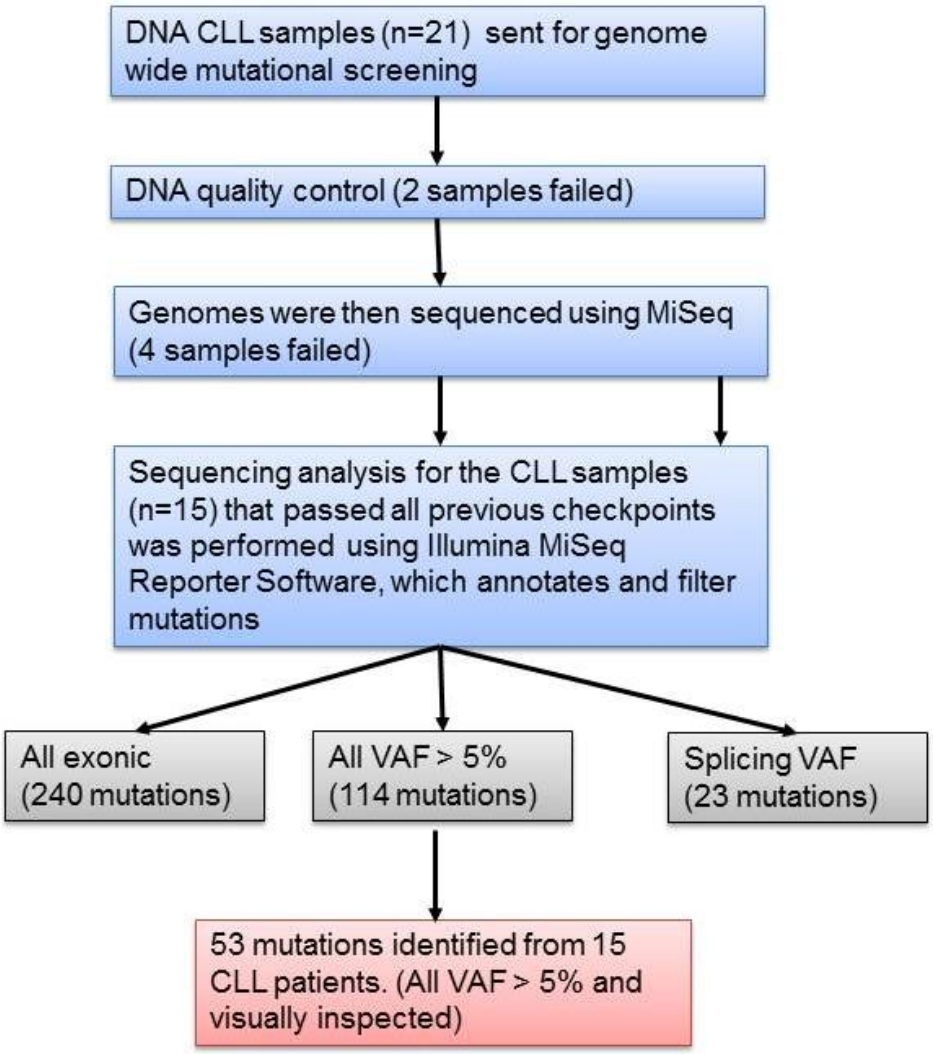

Figure 2.3 Flow chart of the mutation screening process carried out by Oxford University.

3 Complement levels effect MAb efficacy

3.1 Introduction

MAb therapies form an integral part of the treatment regime for CLL patients. MAbs exert anti-tumour activity by harnessing the body's own natural immune response especially ADCC involving the recruitment of NK cells to cause phagocytosis and CDC requiring the activation of the classical complement pathway, and/or apoptosis[284].

Type 1 MAbs, such as RTX and OFA, are potent inducers of CDC as they are able to localise CD20 into lipid rafts enhancing C1q recruitment[255]. CDC induction is critically dependent on the distance between MAb binding site and the plasma membrane, close binding allows efficient coating of active complement components onto the target cell[1]. OFA is a more potent inducer of CDC than RTX. OFA more readily binds to C1q, has a longer disassociation rate and the novel binding site allows more effective deposition of C3b onto the surface of the membrane[254,255,315,316]. The ability to induce CDC is of particular importance in CLL, as CD20 expression levels, which are relatively low compared to B-cell lymphomas, linearly correlate with the lytic response of RTX[310,311]. In addition, recent studies demonstrate that CLL cells can evade RTX, through sequestration of CD20-RTX complexes by phagocytic cells, resulting in trogocytosis. Trogocytosis causes CD20 depletion from the surface of the lymphocytes in circulation, which are no longer responsive to OFA or RTX treatment[318-320]. These findings highlight the importance of generating a MAb capable of effectively inducing CDC and ADCC.

To maximise the clinical effect, it is important to consider whether the patient will be able to elicit a healthy CDC and ADCC responses to MAb immunotherapy. Early reports indicated that CLL patients harbour deficiencies in classical complement components C1 and C4 resulting in defective immune complex clearance[326]. Deficiencies in classical complement components have also been linked to CLL patients being more susceptible to infections with organisms such as *S. pneumonia,* and exhibiting a propensity to developing autoimmune syndromes[325-327]. Complement deficiencies could greatly impact upon the clinical

efficacy of OFA and RTX. Therefore it is important to establish the prevalence and impact of complement deficiencies within CLL patients.

3.2 Aim

The main focus of this research is to establish whether CLL patients are prone to deficiencies in classical complement components. If complement deficiencies do occur then we also aim to determine:

- How frequently they occur;
- How they impact upon the efficacy of MAb treatment;
- If CDC activity is reduced, can we enhance it?;
- Is a reduction in complement levels or CDC activity observed *in vivo* following MAb therapy.

3.3 Results

3.3.1 CLL patient sera display multiple deficiencies in components of the classical complement cascade

Complement component levels C1, C2, C3 and C4 were assessed in CLL patient sera alongside NHS and sera from AMS controls. NHS was provided by healthy volunteers with an age range of 22-50 years, similar to those donating fresh frozen plasma (FFP). CLL is a late onset disease therefore the age range for our CLL sera cohort was 67.9 years ± 6.78 years (age range 48-88 years, 57.9% males). To determine whether the predominance of any complement deficiencies were CLL related and not age related AMS was used. AMS had an average age of 64.8 years ± 12.91 (age range 47-84 years, 41.7% males).

Patients displaying single deficiencies/reduced levels were noted in all complement components screened (Figure 3.1A). In the AMS samples (n=12), complement deficiencies slightly below normal range for C1, C2 and C3/C4 were observed in a minority of donors (n=3), a single deficiency in C4 was also observed in one NHS control sera. The CLL sera screened displayed a much wider range of complement values than either controls, with complement concentrations falling outside the normal range. Of the CLL patients screened, 15.4% exhibited levels lower than the normal range of C1q in their sera (n=52) and approximately 20% of patients displayed deficiencies in the levels of C2 and C4 (17.5%, n=57 and 20.3% n=64 respectively). Analysis of C3 levels revealed that 10.9% of patient sera (n=64) were deficient in this component. Double deficiencies of C1/C4, C2/C4 and C3/C4 also occurred, at a frequency of 3.1%, 3.1% and 4.7% respectively. Triple deficiency of C2/C3/C4 was seen in 3.1% of CLL patients screened, and deficiency of C1q/C2/C3/C4 was observed in one patient within our cohort. Due to the large range of CLL sera complement levels, no statistically significant differences were observed between the mean complement levels from CLL sera and either NHS or AMS. In total 37.5% of CLL sera tested were deficient in at least one complement component (n=64; Figure 3.1A). To determine how these deficiencies impacted on the sequential activation of the classical complement cascade in the CLL sera we performed a CH100 assay. Surprisingly only 19.4% of CLL sera exhibited reduced complement

activity levels (Figure 3.1B), despite the high proportion displaying at least one component deficiency.

To establish whether there was an association with abnormal complement levels, either above or below the normal range, we compared complement levels vs different prognostic markers in CLL. Complement concentrations and prognostic information for each CLL patient sera screened is shown in Table 2.2. Firstly complement levels were stratified against the Binet stage of disease at the point of sample collection. We observed no correlation between the different clinical stages and complement levels (Figure 3.2). Interestingly when the different mutational or cytogenetic sub-groups in CLL were compared to complement levels, we observed an elevation of C1q and C4 concentrations in $NOTCH1^{MUT}$ CLL patients. When comparing the mean complement levels for $NOTCH1^{MUT}$ vs. cytogenetically normal CLL patients the values were near significance using a two-tailed unpaired t-test, p= 0.069 (C1q) and p=0.056 (C4), however a larger sample size is required to determine if this is a significant trend (Figure 3.3). ZAP-70 status groups revealed no statistical significance between complement levels for our CLL patient cohort (Figure 3.4). However the majority of C2 and C4 complement deficiencies were observed in the ZAP-70 positive cohort, but again a larger sample size is required to determine if this is a significant trend.

3.3.2 Optimisation of CDC in CLL cell lines

Two CLL cell lines, HG3 and WAC were used to determine the optimal experimental conditions to achieve maximal CDC with OFA using RTX as a comparator. CDC was determined by the percentage of cells positive for PI staining (Figure 3.5). We determined that the highest efficacy was reached at 20 µg/ml for OFA in HG3 cells (Figure 3.5A) and using 50% NHS (to approximate physiological conditions; Figure 3.5B) in both CLL cell lines. Longer serum incubation times made no significant difference to enhancing CDC levels (Figure 3.5C), therefore 2 hr incubation time was used for maximal CDC. These conditions were then used for all subsequent CDC experiments unless stated. HG3 cell line was also used for all subsequent experiments due to the high levels of CDC observed. These optimisation results also corroborate the increased efficacy of OFA to induce CDC in comparison to RTX, as seen by others[254,255,344].

3.3.3 High exhaustion levels associate with increasing tumour burden

To determine whether CDC was affected by high tumour load, we carried out exhaustion assays using NHS exposed to increasing numbers of primary CLL cells. The efficiency of CDC in primary CLL cells did not decline significantly until 10000 cells/µl were present, at which point CDC activity dropped by 48.1% in the NHS from the primary use (Figure 3.6). Given that CLL sera is more depleted of complement than NHS, CLL sera exhaustion assays carried out in subsequent experiments were performed using 2500 HG3 cells/µl. These findings indicate that tumour load will also have a significant negative impact on CDC activity.

3.3.4 CLL sera readily exhaust of complement activity following MAb therapy

Our findings indicated that low levels of individual complement components observed in CLL patient sera did not always directly impact on CH100 complement activity. We therefore hypothesised that CLL patient serum might exhaust the available complement components more readily after eliciting an initial CDC response. This is an important consideration given the repeated scheduling of MAbs in CLL patients undergoing immunotherapy. To validate complement exhaustion, OFA-mediated CDC was performed on the CLL cell line HG3 using 50% CLL patient sera (n=52), with a NHS control included for comparison. Following 2 hr incubation, cells were pelleted and CDC levels measured by PI staining (Figure 3.7A). The sera removed from this experiment was then re-used to promote a second CDC response on fresh OFA bound HG3 cells (Figure 3.7B). Serum exhaustion was performed on 52 CLL patient sera. The difference between CDC cell kill from the first to the second round of serum use was then plotted (Figure 3.8A), with representative data from three individual patient samples with poor (CLL08), medium (CLL32) and good (CLL85) CDC activity shown (Figure 3.8B). Our results clearly demonstrate that CLL patient sera show significantly more complement exhaustion compared to NHS controls, with 42.3% of CLL patient sera showing more than 30% reduction in CDC activity from primary to secondary use.

As previously shown with complement levels, we determined whether exhaustion levels were associated with poor prognostic markers, also shown in Table 2.2.

Similar to our findings with complement concentration levels, there was no significant correlation between exhaustion and Binet stage (Figure 3.9A) and ZAP-70 status (Figure 3.9C). Interestingly 11q del patients, which had marginally elevated C2 and C4 levels compared to cytogenetically normal CLL samples, also had lower levels of exhaustion bordering on statistical significance when compared against cytogenetically normal CLL sera ($p= 0.056$, using two-tailed paired t-test; Figure 3.9B). This suggests that there is possibly genetic interplay between the different cytogenetic sub-groups and the expression and activity of complement components; however more samples would be required to confirm this.

3.3.5 CLL sera exhaustion is most strongly linked with complement C2 concentration levels

To establish whether complement exhaustion could be attributed to individual complement components, we performed linear regression analysis comparing individual complement components against exhaustion levels (Figure 3.10). The concentration of C2 displayed a significant negative correlation with sera exhaustion levels in CLL patients (Figure 3.10B; $r^2= 0.5260$, $p <0.0001$). The levels of C4 also displayed a significant negative correlation with sera exhaustion in CLL patients (Figure 3.10D; $r^2= 0.1559$, $p= 0.0192$), albeit to a lesser degree than C2. The concentrations of C1 and C3 appeared to have marginal influence over the level of CDC exhaustion observed.

3.3.6 CLL sera exhaustion can be reduced by the addition of a complement source

To determine whether CDC could be improved in patients deficient in one or more complement component, individual components were added back to CLL patient sera. We added back both C2 and C4 as they showed significant correlation with exhaustion levels. Similar to a report by Kennedy A.D., *et al.*, we identified C2 as being the limiting factor [319]. Upon addition of C2 to patient sera we were able to abrogate complement exhaustion (Figure 3.11A). Only C2 alone or in combination with C4 was able to augment CDC in deficient sera, supporting previous findings that C2 is the limiting factor. Interestingly C2 was also important for improving CDC in CLL patients deficient in C4 alone (Figure 3.11B). In a larger patient cohort, supplementing the sera with C2 restored CDC

cell kill from primary to secondary sera use to levels observed for the NHS control (Figure 3.12), whereas the addition of C4 only showed improvement in CDC levels during the primary sera use. To determine whether we could protect against complement consumption in a clinically-relevant manner, we added back 10% and 20% NHS (equivalent to FFP, an available source of complement for CLL sera), prior to the first round of CDC. Our results clearly demonstrate that adding back 20% NHS not only gave significant improvement to the initial level of CDC but also decreased the amount of complement exhaustion on secondary use (Figure 3.13).

3.3.7 CLL sera exhaustion is observed *in vivo* with RTX

Next we screened the sera of CLL patients undergoing RTX immunotherapy to establish whether complement levels were severely diminished following RTX treatment *in vivo*. The standard dosing schedule for RTX is shown in Figure 3.14A, along with sera collection points. All except one CLL patient displayed complement levels falling below the expected normal range 24 hr post RTX infusion (Figure 3.14B-D). For the majority of patients, 28 days was sufficient for complement levels to be replenished following treatment, however this was not true for the patient already deficient in C2 (CLL106). In addition, *in vitro* CDC assays were carried out using OFA treated HG3 cells, using the RTX treated patient sera. OFA was chosen due to its ability to elicit higher levels of CDC *in vitro* than RTX, enabling a better range of CDC response to be measured. Analysis 24 hr following RTX infusion revealed that reduced complements levels correlated with an inability to elicit a CDC response (Figure 3.15A). The one CLL patient serum sample (CLL108) which did not have reduced complement levels also demonstrated good CDC activity on OFA treated HG3 cells which correlated with no complement exhaustion following RTX treatment (Figure 3.14B-D and Figure 3.15). Interestingly CLL108 was identified as being positive for $NOTCH1^{MUT}$. Retrospective analysis of the CLL8 trial demonstrated that the addition of RTX to FC provided no additional benefit to $NOTCH1^{MUT}$ CLL patients[108]. Therefore it was not surprising that very little RTX CDC activity was observed for this patient within their sera. Individual complement component levels also reflected how readily patient sera exhausted following subsequent CDC challenge on OFA treated HG3 cells, with CLL106 displaying a marked reduction in CDC cell kill *in vitro* prior to RTX infusion (Figure 3.15Bi). This was

more apparent post RTX infusion with the majority of patients showing complete ablation of complement activity *in vivo* (Figure 3.15Bii). These findings highlight important implications for the future management of CLL patients receiving MAb therapy.

3.3.8 OFA also induces complement consumption *in vivo*

When this study was carried out, pre-April 2014, OFA was registered for use only in patients that were double refractory to both fludarabine and alemtuzumab treatment. Therefore the number of CLL patients receiving OFA treatment was scarce in the Glasgow area, however we were fortunate to receive sera from two CLL patients undergoing OFA immunotherapy. As we and others have shown OFA is a more potent inducer of CDC than RTX due to its novel epitope binding site (Figure 3.5). The scheduling for OFA is different from RTX with weekly cycles of MAb infusion followed by monthly doses. This scheduling, in combination with OFA's potent CDC induction could therefore potentially lead to more excessive complement exhaustion. The standard dosing schedule for OFA is show in Figure 3.16A, including the time points at which serum samples were collected for CLL111. 24 hr post the first 300 mg infusion of OFA, complement levels C2 and C4 were completely abolished, and C3 dropped below the normal range (Figure 3.16B-D). For this patient OFA demonstrates excessive complement consumption similar to what we observe with CLL patients receiving RTX immunotherapy (Figure 3.14). 7 days after the 300 mg small dose of OFA complement levels were restored back to within the normal range. Interestingly when the dose of OFA increased to 2000 mg, 7 days post this infusion CLL111 still had no detectable C2 or C4 complement levels and C3 remained below the normal range (Figure3.16B-D). The reduction in complement levels were reflected in the CDC activity of the sera, with no detectable CDC observed in the primary or secondary use of the sera following OFA infusion (Figure 3.17). These *in vitro* findings potentially have a clinical impact, as they highlight that any further dose of OFA would likely have little effect on CDC lysis of tumour cells.

The serum collection points for the second CLL patient that underwent OFA immunotherapy, CLL127, are shown in Figure 3.18A. CLL127 displayed a very high expression of complement components C2, C3 and C4, and after the start of OFA treatment, while complement levels dropped, they remained within the

normal range (Figure 3.18B-D). CDC analysis of the sera revealed that serum extracted from CLL127 still showed no complement exhaustion (Figure 3.19). CLL127 CDC results also demonstrated that there was enough OFA circulating within the peripheral blood to induce high levels of CDC *in vitro* upon HG3 cells incubated with this patient's serum (i.e. no additional OFA added *in vitro*) to be used as a control. After the first 300 mg dose of OFA we observed an increase in CDC by 33.7% on untreated HG3 cells and 7 days after the large 2000 mg dose of OFA, CDC on untreated HG3 cells was maximal. This data shows that OFA is likely to be stable and circulate within the body for at least 7 days post treatment.

3.4 Discussion

MAbs are now firmly established in the treatment of CLL, both as a first-line therapy and in the relapse setting. Type 1 anti-CD20 MAbs mediate their toxicity effects against CLL cells by using the patient's natural immune responses to induce cell death through ADCC and CDC. Previous reports have shown that CDC is a finite process with complement becoming exhausted following MAb induced cell lysis[329]. Earlier research indicated that around 50% of CLL patients are deficient in C1 and C4, key components of the classical complement cascade, and this low complement activity is associated with advanced disease and shorter survival time[325,326,328,338]. Despite these early reports there has been little follow up to determine how these complement deficiencies influence the efficacy of MAb treatment, with immunotherapies such as OFA and RTX that are potent inducers of CDC.

3.4.1 CLL patients have lower classical complement levels

Our comprehensive assessment of the levels of all complement components involved in the first stage of the classical cascade in CLL patient sera revealed that a high proportion of CLL patients harbour deficiencies, with 37.5% displaying a reduced level of either C1, C2, C3 or C4. Patients exhibited a range of deficiencies from one to multiple complement components, with one individual demonstrating a deficiency in all classical complement components examined. Levels of C1 and C3 were often within the normal range, whereas subnormal levels of C2 (17.5% deficient) and C4 (20.3% deficient) were more prevalent in the CLL patient cohort examined. We were unable to define any significant differences in complement concentration within CLL patient clinical stage, or ZAP-70 status. Interestingly NOTCH1^{MUT} CLL samples displayed a trend towards elevated concentration levels of C1 and C4. NOTCH1^{MUT} CLL cells have previously been reported to be resistant against anti-CD20 MAb therapies; therefore our data indicates that impaired complement levels are not limiting CDC activity[108,109]. C2 and C4 are both cleaved into two fragments during classical complement activation, with C4b and C2a then forming a complex termed C3-convertase. C3-convertase is essential for cleaving C3, which enables the C3b fragment to opsonise the target cell and act as a scaffold for the MAC to assemble so that the target cell can be lysed. C3b also functions to opsonise

bacteria strains, for clearance by the classical pathway[284]. CLL patients are frequently unable to effectively coat bacterial pathogens with C3b, making them more susceptible to infection[327]. Therefore these deficiencies could increase the risk of life threatening infection, already a major concern in CLL patients[338,345].

3.4.2 CLL patient sera more readily exhaust of complement, abrogating CDC activity

Although the high frequency of defects in complement levels did not correlate closely to overall classical complement activity *in vitro*, analysis of patient sera revealed that significantly more CLL patient sera samples underwent complement exhaustion on secondary challenge with bound MAb, compared to the NHS controls (42.3%; n=52). CLL patients with 11q del have been shown to respond well to RTX when added to FC treatment[346], this could be in part due to the reduced level of complement exhaustion we observed in this cytogenetic subset. 11q del patients show 16.9% less complement exhaustion than CLL patients with no cytogenetic abnormalities (p=0.0529), suggesting there will be more effective clearance of cancer cells via RTX induced CDC.

In addition tumour burden impacted on CDC efficiency, with high levels of sera exhaustion observed at medium-low tumour burden levels typically observed for CLL, 1 x 10^4 CLL cells/μl. These findings are corroborated by Beurskens F.J. *et al.*, who also observed an elevated complement consumption with high cell counts. Moreover they demonstrated that administering high concentrations of OFA did not substantially augment initial CDC induction, but did affect the ability to induce a second round of CDC due to exaggerated complement activation and consumption[329]. Therefore any MAb treatments requiring CDC for potency will be limited by tumour burden, and low complement component levels within CLL patient sera.

3.4.3 CDC activity can be restored in CLL patient sera with limited complement levels

Complement exhaustion has important implications for the dosing schedule of MAb treatment within CLL as frequent dosing, which in addition to limiting the efficacy of the drug, will lead to sustained complement exhaustion making patients more susceptible to infections. Having confirmed previous findings that

C2 was depleted at a high frequency in CLL[319], we established that impaired CDC could be restored to a normal NHS level by supplementing patient sera with C2. In addition, supplementing patient sera with 10 and 20% NHS was also sufficient to substantially improve OFA mediated CDC and enable protection against complement exhaustion. Other studies suggest that RTX is not as effective at depositing C3b onto the surface of cancer cells and is not as effective as OFA as a single agent in CLL[254,255,344]. Despite this, RTX still showed significant improvement when administered together with FFP in a clinical trial of fludarabine-refractory CLL patients, with minimal toxicity[255,347-349]. This suggests that complement could be one of the limiting factors in RTX efficacy as a single agent.

OFA is currently licensed for treatment in combination with chlorambucil for previously untreated CLL patients, when fludarabine based therapy is not suitable and as a single agent for CLL patients that are double refractory. OFA shows significant activity as a single agent, effectively targeting CLL cells previously treated with RTX[256,257]. The improvement reported for the small cohort of patients treated with RTX in combination with FFP, lend support for further investigation of MAb therapy in combination with FFP infusions in clinical trials in the context of enhancing classical complement pathway activity. This would be of particular importance for MAbs like OFA, which are highly effective at using the complement system to induce cell death. Moreover, enhancement of CDC by supplementing MAb therapy with FFP may also reduce the level of trogocytosis thus preventing immune evasion of CLL cells. Indeed, our data highlight the importance of considering tumour burden and patient complement levels prior to MAb therapy, as these factors could negatively impact on the ability of the patient's natural immune system to clear the malignant cells, thus reducing clinical efficiency of the administered MAbs. Significantly, we demonstrate that complement exhaustion can occur following RTX therapy *in vivo*, reducing both complement activity as shown previously[319], and the serum concentrations of complement components, particularly C2 and C4. Analysis of sera from CLL patients undergoing RTX immunotherapy, showed that 24 hr post RTX infusion, complement was rapidly consumed by OFA treated HG3 cells, leading to a substantial decrease in CDC activity. Only one CLL patient, identified as being NOTCH1^{MUT}, did not display depleted complement levels with

high CDC activity and marginal exhaustion with secondary sera use. This was not surprising as NOTCH1^{MUT} patients have previously been shown to display no improvement in PFS or OS when RTX was added to FC[108]. Therefore it is understandable that there would be no complement consumption if the cells are resistant to RTX. We have shown that the lack of RTX activity for this NOTCH1^{MUT} CLL patient is not due to low complement levels or the inability to elicit CDC following OFA binding to HG3 cells. This suggests that the inhibitory mechanism for anti-CD20 MAb CDC efficacy is cellular rather than serum based. However in the majority of patients by day 28 CDC activity was restored, in line with complement levels. Interestingly the patient whose CDC activity remained low at day 28 was deficient in C2, which dropped even lower following RTX treatment and remained at low levels by day 28. We observed that sera from this patient, CLL106, exhausted readily *in vitro*, corroborating what was observed *in vivo*. In contrast to RTX, OFA is typically administered as 8 weekly doses followed by 4 monthly treatments[256,257].

In one of the two CLL patients undergoing OFA treatment, 7 days after the infusion of OFA complement levels still were not restored to normal. This suggests that complement levels take between 7-28 days after MAb infusion to be restored, leaving CLL patients vulnerable to infection during these depleted periods and calls into question the effectiveness of the dosing schedule for OFA. In a previous study, patient complement levels were also reduced considerably following OFA infusion, especially after the first dose when CD20 levels were initially high[23]. These findings have recently been confirmed by Baig et al., who demonstrate that there is a rapid decrease in serum complement levels following OFA treatment, which is sustained 24h post-treatment. In addition CLL cells lose CD20 expression and become insensitive to *in vitro* OFA-mediated CDC, whilst retaining their ability to undergo alemtuzumab-mediated CDC when supplemented with 10% NHS[28]. The higher dose-intensity, coupled with the greater induction of CDC with OFA, suggests that sustained complement depletion is more likely to occur during OFA treatment, in susceptible patients. As observed in our second CLL patient undergoing OFA immunotherapy, OFA appears to be stable within peripheral blood up to and possibly exceeding 7 days. Therefore the addition of FFP could lead to more effective clearance of CLL cells that are entering the peripheral blood from the LNs several days after

OFA infusion. In patients with complement deficiencies, ineffective CDC may also result in non-lethal complement deposition on CLL cells, allowing excessive CD20 depletion through trogocytosis by effector cells, and subsequent resistance to OFA-mediated CDC.

This research demonstrates how important complement levels are in CLL and how this will limit the efficacy of MAb therapies, and gives warrant to a clinical study to assess the impact of complement replenishment using FFP in CLL patients receiving MAb therapy.

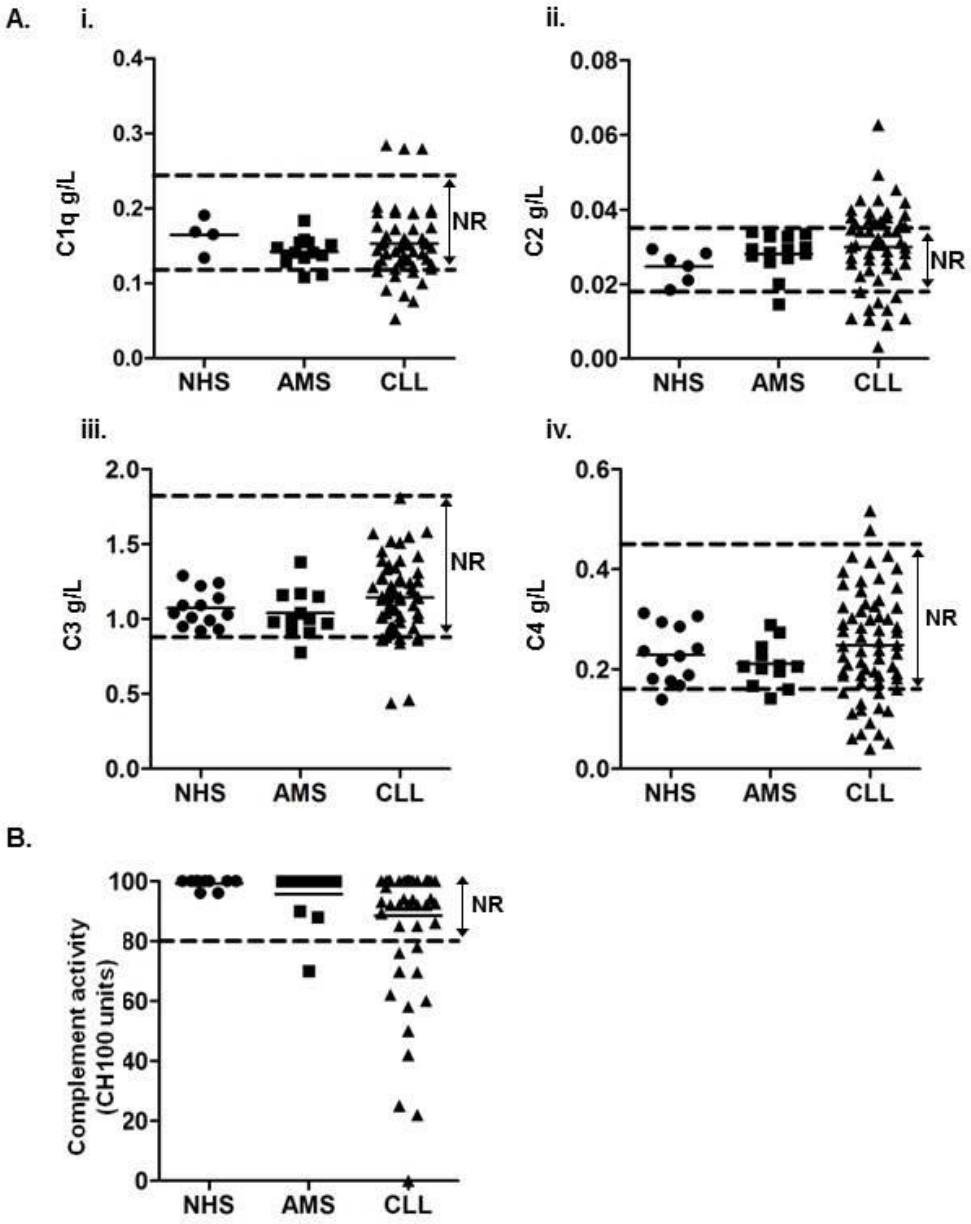

Figure 3.1 CLL patient sera exhibit deficiencies in key components of the classical complement cascade and reduced complement activity

A. The concentrations of complement components of the classical cascade were assessed. Mean of individual patient samples, NHS and AMS controls is shown. NR: Normal Range. i. C1q levels were determined by RID. NR was established from the manufacturer's guidelines (NHS, n=4; AMS, n=12; CLL sera, n=52). ii, C2 levels were determined by RID. NR was established from our AMS controls (NHS, n=6; AMS, n=12; CLL sera, n=57). iii & iv. C3 & C4 concentrations respectively were determined by immunonephelometry performed by the clinical diagnostic laboratory (NHS, n=13; AMS, n=12; CLL sera, n=64). B. Activity of the classical complement cascade was measured using the CH100 assay in CLL sera (n=62), NHS (n=10) and AMS control (n=12). CH100 units were determined against a standard curve following lytic ring measurement produced by serum measured against a calibrator of known activity levels. An unpaired t test revealed no significant difference in the mean complement levels and complement activity when comparing AMS controls with CLL patient sera.

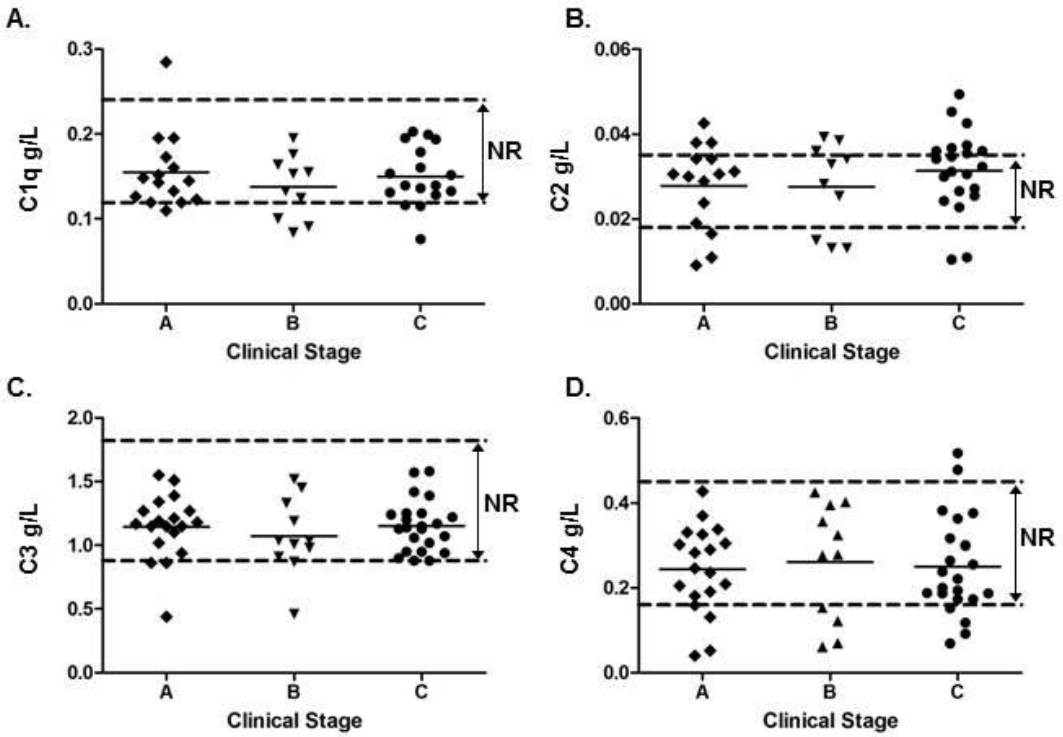

Figure 3.2 Complement concentrations in CLL patient sera are not significantly affected by Binet stage

The concentrations of complement components of the classical cascade were compared against Binet stage of disease at the point of sample collection. Mean of individual patient samples is shown. A. C1q levels compared against clinical stage (n=42). B. C2 levels compared against clinical stage (n=46). C. C3 levels compared against clinical stage (n=53). D. C4 levels compared against clinical stage (n=53). An unpaired t test was performed, with no significant difference observed between the mean complement levels or the level of CLL sera exhaustion and the different clinical stages of disease.

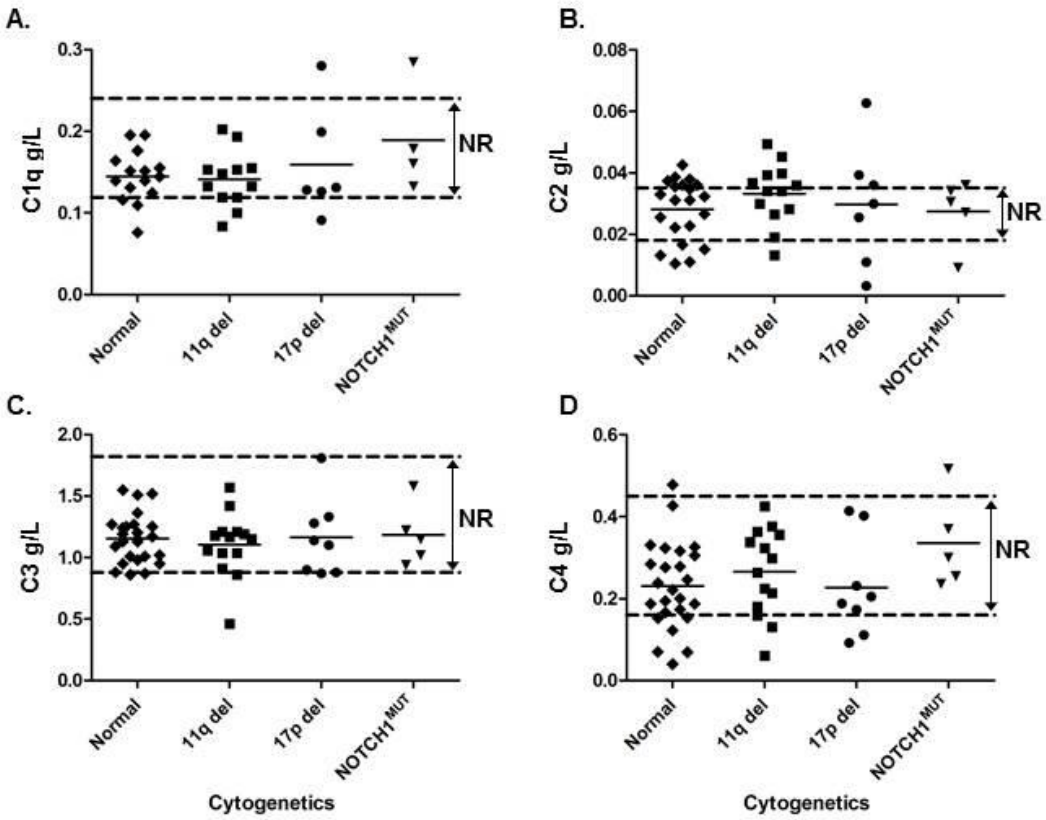

Figure 3.3 Complement concentrations in CLL patient sera are not significantly affected by poor prognosis cytogenetics/mutation

The concentrations of complement components of the classical cascade were compared against the different CLL cytogenetic subgroups normal/13q, 11q del 17p del and NOTCH1^{MUT}. Mean of individual patient samples is shown. A. C1q levels compared against cytogenetic subgroups (n=41). B. C2 levels compared against cytogenetic subgroups (n=46). C. C3 levels compared against cytogenetic subgroups (n=52). D. C4 levels compared against cytogenetic subgroups (n=52). An unpaired t test was performed, with no significant difference observed between the mean complement levels or the level of CLL sera exhaustion and the different cytogenetic subgroups.

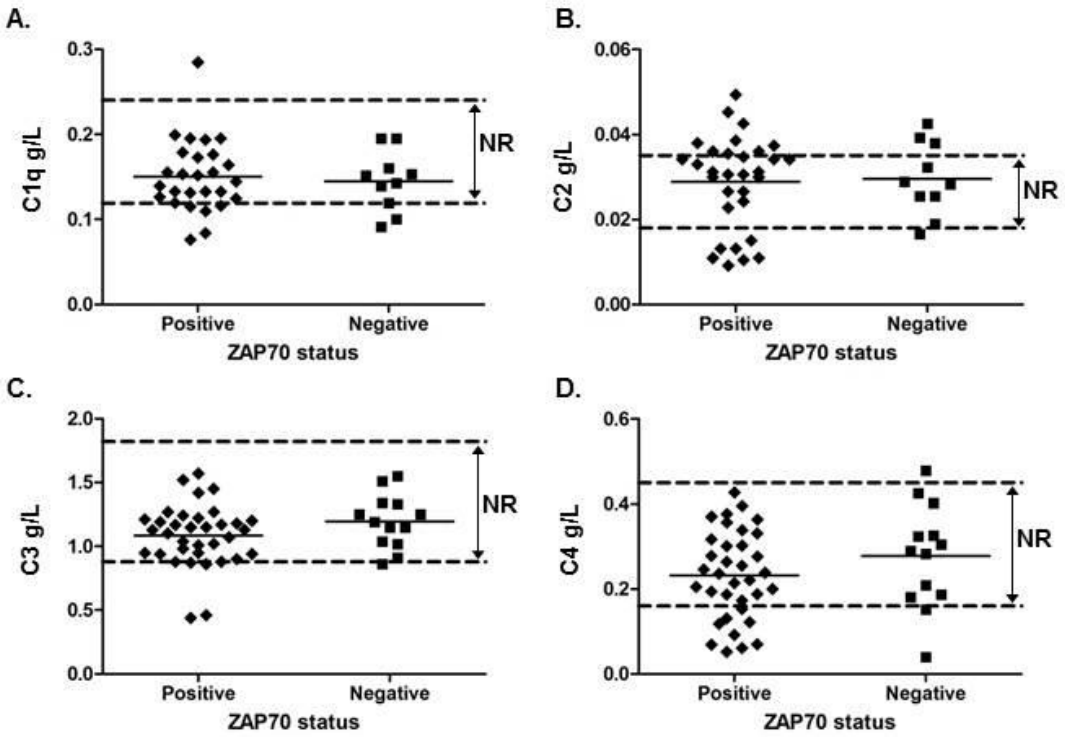

Figure 3.4 Complement concentrations in CLL patient sera are not significantly affected by ZAP-70 status

The concentrations of complement components of the classical cascade were compared against the ZAP-70 status. Mean of individual patient samples is shown. A. C1q levels compared against ZAP-70 status (n=37). B. C2 levels compared against ZAP-70 status (n=41), 25% ZAP-70 positive CLL patients are deficient in C2 compared to 10% that are ZAP-70 negative. C. C3 levels compared against ZAP-70 status (n=48). D. C4 levels compared against ZAP-70 status (n=48). An unpaired t test was performed, with no significant difference observed between the mean complement levels or the level of CLL sera exhaustion and ZAP-70 status.

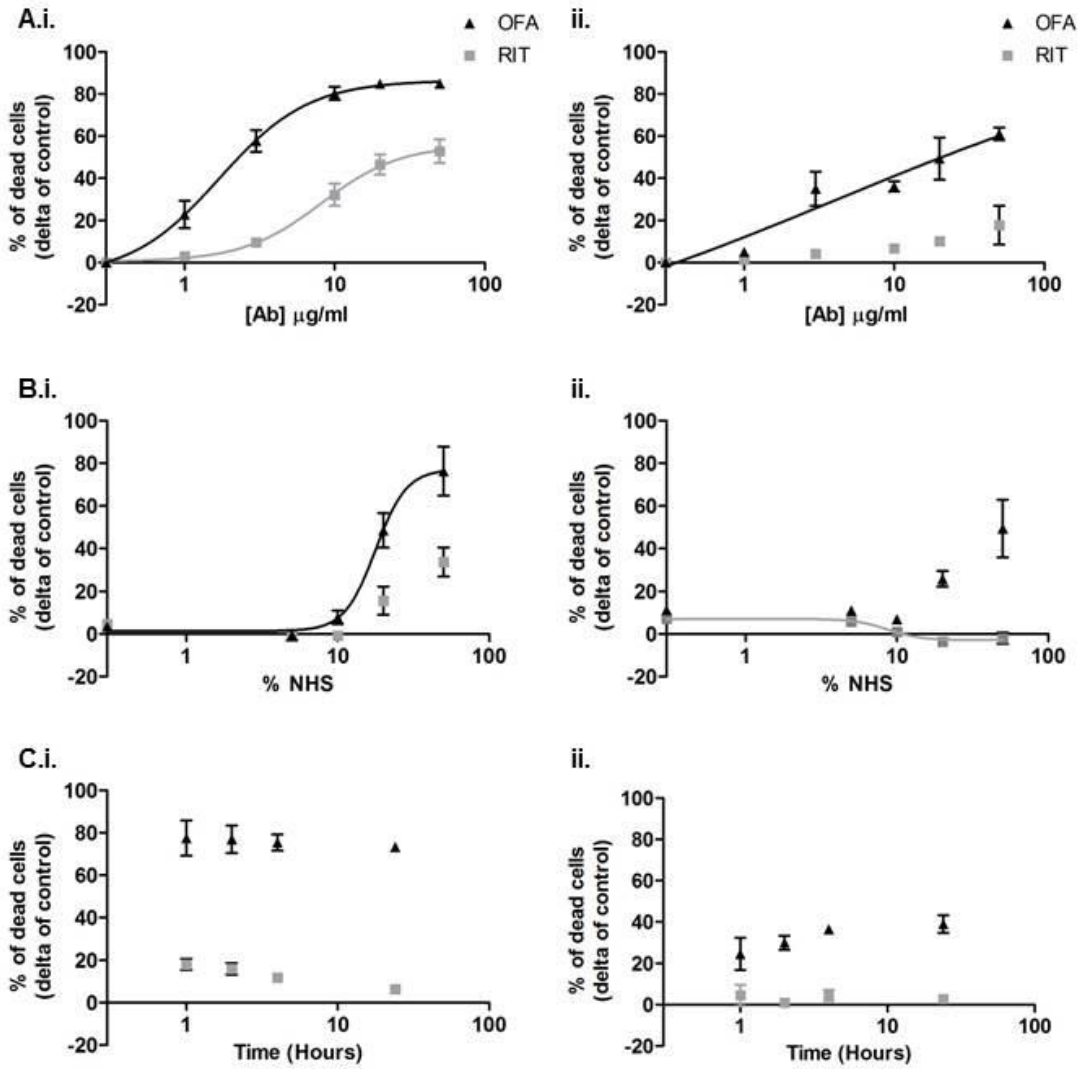

Figure 3.5 Optimisation of experimental conditions using two CLL cell lines

Optimisation of CDC was carried out using two CLL cell lines, HG3 and WAC. 2.5 x 10^6 cells/ml were cultured with different concentrations of MAb and the optimal concentration was then used to determine the % NHS required to produce maximal CDC, once the % NHS was defined the time in which CLL cells incubated with NHS was altered. The level of CDC cell death was measured by flow cytometry (% PI+ cells). The percentage of dead cells is expressed relative to untreated control. A. Varying MAb concentrations with 50% pooled NHS and 2 hr incubation. i. HG3 cell line. ii. WAC cell line. B From these results (A) 20 µg/ml of OFA or RTX was decided as optimal, and cells were then incubated for 2 hr with different percentages of NHS. i. HG3 cell line. ii. WAC cell line. C. From (B) 50% pooled NHS was chosen as optimal and incubation time with NHS was varied between 1 and 24 hr. All experiment conditions were repeated in duplicate and representative data is shown. Each data point has been repeated in triplicate, with mean ± S.D shown.

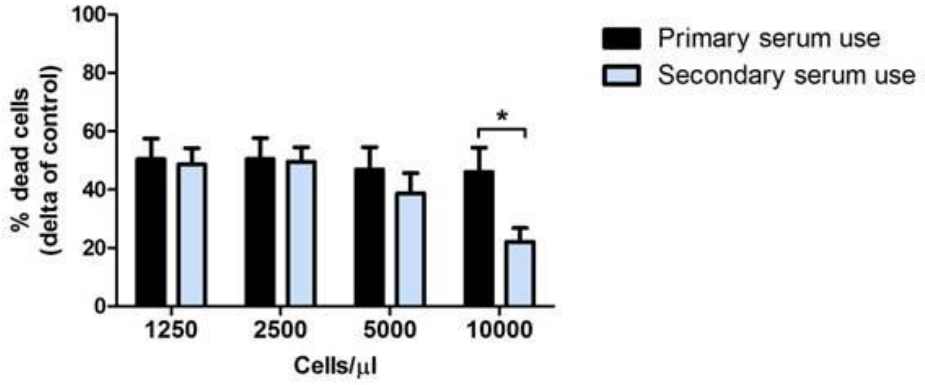

Figure 3.6 Increasing tumour burden results in excessive complement consumption

CLL primary cells (n=4 ± SEM) of different cell densities were treated with 20 µg/ml OFA. Sera were removed and re-challenged with fresh CLL cells of matching cell density treated with 20 µg/ml OFA. CDC was measured at both stages. The level of CDC cell death was measured by flow cytometry (% PI+ cells). p values were determined by a paired t-test (*, $p<0.05$).

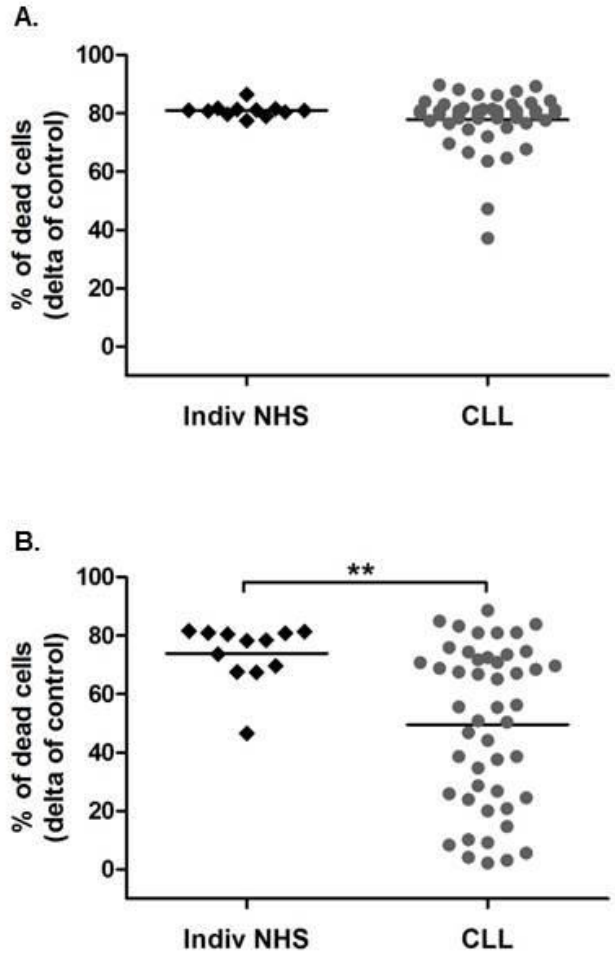

Figure 3.7 CLL patient sera displays reduced CDC activity when used for a second time

HG3 cells were treated with 20 µg/ml OFA and then incubated with 50% CLL patient sera or NHS and the level of CDC cell death measured by flow cytometry (% PI+ cells). The percentage of dead cells is expressed relative to untreated control. A. Induction of CDC from CLL patient sera for the first set of OFA-treated HG3 cells was assessed by PI staining (NHS, n=12; CLL, n=48). Serum that caused ≥40% CDC was used for secondary CDC. B. Sera from the first set of OFA-treated HG3 cells were removed from the cells and used for a second time to determine the CDC activity induced on fresh HG3 cells treated with 20 µg/ml OFA (2° use) (NHS, n=12; CLL, n=48). p values were determined by an unpaired t-test (** $p<0.01$).

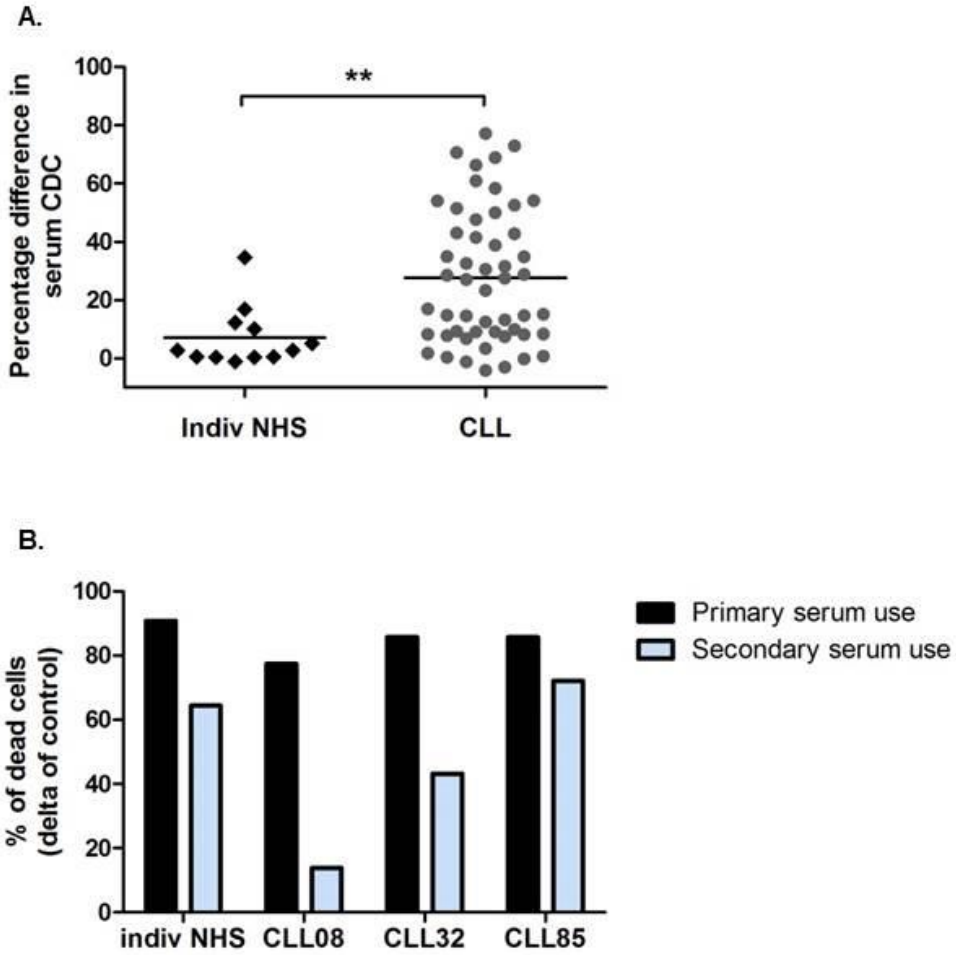

Figure 3.8 CLL patient sera exhausts more readily than NHS

HG3 cells were treated with 20 µg/ml OFA and then incubated with 50% CLL patient sera or NHS and the level of CDC cell death measured by flow cytometry (% PI+ cells). The percentage of dead cells is expressed relative to untreated control. A. CLL serum that caused ≥40% CDC in OFA treated HG3 cells in 1° use, was used again (2° use) and the percentage difference in CDC from 1° to 2° sera use enabled calculation of exhaustion levels (n=52 CLL patient sera vs. n=12 individual NHS). p values were determined by an unpaired t-test (** $p<0.01$). B. After induction of CDC from the first set of OFA-treated HG3 cells (1° use) sera were removed from the cells and used for a second time to determine the CDC activity induced on fresh HG3 cells treated with 20 µg/ml OFA (2° use). Representative data are shown from the sera of 3 CLL patients and NHS control. p values were determined by a paired t-test (*, $p<0.05$).

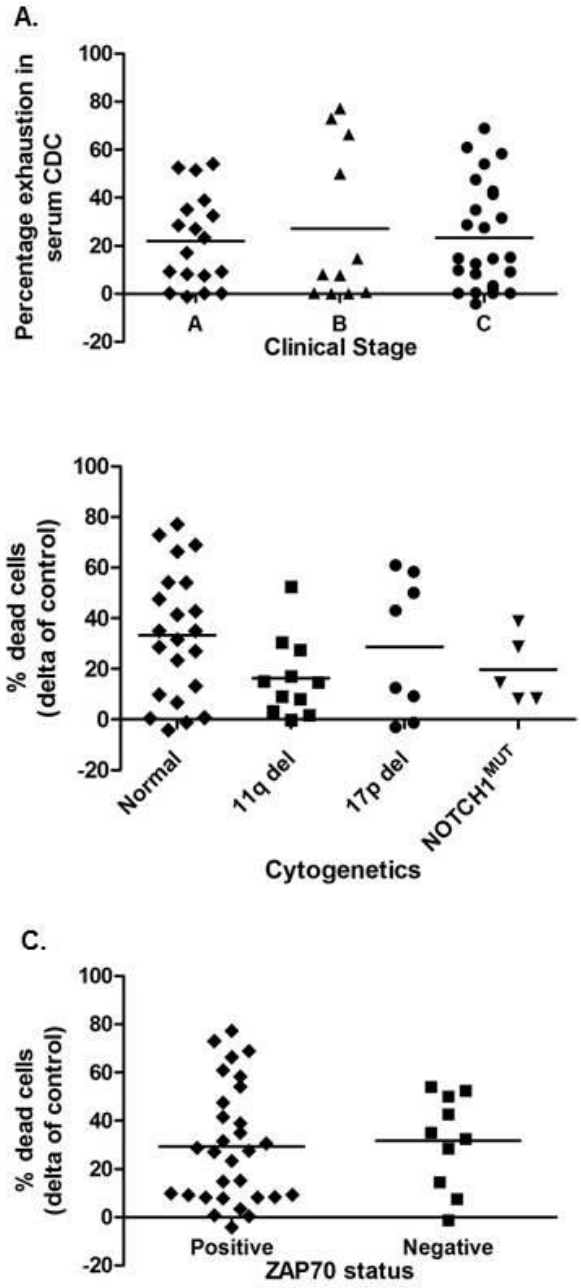

Figure 3.9 Exhaustion levels are not significantly linked with any poor prognostic markers in CLL

CLL patient sera exhaustion levels were compared against different poor prognostic markers. Mean of individual patient samples is shown. A. Binet stage of the disease at the point of sample collection (n=54). B. CLL cytogenetic subgroups normal/13q, 11q del,17p del and NOTCH1^{MUT} (n=46). C. ZAP-70 status (n=40). An unpaired t test was performed, with no significant difference observed between the mean CLL sera exhaustion levels and the different poor prognostic markers.

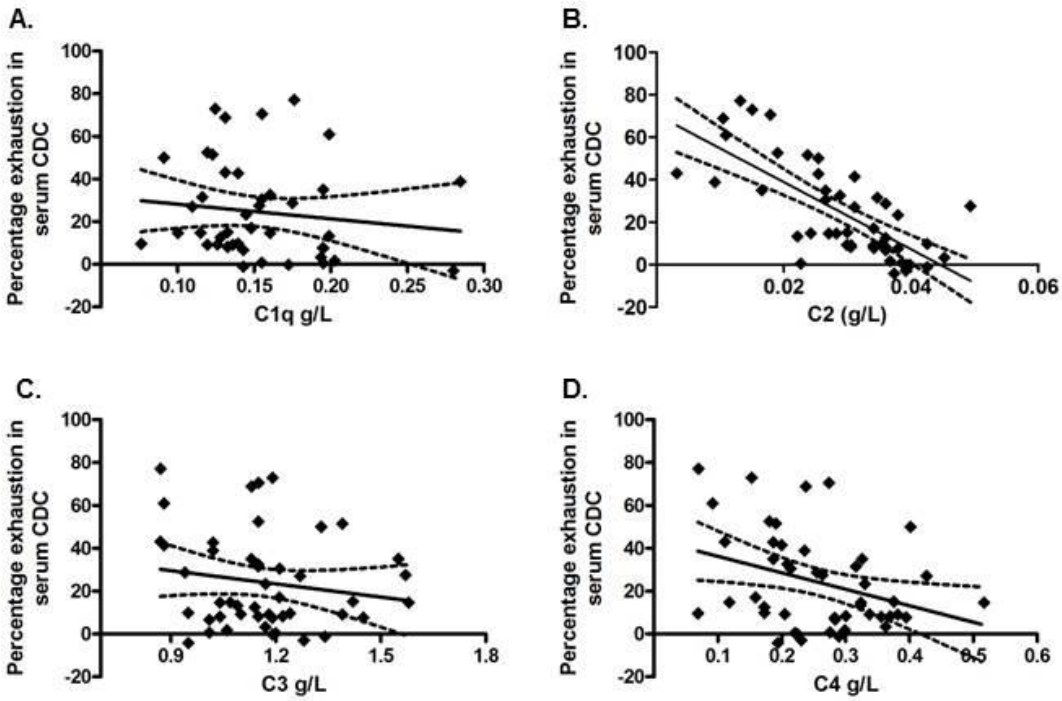

Figure 3.10 Complement C2 levels strongly correlates with CLL sera exhaustion

Complement concentration levels were compared against the levels of CLL sera exhaustion to determine whether one or more complement component displayed the strongest association. A. C1q levels in CLL patient sera were compared against CLL patient sera exhaustion (n=43). Linear regression was applied to obtain values for r^2, 0.01681 and p value, 0.4073. B. C2 levels in CLL patient sera were compared against CLL patient sera exhaustion (n=47). Linear regression was applied to obtain values for r^2, 0.5260 and p value, <0.0001. B. C3 levels in CLL patient sera were compared against CLL patient sera exhaustion (n=47). Linear regression was applied to obtain values for r^2, 0.02727 and p value, 0.2673. C. C4 levels in CLL patient sera were compared against CLL patient sera exhaustion (n=43). Linear regression was applied to obtain values for r^2, 0.1559 and p value, 0.0192.

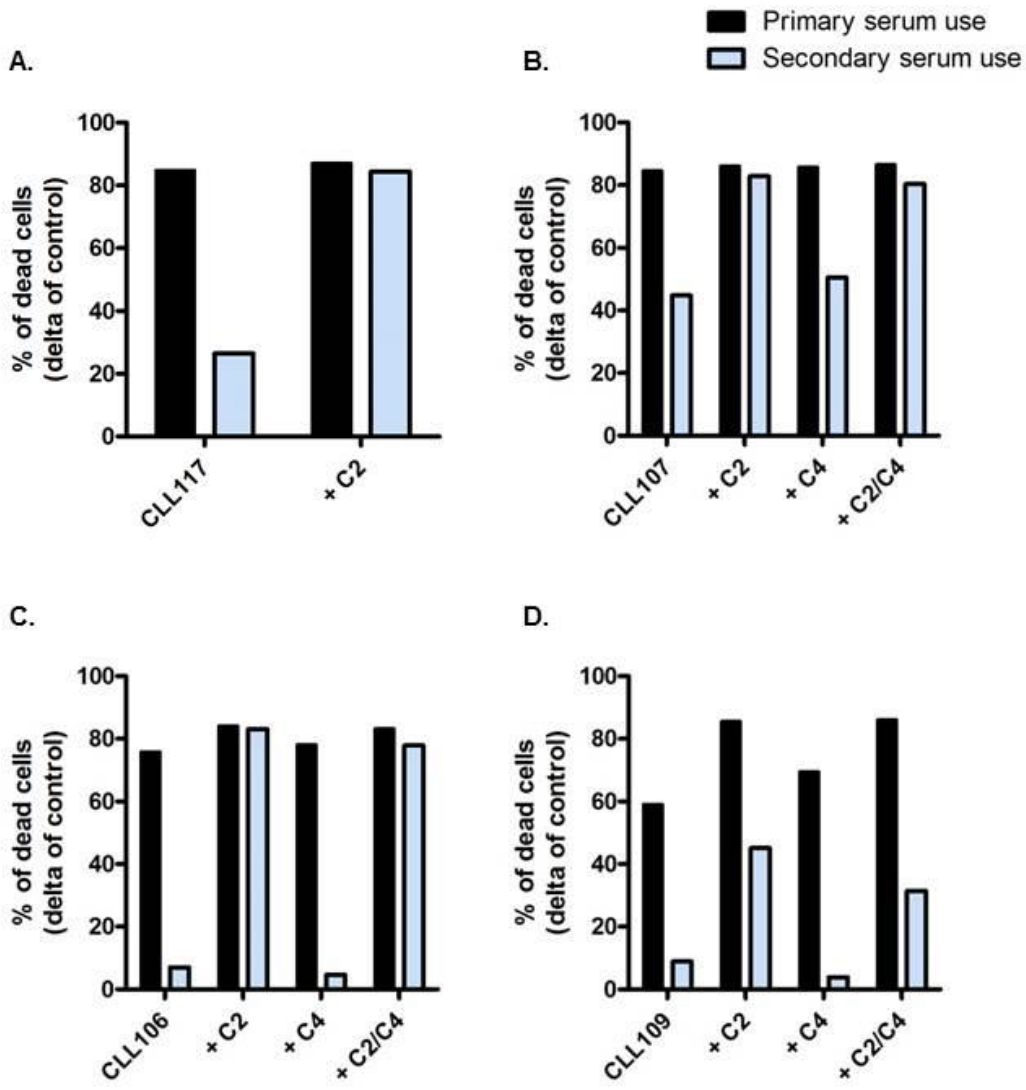

Figure 3.11 CLL sera exhaustion in complement deficient serum can be restored with the addition of complement components

CLL sera that had complement deficiencies in C2, C3 and/or C4 were supplemented with C2 (50 µg/ml), C4 (700 µg/ml) or both C2/C4 (25 µg/ml/350 µg/ml respectively), before being used to induce CDC in HG3 cells treated with 20 µg/ml OFA (1° use). After the incubation period, sera was removed and re-challenged with HG3 cells treated with 20 µg/ml OFA (2° use). Percentage of dead cells is relative to untreated control. A. Representative CLL patient serum sample deficient in C2 alone. B. Representative CLL patient serum sample deficient in C4 alone. C. Representative CLL patient serum sample deficient in C2 and C4.

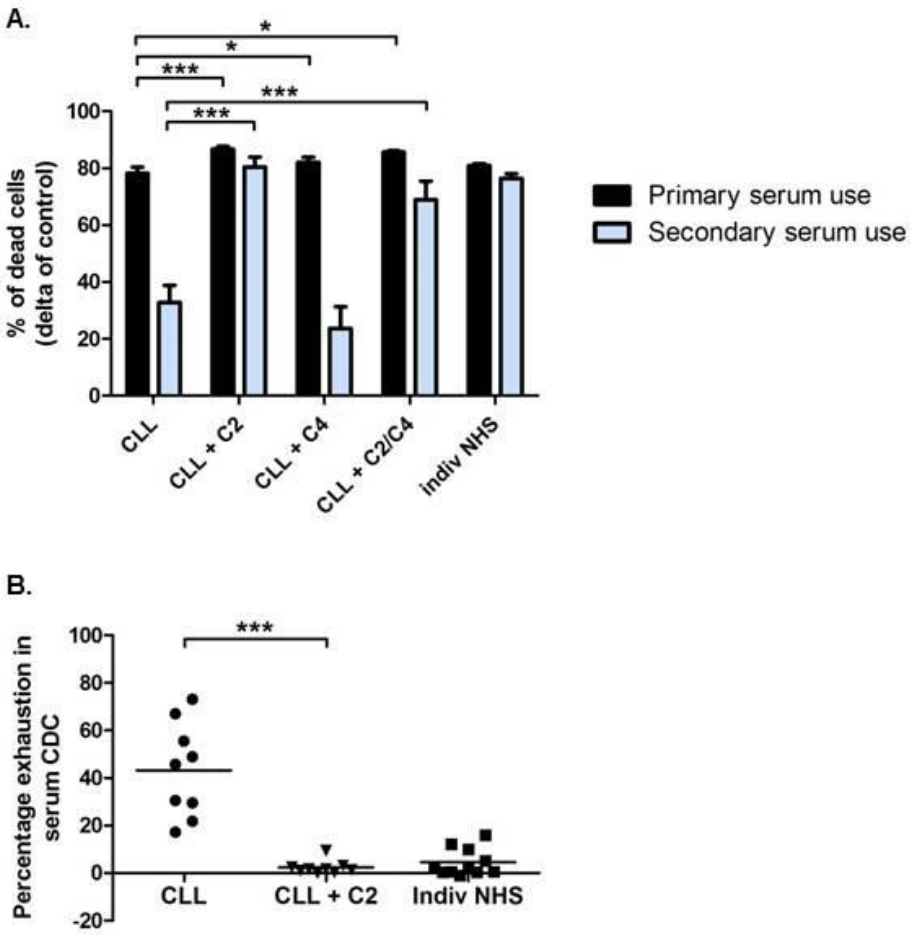

Figure 3.12 CDC activity in complement deficient serum can be restored with the addition of C2 alone

CLL sera that exhibited high levels of serum exhaustion was supplemented with C2 (50 µg/ml), C4 (700 µg/ml) or both C2/C4 (25 µg/ml/350 µg/ml respectively), before being used to induce CDC in HG3 cells treated with 20 µg/ml OFA (1° use). After the incubation period, sera was removed and re-challenged with HG3 cells treated with 20 µg/ml OFA (2° use). Percentage of dead cells is relative to untreated control. A. CLL sera (n=16) were supplemented with C2 (n=14), C4 (n=9), C2 and C4 combined (n=8). Mean cell death $\pm$ SEM are shown. p value were obtained by paired t test (* $p<0.05$, ** $p<0.01$, *** $p<0.001$). B. CLL sera were supplemented with C2 alone. Analysis is shown for the percentage change in CDC from the 1° to 2° use. p value was obtained from a paired t-test (*** $p<0.001$).

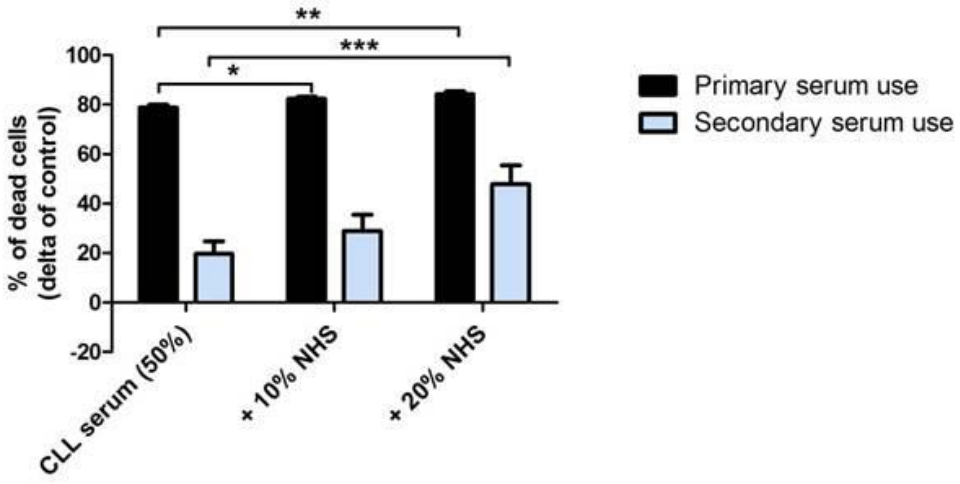

Figure 3.13 The addition of NHS to CLL sera significantly abrogates serum exhaustion

CLL sera that exhibited high levels of serum exhaustion was supplemented with 10 or 20% NHS (n=9 ± SEM), before being used to induce CDC in HG3 cells treated with 20 µg/ml OFA (1° use). After the incubation period, sera was removed and re-challenged with HG3 cells treated with 20 µg/ml OFA (2° use). Percentage of dead cells is relative to untreated control. p value was obtained from paired t test. (* $p<0.05$; ** $p<0.01$; *** $p<0.001$). Percentage of dead cells is relative to untreated control.

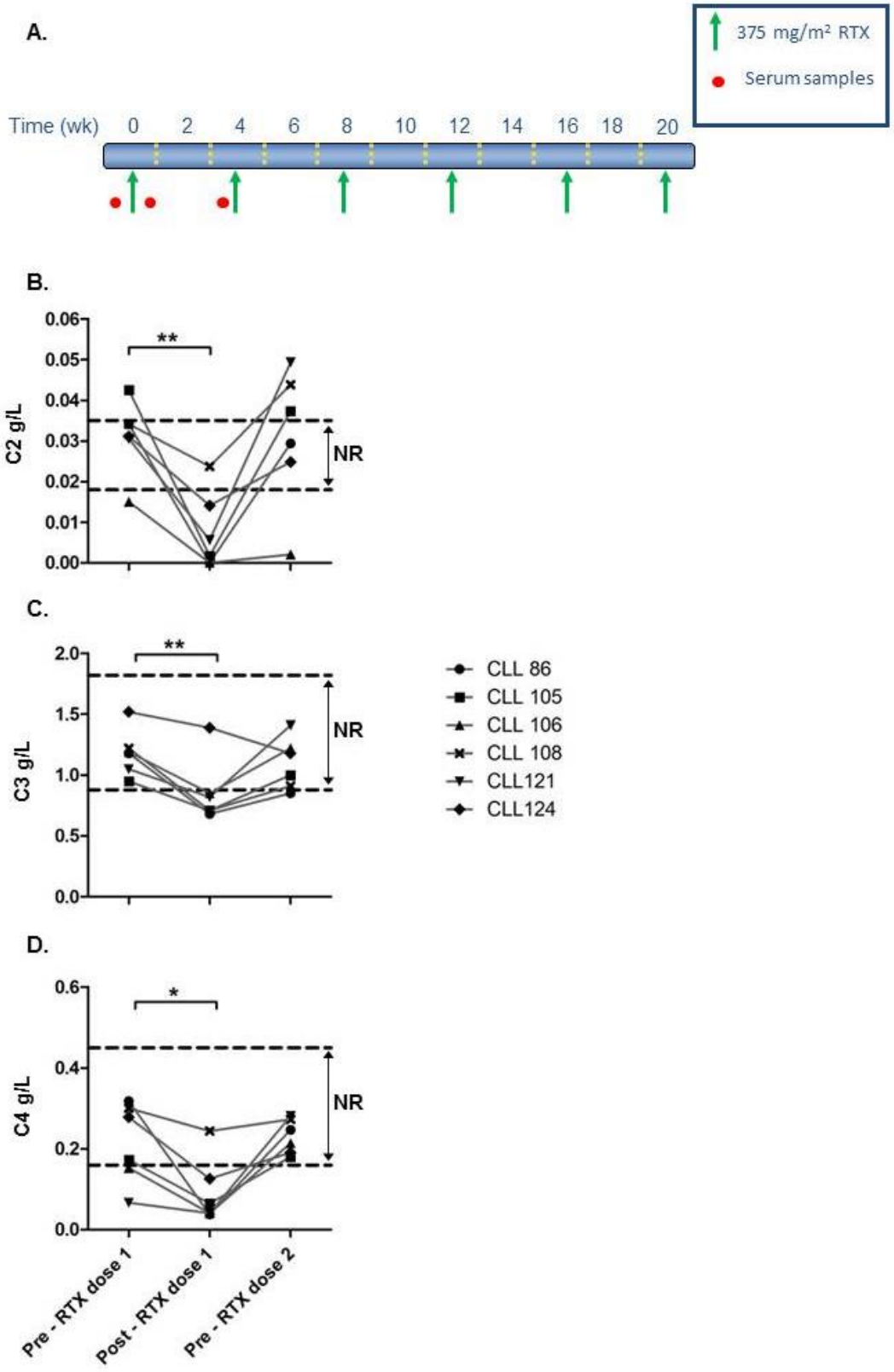

Figure 3.14 Complement levels are exhausted *in vivo* following RTX immunotherapy

A. RTX dosing schedule and serum sample collection points. B-D. Concentrations of complement levels from sera samples collected from CLL patients undergoing RTX immunotherapy (concentration shown in Table 3.1; n=6). Sera were collected prior to RTX therapy (pre – RTX dose 1), 24 hr after treatment (post – RTX dose 1) and prior to the second dose of RTX, 28 days after dose 1 (pre – RTX dose 2). A. C2 levels were determined by RID. B. & C. C3 & C4 concentrations were determined by immunonephelometry. p value was obtained from paired t test (* $p<0.05$; ** $p<0.01$).

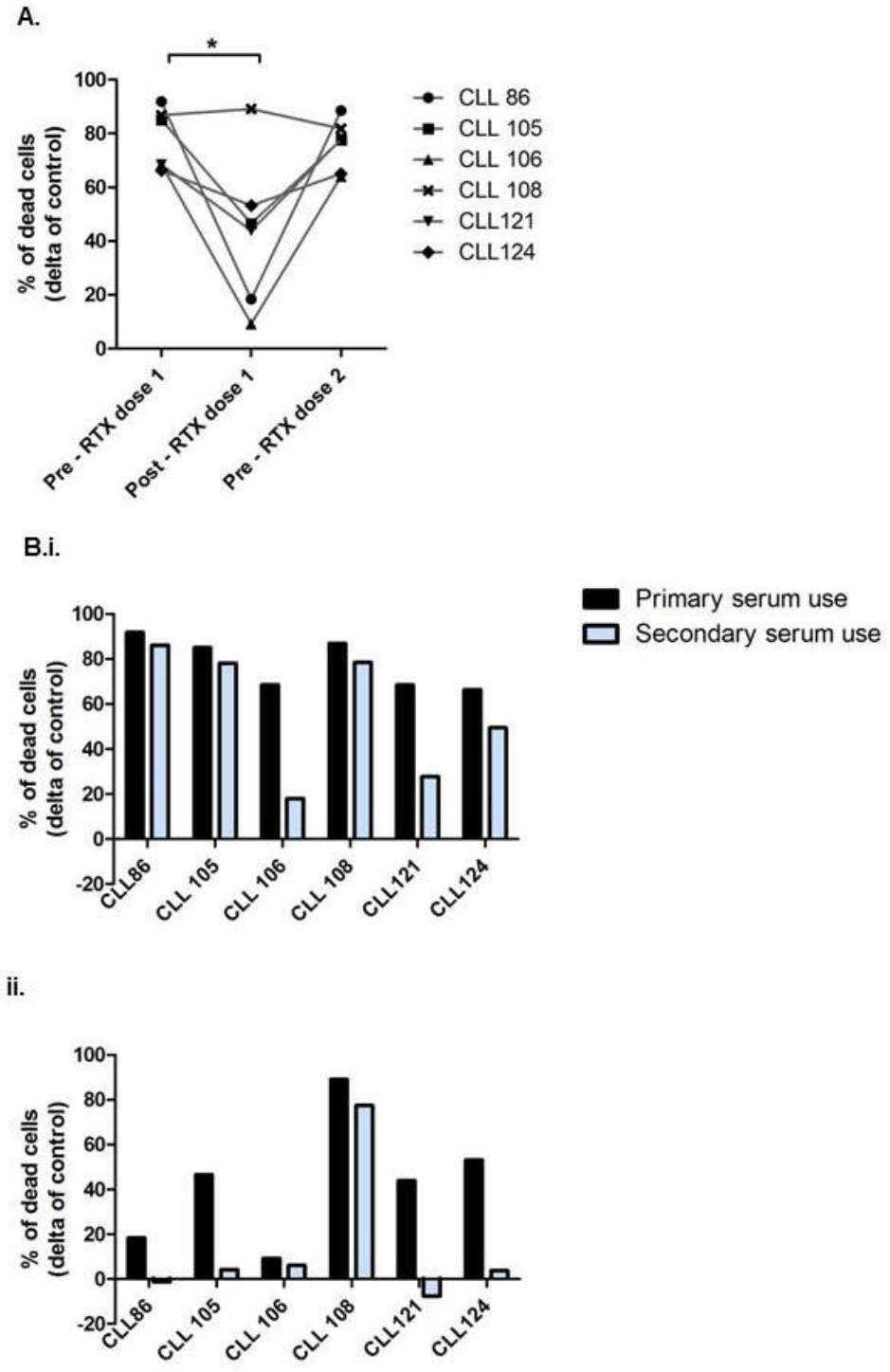

Figure 3.15 CDC activity is exhausted *in vivo* following RTX immunotherapy

CDC activity of sera from CLL patients undergoing RTX immunotherapy (concentration shown in Table 3.1; n=6). Sera were collected prior to RTX therapy (pre – RTX dose 1), 24 hr after treatment (post – RTX dose 1) and prior to the second dose of RTX, 28 days after dose 1 (pre – RTX dose 2). A. CDC was measured on HG3 cells treated with 20 µg/ml OFA in 50% CLL sera. p value was obtained from paired t test (* $p<0.05$; ** $p<0.01$). B. Exhaustion was measured in sera collected i, prior to RTX therapy and ii, post – RTX dose 1. After induction of CDC from the first set of OFA treated HG3 cells (1° use) sera were removed from the cells and re-challenged with HG3 cells treated with 20 µg/ml OFA and CDC measured (2° use). Percentage of dead cells is relative to untreated control.

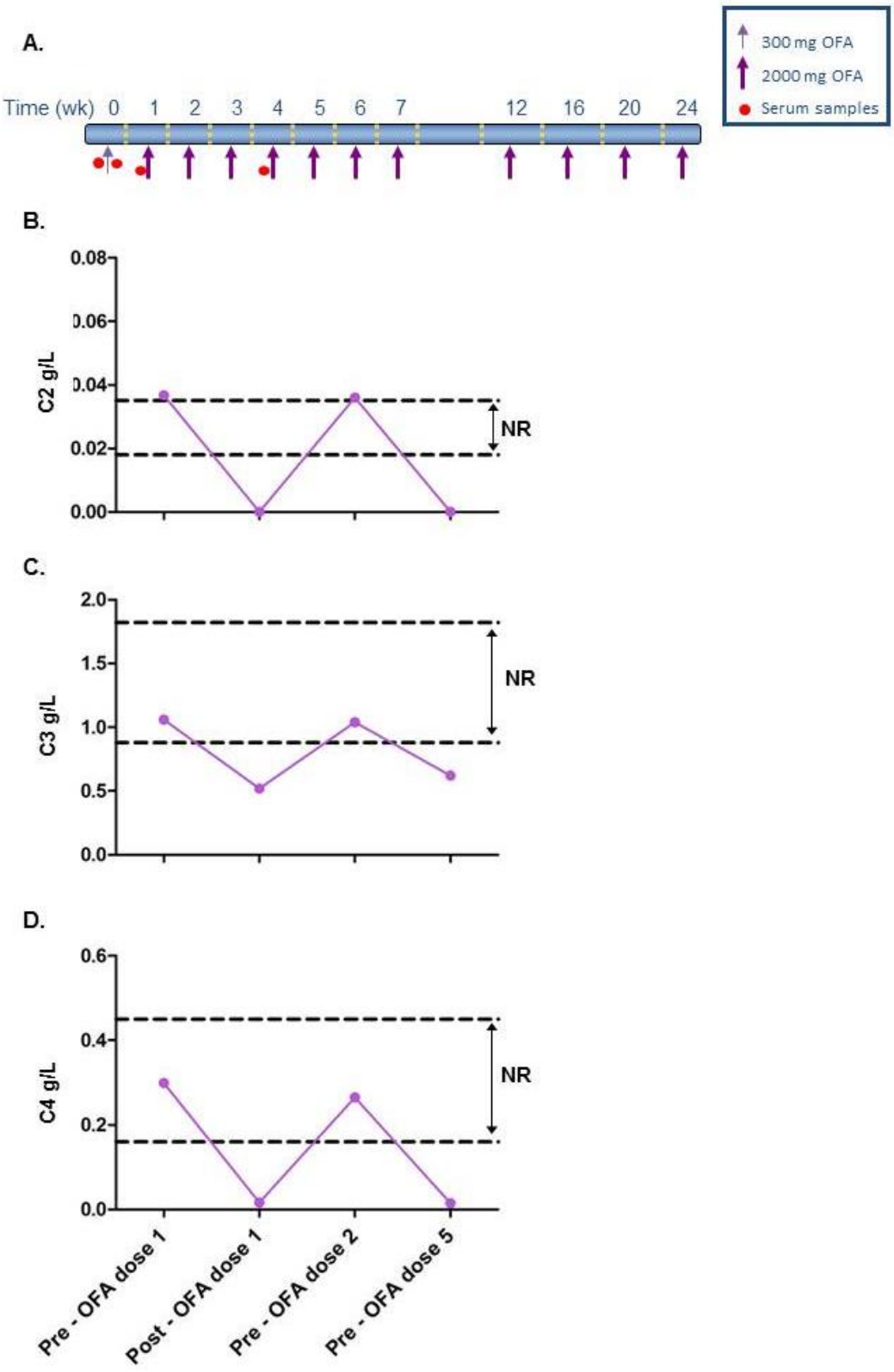

Figure 3.16 Complement levels are exhausted *in vivo* following OFA immunotherapy

A. OFA dosing schedule and serum sample collection points B-D. Concentrations of complement levels from sera collected from one CLL patient (CLL111) undergoing OFA immunotherapy. Sera were collected prior to OFA therapy (pre – OFA dose 1), 24 hr after treatment (post – OFA dose 1), prior to the second dose of OFA, 7 days after dose 1 (pre – OFA dose 2) and 7 days after the fourth dose of OFA (Pre-OFA dose 5). A. C2 levels were determined by RID. B. & C. C3 & C4 concentrations were determined by immunonephelometry.

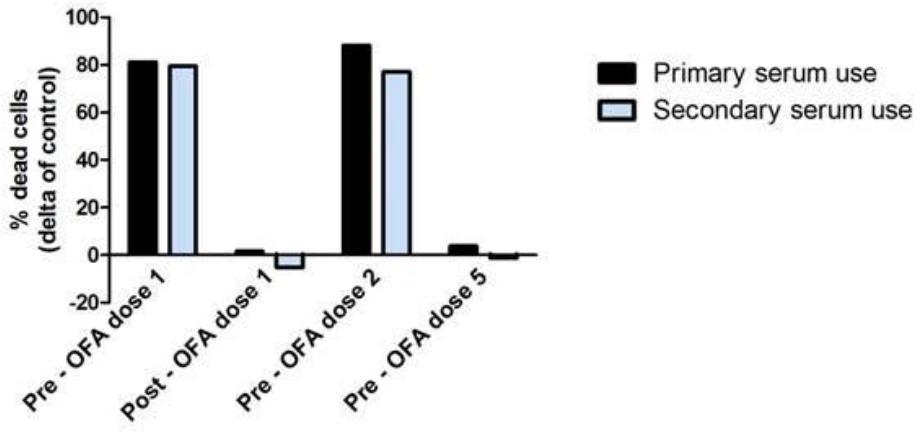

Figure 3.17 CDC activity is exhausted *in vivo* following OFA immunotherapy

CDC activity of sera from one CLL patient (CLL111) undergoing OFA immunotherapy. Sera were collected prior to OFA therapy (pre – OFA dose 1), 24 hr after treatment (post – OFA dose 1), prior to the second dose of OFA, 7 days after dose 1 (pre – OFA dose 2) and 7 days after the fourth dose of OFA (pre-OFA dose 5). Exhaustion was measured in sera collected at each time point, after induction of CDC from the first set of OFA treated HG3 cells (1° use) sera were removed from the cells and re-challenged with HG3 cells treated with 20 µg/ml OFA and CDC measured (2° use). Percentage of dead cells is relative to untreated control.

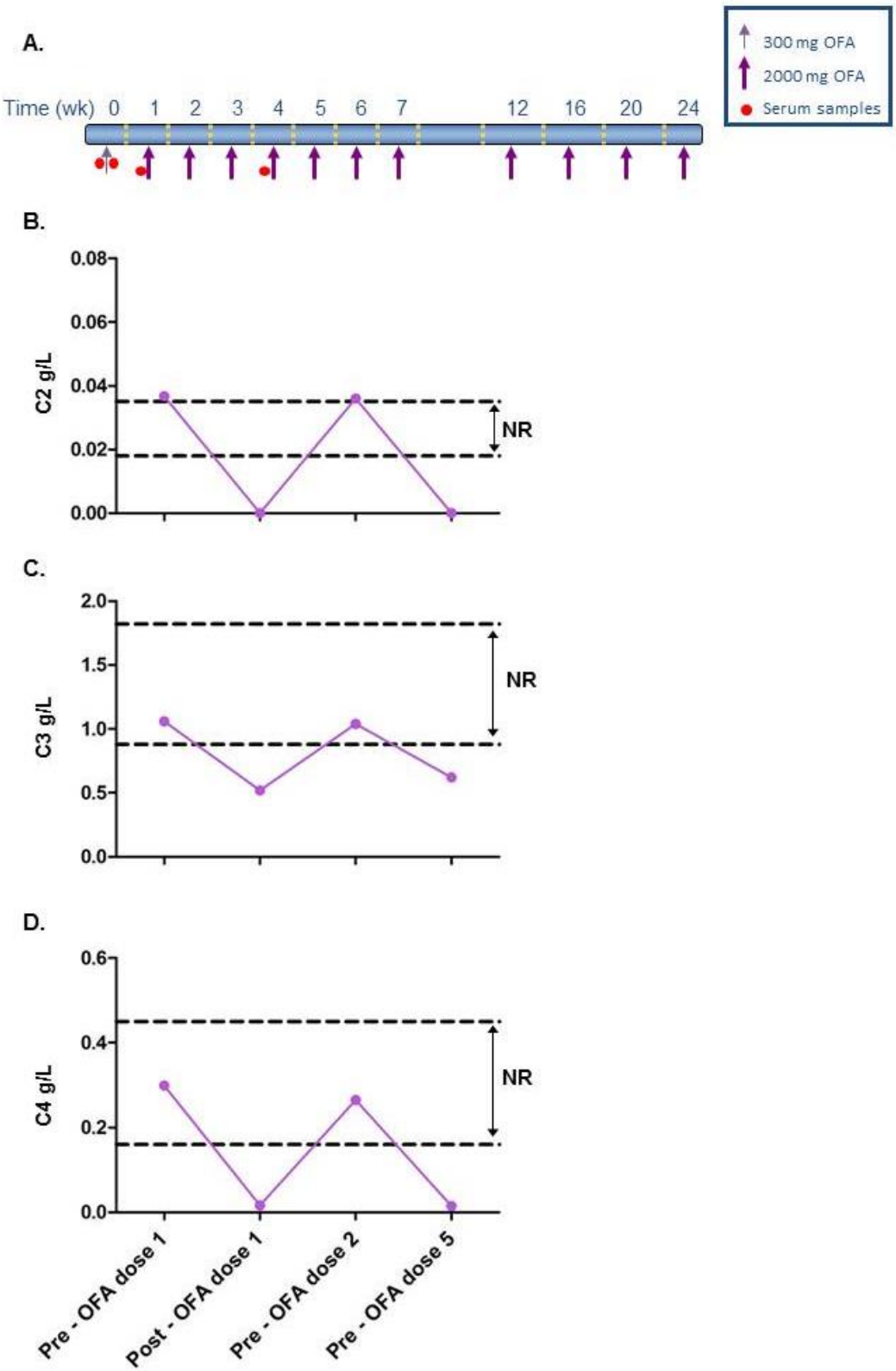

Figure 3.18 Complement levels are reduced *in vivo* following OFA immunotherapy

A. OFA dosing schedule and serum sample collection points. B-D. Concentrations of complement levels from sera collected from one CLL patient (CLL127) undergoing OFA immunotherapy. Sera were collected prior to OFA therapy (pre – OFA dose 1), prior to the second dose of OFA, 7 days after dose 1 (pre – OFA dose 2), 7 days after dose 2 (Pre-OFA dose 3), 7 days after dose 3 (pre-OFA dose 4) and 7 days after the sixth dose of OFA (pre-OFA dose 7). A. C2 levels were determined by RID. B. & C. C3 & C4 concentrations were determined by immunonephelometry.

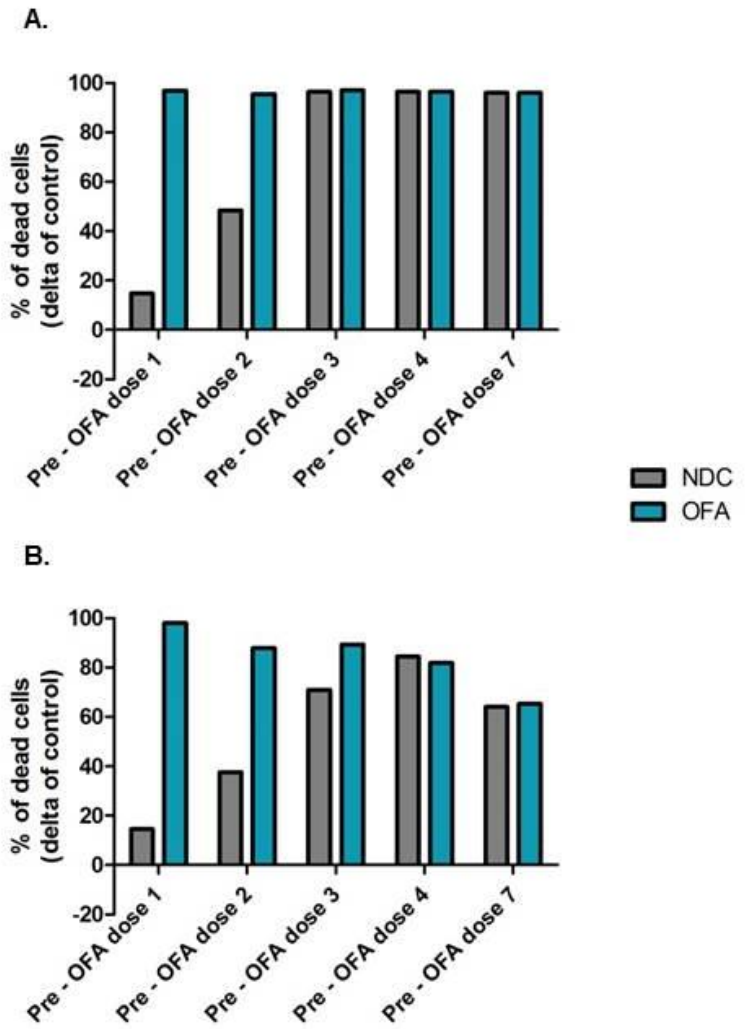

Figure 3.19 OFA is stable within peripheral blood for up to 7 days in vivo following OFA immunotherapy

CDC activity of sera from one CLL patient (CLL127) undergoing OFA immunotherapy. Sera were collected prior to OFA therapy (pre – OFA dose 1), prior to the second dose of OFA, 7 days after dose 1 (pre – OFA dose 2), 7 days after dose 2 (Pre-OFA dose 3), 7 days after dose 3 (pre- OFA dose 4) and 7 days after the sixth dose of OFA (pre-OFA dose 7). Exhaustion was measured in sera collected at each time point. A. CDC induction from the first set of OFA treated HG3 cells (1° use). B After the induction of CDC from the 1° use sera were removed from the cells and re-challenged with HG3 cells treated with 20 µg/ml OFA and CDC measured (2° use).

4 Anti-CD20 MAb activity on CLL cells

4.1 Introduction

As described in the previous chapter MAbs exert anti-tumour activity via harnessing the body's own natural immune response especially ADCC involving the recruitment of NK cells to cause phagocytosis and CDC requiring the activation of the classical complement pathway, and/or apoptosis[284]. RTX and OFA are Type 1 MAbs which exert anti-tumour activity mainly through ADCC and CDC induction and rarely through apoptosis. Therefore the focus of this chapter is to assess CDC and ADCC induction in CLL cells following RTX and OFA treatment.

4.1.1 Surface expression markers and anti-CD20 MAb activity

Research has shown that RTX induced CDC is greatly hindered by low CD20 expression levels and high expression of complement inhibitory proteins CD55 and CD59, which aid CLL cells resistance to RTX mediated killing. CD55 and CD59 both prevent uncontrolled complement activation[311,319,350]. CD55 acts to accelerate the decay of C3 convertase, whereas CD59 inhibits the formation of the MAC pore thus preventing cell lysis by CDC[306]. However, in the case of RTX, the most important determinant in inducing CDC is the expression levels of CD20[310,311]. In CLL patients that had low CD20 expression levels, CDC induction by RTX was improved with the use of inhibitor molecules against one or both of these proteins[310,311]. Further research has also suggested that OFA is less dependent on these inhibitory proteins and is more effective at inducing CDC at lower CD20 levels. This is important as CLL cells are known to express lower levels of CD20 than other B-cell malignancies[254,255,315,344,351,352]. CD52 glycoprotein is the target for alemtuzumab MAb. CD52 displays high expression on both B and T cells, there are thought to be around 500,000 CD52 molecules/cell, encompassing 5% of the cells surface[353]. The physiological function of CD52 is relatively unknown, however it is thought to function in T cell activation, cell to cell adhesion and signal transduction[353]. CD55 and CD59 both possess GPI tails, CD52 is also anchored to the cellular membrane through the GPI tail[354]. One research group postulated that it may also function as a complement inhibitor[354]. When they created RTX resistant cell lines from Raji

and RL cells, it was found that CD52 expression was up-regulated. Complete inhibition of CD52 resulted in partial rescue of RTX CDC sensitivity in these cell lines[354]. Therefore although CD52 does not appear to be a potent complement inhibitory protein it may function in conjunction with CD55 and CD59 expression to increase OFA/RTX related resistance. Although substantial research has been carried out to determine the effect of these surface proteins on RTX activity little is known about the effect they have on OFA activity in CLL.

Well documented cytogenetic aberrations such as 17p (targeting *TP53*) and 11q (targeting *ATM)* deletions have long provided a difficult paradigm for the treatment of CLL. ATM is a key component of the DNA damage response pathway and p53 is a critical component for driving apoptosis in the presence of DNA damage[83]. Chemotherapeutic agents such as alkylating agents and purine analogues rely upon this pathway for their clinical efficacy[246,248]. Therefore it is not surprising that 17p del CLL displays aggressive clinical course with limited therapeutic options. Alemtuzumab is most commonly used for CLL patients with either a *TP53* mutation and/or refractory to fludarabine based treatment[86,354,355]. Recent identifications of novel genetic mutations are also shedding light upon chemotherapy resistance not contributable to 17p del. *BIRC3* mutations for instance are extensively observed within CLL patients relapsed refractory to fludarabine whom are p53 wild-type[113].

Emerging data is now contributing NOTCH1^{MUT} with resistance against type I anti-CD20 MAbs. NOTCH1^{MUT} were recently identified as an independent poor prognostic marker for CLL patients, present in approximately 10-12% of CLL cases[96]. The majority of mutations, 80%, are generated from a 2 base pair frameshift deletion c.7544_7545delCT, resulting in a truncated protein lacking the C-terminal PEST domain[98]. This mutation results in Notch1 escaping ubiquitination leading to an accumulation of active Notch1 in the nucleus. Active Notch1 in the nucleus is known to result in deregulated activation of various different cellular pathways, especially those involved in cell cycle and cell survival such as NF-κB1 and MYC[210,217].

A retrospective study of the CLL8 trial identified the patients within the trial which had NOTCH1^{MUT}, and then determined how this predicted their response to FC vs FCR treatment. From these data it was determined that there was no

advantage to combining RTX with FC treatment, similar to results obtained from the 17p deleted cohort[108]. Interestingly, research presented from a trial investigating the effect of chlorambucil with or without OFA on PFS, observed an improvement in PFS with chlorambucil plus OFA in NOTCH1^{MUT}. However this response only occurred during the first 18 months, after which the affect was lost and PFS followed patients treated with chlorambucil alone in the NOTCH1^{MUT} cohort[109]. Although the initial response was lost, it is important to identify why the NOTCH1^{MUT} patients respond briefly to OFA treatment and not RTX. Especially since other poor prognostic cytogenetics such as 11q del respond well to this type of treatment[346].

4.2 Aim

The main focus was to investigate anti-CD20 MAb activity in poor prognosis NOTCH1^{MUT} CLL patient cells. In order to do this the differences in CDC and ADCC activation in CLL cells between RTX and OFA was characterised, and analysis of surface protein expression markers CD20, CD52, CD55 and CD59 linked to anti-CD20 MAb activity was performed. Key aims:

- Distinguish surface protein expression levels between normal healthy B-cells and CLL cells and the different cytogenetic sub-groups;
- Determine whether OFA displays significantly improved CDC compared to RTX in all the different CLL cytogenetic sub-groups;
    - If so are CDC levels limited by CD20, CD52, CD55 and CD59 expression levels?
- Establish ADCC induction levels in NOTCH1^{MUT} CLL cells and if induction is lower than in the other cytogenetic groups.

4.3 Results

4.3.1 Identification of NOTCH1^{MUT} CLL patients

FISH analysis was performed on CLL patients at the point of diagnosis by the regional haematology laboratory, to determine whether patients harboured 11q del or 17p del. Identification of NOTCH1^{MUT} was carried out in the laboratory using ARMS PCR screening. Of the 89 patients screened by ARMS PCR (Figure 4.1) *NOTCH1* mutations were identified in 8.0% of our CLL patients that had no 11q or 17p de. Surprisingly we also identified a small cohort of CLL patients harboured both 17p del and NOTCH1^{MUT} (3.3%). This assay is sensitive enough to detect the mutation allele if present in at least 10% of the clonal population; we detected samples that had a stronger band present in the wild type allele, and a faint band for the mutant allele (CLL122; Figure 4.1). These samples were excluded from further analysis. Cytogenetically normal CLL cells were classified as CLL cells with no detectable 17p or 11q del or NOTCH1^{MUT}.

4.3.2 Surface expression levels for specific proteins differ between healthy B-cells and CLL cells

We next investigated how surface protein expression levels of CD20, CD52, CD55 and CD59 differ between CLL cells and those from healthy B-cells (n=10). Protein expression levels were determined by mean fluorescent intensity (MFI) ratio (MFI stained cells / MFI unstained cells). CD20 expression levels show the most marked difference in expression between B cells and CLL cells (Figure 4.2A), with healthy B cells having approximately 30 fold higher expression of CD20 compared with CLL cells. It is widely known that CLL cells have reduced CD20 expression levels compared to other B cell malignancies such as non-Hodgkins lymphomas. These results further highlight the low levels of CD20 expression and the importance of antibody binding affinity and its proximity to the cell surface when considering anti-CD20 MAb treatment in CLL[254,311]. As observed with CD20 expression, levels of CD52, another protein targeted frequently in the treatment of CLL patients, also had significantly less expression, with around 3 fold less observed in CLL cells compared to healthy B cells (Figure 4.2B). This finding implies that the MAbs used in CLL will also target any healthy B cells present in CLL patients. Interestingly comparing expression levels of the two complement inhibitory proteins CD55 and CD59, expression was variable with CD55 having an

approximate 2 fold higher expression in CLL cells than B cells, while there was little difference between the two populations for CD59 expression (Figure 4.2C&D). Higher expression levels of CD55 may act to further inhibit the classical complement pathway making CLL cells less susceptible to CDC induction by MAbs.

4.3.3 Different cytogenetic sub-groups de-regulate surface protein expression

To further characterise CD20, CD52, CD55 and CD59 expression in our CLL patient cohort we separated the CLL samples based on cytogenetic status. Interestingly when we compared CD20 expression levels, CLL cells with no reported cytogenetic abnormalities or those with 11q del had the highest expression levels, and 17p del had significantly lower expression of CD20 (Figure 4.3A). Similar to other reports[356], we also found NOTCH1^{MUT} CLL patients to have lower expression levels of CD20, having on average 30% lower expression levels than cytogenetically normal CLL cells. Although with a larger NOTCH1^{MUT} patient cohort this may become statistically significant. Our findings demonstrate that although NOTCH1^{MUT} patients do have lower CD20 expression levels this is unlikely to be the only contributing factor leading to their reduced CDC activity with anti-CD20 MAb's. 17p del patients also express lower CD20 expression levels and reports have shown that these patients still show slight improvement in PFS and OS when RTX is added to FC, albeit not to the extent observed with 11q del or cytogenetically normal CLL patients[108,346]. When we compared CD52 expression levels, CLL samples with no cytogenetic abnormalities exhibited the highest expression levels, whilst 11q del CLL cells had the lowest expression levels observed with approximately 40% lower expression than normal CLL cells ($p=0.0795$), which may be a contributing factor to the effectiveness of RTX treatment in 11q del patients[346]. CD55 expression was relatively similar between the different cytogenetic groups with NOTCH1^{MUT} having slightly higher expression than the other cytogenetic groups, (Figure 4.3C) and CD59 displayed no difference between the cytogenetic groups (Figure 4.3D).

4.3.4 OFA displays significantly higher efficacy at inducing CDC in all cytogenetic sub-groups

CDC was induced for both OFA and RTX in CLL cells from all of the different cytogenetic groups, on average the level of CDC observed with RTX was low at 0.93%, whereas OFA produced significantly more CDC with a mean of 23.13% (Figure 4.4). When we compare the level of CDC produced by OFA between the different prognostic groups we observe that NOTCH1^{MUT} CLL cells produced the lowest levels of CDC, with CDC levels being nearly half that of cytogenetically normal CLL cells (Figure 4.5). These findings are in line with a previous report which also showed that NOTCH1^{MUT} CLL cells exhibited less CDC in response to MAb[233]. Although there are no statistically significant differences between the groups in our study, this is likely due to the small sample size; a larger cohort is required to determine if these findings are statistically significant.

4.3.5 OFA CDC levels display a positive linear correlation with CD20 expression levels only

Next we determined if there was any correlation between CD surface proteins levels and the level of OFA induced CDC. Firstly CD20 MFI ratio was plotted against OFA CDC levels, this showed a strong positive correlation between CDC levels and CD20 expression levels (r^2= 0.4506; p= <0.001) (Figure 4.6A). Analysing these data by the different cytogenetic groups demonstrated that cytogenetically normal CLL cells displayed a significant correlation with CD20 expression levels (r^2= 0.6898; p= 0.01). While 11q and 17p del patients displayed a positive linear correlation, this was not statistically significant, although the results are close to being so (r^2= 0.4342; p= 0.11 and r^2= 0.4881; p= 0.081 respectively) (Figure 4.6Bi-iii). This is in contrast to NOTCH1^{MUT} CLL cells which displayed no correlation (r^2= 0.098; p= 0.49), again corroborating our earlier results that the lack of anti-CD20 MAb activity can not solely be contributed to low CD20 expression levels (Figure 4.6Biv). Comparing CD52, CD55 and CD59 expression levels produced no correlation with % of dead cells from OFA induced CDC. Others have also shown that RTX CDC activity does not correlate with complement inhibitory proteins, but CDC activity was improved with inhibitors of CD55 and CD59 for CLL cells that displayed reduced efficacy towards RTX (Figure 4.7)[308,310,311].

4.3.6 OFA has greater efficacy at inducing ADCC in CLL cells

An ADCC assay was performed on our CLL samples to address potential mechanisms of NOTCH1^{MUT} mediated resistance to RTX[108]. To determine the range of concentrations to use for RTX and OFA the assay was optimised in two cell lines HG3 and Ramos (Burkitt's lymphoma cell line with high expression levels of CD20). We analysed the results in two ways; using the luminescence read and calculating the fold of induction of ADCC (MAb luminescence/no drug control (NDC) luminescence –background luminescence). As the fold of induction was more informative this was used for all further analysis. Ramos displayed a greater induction of ADCC than HG3 cells, with OFA being more potent at a lower concentration than RTX (OFA at 100 ng/ml as opposed to RTX at 1 μg/ml). However RTX induced a higher fold of induction than OFA (Figure 4.8).

Comparing the response of cytogenetically normal CLL cells with RTX and OFA (Figure 4.9), there was a slightly higher induction of ADCC for OFA than RTX and OFA was more potent, with maximal fold of induction observed at 100 ng/ml as opposed to RTX at 1 μg/ml, as seen with the cell lines. A similar trend with OFA being more potent at lower concentrations was observed in our 11q del CLL patients (Figure 4.10), although only 1 of 3 patients displayed a clear induction of ADCC. Minimal ADCC induction was observed for both RTX and OFA in our 17p del patients (Figure 4.11). Comparing the MAbs in our NOTCH1^{MUT} samples (Figure 4.12), there was a slightly higher maximal fold of induction for OFA and again OFA had higher potency at 100 ng/ml. To determine if there was significant difference in the efficacy at inducing ADCC between OFA and RTX the fold induction at the highest potency for the two MAbs was compared, for OFA 100 ng/ml and RTX 1 μg/ml. For all the different cytogenetic groups, OFA had the higher fold of induction, but this was only statistically significant for 11q del CLL cells ($p=0.0057$) (Figure 4.13A-D). Comparing all the CLL samples together, OFA significantly induced higher amounts of ADCC than RTX, with approximately 30% more ADCC observed with OFA than RTX ($p=0.0068$). When the maximal fold of induction for both RTX and OFA was compared between the different cytogenetic groups, cytogenetically normal CLL cells had the higher ADCC induction, similar to our findings for CDC activation in this group. However unlike with CDC, 17p del patients had the lowest levels of induction, lower than NOTCH1^{MUT} CLL cell ADCC induction, although a larger patient cohort is required

to determine if there are any statistically significant differences between the different cytogenetic subsets (Figure 4.14).

4.3.7 ADCC induction does not correlate with expression levels of CD20 nor CDC induction.

Comparing CD20 expression levels against CDC demonstrated there was a strong positive linear correlation between CD20 expression levels and the % of dead cells produced by CDC induction. However, the same was not true for ADCC. Comparing the maximal fold of ADCC induction produced with OFA at 100 ng/ml for all the CLL samples in comparison to CD20 expression levels produced no correlation (Figure 4.15A). To determine whether the higher levels of CDC activation would relate to higher ADCC induction this was also plotted, however no correlation was found (Figure 4.15B). Therefore our results indicate that when CLL samples are susceptible to OFA induced CDC, this does not necessarily result in similar susceptibly to OFA induced ADCC.

4.4 Discussion

Notch1 mutations are a recently identified independent poor prognostic marker in CLL, with mutations resulting in increased CLL cell survival and proliferation[98,229,357]. Notch expression has been shown to result in suppression of p53 and pro-apoptotic proteins Bax, Bim and Noxa, whilst activating PI3K/Akt, NF-κB and anti-apoptotic proteins Bcl-2 and Bcl-X_L[210]. Over activation of pro-survival pathways in NOTCH1^{MUT} CLL cells, presents an obstacle for chemotherapeutic agents, especially through the suppression of p53 activity limiting the induction of apoptosis. However immunotherapeutic agents such as RTX, that induce CDC and ADCC and have limited efficacy at inducing programmed cell death, could have provided a viable treatment option for NOTCH1^{MUT} CLL cells. Therefore it was surprising that a retrospective investigation of the CLL8 trial identified that NOTCH1^{MUT} confers a resistance to RTX when RTX is added to FC treatment strategy, which is not observed in any other poor cytogenetic subset[108]. Importantly there was improvement in PFS observed in NOTCH1^{MUT} patients treated with chlorambucil plus OFA, although this improvement was relatively short lived, 18 months. Therefore, it is important to understand the mechanism surrounding CD20 MAb treatments that result in diminished efficacy in NOTCH1^{MUT} CLL patients and whether a potent inducer of CDC may be able to overcome this resistance[109].

4.4.1 The level of CD20 expression is the most important determinant in CDC induction with RTX/OFA

Comparing surface expression levels of CD20 from healthy B cell donors and CLL cells demonstrated as expected that CLL cells had significantly lower levels of CD20, which is a well-documented phenotype of CLL cells[310,318]. Interestingly there was also lower expression levels of CD52. However the mean CD52 MFI ratio in CLL cells was 67.29, which was still substantially larger than the mean MFI ratio for CD20 which was 4.388. Therefore although expression levels are lower, it would seem likely that the number of CD52 molecules on the surface of the CLL cell are still above a critical level required for CDC and ADCC activation, which makes alemtuzumab such a successful treatment regime[86,358]. Interestingly only CD55 displayed a significant up-regulation in CLL cells, whereas with CD59 there was little difference in expression levels from normal B cells to CLL cells.

Others have also observed a skew in CLL cells towards up-regulating CD55 more than CD59[311].

4.4.2 Surface protein expression levels do not fully explain the lack of activity of RTX and OFA against NOTCH1^{MUT}

When CD20 expression levels were separated based on CLL cytogenetic subsets, 17p del CLL cells displayed significantly less CD20 expression than CLL cells with no cytogenetic abnormality. Although NOTCH1^{MUT} cells also had lower levels of CD20 than normal CLL cells this was not statistically significant, with a larger population of NOTCH1^{MUT} CLL cells this may change. Importantly 11q del patients did not display reduced CD20 expression levels, and responded well to OFA induced CDC, therefore low CD20 expression levels are not uniformly observed in all poor prognostic CLL patients. The retrospective CLL8 trial demonstrated no improvement in PFS or OS in NOTCH1^{MUT} CLL cells with FC vs FCR. However there was a slight improvement observed in PFS and OS within 17p del patients receiving FCR compared to FC[108]. When the mean OFA induced CDC levels were compared between all cytogenetic sub-groups, NOTCH1^{MUT} CLL cells demonstrated the lowest CDC induction of all the cytogenetic subgroups. This indicates that low CD20 expression levels alone do not entirely contribute to the lack of activity of anti-CD20 MAb in NOTCH1^{MUT} CLL cells. Recent research of a large cohort of CLL patients (n=692) of which 87 were NOTCH1^{MUT} suggests the reduced activity of anti-CD20 MAbs in NOTCH1^{MUT} CLL cells is due to reduced expression of CD20[356]. When CLL samples were sorted for lowest and highest expression of CD20 they identified that the population with the lowest CD20 expression was enriched for NOTCH1^{MUT}. They attributed the lower expression of CD20 to increased expression at the mRNA and protein level of *HDAC1* and *HDAC2*[356]. HDACs act as epigenetic regulators of gene expression by catalysing the removal of acetyl groups from core histones. This in turn results in chromatin compaction leading to the repression of gene transcription[359,360]. HDAC inhibitors, such as valporic acid (VPA) have been shown to result in the up-regulation of CD20 expression and potentiate the activity of RTX mediated CDC in B cell lymphoma cell lines[361]. Low CD20 expression levels have been associated with innate and acquired RTX related resistance, and HDAC inhibitors have been shown to augment the CDC activity of RTX. However our results would suggest that even if CD20 expression levels were able to be raised in NOTCH1^{MUT}

CLL cells this would not necessarily result in the complete return in activity of OFA/RTX. This is highlighted when comparing CD20 expression and CDC linear regression, with no detectable correlation between the two in NOTCH1^{MUT} CLL cells.

CD55 was the only other molecular marker investigated that could contribute to reduced MAb activity in NOTCH1^{MUT} CLL cells, as CD55 expression was highest within NOTCH1^{MUT} CLL samples. Higher CD55 complement inhibitory protein expression in conjunction with low CD20 expression levels could result in resistance to RTX. Although OFA CDC levels did not display any correlation with expression of CD55 or CD59, others have also observed similar results with RTX [311]. Despite a lack of correlation between CD55 and CD59 expression with RTX induced CDC within their study, in CLL cells with basal response to RTX there was improvement in RTX CDC induction when antibodies against CD55 and CD59 were used. The improved efficacy was cumulative when antibodies against both proteins were used in conjunction with RTX, displaying a 6-fold increase in CDC induction in the previously basal level responders[311]. In the CLL cells that responded well to RTX within the first instance, inhibition of either CD55 or CD59 was sufficient to produce maximal CDC induction[311]. The lack of correlation with expression levels and induction of CDC suggests that even the lowest expression of these complement inhibitors is sufficient for them to limit complement activation and higher expression levels provide no further inhibitory effect. As NOTCH1^{MUT} CLL cells demonstrate poor CDC induction with OFA, inhibition of CD55 and CD59 may lead to increased efficacy. RTX displays little efficacy as a single agent, whereas when in combination with FC superior responses are produced[349]. One of the mechanisms behind this is thought to be that fludarabine may potentially cause the down-regulation of CD55. Within a non-Hodgkin's lymphoma cell line resistant to RTX it was identified that exposure to fludarabine caused a reduction in CD55 from 96% to 55% positive cells and synergised with the efficacy of RTX[362]. OFA however does not demonstrate the same level in improvement in CDC induction with inhibitors against CD55 and CD59, presumably because it is a more effective inducer of CDC in the presence of low CD20 expression levels[363]. CD55 competes for binding to complement component C4b so that C2a is displaced and C3 convertase can no longer be formed, whereas CD59 prevents the formation of the MAC through

stopping the polymerisation of complement C9[1]. This suggests that the closer binding site of OFA allows more effective deposition of active complement components onto the surface of the cell so even in the presence of these complement inhibitory proteins CDC is still induced. The brief time period in which OFA showed clinical efficacy in NOTCH1^{MIUT} CLL patients could be explained by the heterogeneous population of CLL cell being treated[254,255,315,316]. Within NOTCH1^{MUT} CLL patients OFA infusion could effectively have cleared the CLL cells not expressing NOTCH1^{MUT} which had higher levels of CD20 expression. This would leave the malignant NOTCH1^{MUT} clone to escape into the BM/LN. Within the BM/LN microenvironment stimulation of the Notch pathway would provide enhanced activation of the NOTCH1^{MUT} clone leading to its expansion. After 18 months the NOTCH1^{MUT} clone would then represent the majority of the CLL cell population resulting in a loss of susceptibility against OFA activity.

4.4.3 ADCC levels do not correlate with CD20 expression

Investigating the efficacy of RTX and OFA at inducing ADCC in CLL cells demonstrated that OFA is more potent than RTX and also shows significantly higher ADCC induction, although this induction is not as notable as with CDC. Others have seen that OFA is marginally more effective than RTX at inducing ADCC[364]. Interestingly 17p del displayed the lowest levels of ADCC induction, lower than results obtained from NOTCH1^{MUT} CLL cells, but a larger patient cohort would be required to determine if this is a significant trend. Again NOTCH1^{MUT} CLL cells displayed less ADCC induction with RTX/OFA than cytogenetically normal CLL cells, indicating that the resistance observed *in vivo* is also observed *in vitro* without Notch1 stimulation. Interestingly, unlike CDC activation the ADCC fold of induction did not correlate with CD20 expression levels. The Ramos cell line has a much higher expression level of CD20 than CLL cells, and it displays a strong fold of induction with RTX/OFA. Therefore it is possible that the surface expression of CD20 on CLL cells is too low and only above a certain threshold can CD20 expression levels affect the level of ADCC induction. Furthermore high CDC activation did not correlate with high ADCC induction, others have also found this characteristic of ADCC with RTX[365]. This indicates that CLL cells may be susceptible to either CD20 MAb induced CDC/ADCC but not necessarily both of these pathways.

This work provides important evidence that CD20 expression levels could be to blame for some, but not all of the reduced activity of anti-CD20 MAb in NOTCH1^{MUT} CLL cells. Therefore further research is required to determine the precise mechanisms responsible for poor activity of these MAbs against NOTCH1^{MUT} CLL cells.

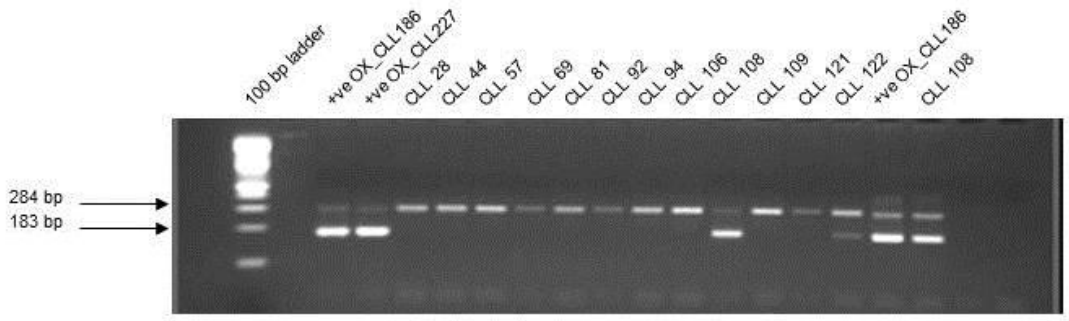

Figure 4.1 Identification of NOTCH1^{MUT} by ARMS PCR

ARMS PCR detects NOTCH1 c.7544_7545delCT mutation using two forward primers, one for the normal NOTCH1 sequence producing a band at 284 bp and one for the NOTCH1 mutation giving a band at 183 bp. Representative data is shown here from twelve of our CLL patients along with two NOTCH1^{MUT} positive samples received from Oxford University (+ve OX_CLL). A total of 89 CLL patients were screened, with seven found to be NOTCH1^{MUT} positive with no 11q or 17p deletions detected by FISH.

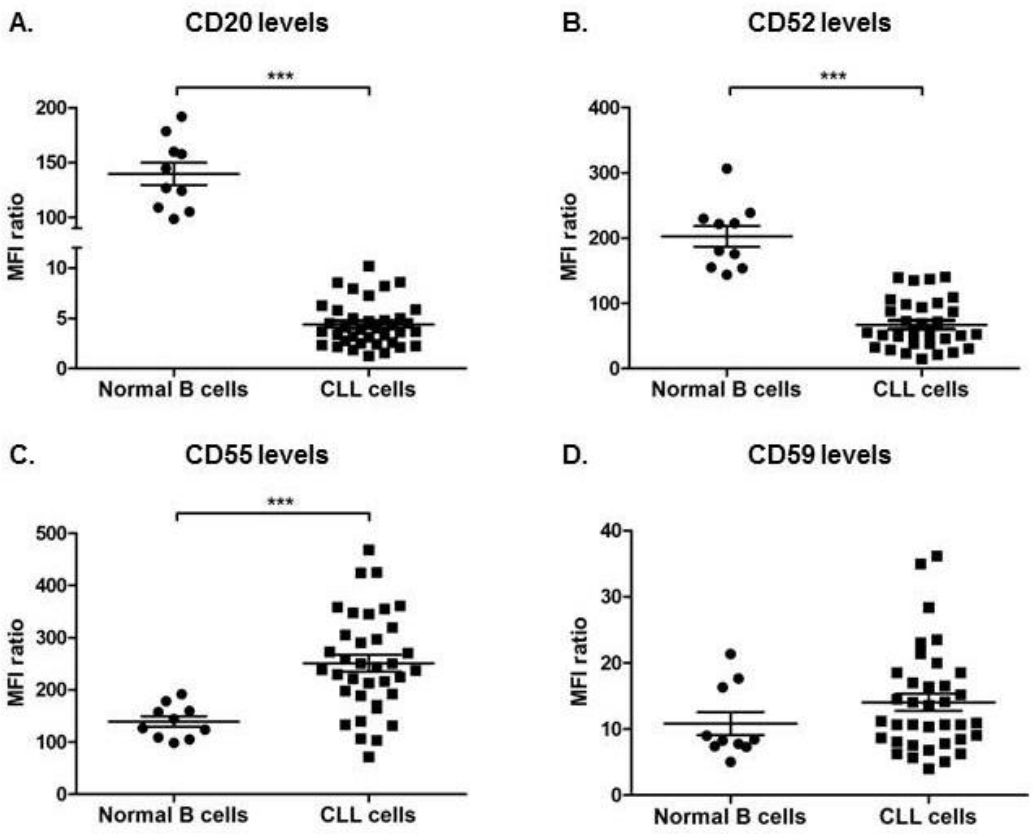

Figure 4.2 Cluster of differentiation surface protein expression is skewed in CLL patients

Normal healthy B cells were selected by gating on the $CD19^+$ and $CD20^+$ population of cells. B cells and CLL cells were either unstained or stained with Ab, cells were left on ice with Ab for 30 min and then washed with PBS. All cells then underwent flow cytometry analysis. MFI ratio was obtained by taking the ratio of unstained vs stained cells. A. CD20 expression in normal B cells (n=10) vs CLL cells (n= 37). B. CD52 expression in normal B cells (n=10) vs CLL cells (n= 33). C. CD55 expression in normal B cells (n=10) vs CLL cells (n= 36). D. CD59 expression in normal B cells (n=10) vs CLL cells (n= 36). p values were determined by an unpaired t-test (*** $p<0.001$).

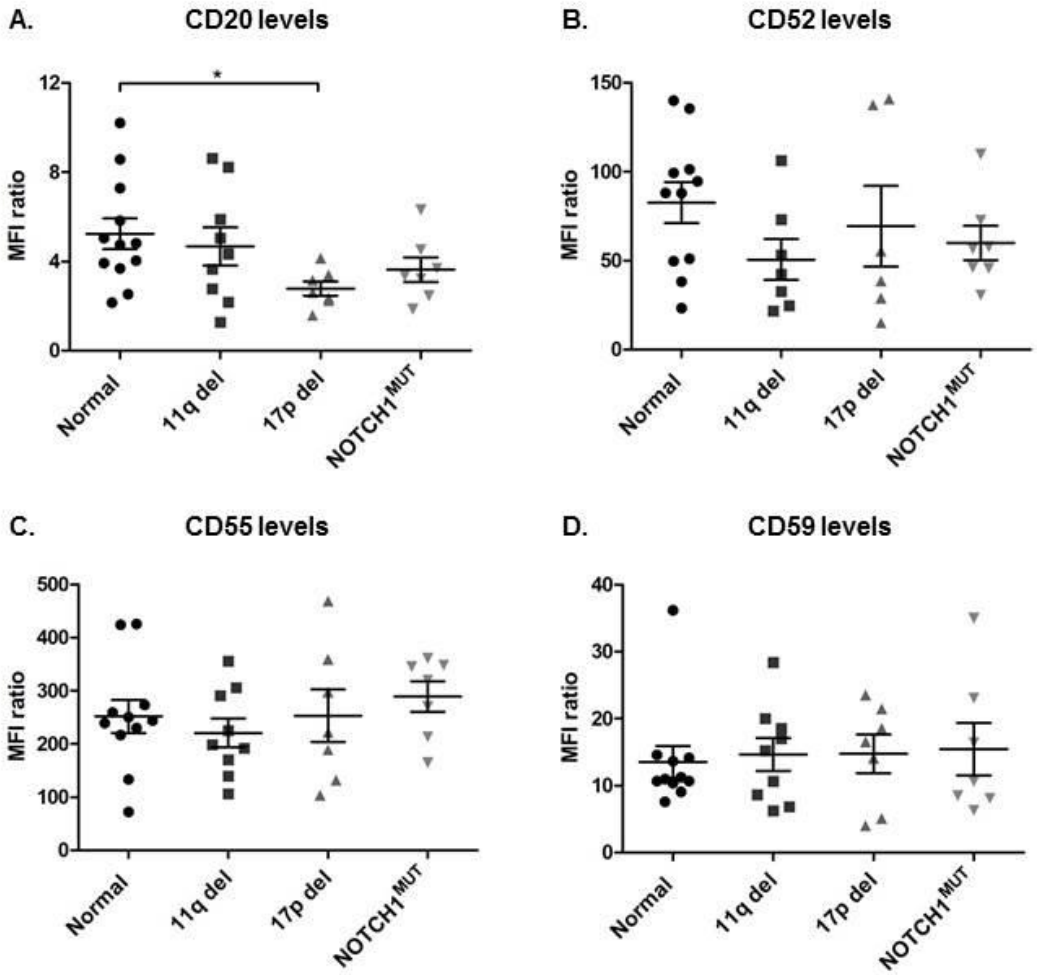

Figure 4.3 Only CD20 expression levels display significant differences between the different CLL cytogenetic subsets

CLL cells were either unstained or stained with Ab, cells were left on ice with Ab for 30 min and then washed with PBS. All cells then underwent flow cytometry analysis. MFI ratio was obtained from taking the ratio of unstained vs stained cells. A. CD20 expression in cytogenetically normal (n=8), 11q del (n= 7), 17p del (n=7) and NOTCH1^{MUT} (n=7) CLL cells. B. CD52 expression in cytogenetically normal (n=8), 11q del (n= 6), 17p del (n=6) and NOTCH1^{MUT} (n=7) CLL cells. C. CD55 expression in cytogenetically normal (n=8), 11q del (n= 7), 17p del (n=7) and NOTCH1^{MUT} (n=7) CLL cells. D. CD59 expression in cytogenetically normal (n=8), 11q del (n= 7), 17p del (n=7) and NOTCH1^{MUT} (n=7) CLL cells. p values were determined by an unpaired t-test (* $p<0.05$). MFI ratio ± SEM is shown.

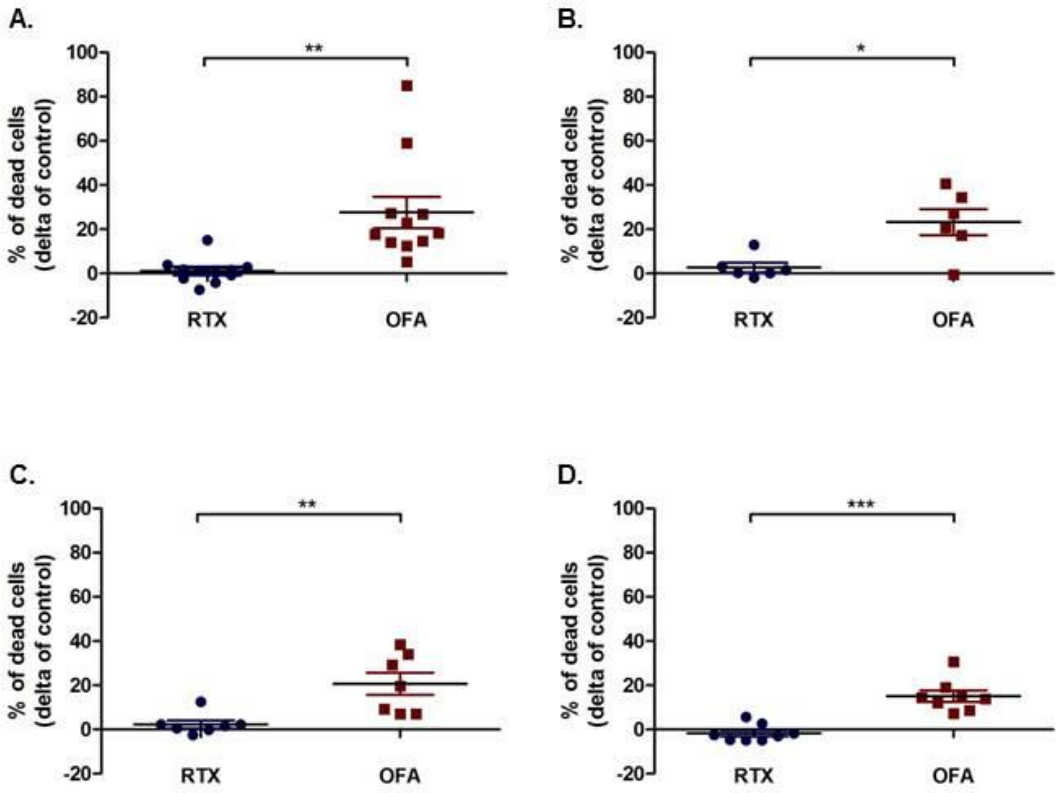

Figure 4.4 OFA is a superior inducer of CDC than RTX in all cytogenetic sub-groups of CLL

CLL patient cells were treated with 20 µg/ml OFA or RTX and then incubated with 50% NHS and the level of CDC cell death measured by flow cytometry (% PI+ cells). The percentage of dead cells is expressed relative to untreated control, p values were determined by a paired t-test (*, $p<0.05$, ** $p<0.01$, *** $p<0.001$). A. Cytogenetically normal CLL cells (n=11). B. 11q del CLL cells (n=6). C. 17p del CLL cells (n=7).D. $NOTCH1^{MUT}$ CLL cells (n=8). Mean cell death $\pm$ SEM is shown.

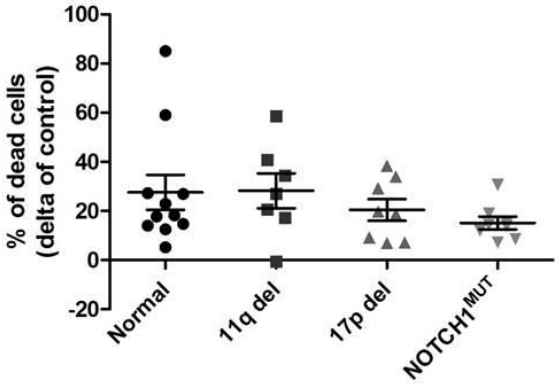

Figure 4.5 OFA has higher CDC potency in cytogenetically normal and 11q del CLL patients

CLL patient cells (n=32) were treated with 20 µg/ml OFA and then incubated with 50% NHS and the level of CDC cell death measured by flow cytometry (% PI+ cells). The percentage of dead cells is expressed relative to untreated control. CLL samples are categorised by the type of cytogenetic abnormalities they harbour. Mean cell death ± SEM is shown.

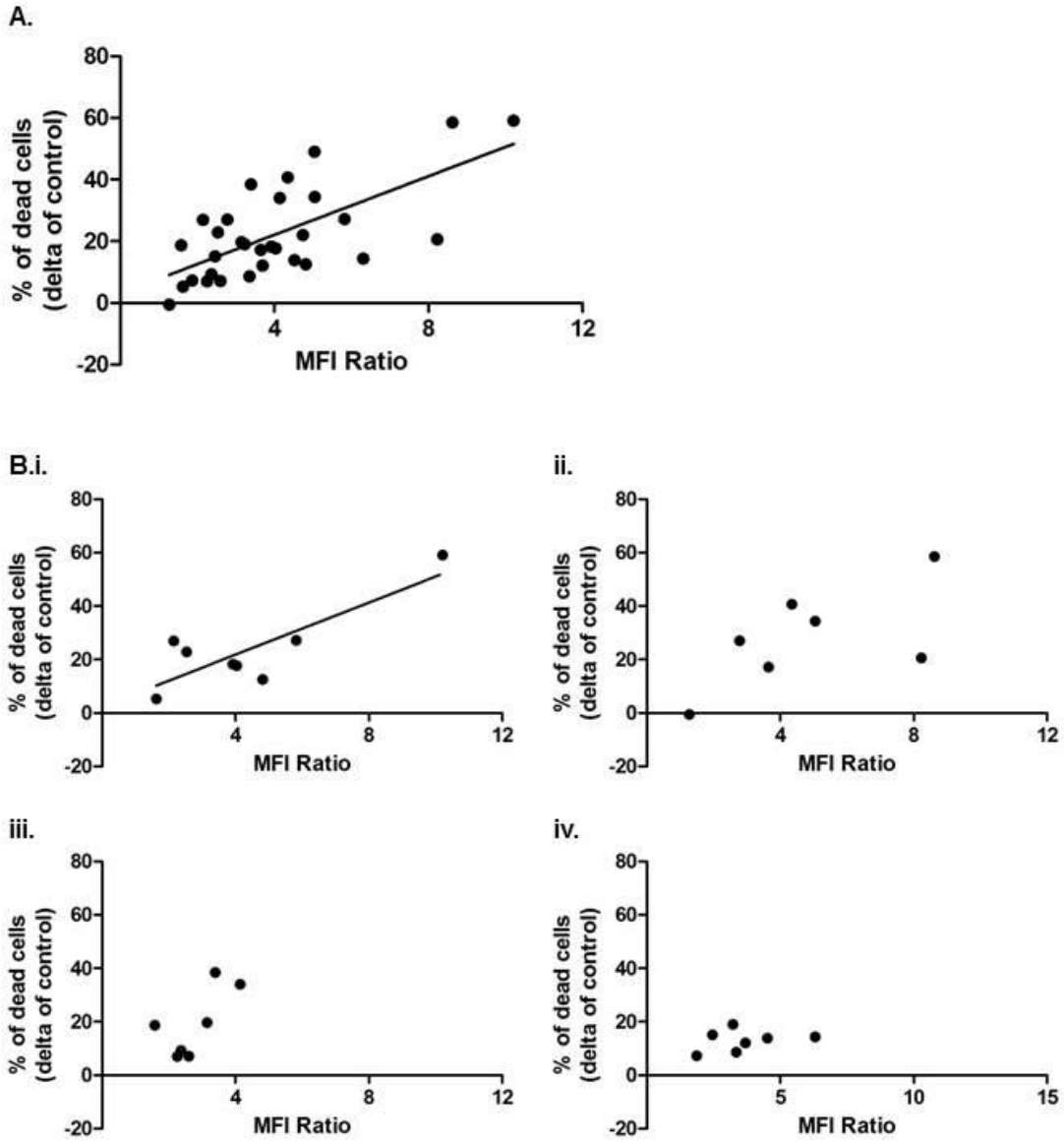

Figure 4.6 NOTCH1^{MUT} CLL cells display no correlation with CD20 expression levels and OFA induced CDC

CD20 expression levels was determined by flow cytometry and MFI ratio was calculated from the MFI signal from stained divided by unstained CLL cells and plotted against the CDC percentage dead cells observed with 20 µg/ml OFA. Linear regression analysis was applied. A. All CLL cells (n=31), r^2, 0.4506 and p value, <0.0001. B. CDC vs CD20 expression separated by CLL cytogenetics. i. Cytogenetically normal CLL cells (n=8), r^2, 0.6898 and p value, 0.0107. ii. 11q del CLL cells (n=7), r^2, 0.4342 and p value, 0.1075 (not statistically significant). iii. 17p del CLL cells (n=7), r^2, 0.4881 and p value, 0.0808 (not statistically significant). iv. NOTCH1^{MUT} CLL cells (n=7), r^2, 0.09824 and p value, 0.4937 (not statistically significant).

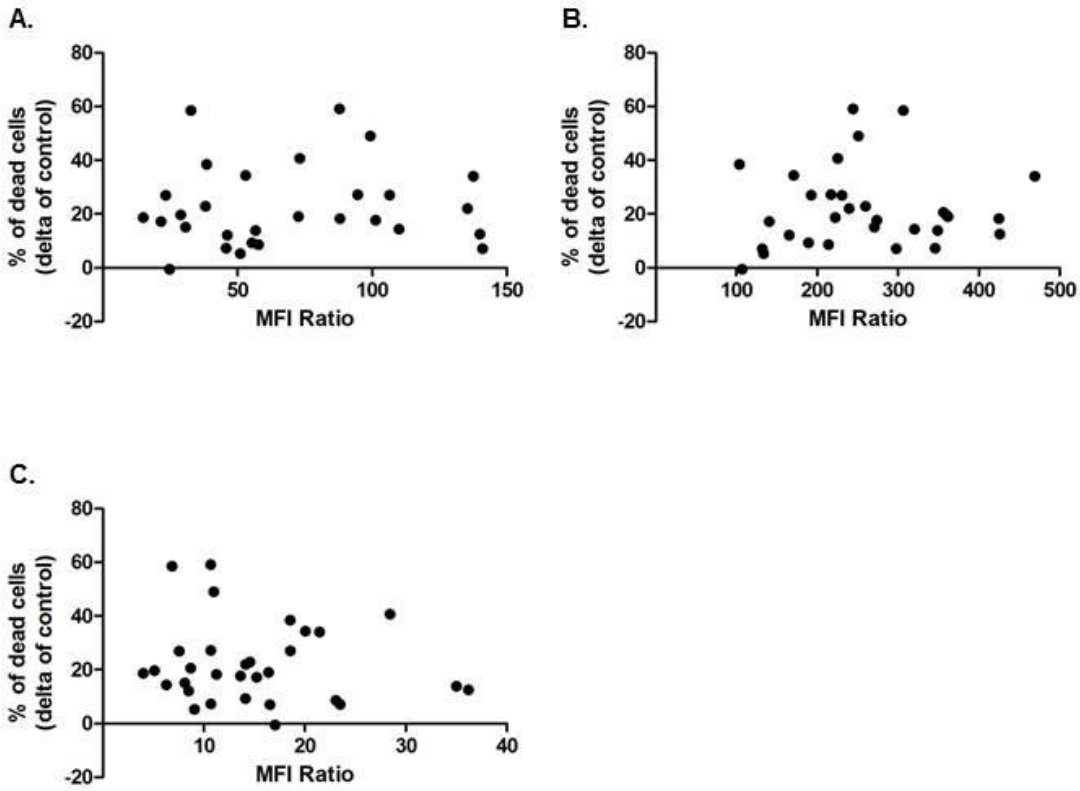

Figure 4.7 No correlation was observed with surface expression levels of complement inhibitory proteins and OFA induced CDC

Surface expression levels were determined by flow cytometry and MFI ratio was calculated from the MFI signal from stained divided by unstained CLL cells and plotted against the CDC percentage dead cells observed with 20 µg/ml OFA. Linear regression analysis was applied and no statistical significance was observed. A. CD52 expression vs CDC induction in CLL cells (n=29), r^2, 0.0048 and p value, 0.712. B. CD55 expression vs CDC induction in CLL cells (n=31), r^2, 0.012 and p value, 0.558. C. CD59 expression vs CDC induction in CLL cells (n=31), r^2, 0.0054 and p value, 0.705.

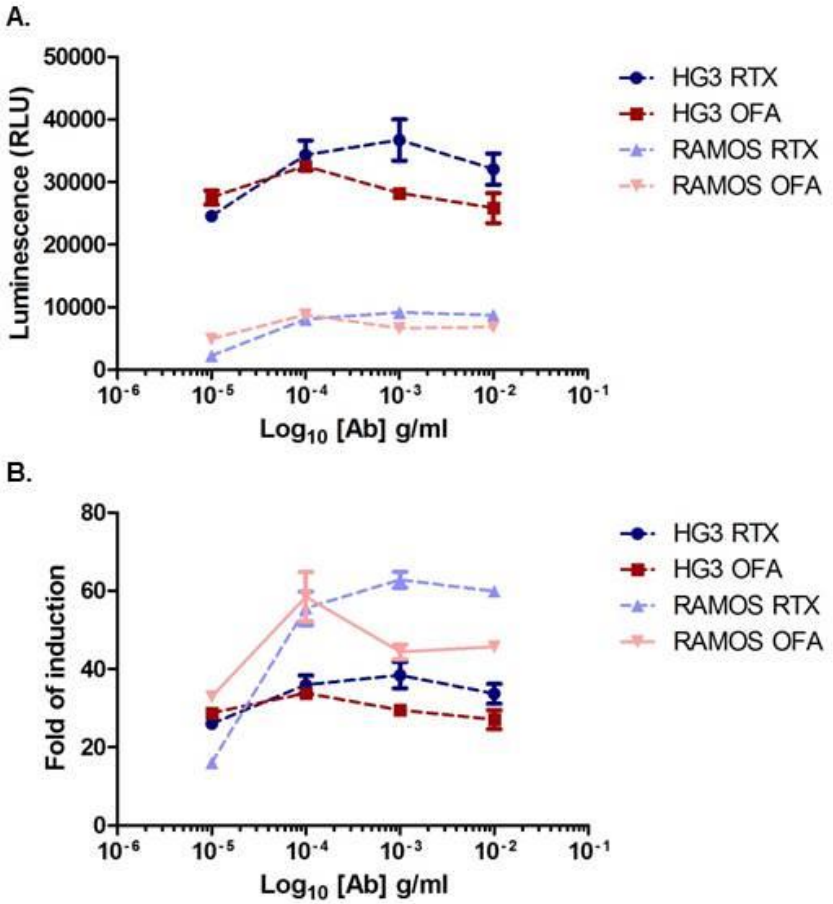

Figure 4.8 ADCC optimisation in two cell lines

HG3 and Ramos cell line were cultured on plastic for 18 hr. ADCC luciferase reporter bioassay was performed with a ratio of effector: target cells of 6:1. A. Luminescence signal. B. Fold of induction was calculated by dividing the luminescence signal from MAb treatments by the luminescence signal from NDC. Mean ± SD are shown.

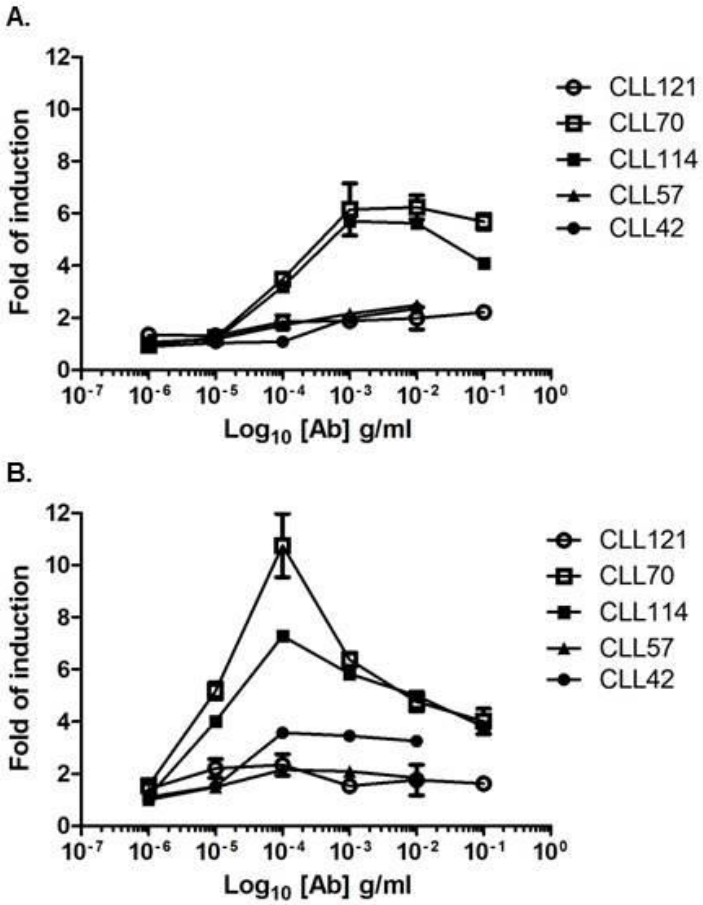

Figure 4.9 OFA has higher ADCC efficacy in normal CLL cells than RTX

Cytogenetically normal CLL cells (n=5) were cultured on plastic for 18 hr. ADCC luciferase reporter bioassay was performed with a ratio of effector: target cells of 6:1. Fold of induction was calculated by dividing the luminescence signal from MAb treatments by the luminescence signal from NDC. A. RTX treatment. B. OFA treatment. Mean ± SD are shown.

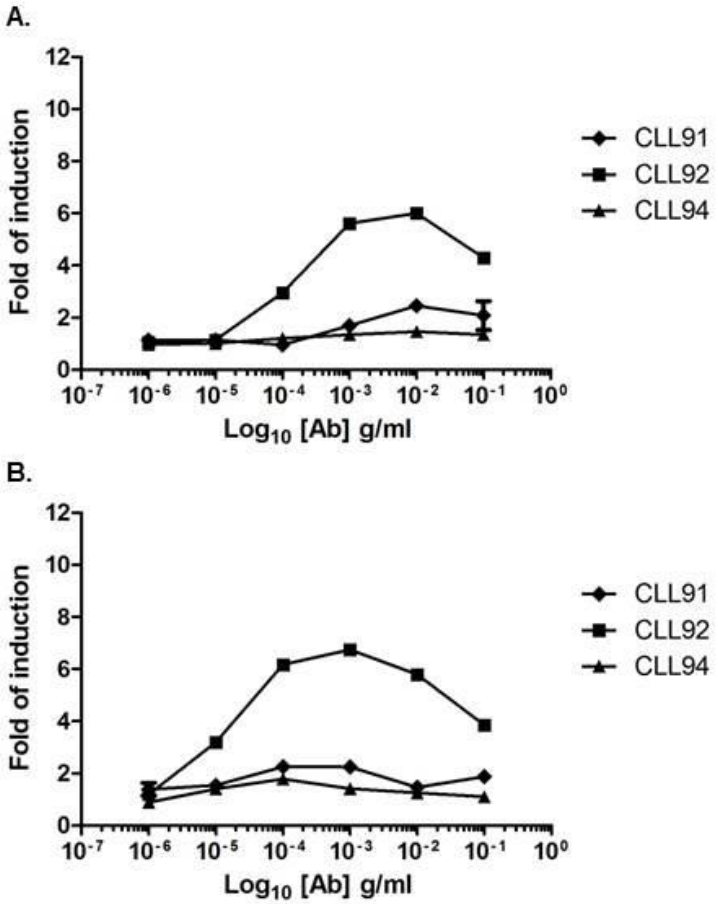

Figure 4.10 OFA has higher ADCC efficacy in 11q del CLL cells than RTX

11q del CLL cells (n=3) were cultured on plastic for 18 hr. ADCC luciferase reporter bioassay was performed with a ratio of effector: target cells of 6:1. Fold of induction was calculated by dividing the luminescence signal from MAb treatments by the luminescence signal from NDC. A. RTX treatment. B. OFA treatment. Mean ± SD are shown**.**

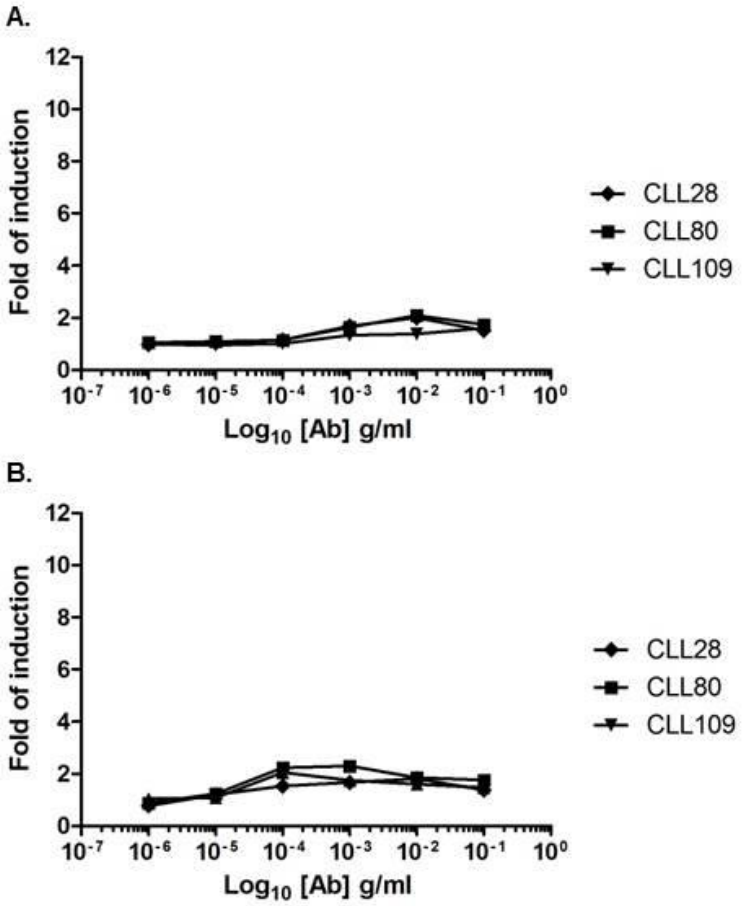

Figure 4.11 CLL cells with 17p del display minimal ADCC induction

17p del CLL cells (n=3) were cultured on plastic for 18 hr. ADCC luciferase reporter bioassay was performed with a ratio of effector: target cells of 6:1. Fold of induction was calculated by dividing the luminescence signal from MAb treatments by the luminescence signal from NDC. A. RTX treatment. B. OFA treatment. Mean ± SD are shown.

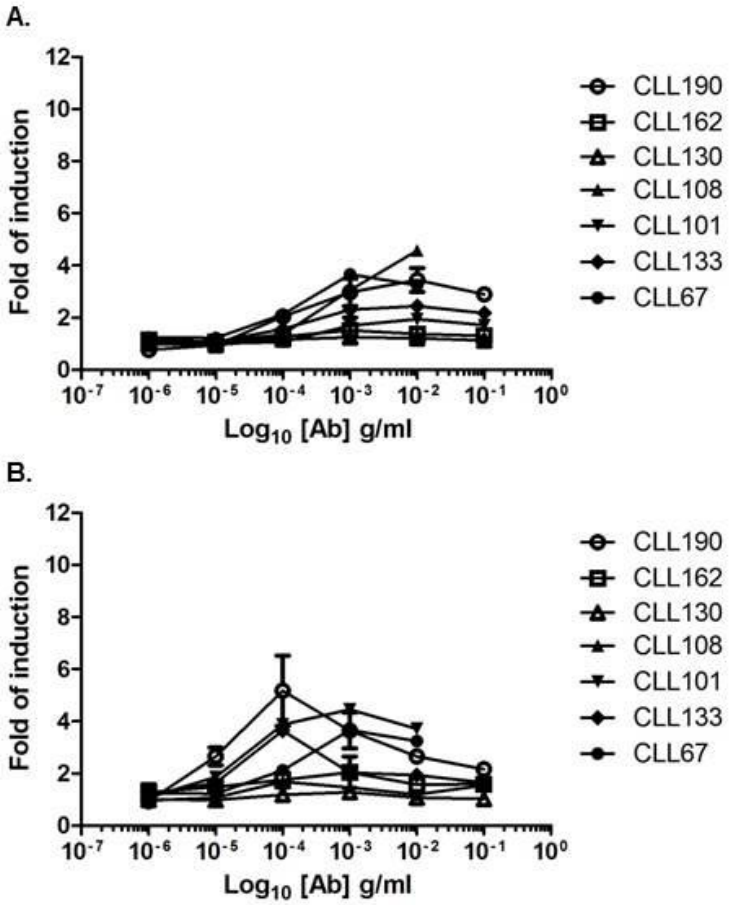

Figure 4.12 OFA has higher ADCC efficacy in NOTCH1^{MUT} CLL cells than RTX

NOTCH1^{MUT} CLL cells (n=7) were cultured on plastic for 18 hr. ADCC luciferase reporter bioassay was performed with a ratio of effector: target cells of 6:1. Fold of induction was calculated by dividing the luminescence signal from MAb treatments by the luminescence signal from NDC. A. RTX treatment. B. OFA treatment. Mean ± SD are shown.

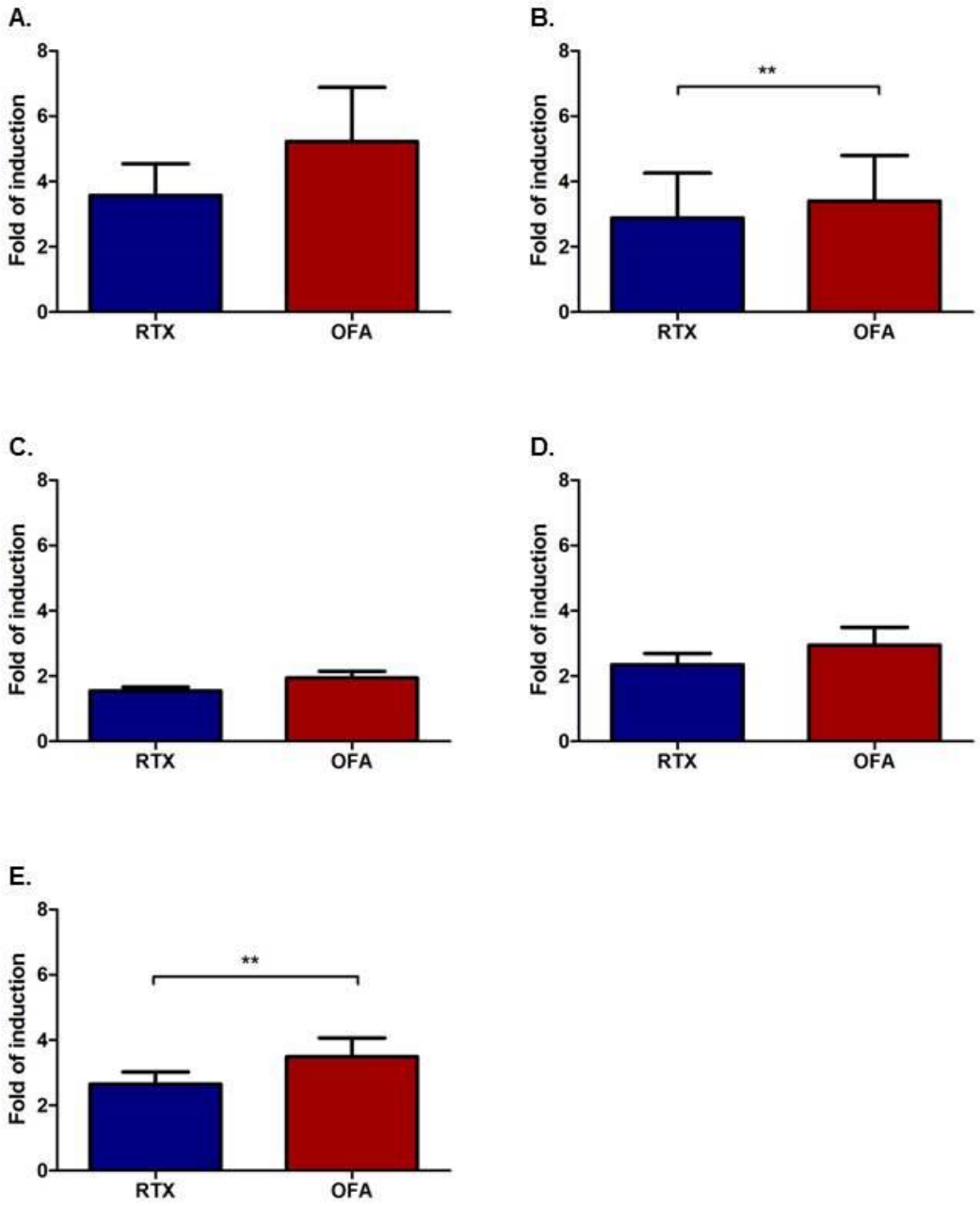

Figure 4.13 OFA is a more potent inducer of ADCC than RTX in CLL cells

CLL cells (n=18) were cultured on plastic for 18 hr. ADCC luciferase reporter bioassay was performed with a ratio of effector: target cells of 6:1. Fold of induction was calculated by dividing the luminescence signal from MAb treatments by the luminescence signal from NDC. The fold of induction at the optimal concentration of RTX (1 µg/ml) and OFA (100 ng/ml) is plotted, p values were determined by a paired t-test (** $p<0.01$) A. Cytogenetically normal CLL cells (n=5). B. 11q del CLL cells (n=3). C. 17p del CLL cells (n=3). D. $NOTCH1^{MUT}$ CLL cells (n=7). E. All CLL cells (n=18). Mean ± SEM are shown.

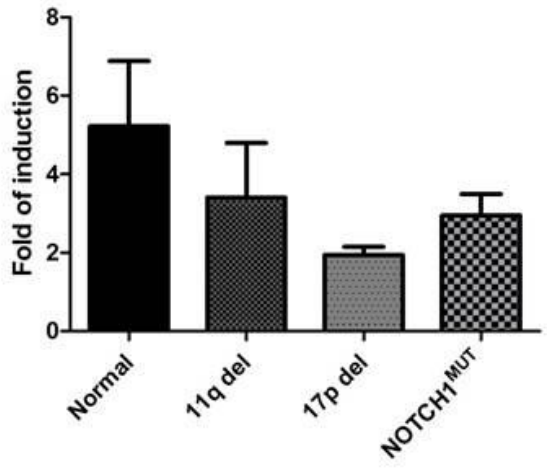

Figure 4.14 17p del patients display lowest levels of ADCC induction

CLL cells were cultured on plastic for 18 hr. ADCC luciferase reporter bioassay was performed with a ratio of effector: target cells of 6:1. Fold of induction was calculated by dividing the luminescence signal from MAb treatments by the luminescence signal from NDC. The fold of induction at the optimal concentration of OFA (100 ng/ml) is plotted for each of the cytogenetic sub-groups, normal (n=5), 11q del (n=3), 17p del (n=3), $NOTCH1^{MUT}$ (n=7) CLL cells. Mean ± SEM are shown.

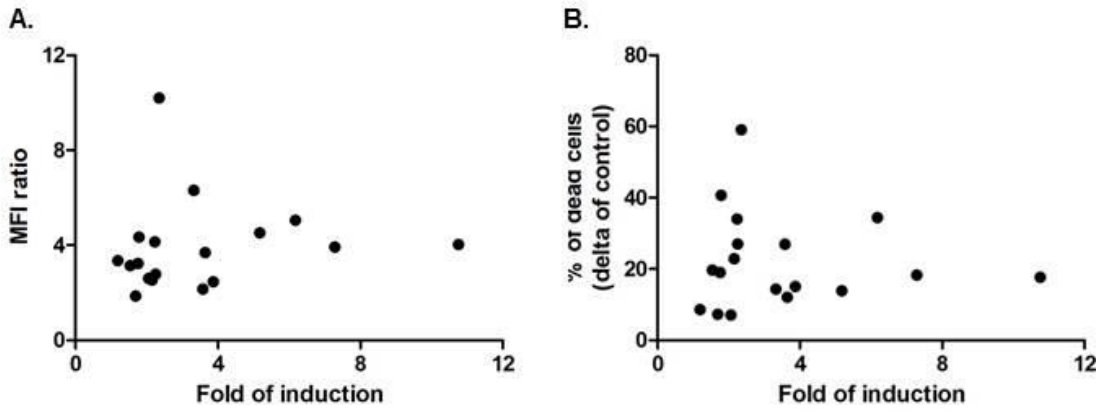

Figure 4.15 ADCC induction displays no correlation with CD20 expression levels or CDC activation

CLL cells (n=18) were cultured on plastic for 18 hr. ADCC luciferase reporter bioassay was performed with a ratio of effector: target cells of 6:1. Fold of induction was calculated by dividing the luminescence signal from MAb treatments by the luminescence signal from NDC. The fold of induction at the optimal concentration of OFA (100 ng/ml) is plotted. A. CD20 expression levels was determined by flow cytometry and MFI ratio was calculated from the MFI signal from stained divided by unstained CLL cells and plotted against ADCC fold of induction. B. CLL patient cells were treated with 20 µg/ml OFA and then incubated with 50% NHS and the level of CDC cell death measured by flow cytometry (% PI+ cells). The percentage of dead cells is expressed relative to untreated control and plotted against the ADCC fold of induction.

5 Microenvironmental stimulation and anti-CD20 MAb activity

5.1 Introduction

CLL cells are known to migrate between the BM, LN and the peripheral blood. Within the BM and LN CLL cells gain pro-survival and pro-proliferative signals. CLL cells are also dependent on microenvironmental stimulation *in vitro*, with isolated CLL cells undergoing spontaneous apoptosis unless rescued through co-culture with stromal-derived cells[136]. Malignant CLL cells have been shown to tailor their microenvironment to aid in their survival and proliferation[138]. The interaction of CLL cells with the other components of this niche, such as stromal cells, T cells and soluble factors, can also promote drug resistance[140,231]. Chlorambucil and fludarabine *in vitro* demonstrate reduced efficacy at inducing apoptosis in CLL cells when co-cultured with BM stromal cells[141,190]. This close association of CLL cells with the microenvironment leads to CLL cells interacting with other cell types and secreted factors which aid malignant CLL cell survival and proliferation. T cells expressing CD154, support the proliferation of CLL cells and cytokine IL-4 secretion by T cells promotes the expansion of CLL cell clones and aids survival[138,139,366]. CD40 stimulation in combination with IL-4R signalling causes the up-regulation of anti-apoptotic Bcl-2 family proteins, Bcl-X_L, Bfl-1, A1 and MCL-1[168]. Therefore with the up-regulation of anti-apoptotic proteins it is not surprising that drug resistance is observed *in vitro*[141,190]. Fludarabine and chlorambucil also induce DNA damage to cause CLL cell death[246,248]. Cytogenetic abnormalities 17p and 11q del encompasses genes *TP53* and *ATM* respectively, which results in impaired DNA damage response pathway, limiting the efficacy of agents that cause DNA damage[77,367]. This highlights the need for treatments such as anti-CD20 MAbs that do not cause cell death through DNA damage and do not function principally through the induction of apoptosis.

LN/BM interactions could therefore greatly impact on the efficacy of MAb treatment. CLL cells may differentially regulate the surface expression of CD20 or complement inhibitory proteins upon cross-talk within the LN or BM. A recent publication suggested that long term culture of CLL cells with BM derived stromal cells causes both a reduction in CD20 expression and an increase in CD59 expression, which resulted in a reduced susceptibility to RTX[144]. Different

cytogenetic abnormalities or mutations may also alter the way CLL cells respond to their microenvironment[232,368]. Our lab has previously established that upon NTL/CD154+IL-4 stimulation of CLL cells, there is increased activation of the NF-κB pathway[369]. Others have identified that NF-κB is able to induce the expression of the Notch1 receptor ligand, Jagged1, in B cells, which results in the activation of Notch1[217,230]. BM stromal cells are known to express Notch ligands Jagged 1 and DLL1, and an up-regulation of Notch is observed *in vivo* within the LN and *in vitro* with microenvironmental stimulation[226-228,232,368]. Therefore chronic activation of Notch1 within LN/BM microenvironment may be a cause of impaired susceptibility of CLL cells to anti-CD20 MAbs in patient lymphoid organs.

To further investigate the action of anti-CD20 MAbs and why they are ineffective against NOTCH1^{MUT} CLL cells, analysis of the effect the tissue microenvironment has on anti-CD20 MAb activity will be assessed. For microenvironmental stimulation we will use three different culture systems; plastic (containing no stromal cell support), NTL (stromal cells) and NTL/CD154+IL-4 (NTL stromal cells expressing CD154 supplemented with IL-4).

5.2 Aim

The focus was to determine whether the microenvironment played a role in the mechanism behind NOTCH1^{MUT} mediated resistance to anti-CD20 MAbs, and what effects microenvironmental stimulation has on the efficacy of MAbs against other poor cytogenetic CLL groups. To do this CLL cells will be cultured in conditions which mimic the circulating compartment (co-culture with NTL), or the tissue microenvironment (co-culture with NTL/CD154+IL-4). Following stimulation CLL cells will be assessed for:

- Changes in the surface protein expression levels of CD20, CD52, CD55 and CD59 upon co-culture in our different systems;
    - In particular analysis will be conducted to determine whether there are any differences between the CLL cytogenetic sub-groups.
- Differences in the induction of CDC by RTX and OFA when CLL subtypes are stimulated on the different co-culture systems;
- Modulations of CDC induction between the CLL cytogenetic subsets on the different co-culture systems.

5.3 Results

5.3.1 Microenvironmental stimulation differentially regulates the expression of selected surface markers within CLL prognostic subgroups

Chapter 4 demonstrated that different surface proteins were deregulated in CLL cells and for CD20 expression levels this significantly impacted on amount of OFA or RTX induced CDC. Using conditions which recapitulates the LN microenvironment CLL cells were stimulated to establish the impact upon the expression of the surface proteins CD20, CD52, CD55 and CD59. CLL cells were either cultured on plastic (no stimulation), or co-cultured on NTL or NTL cells expressing CD154 with IL-4 added (NTL/CD154+IL-4) for 24-72 hr. After this time CLL cells were removed and the surface expression was analysed. The MFI produced from plastic at each time point was subtracted from the MFI ratio produced from either NTL or NTL/CD154+IL-4.

5.3.1.1 CD20 expression

Cytogenetically normal cells were those with no 17p del, 11q del or NOTCH1^{MUT} detected. Analysis of CD20 expression levels showed that for cytogenetically normal CLL cells there is little change in CD20 expression levels for all samples when cultured on NTL. However two CLL samples displayed an increase in CD20 expression when co-cultured on NTL/CD154+IL-4 (CLL57 and CLL70). For CLL57 there is minimal increase in CD20 expression but for CLL70 there is a rapid increase in CD20 expression levels with an 8 fold increase in CD20 MFI ratio from 24 to 72 hr (Figure 5.1A). For 11q del CLL patients there was little change in CD20 expression levels on NTL, whereas on NTL/CD154+IL-4 for one CLL patient, CLL86, CD20 expression levels decreased in comparison to plastic. For two of the 11q del CLL samples expression levels of CD20 increased (Figure 5.1B). For 17p del CLL patients CD20 expression levels did not change on either of the two co-culture systems (Figure 5.1C). Interestingly in NOTCH1^{MUT} CLL cells, there was an increase in CD20 expression at 24 hr on NTL for CLL101 and 50% of the NOTCH1^{MUT} CLL samples analysed displayed reduced CD20 surface expression when co-cultured on NTL/CD154+IL-4.

5.3.1.2 CD52 expression

Following 24, 48, and 72 hr culture on plastic and co-culture on NTL or NTL/CD154+IL-4 CD52 expression levels were measured. There was a small increase in expression of CD52 for cytogenetically normal CLL samples following NTL stimulation. However upon NTL/CD154+IL-4 stimulation there was a slight down-regulation of CD52 in 75% of the normal CLL cells, from 24 to 72 hr the mean fold reduction in CD52 expression was 0.8 (Figure 5.2A). 11q del CLL cells displayed differential regulation on NTL and similar to normal CLL cells 75% of the CLL samples displayed down-regulation of CD52 when co-cultured on NTL/CD154+IL-4, although the down-regulation in 11q del CLL cells was more prominent (Figure 5.2B). 17p del CLL samples all display down-regulation on NTL/CD154+IL-4, contrasting the up-regulation they display on NTL stromal cells (Figure 5.2C). NOTCH1^{MUT} CLL cells displayed a similar pattern to 17p del patients with a prominent down-regulation of CD52 on NTL/CD154+IL-4, and up-regulation on NTL (Figure 5.2D). Intriguingly the down-regulation of CD52 was more notable and consistent in the poorer prognostic subgroups especially in 17p del and NOTCH1^{MUT} CLL cells.

5.3.1.3 CD55 and CD59 expression

CD55 and CD59 are known to confer resistance to complement fixation and CDC induction, therefore it was important to establish how LN microenvironmental stimulation altered the expression patterns of CD55 and CD59. For cytogenetically normal CLL cells CD55 displayed little change in expression levels on either NTL or NTL/CD154+IL-4 (Figure 5.3A). For 11q del CLL patients there was little difference in CD55 expression when cells are cultured on NTL or NTL/CD154+IL-4, with 75% of the samples showing an up-regulation of CD55 when we mimic the tissue microenvironment (Figure 5.3B). 17p del CLL samples displayed the highest up-regulation of the complement inhibitory protein CD55 on NTL, and 40% of the samples examined displayed a down-regulation of CD55 upon stimulation with NTL/CD154+IL-4 (Figure 5.3C). All of the NOTCH1^{MUT} CLL samples displayed an up-regulation of CD55 on both NTL and NTL/CD154+IL-4 and for CLL101 there was a large increase in CD55 expression level (Figure 5.3D). These results indicate that up-regulation of CD55 following LN

microenvironmental stimulation may play a key role in conferring resistance and warrants further investigation.

CD59 expression levels appear to differentially regulate between CLL samples from all the cytogenetic subsets. In comparison to CD59, CD55 expression is more readily up-regulated with an MFI ratio approximately 100 fold or above, whereas CD59 MFI ratio displayed approximately 20-30 fold up-regulation. For cytogenetically normal CLL samples following co-culture with NTL there appeared to be a gradual increase in expression of CD59 over time, and on NTL/CD154+IL-4 50% of the CLL samples displayed a rapid increase in CD59 expression whilst the other 50% of samples remained the same (Figure 5.4A). 11q del CLL cells displayed no specific pattern for CD59 regulation on NTL whilst on NTL/CD154+IL-4 there was a trend for a small peak in CD59 expression at 48 hr (Figure 5.4B). There was little change in expression on NTL in 17p del CLL samples and on NTL/CD154+IL-4 40% of the CLL samples displayed increased expression of CD59. In one patient sample, CLL109, there was a substantial increase in CD59 expression (Figure 5.4C). For NOTCH1^{MUT} CLL cells when co-cultured on NTL/CD154+IL-4 only one CLL patient displayed an increase in CD59 expression over time (Figure 5.4D).

5.3.1.4 Simulating the tissue microenvironment impacts the surface expression of different markers depending on the CLL cytogenetics

To evaluate the observed changes in MFI ratios for CD20, CD52, CD55 and CD59 in more detail the mean values ± SEM were compared for all cytogenetic subsets following NTL/CD154+IL-4 stimulation. CD20 expression levels gradually increased over time for 11q del CLL cells following NTL/CD154+IL-4 co-culture. Cytogenetically normal CLL cells displayed a similar trend however the mean is skewed by the high up-regulation of CD20 in sample CLL70. In 17p del patients CD20 expression remained the same and for NOTCH1^{MUT} CLL cells expression was reduced. Previous results from Chapter 4 demonstrated that 17p del had the lowest expression levels of CD20 shortly followed by NOTCH1^{MUT} CLL cells (Figure 4.3). In combination with this data it would appear that in both these two poor prognostic subsets there is de-regulation of CD20 expression so that lower expression is exhibited (Figure 5.5A). Interestingly for all the CLL cytogenetic subsets there was a down-regulation of CD52 when co-cultured with

NTL/CD154+IL-4, although this was only marginal with cytogenetically normal CLL samples. At 48 and 72 hr NOTCH1^{MUT} displayed significantly lower CD52 expression, approximately 40 fold and 5 fold less expression respectively, than cytogenetically normal CLL cells. Anti-CD52 MAb alemtuzumab is known to be less effective at targeting CLL cells that have migrated to the LN[260,370], our data would suggest that this is due to rapid down-regulation of CD52 within the LN, which is more prominent in CLL cells with poor prognostic cytogenetics (Figure 5.5B). Chapter 4 results demonstrated that within primary CLL samples NOTCH1^{MUT} CLL cells displayed the highest levels of CD55 expression (Figure 4.3) and with NTL/CD154+IL-4 co-culture NOTCH1^{MUT} CLL displayed the largest up-regulation of CD55. This indicates that NOTCH1^{MUT} CLL cells favour an up-regulation of CD55 compared to other CLL cytogenetic subsets and may explain some of the reduced activity against anti-CD20 MAbs (Figure 5.5C). CD59 expression did not display as large a range in MFI ratio in comparison to CD55, cytogenetically normal CLL cells and 17p del CLL cells displayed a similar gradual increase in CD59 expression whereas 11q del and NOTCH1^{MUT} CLL cells increased CD59 expression which peaked at 48 hr (Figure 5.5D). The ability to down-regulate CD20 and CD52 whilst up-regulating CD55 and CD59 following microenvironmental stimulation may play a key role in resistance to immunotherapy in CLL.

5.3.2 Anti-CD20 MAb CDC activity is enhanced with microenvironmental stimulation in CLL cells

The differential regulation of surface markers on CLL cells following LN microenvironment simulation was assessed for the impact upon the ability of RTX and OFA to induce a CDC response on CLL cells. CLL cells were cultured with or without MAb on plastic, NTL or NTL/CD154+IL-4 for 24 to 72 hr. CLL cells cultured without MAb were removed from culture and treated with MAb prior to carrying out CDC analysis, as previously described in section 2.4.1. In chapter 3 data from one CLL patient (CLL127) indicate the high dose at which OFA is administered during immunotherapy results in OFA remaining within the circulating peripheral blood for up to 7 days after infusion and that it is stable enough to result in high levels of CDC on untreated HG3 cells (Figure 3.19). For this reason CLL cells were also co-cultured with MAbs to determine what effect leaving anti-CD20 MAbs in culture had on CDC activation.

5.3.2.1 Microenvironmental CDC activity of RTX

Cytogenetically normal CLL cells displayed a slight increase in RTX CDC activity when co-cultured on NTL/CD154+IL-4. As previously shown little CDC activity was observed on plastic and similar results were obtained with NTL co-culture. As predicted from CD20 expression data there was an increase in CDC activity when CLL cells were cultured with NTL/CD154+IL-4, this was also observed when RTX was incubated with CLL cells over 72 hr (Figure 5.6).

11q del CLL cells displayed a small percentage of cell death following RTX induced CDC activity on plastic and NTL over the 72 hr time period, however following co-cultured with NTL/CD154+IL-4 there was a notable increase in CDC at 24 hr, and by 48 hr CDC activity improved by 30.17% for cells cultured in the absence of RTX and 42.5% for CLL cells cultured in the presence of RTX (p value; 0.0747 and 0.0992 respectively). This increase in CDC activity was maintained at the 72 hr time point although there was a slight drop in CDC activity, 8.25% less dead cells, for cells cultured with RTX (Figure 5.7).

17p del CLL cells only displayed a small amount of cell death following CDC activity with RTX when co-cultured on NTL/CD154+IL-4 (Figure 5.8). These results in conjunction with those from Chapter 4 which indicated that 17p del patients displayed the lowest levels of CD20, and the second lowest levels of CDC with OFA (Figure 4.3 and 4.5), suggest 17p del patients like NOTCH1^{MUT} CLL cells have reduced susceptibility to anti-CD20 MAbs . Unlike cytogenetically normal and 11q del CLL cells the 17p del CLL cells showed no increase in CD20 over the 72 hr time period, and both complement inhibitory proteins CD55 and CD59 were up-regulated, which may explain why CDC activity was limited.

NOTCH1^{MUT} CLL cells display no clinical efficacy to RTX treatment[108], we and others have demonstrated that NOTCH1^{MUT} CLL cells have low CD20 expression levels[233] (Figure 4.3) and demonstrate the lowest levels of CDC induction with OFA (Figure 4.5). NOTCH1^{MUT} CLL samples displayed a reduction in CD20 expression over time when co-cultured on NTL/CD154+IL-4, and a large up-regulation of CD55. Despite this by 72 hr there was an increase in CDC by 18.67% cell death when co-cultured with RTX on NTL/CD154+IL-4 (p value 0.0621) (Figure 5.9).

Combining these data, the mean RTX induced CDC when co-cultured with NTL/CD154+IL-4 over the 72 hr time period was compared between the different cytogenetic groups. 11q del CLL patients had significantly higher RTX induced CDC, for CLL cells cultured without RTX, than other poor prognostic CLL cells from 48 hr of co-culture onwards (Figure 5.10A). Despite the increase in CDC in cytogenetically normal CLL cells by 72 hr the effect was lost, even though CD20 expression levels continuing to increase over the 72 hr time period. This drop in CDC activity could be explained by the increase in CD59 expression in cytogenetically normal CLL cells. RTX CDC activity was also compared between CLL cells cultured in the presence of RTX on NTL/CD154+IL-4. Initially significantly lower levels of CDC was observed when comparing NOTCH1^{MUT} CLL cells with cytogenetically normal CLL cells, but then gradually an increase in RTX activity occurred, despite a reduction in CD20 expression levels and high CD55 expression. Cytogenetically normal, 11q del and 17p del all displayed a CDC peak at 48 hr (Figure 5.10B). Again 11q del CLL patients displayed the highest levels of CDC and had significantly higher levels than 17p del patients at 48 to 72 hr. As previously stated 11q del CLL patients have been clinically shown to respond well to RTX treatment[346], and our research supports these findings.

5.3.2.2 Microenvironmental CDC activity of OFA

Cytogenetically normal CLL cells display enhanced CDC activity with OFA in all the co-culture systems, compared to RTX. Although one CLL patient CLL81 displayed no enhancement in CDC activity, which corresponded to low CD20 expression levels with an MFI ratio of 1.6 on plastic culture. The enhanced CDC induction with OFA makes the drop in CDC activity when OFA is present in culture with CLL cells more prominent, this was observed even at 24 hr on plastic where there was 15.34% less cell death ($p=0.0272$) when OFA was left in culture. This suggests that OFA bound to CD20 is being removed over time in culture, either through internalisation or loss from the surface of the CLL cell. Once again the enhanced CDC effect on NTL/CD154+IL-4 peaked at 48 hr and then diminished (Figure 5.11).

As observed with RTX cultures, 11q del CLL cells displayed high susceptibility to OFA induced CDC, which was observed in all three of the CLL samples (Figure 5.12). Interestingly for 11q del CLL samples there was a more pronounced drop

in CDC activity when OFA was present in co-culture on plastic and NTL, the percentage of dead cells did not rise above 9%, whereas there was no drop in CDC when OFA was present in co-cultured with NTL/CD154+IL-4. This suggests that for 11q del CLL cells there are protective interactions with NTL/CD154+IL-4 stimulation that stop OFA bound to CD20 from being removed or internalised by the CLL cell.

CLL cells with 17p del, as with the other cytogenetic sub-sets analysed, displayed either internalisation or loss of OFA-CD20 complex in culture. For 17p del CLL cells there was significant benefit to OFA induced CDC at 24 hr on NTL/CD154+IL-4 when OFA was not present in culture. There does not seem to be a dramatic peak in CDC activity at 48 hr as seen with cytogenetically normal and 11q del CLL cells. There was a gradual increase in CDC observed when OFA was co-cultured with NTL/CD154+IL-4 which continued to rise at each time point (Figure 5.13).

Finally, NOTCH1^{MUT} CLL cells displayed significantly more CDC on co-culture with NTL/CD154+IL-4 when OFA was not present in the culture at 24 hr only, over time as with 17p del CLL cells there was a gradual increase in CDC when OFA was present in culture. NOTCH1^{MUT} CLL cells displayed significantly more OFA induced CDC when co-cultured on NTL/CD154+IL-4 than when cultured on plastic for 24 hr only. The benefits received from the co-culture started to be lost with longer culture (48 and 72 hr), which could be due to the reduced levels of CD20 that occurred in NOTCH1^{MUT} CLL cells following co-culture.

Combining these data, the mean OFA induced CDC when co-cultured with NTL/CD154+IL-4 over the 72 hr time period was compared between the different cytogenetic groups (Figure 5.15A). For CLL cells not cultured with OFA, 11q del CLL cells were the most susceptible to anti-CD20 MAb CDC as they displayed the highest levels of OFA CDC, with NOTCH1^{MUT} CLL cells demonstrating significantly lower levels of CDC when compared to 11q CLL cells. 11q and cytogenetically normal CLL cells displayed the same CDC peak at 48 hr before losing the benefit of the co-culture at later time points. Interestingly 17p del CLL cells displayed no peak in OFA CDC activity, with activity remaining constant. Whereas NOTCH1^{MUT} CLL cells displayed a gradual loss in CDC activity following 24 hr, which may reflect the reduction in CD20 expression levels observed following

NTL/CD154+IL-4 co-culture. When OFA was present in co-culture cytogenetic subgroups other than 11q del displayed at least a 20% drop in CDC activity at 24 hr (Figure 5.15B). Normal and 11q del CLL cells again displayed the same 48 hr peak trend, but interestingly both 17p del and NOTCH1^{MUT} CLL cells demonstrated an increase in CDC over the 72 hr time period. This suggests that there may be a common phenotype between these two distinct subgroups that results in this gradual increase in CDC when OFA is present in the co-culture only.

5.4 Discussion

CLL currently remains an incurable disease and one likely cause for this is the cross-talk between accessory stromal cells and T cells that interact with the malignant B cells and help promote tumour growth, survival and drug resistance. Chemoterapeutic agents such as fludarabine and chlormabucil function by causing DNA damage which should result in apoptosis to destroy the CLL cell[246,248]. However signals generated from the microenvironement result in up-regulation of the Bcl-2 family of anti-apoptotic within CLL cells, rendering these drugs less effective *in vitro*[141,190]. However type I anti-CD20 MAbs cause CLL cell death through CDC and ADCC primarily, therefore they may be beneficial for targeting CLL cells within the LN/BM. Proliferation centres within the LN and BM provide nurturing pro-survival and pro-proliferative signals, enabling new cells to enter into the circulating, accumulating compartment. The cytoprotective signals generated in the proliferation centres must be overcome in order to provide a promising therapy for CLL[366]. The interaction of CLL cells with other cells within proliferation centres is likely to cause either an up or down-regulation of different surface markers. Interestingly for all the CLL cells analysed there was a prominent loss of CDC activity for both RTX and OFA when these MAbs were present in culture on plastic and importantly in co-culture with NTL cells. NTL cells mimic the interactions observed for the circulating compartment of CLL cells, suggesting there would be internalisation of the MAb/CD20 complex or loss from the surface of the CLL cell *in vivo*. When CLL cells were being stimulated with NTL/CD154+IL-4 there was still a reduction in CDC if OFA or RTX was present in the co-culture but the reduction was far less prominent. This indicates that NTL/CD154+IL-4 stabilises the MAb/CD20 complex, allowing the MAb to remain active overtime. This supports the use of OFA as a first line therapy for all CLL patients due to OFA being a potent inducer of CDC and displaying enhanced efficacy against CLL cells stimulated with NTL/CD154+IL-4. Improved efficacy of chemotherapeutic agents when CLL cells are stimulated with LN microenvironmental signals is not observed with first line therapies such as fludarabine and chlorambucil[140,141,176,190,333,369]. For all the CLL cell cytogenetic subsets analysed there was an increase in OFA induced CDC on NTL/CD154+IL-4, despite the differences in expression of the different surface markers. Others have also shown that CLL cells stimulated with CD40 are

sensitised to RTX and OFA-induced cell death, which occurred independently of any rise in CD20 expression[176]. However programmed cell death only took place when these MAbs were in the presence of a cross-linking antibody[176,333]. Type 1 MAbs such as OFA and RTX are not known potent inducers of apoptosis, and therefore require a cross-linking antibody for this to occur[254,255]. Therefore not only is there an increase in the activity of these MAbs to induce CDC but there is also an increase in apoptosis. This suggest that there is activation of one or several molecular pathways when CLL cells are co-cultured with NTL/CD154+IL-4 that results in greater susceptibility to the activity of OFA or RTX independently of CD20 expression levels.

These results in conjunction with our previous data has implications for OFA immunotherapy, which after the first initial low dose is administered at high doses of 2000 mg. Data from CLL127 (Figure 3.21) has shown that OFA is still stable within the peripheral blood 7 days after infusion with serum resulting in high levels of CDC on untreated HG3 cells. Chapter 3 demonstrated that complement levels are rapidly exhausted *in vivo* following anti-CD20 MAb infusion, this may therefore potentially lead to OFA remaining in circulation. Our results show that when OFA was present within co-culture with CLL and NTL cells, there was a dramatic loss in CDC induction possibly through loss of OFA bound to CD20 or internalisation. NTL stimulation of CLL cells mimics the circulating compartment; therefore it is possible that *in vivo* after OFA infusion there is complement depletion resulting in incomplete clearance of CLL cells. Circulating CLL cells then lose OFA bound to CD20 through shaving, internalisation and trogocytosis. Trogocytosis occurs when effector cells such as phagocytic cells remove OFA bound to CD20 from the surface of the CLL cell[317,371]. When complement levels within the peripheral blood have restored CDC induction will be impaired due to loss of OFA bound to CD20 on the remaining circulating CLL cells. Therefore despite the more efficient clearance of CLL cells co-cultured with NTL/CD154+IL-4 by OFA, once these cells have been removed the CLL cells in circulation that have escaped OFA CDC will be able to take their place, possibly leading to clonal evolution of CLL cells more resistant to OFA treatment. This suggests that lower doses of OFA may be more beneficial to CLL patients undergoing immunotherapy.

5.4.1 CD52 expression levels on NTL/CD154+IL-4 indicate why alemtuzumab is not effective against CLL cells within the LN

Interestingly when CLL cells are co-cultured with NTL/CD154+IL-4 a down-regulation of CD52 was observed, which was most prominent in our CLL cells with poor prognostic genetics. Alemtuzumab is known to be less clinically active against CLL cells that are located within the LN as opposed to the peripheral blood or BM, and our results indicate that this is at least in part due to the down-regulation of CD52[260,370]. Research by Jak M. *et al.*, also analysed the ability of CD52 to cause apoptosis on CLL cells stimulated with CD40. RTX displayed enhanced programmed cell death induction with CD40 stimulation, whereas there was no significant induction in programmed cell death with alemtuzumab and CD40 stimulation[176]. Therefore it would be interesting to also analyse whether there was a drop in the CDC activity of anti-CD52 MAbs on these CLL cells. Cytogenetically normal CLL cells did not display a prominent down-regulation of CD52 expression, suggesting that these cells would still be susceptible to alemtuzumab. This highlights that different pathways are de-regulated within CLL cells and this corresponds to the cytogenetic abnormality, which also affects the response of CLL cells to the microenvironment and their susceptibility to different treatments.

5.4.2 Anti-CD20 MAbs are an effective treatment for 11q del CLL patients

Chapters 3 and 4 have shown that 11q del CLL patients have reduced complement exhaustion, high CD20 expression and good CDC induction with OFA. This suggests that despite 11q del being a more aggressive form of CLL, they are still susceptible to anti-CD20 MAbs, which is also observed clinically[346]. Further to this, 11q del CLL cells also demonstrate susceptibility to anti-CD20 MAbs even when they undergo tissue microenvironment stimulation. In addition 11q del CLL cells displayed an up-regulation of CD20 upon co-culture with NTL/CD154+IL-4 and a down-regulation of the complement inhibitory protein CD55, which may explain why 11q del cells displayed superior CDC with both RTX and more prominently with OFA than even cytogenetically normal CLL cells. As expected from our previous CDC data, OFA is more potent at inducing CDC than RTX in cells co-cultured with NTL/CD154+IL-4. Our data supports OFA as an effective

treatment regime for 11q del CLL patients, resulting in effective clearance of CLL cells that are both in circulating and tissue compartments.

5.4.3 NOTCH1^{MUT} CLL cells

Chapter 4 identified that NOTCH1^{MUT} CLL cells displayed low levels of CDC and ADCC with OFA and RTX compared to cytogenetically normal CLL cells, and they also had low CD20 expression levels and high expression of CD55 (Figure 4.3 & 4.5). Our complement analysis did not reveal any deficiencies to explain this resistance against anti-CD20 MAbs. Here we demonstrate that when NOTCH1^{MUT} CLL cells were stimulated with NTL/CD154+IL-4, the mean CD20 expression falls which, in conjunction with the already low CD20 expression levels help build resistance to anti-CD20 MAbs. It is also important to establish at the molecular level whether ICN expression is up-regulated within CLL cells upon NTL/CD154+IL-4 stimulation. Research by Pozza *et.al.,* suggests that chronic activation of ICN within NOTCH1^{MUT} CLL cells causes competition between ICN and the epigenetic gene silencer HDAC for binding to the CSL transcriptional complex[233]. ICN preferentially binds to the CSL complex, unbound HDAC is then free to bind to the promoter of CD20 causing epigenetic silencing of the gene resulting in the down-regulation of CD20 surface expression on NOTCH1^{MUT} CLL cells[233]. If ICN is over expressed with NTL/CD154+IL-4 stimulation then there would be an expected down-regulation of CD20 within the NOTCH1^{MUT} CLL cells, which was observed within 50% of our NOTCH1^{MUT} CLL cohort. Recent research into CLL co-culture with BM derived stromal cells demonstrated that a significant down-regulation of CD20 was observed within CLL cells only after a 2 week time period[144]. Therefore future experiments with NOTCH1^{MUT} CLL cell co-culture with NTL/CD154+IL-4 might demonstrate more pronounced results with longer co-culture times. Interestingly results from the CLL co-culture study also showed that after 2 weeks of co-culture with BM derived stromal cells there was also an increase in CD59 expression on CLL cells, however they did not assess CD55 expression[144]. Our results suggest that CD55 is more prominently up-regulated with NTL/CD154+IL-4 stimulation which is most notable within NOTCH1^{MUT} CLL cells. NOTCH1^{MUT} CLL cells in co-culture with NTL/CD154+IL-4 stimulation displayed approximately 65% higher expression of CD55. Previous results demonstrate that there is no statistical correlation between CD55 and CD59 expression and CDC induced cell death (Figure 4.7). Therefore any changes of

CD55 and CD59 expression with NTL/CD154+IL-4 co-culture may cause no changes to anti-CD20 MAb induced CDC for CLL cells. Performing CD55 and CD59 inhibition assays in combination with OFA induced CDC on CLL cells co-cultured with NT/CD154+IL-4 stimulation may provide more insight into the effect the expression levels of these two complement inhibitory proteins have upon OFA induced CDC induction.

Experiments with NOTCH1^{MUT} CLL cells demonstrated that at 24 hr there was a rise in OFA CDC activity, indicating there is an interaction between CLL cells and NTL/CD154+IL-4 that results in an increase in CDC induction independently of changes in CD20, CD55 and CD59 expression. Therefore it would be of interest to analyse the CLL cells at the molecular level to establish if there is an activation of the *NOTCH1* pathway on NTL/CD154+IL-4 that could result in the resistance of NOTCH1^{MUT} CLL cells after 48 hr. Interestingly when OFA and RTX were co-cultured with NOTCH1^{MUT} CLL cells and NTL/CD154+IL-4 there was a steady increase in CDC overtime, therefore it appears that OFA bound to CD20, interacts or activates one or several molecular pathways that then alters the way in which these cells respond. The same response was not observed on NTL cells; therefore it seems unlikely that NTL cells express a ligand for the Notch1 receptor. Our lab has previously demonstrated an up-regulation of the NF-κB pathway in CLL cells when stimulated with NTL/CD154+IL-4, and others have identified that NF-κB can induce the expression of the Notch1 receptor ligand, Jagged1, in B-cells[217,230,369]. This suggests that NOTCH1^{MUT} CLL cells upon stimulation with NTL/CD154+IL-4 are undergoing autocrine activation of the Notch1 pathway, de-regulating the response to anti-CD20 MAbs. Jak M. *et al*. identified that the increase in RTX induced apoptosis when CLL cells were stimulated with CD40 was possibly due to the role of CD20 as a store-operated Ca^{2+} channel. They found that CD40 stimulation caused CLL cells to be sensitised to RTX-induced cell death through a rise in cytoplasmic Ca^{2+} levels, it would be interesting to establish if this was through CD20 alone or if CD20 couples with another Ca^{2+} channel when bound with RTX[176]. Increased cytoplasmic Ca^{2+} levels caused a Ca^{2+}- dependent increase in ROS production leading to programmed cell death[176]. This further highlights the need to analyse NOTCH1^{MUT} CLL cells response to NTL/CD154+IL-4 stimulation at a molecular level, which could hold the key to understanding their resistance to RTX and OFA.

NOTCH1^{MUT} CLL cells also displayed an increase in RTX mediated CDC when RTX was present in co-culture with NTL/CD154+IL-4, yet there is no clinical benefit observed for RTX when added to FC[108,372]. This suggests that the brief clinical efficacy observed with OFA is not due to OFA being bound to CLL cells within the LN for long periods of time before undergoing CDC[109].

It would appear that the reduced activity of anti-CD20 MAbs against NOTCH1^{MUT} CLL cells is due to a combination of several different factors, and not just one clear difference between these CLL cells and others. A trial investigating the effect of chlorambucil with or without OFA, observed an improvement in PFS with chlorambucil plus OFA in NOTCH1^{MUT}CLL patients[109]. However this response only occurred during the first 18 months, after which the affect was lost and PFS mirrored patients treated with chlorambucil alone in the NOTCH1^{MUT} cohort[109]. NOTCH1^{MUT} CLL cells returning into circulation after receiving Notch1 activating signals within the LNs, may have conferred resistance to anti-CD20 MAbs due to low CD20 expression. A potential explanation for the short period of effectiveness of OFA in combination with chlorambucil may be due to its high efficacy at inducing CDC on the circulating CLL cells, which will likely be a combination of CLL cells with and without NOTCH1^{MUT}. But after the clearance of these cells there is no longer effective killing of the CLL cells leaving the LNs allowing the malignant NOTCH1^{MUT} clone to emerge. Others have also reported that CLL cells with the highest expression levels of Notch1 are those located within the LNs[101].

In conclusion we have further characterised how the different CLL cytogenetic subsets affect the efficacy of anti-CD20 MAbs. For the majority of poor prognosis CLL cells, except those with NOTCH1^{MUT}, stimulation via the tissue microenvironment proves beneficial to anti-CD20 MAb activity, making OFA and RTX better immunotherapy options for targeting CLL cells within the LN than alemtuzumab.

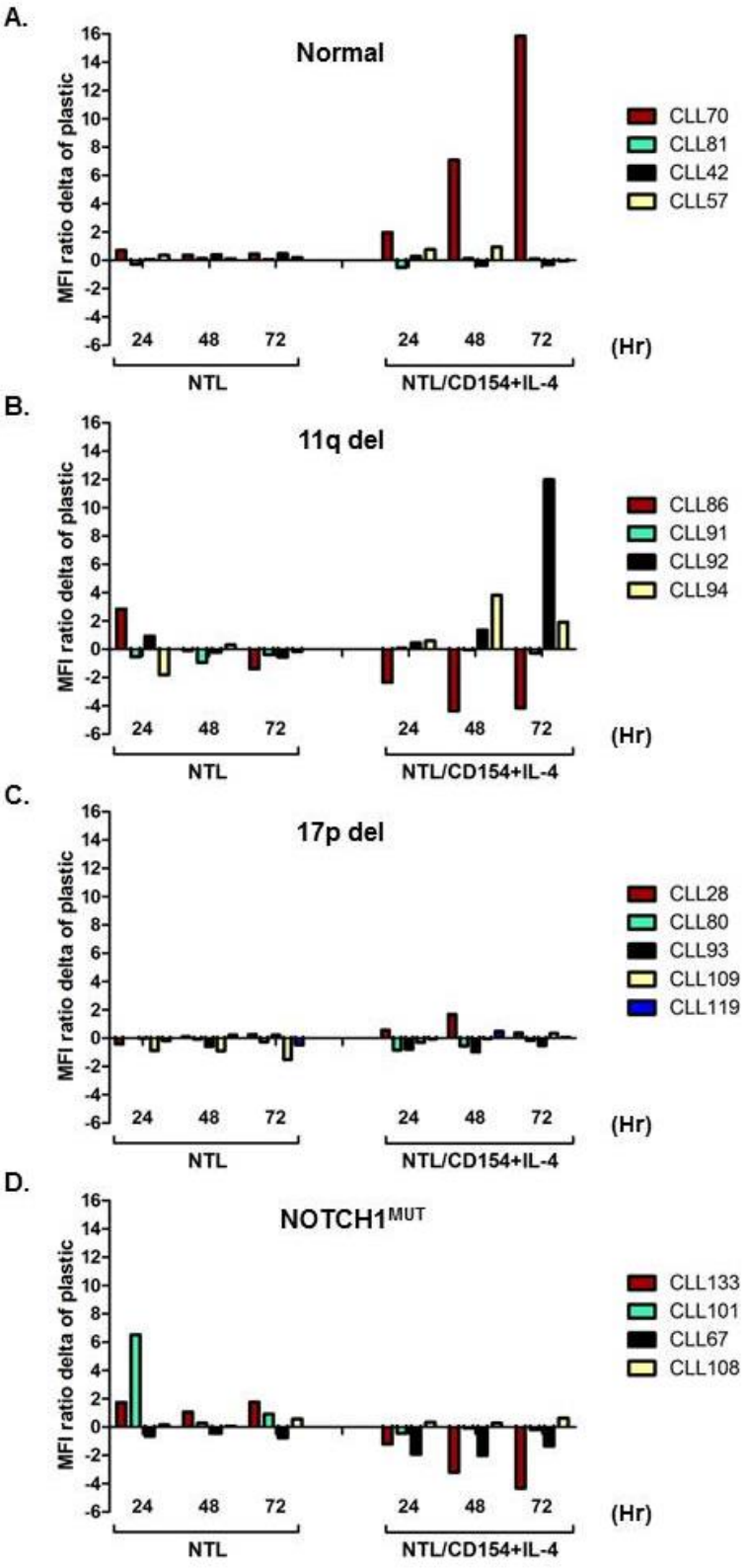

Figure 5.1 CD20 expression levels change differentially depending on the cytogenetic subset and microenvironmental stimulation

CLL cells were cultured in the three different culture systems for 24 to 72 hr. Changes in expression of CD20 was determined by flow cytometry and MFI ratio was calculated from the MFI signal from stained divided by unstained CLL cells. The MFI ratio produced on plastic was subtracted from the MFI ratios produced on NTL and NTL/CD154+IL-4. A. Cytogenetically normal (n=4). B. 11q del (n=4). C. 17p del (n=5). D. NOTCH1^{MUT} (n=4).

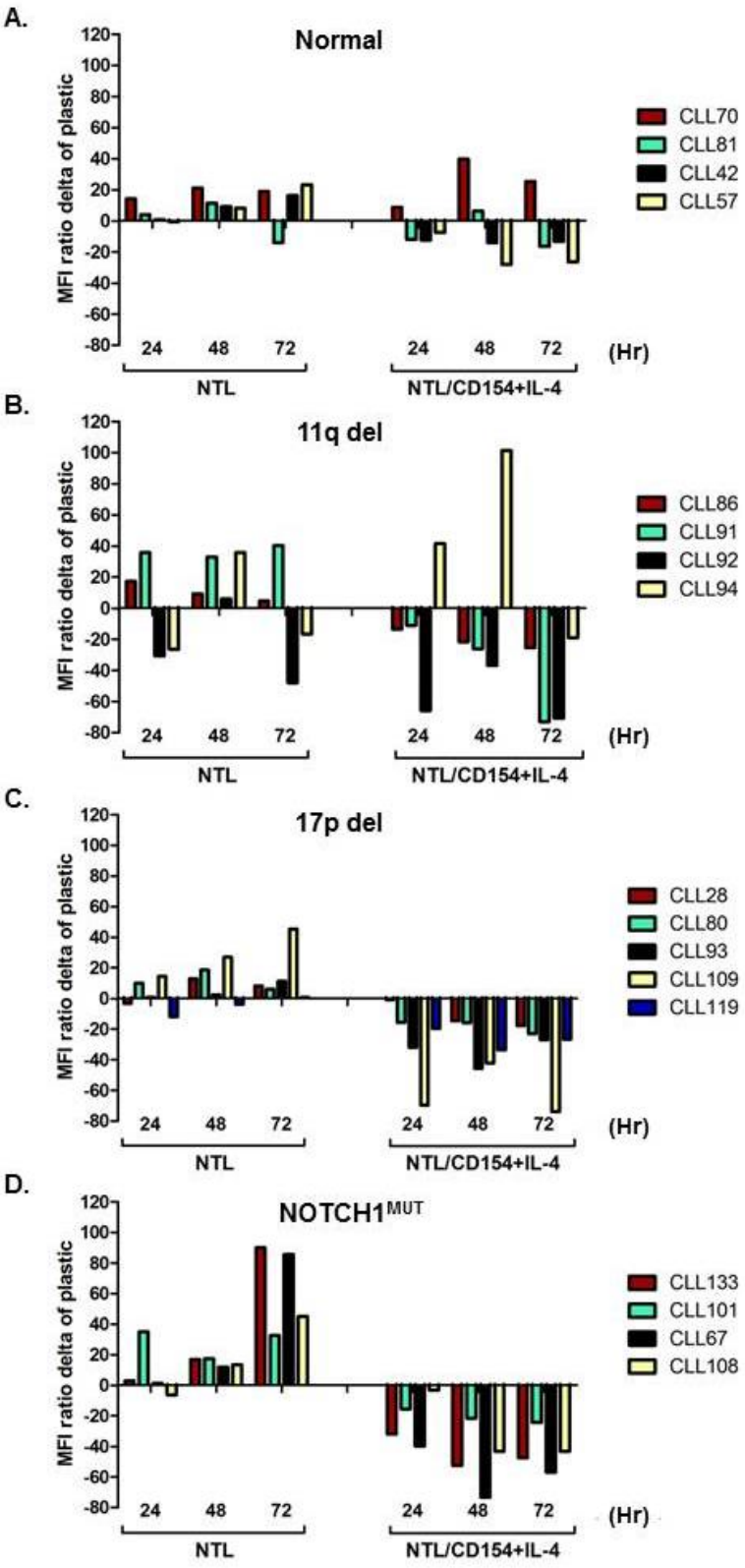

Figure 5.2 CD52 expression is down-regulated on CLL cells when cultured with NLT/CD154+IL-4

CLL cells were cultured in the three different culture systems for 24 to 72 hr. Changes in expression of CD52 was determined by flow cytometry and MFI ratio was calculated from the MFI signal from stained divided by unstained CLL cells. The MFI ratio produced on plastic was subtracted from the MFI ratios produced on NTL and CD154/IL-4. A. Cytogenetically normal (n=4). B. 11q del (n=4). C. 17p del (n=5). D. NOTCH1^{MUT} (n=4).

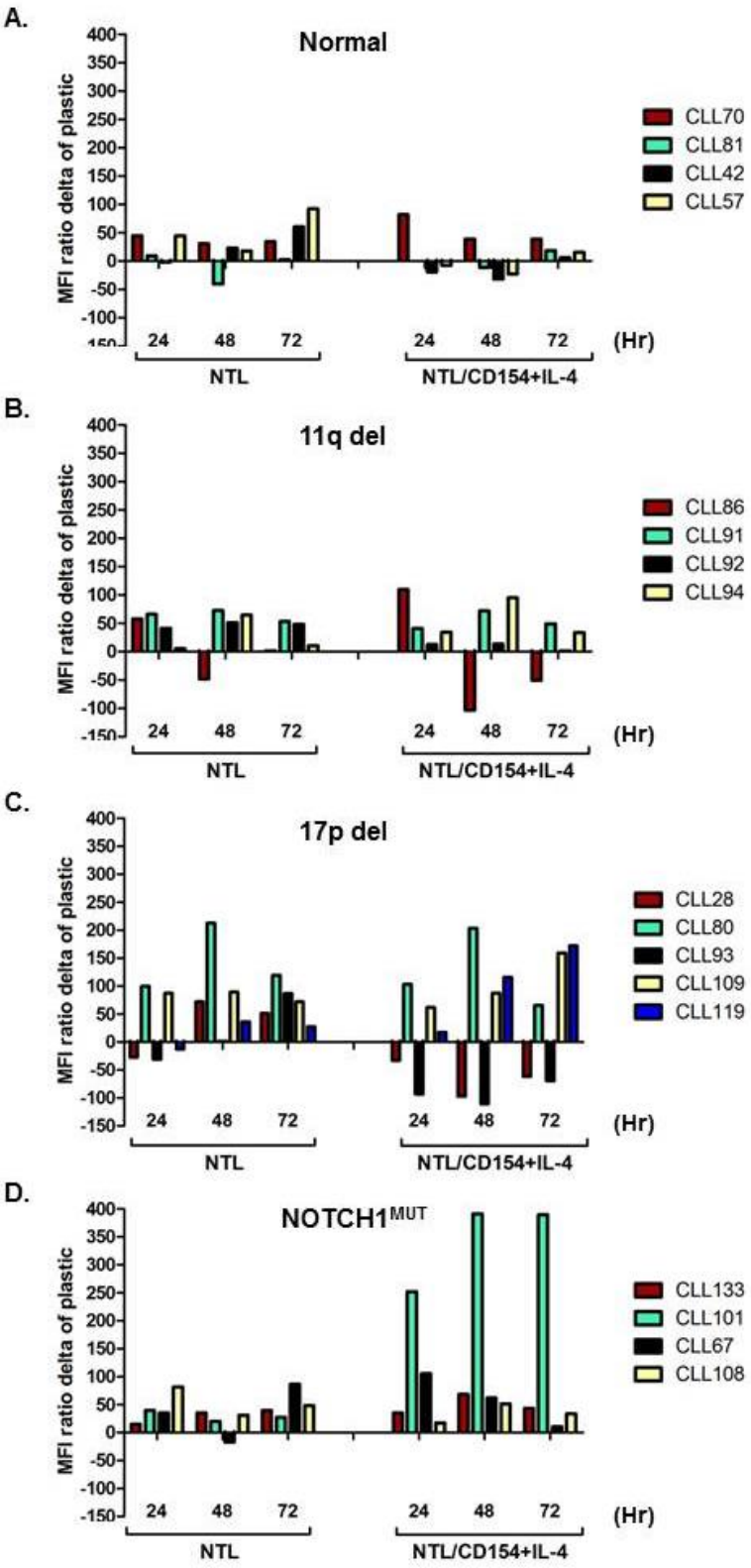

Figure 5.3 CD55 expression levels are de-regulated in poor prognostic CLL cells with microenvironmental stimulation

CLL cells were cultured in the three different culture systems for 24 to 72 hr. Changes in expression of CD55 was determined by flow cytometry and MFI ratio was calculated from the MFI signal from stained divided by unstained CLL cells. The MFI ratio produced on plastic was subtracted from the MFI ratios produced on NTL and CD154/IL-4. A. Cytogenetically normal (n=4). B. 11q del (n=4). C. 17p del (n=5). D. NOTCH1^{MUT} (n=4).

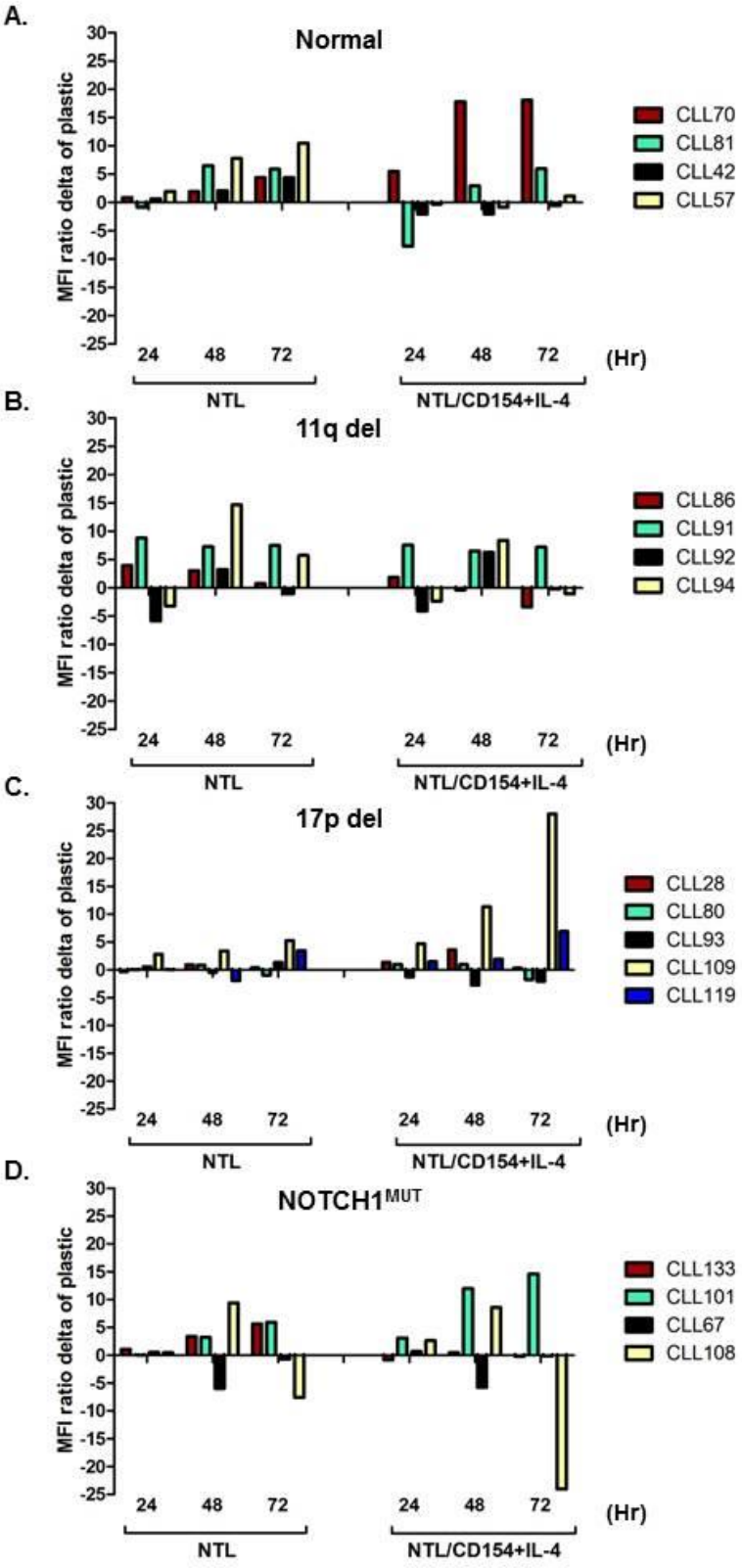

Figure 5.4 CD59 expression levels are de-regulated in CLL cells upon microenvironmental stimulation

CLL cells were cultured in the three different culture systems for 24 to 72 hr. Changes in expression of CD59 was determined by flow cytometry and MFI ratio was calculated from the MFI signal from stained divided by unstained CLL cells. The MFI ratio produced on plastic was subtracted from the MFI ratios produced on NTL and CD154/IL-4. A. Cytogenetically normal (n=4). B. 11q del (n=4). C. 17p del (n=5). D. NOTCH1^{MUT} (n=4).

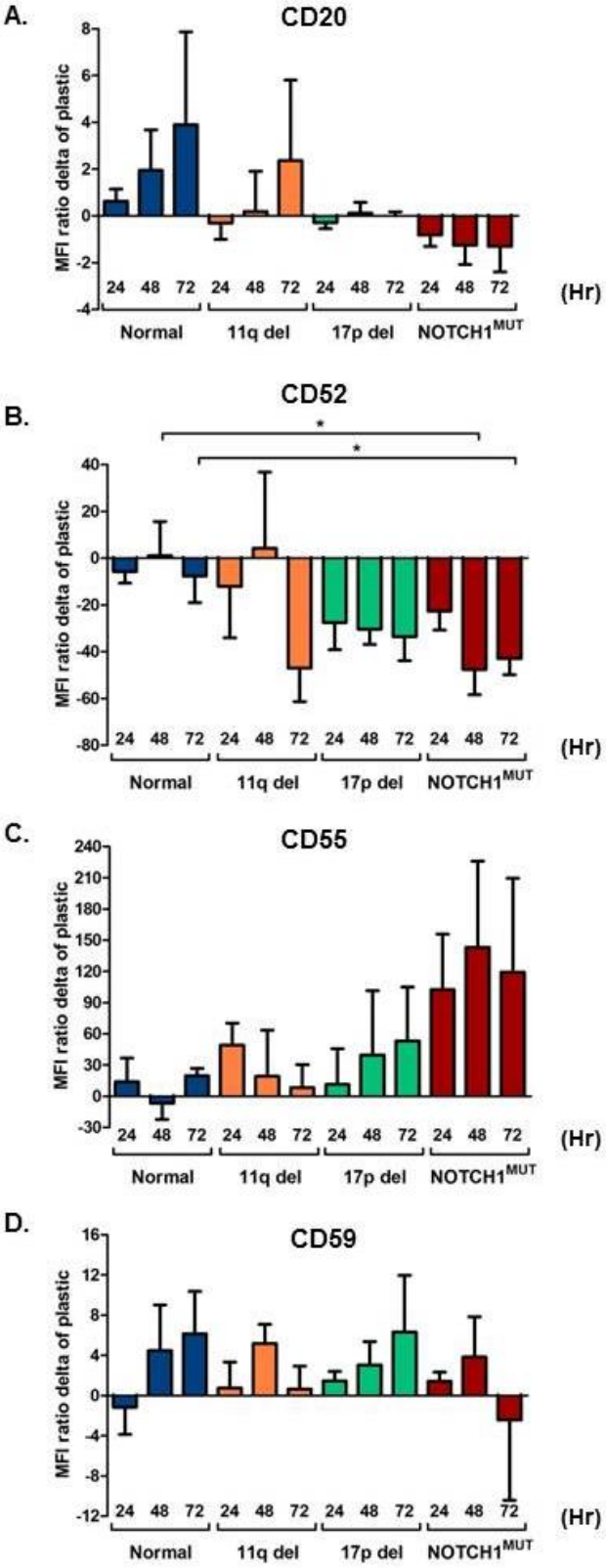

Figure 5.5 NTL/CD154+IL-4 microenvironmental stimulation alters the expression of surface markers

CLL cells were cultured on NTL/CD154+IL-4 for between 24 to 72 hr. Changes in expression of CD20, CD52, CD55 and CD59 were determined by flow cytometry and MFI ratio was calculated from the MFI signal from stained divided by unstained CLL cells. The MFI ratio produced on plastic was subtracted from the MFI ratios produced on NTL/CD154+IL-4. The mean $\pm$ SEM MFI ratio are shown from cytogenetically normal CLL samples (n=4), 11q del (n=4), 17p del (n=5) and NOTCH1^{MUT} (n=4). A. CD20 expression levels. B. CD52 expression levels. C. CD55 expression levels. D. CD59 expression levels. p values were determined by an un-paired t-test (*, $p<0.05$).

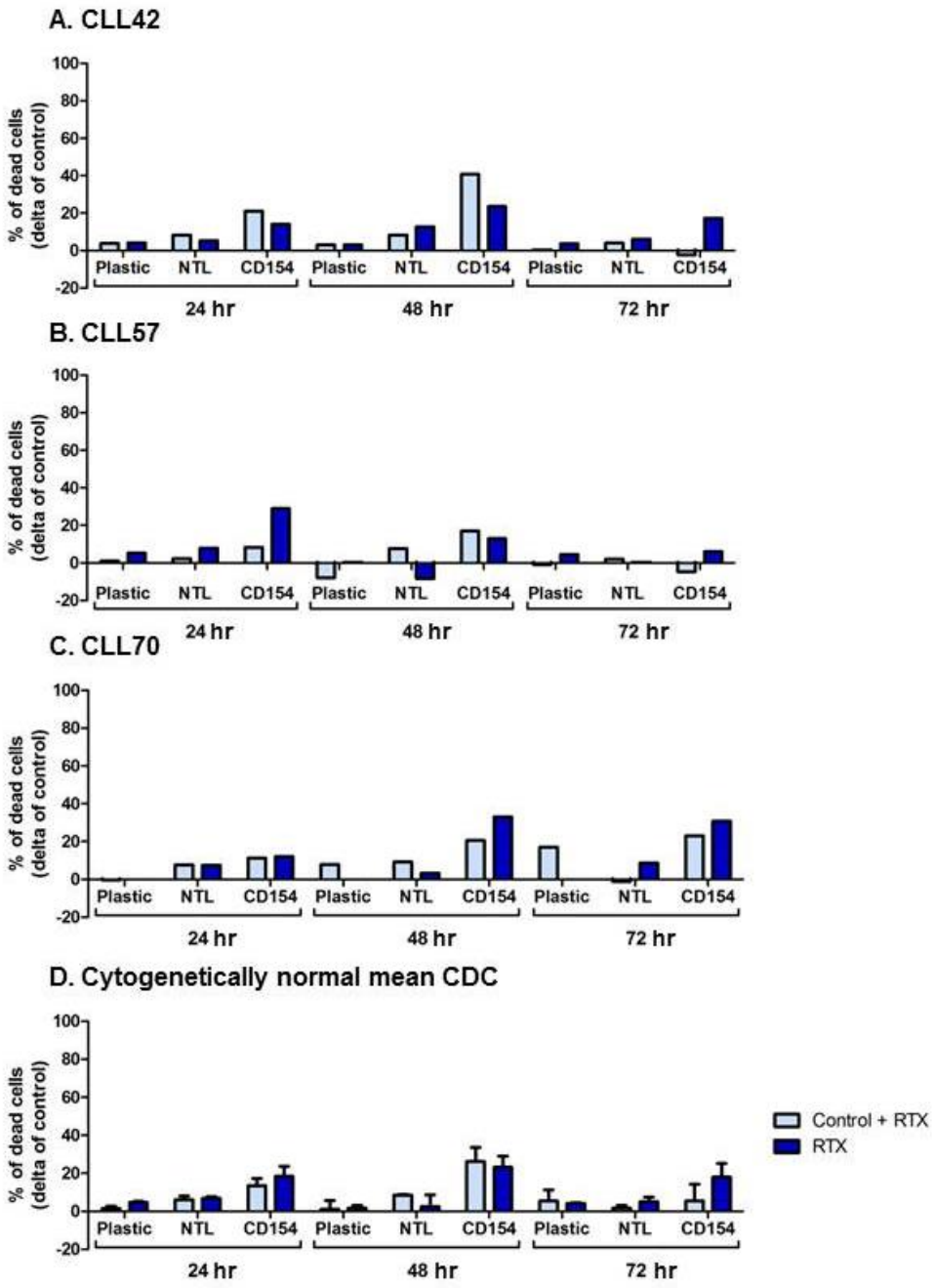

Figure 5.6 RTX CDC activity is marginally improved in cytogenetically normal CLL samples upon microenvironmental stimulation

Cytogenetically normal CLL cells were cultured on the three different culture systems; plastic , NTL or CD154 (NTL/CD154+IL-4) and were either incubated with or without RTX for between 24-72 hr. At each 24 hr interval CLL cells were removed and cells not cultured with MAb were either left without MAb or incubated for 30 min with 20 µg/ml of RTX (control + RTX), all cells then underwent CDC. The percentage of dead cells is relative to untreated control. A. CLL42. B. CLL57. C. CLL70. D. Cytogenetically normal CLL cells, mean $\pm$ SEM (n=3).

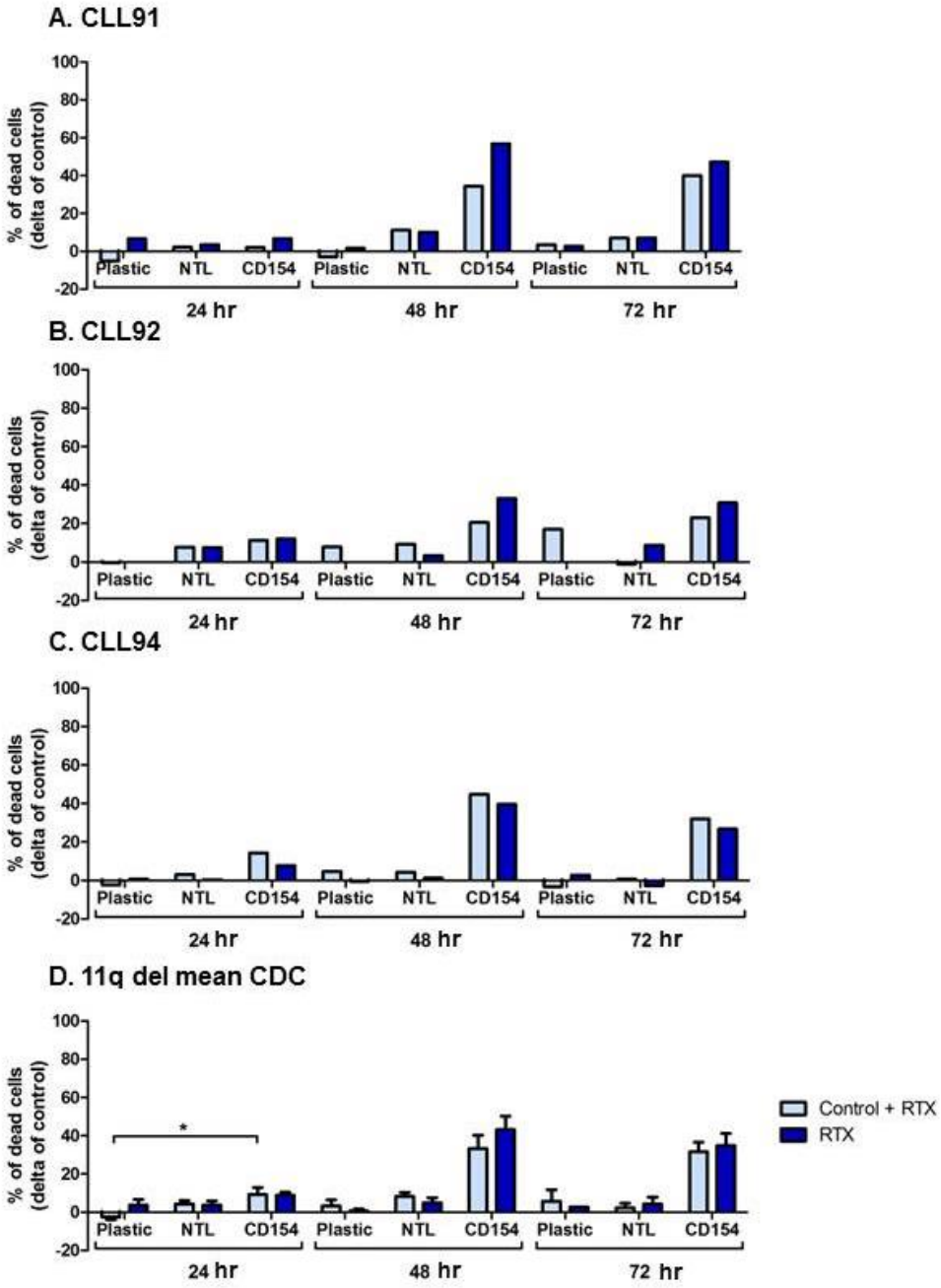

Figure 5.7 RTX CDC activity is significantly improved in 11q del CLL samples upon microenvironmental stimulation

11q del CLL cells were cultured on the three different culture systems; plastic , NTL or CD154 (NTL/CD154+IL-4) and were either incubated with or without RTX for between 24-72 hr. At each 24 hr interval CLL cells were removed and cells not cultured with MAb were either left without MAb or incubated for 30 min with 20 μg/ml of RTX (control + RTX), all cells then underwent CDC. The percentage of dead cells is relative to untreated control. A. CLL91. B. CLL92. C. CLL94. D. 11q del CLL cells, mean $\pm$ SEM (n=3). p value was determined by a paired t-test (*, $p<0.05$).

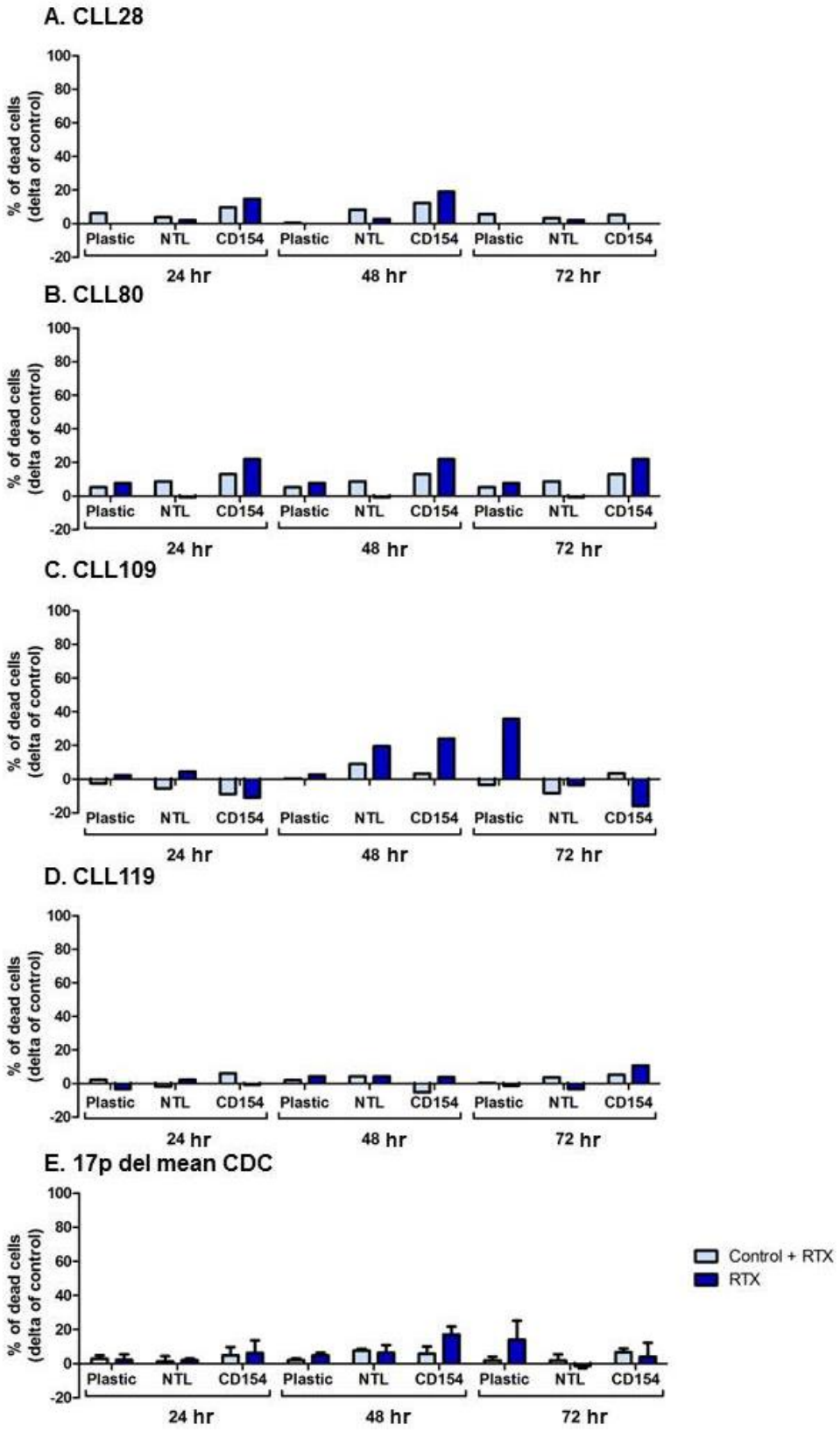

Figure 5.8 RTX CDC activity is minimal in 17p del CLL samples upon microenvironmental stimulation

17p del CLL cells were cultured on the three different culture systems; plastic , NTL or CD154 (NTL/CD154+IL-4) and were either incubated with or without RTX for between 24-72 hr. At each 24 hr interval CLL cells were removed and cells not cultured with MAb were either left without MAb or incubated for 30 min with 20 μg/ml of RTX (control + RTX), all cells then underwent CDC. The percentage of dead cells is relative to untreated control. A. CLL28. B. CLL80. C. CLL109. D. CLL119. E. 17p del CLL cells, mean $\pm$ SEM (n=4).

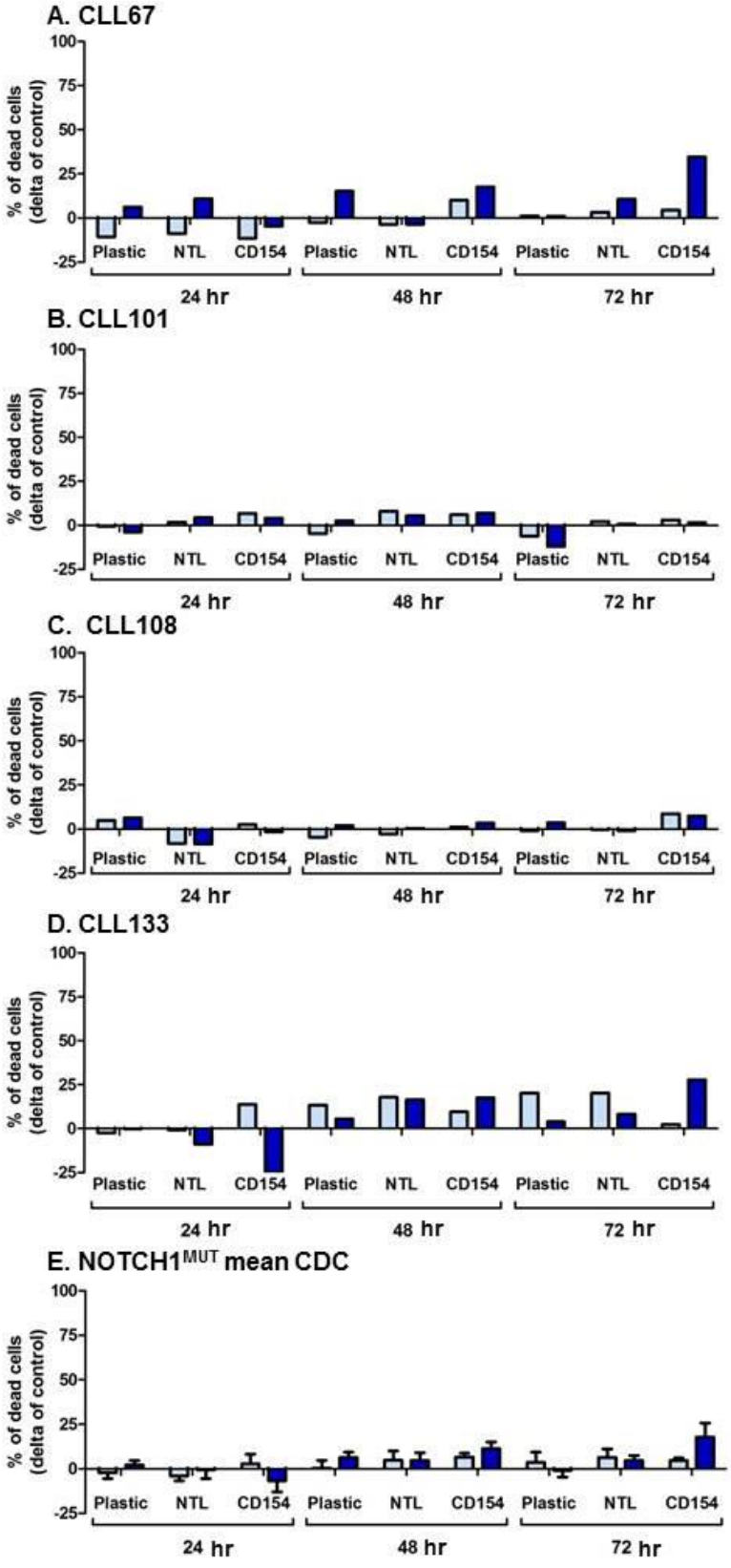

Figure 5.9 RTX CDC activity is minimal in NOTCH1^{MUT} CLL samples upon microenvironmental stimulation

NOTCH1^{MUT} CLL cells were cultured on the three different culture systems; plastic , NTL or CD154 (NTL/CD154+IL-4) and were either incubated with or without RTX for between 24-72 hr. At each 24 hr interval CLL cells were removed and cells not cultured with MAb were either left without MAb or incubated for 30 min with 20 µg/ml of RTX (control + RTX), all cells then underwent CDC. The percentage of dead cells is relative to untreated control. A. CLL67. B. CLL101. C. CLL108. D. CLL133. E. NOTCH1^{MUT} CLL cells, mean $\pm$ SEM (n=4).

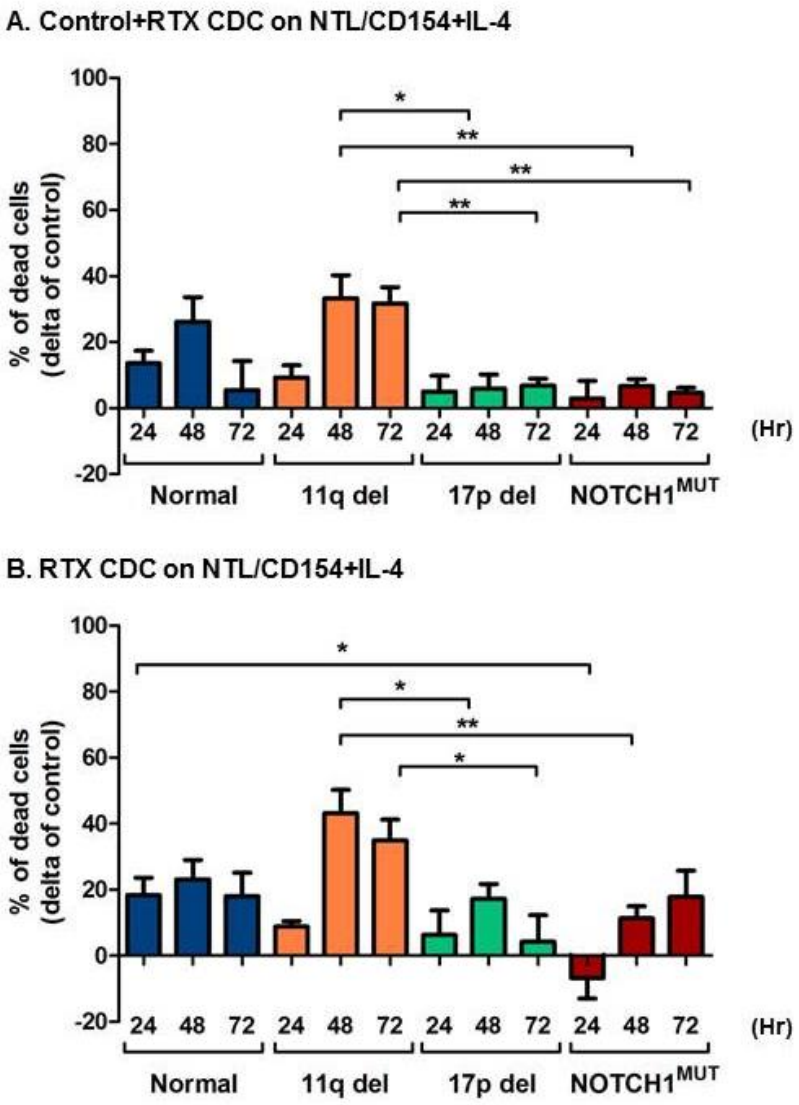

Figure 5.10 11q del CLL cells display the highest level of RTX induced CDC upon microenvironmental stimulation, and co-culture with RTX produces the highest efficacy for most CLL samples

Primary CLL cells were cultured on CD154 (NTL/CD154+IL-4) and were either incubated with or without RTX for between 24-72 hr. At each 24 hr interval CLL cells were removed and cells not cultured with MAb were either left without MAb or incubated for 30 min with 20 µg/ml of RTX (control + RTX), all cells then underwent CDC. The mean $\pm$ SEM percentage of dead cells are shown from cytogenetically normal CLL samples (n=3), 11q del (n=3), 17p del (n=4). D. NOTCH1^{MUT} (n=4). The percentage of dead cells is relative to untreated control. A. CLL cells cultured on CD154 without MAb (control + RTX). B. CLL cells cultured with MAb. p values between different cytogenetic subsets were determined by an un-paired t-test, and p values within a cytogenetic subset were determined by a paired t test (*, $p<0.05$; **, $P<0.01$).

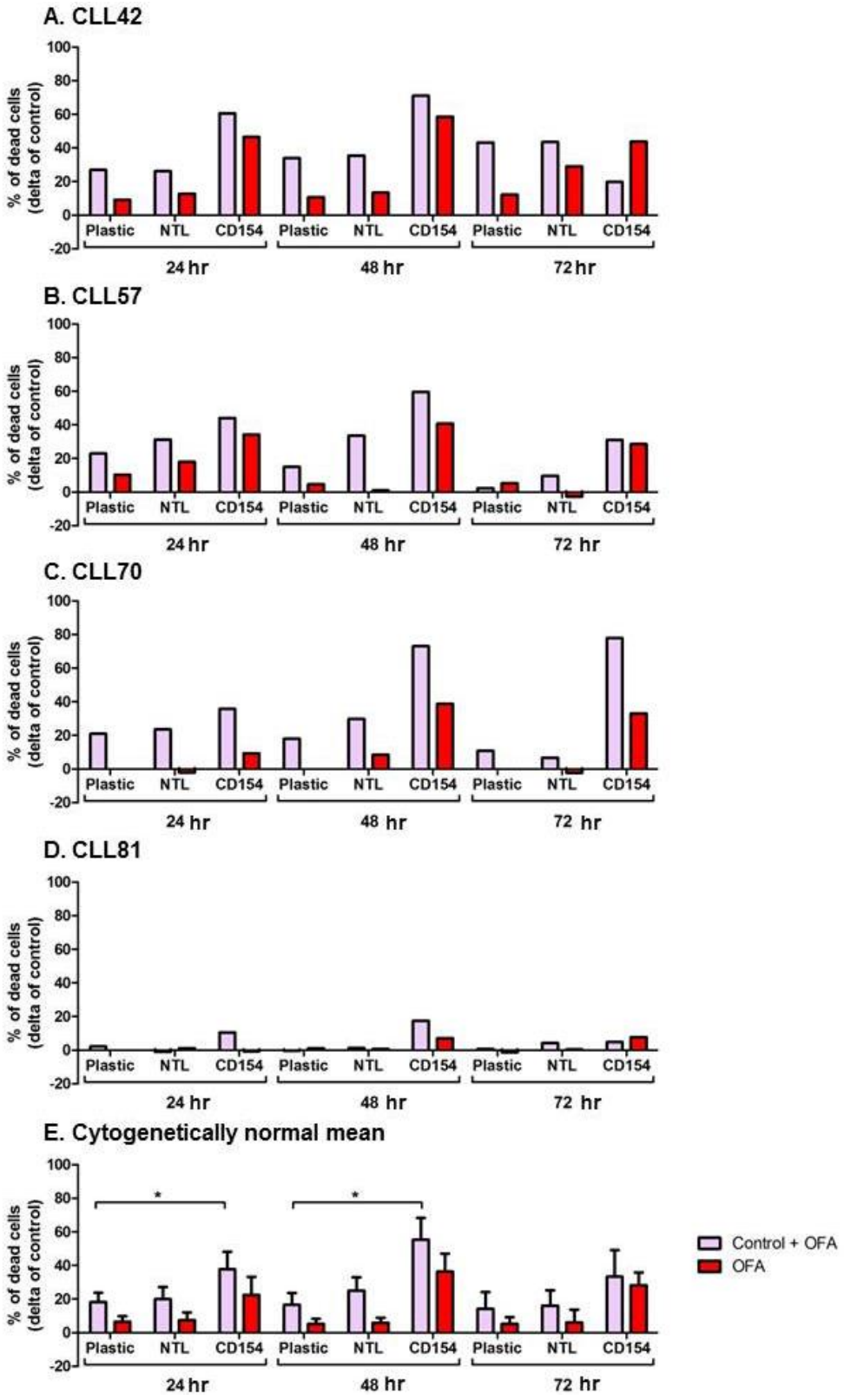

Figure 5.11 OFA CDC efficacy is significantly improved in cytogenetically normal CLL samples upon microenvironmental stimulation

Cytogenetically normal CLL cells were cultured on the three different culture systems; plastic , NTL or CD154 (NTL/CD154+IL-4) and were either incubated with or without OFA for between 24-72 hr. At each 24 hr interval CLL cells were removed and cells not cultured with MAb were either left without MAb or incubated for 30 min with 20 μg/ml of OFA (control + OFA), all cells then underwent CDC. The percentage of dead cells is relative to untreated control. A. CLL42. B. CLL57. C. CLL70. D.CLL81. E. Cytogenetically Normal CLL cells, mean $\pm$ SEM (n=4). p values were determined by a paired t-test (*, $p<0.05$).

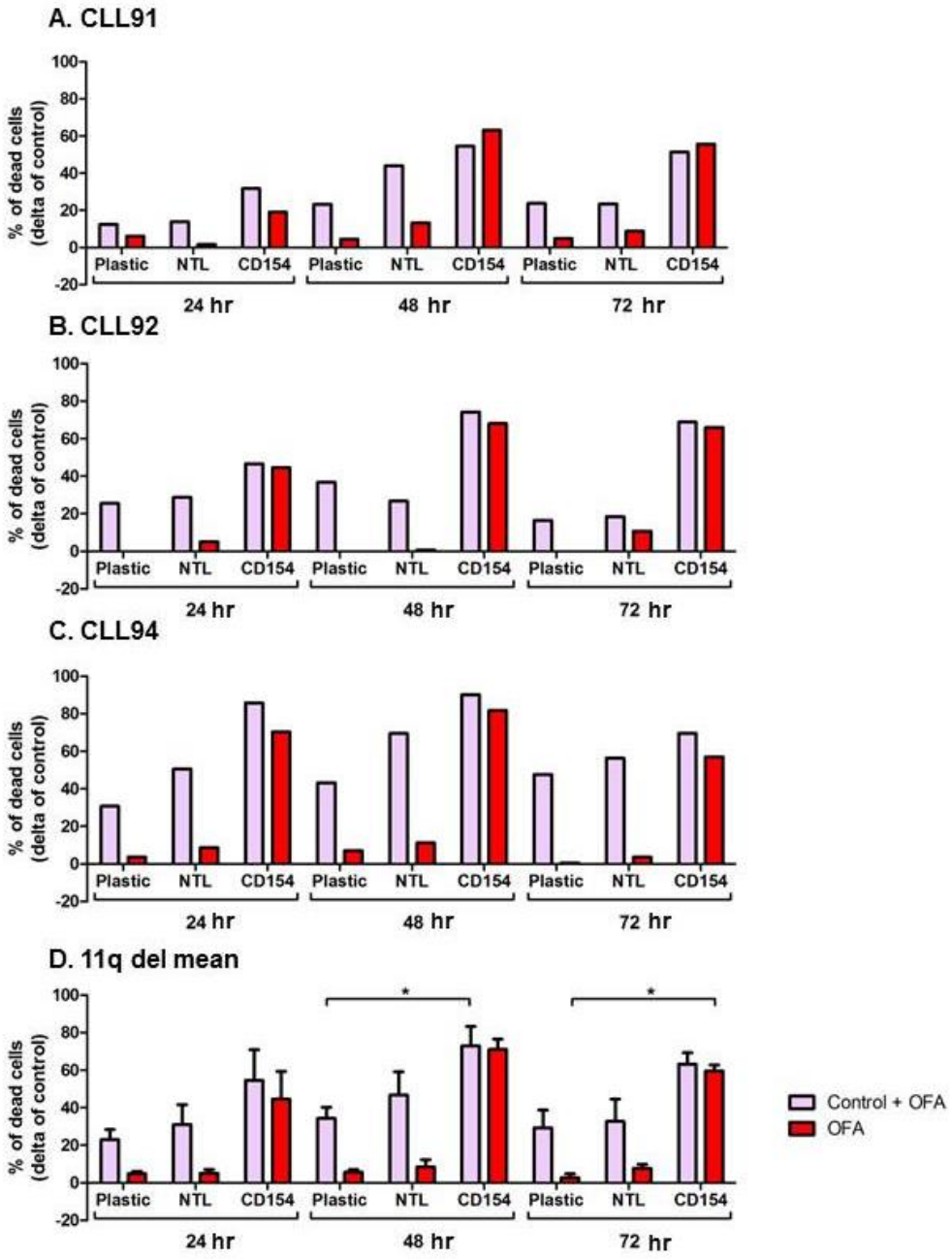

Figure 5.12 OFA CDC activity is significantly improved in 11q del CLL samples upon microenvironmental stimulation

11q del CLL cells were cultured on the three different culture systems; plastic , NTL or CD154 (NTL/CD154+IL-4) and were either incubated with or without OFA for between 24-72 hr. At each 24 hr interval CLL cells were removed and cells not cultured with MAb were either left without MAb or incubated for 30 min with 20 µg/ml of OFA (control + OFA), all cells then underwent CDC. The percentage of dead cells is relative to untreated control. A. CLL91. B. CLL92. C. CLL94. D. 11q del CLL cells, mean $\pm$ SEM (n=3). p values were determined by a paired t-test (*, $p<0.05$).

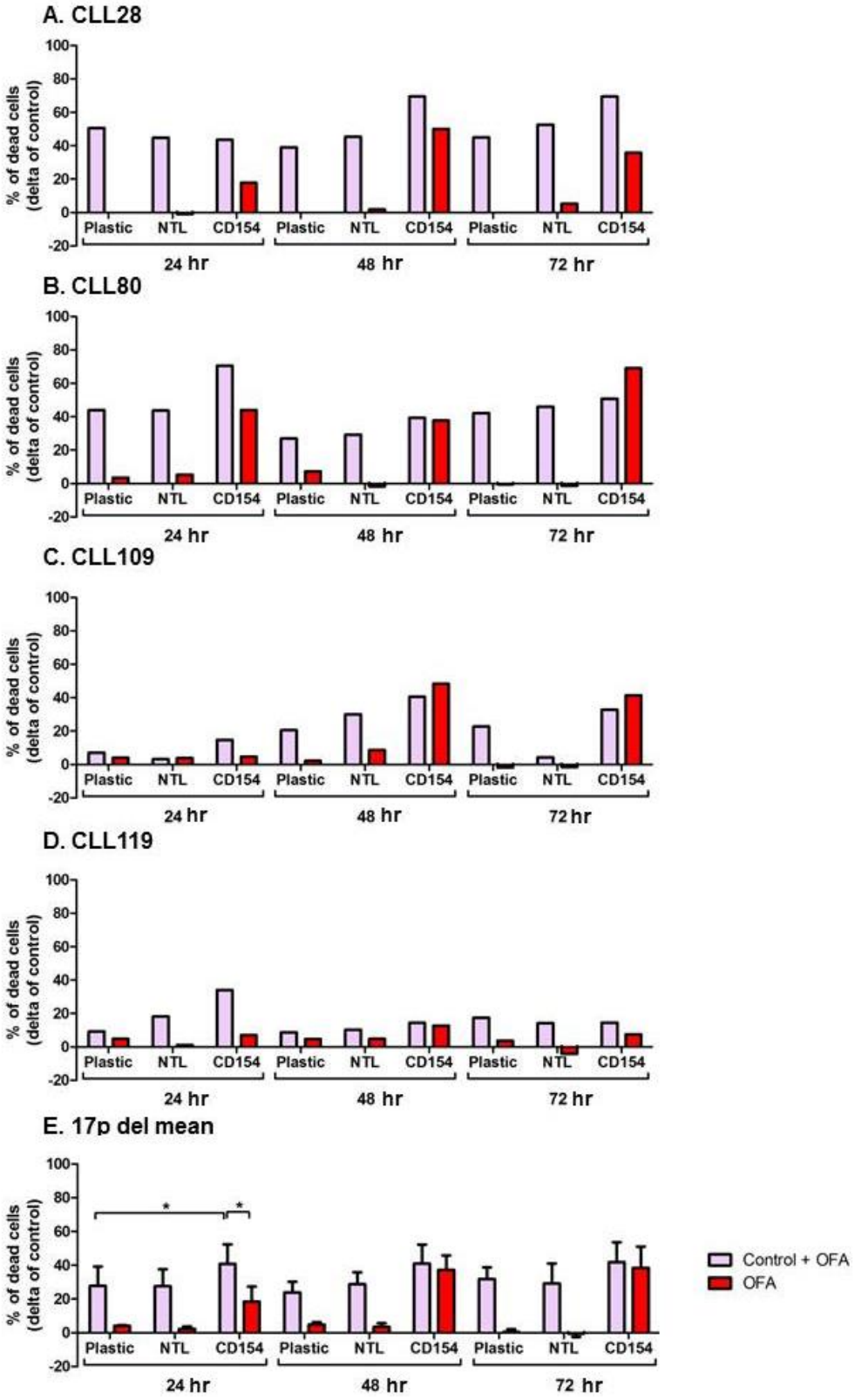

Figure 5.13 The significant improvement in OFA induced CDC in 17p del CLL samples upon microenvironmental stimulation is relatively short lived

17p del CLL cells were cultured on the three different culture systems; plastic , NTL or CD154 (NTL/CD15+/IL-4) and were either incubated with or without OFA for between 24-72 hr. At each 24 hr interval CLL cells were removed and cells not cultured with MAb were either left without MAb or incubated for 30 min with 20 μg/ml of OFA (control + OFA), all cells then underwent CDC. The percentage of dead cells is relative to untreated control. A. CLL28. B. CLL80. C. CLL109. D. CLL119. E. 17p del CLL cells, mean $\pm$ SEM (n=4). p values were determined by a paired t-test (*, $p<0.05$).

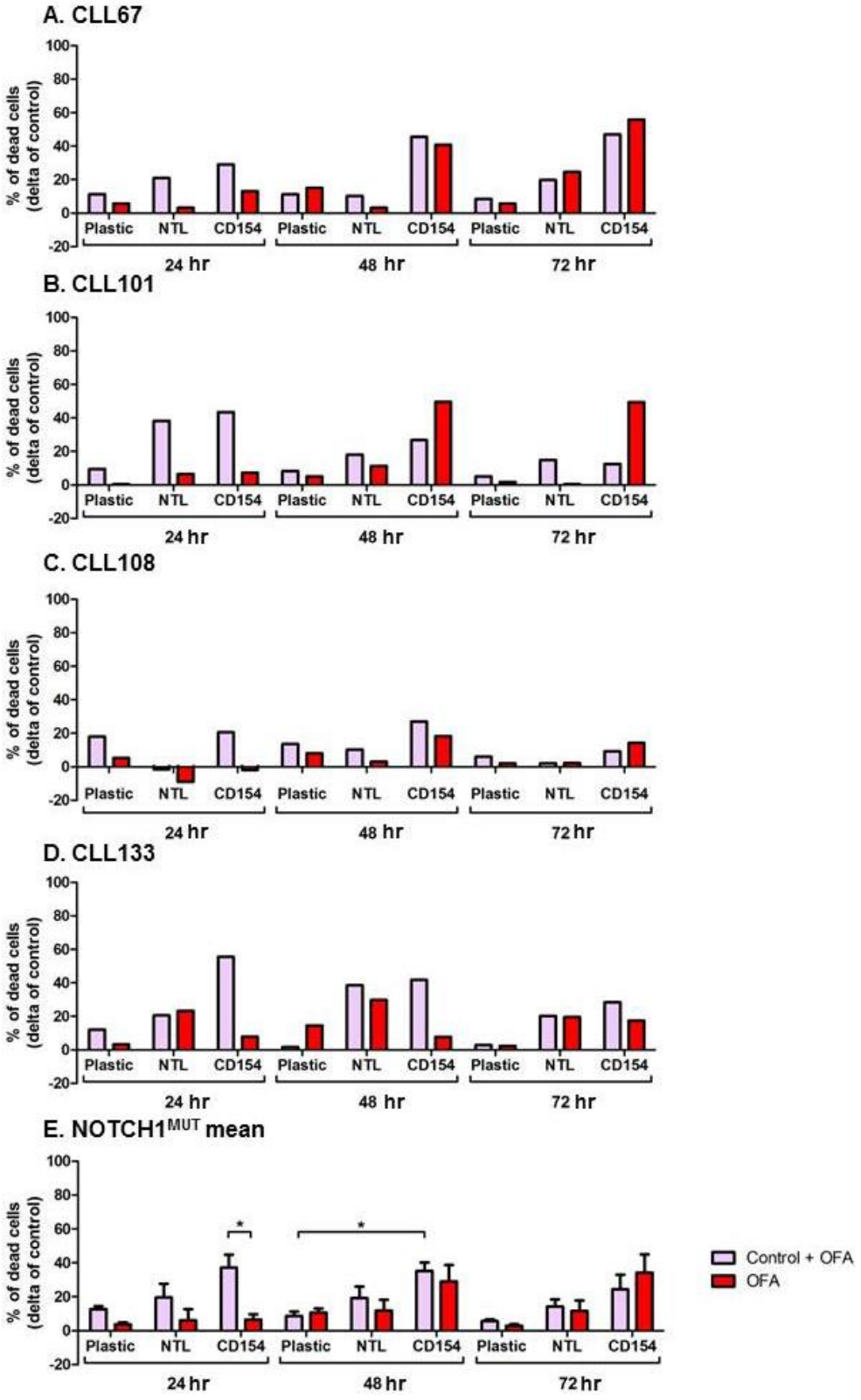

Figure 5.14 OFA CDC activity is significantly improved in NOTCH1^{MUT} CLL samples upon microenvironmental stimulation

NOTCH1^{MUT} CLL cells were cultured on the three different culture systems; plastic , NTL or CD154 (NTL/CD154/IL-4) and were either incubated with or without OFA for between 24-72 hr. At each 24 hr interval CLL cells were removed and cells not cultured with MAb were either left without MAb or incubated for 30 min with 20 µg/ml of OFA (control + OFA), all cells then underwent CDC. The percentage of dead cells is relative to untreated control. A. CLL67. B. CLL101. C. CLL108. D. CLL133. E. NOTCH1^{MUT} CLL cells, mean $\pm$ SEM (n=4). p values were determined by a paired t-test (*, $p<0.05$).

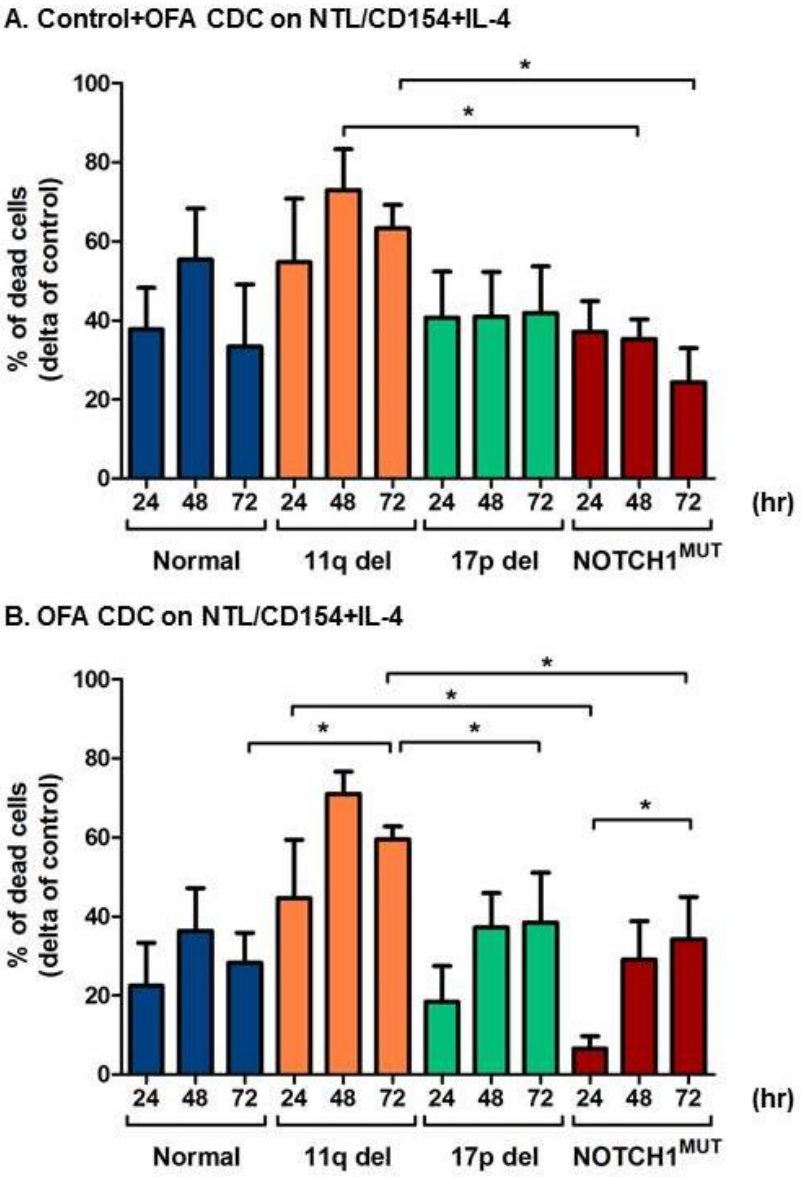

Figure 5.15 11q del CLL cells display the highest level of OFA induced CDC upon microenvironmental stimulation

Primary CLL cells were cultured on CD154 (NTL/CD154/IL-4) and were either incubated with or without OFA for between 24-72 hours. At each 24 hour interval CLL cells were removed and cells not cultured with MAb were either left without MAb or incubated for 30 mins with 20 μg/ml of OFA (control + OFA), all cells then underwent CDC. The mean ± SEM percentage of dead cells are shown from cytogenetically normal CLL samples (n=4), 11q del (n=3), 17p del (n=4). D. NOTCH1^{MUT} (n=4). The percentage of dead cells is relative to untreated control. A. CLL cells cultured on CD154 without MAb (control + OFA). B. CLL cells cultured with MAb. p values between different cytogenetic subsets were determined by an un-paired t-test, and p values within a cytogenetic subset were determined by a paired t test (*, $p<0.05$).

6 Molecular profile of NOTCH1^{MUT} CLL cells

6.1 Introduction

Type I anti-CD20 MAbs function predominantly through harnessing the body's innate immune system for the induction of ADCC, CDC and phagocytosis[262]. Their ability to cause direct cell death through the induction of apoptosis is ambiguous and currently not considered clinically relevant. Previous research into the mechanisms relating to RTX and OFA resistance have focused upon the expression levels of complement inhibitory proteins and CD20[308,310,312]. CDC induction is critically dependent on expression levels of the target antigen and loss of CD20 expression on the surface of the CLL is an important contributing factor in MAb resistance[254,311,317,319]. Recent genome sequencing studies have identified recurrent mutations in *NOTCH1*, observed in 12% of CLL cases[88]. Clinical trials have indicated that addition of OFA and RTX to chemotherapy provides no clinical benefit to NOTCH1^{MUT} CLL patients[108,109]. The genetic mechanisms that could result in resistance to anti-CD20 MAbs are not well elucidated.

Recent research suggests that the mechanism behind the reduced activity of anti-CD20 MAbs observed in NOTCH1^{MUT} CLL cells is due to their reduced expression of CD20[233]. They attributed the lower expression of CD20 to increased expression at the mRNA and protein level of *HDAC1* and *HDAC2*[233]. *HDAC* genes encode for histone deacetylase proteins which act as epigenetic regulators of gene expression by catalysing the removal of acetyl groups from core histones. This in turn results in chromatin compaction leading to the repression of gene transcription[359,360]. Our research confirmed these findings with lower levels of CD20 observed in NOTCH1^{MUT} CLL patients cells when compared to normal cytogenetic CLL cells, however 17p del CLL cells also expressed lower levels of CD20 and yet had marginally higher levels of OFA induced CDC (Figure 4.3 & 4.5). These data suggest that although CD20 levels are an important contributing factor, there is likely to be a complicated interplay with other factors resulting in the reduced activity of anti-CD20 MAbs against NOTCH1^{MUT} CLL cells.

CLL cells within the LN and BM receive pro-survival signals from cross-talk with accessory cells within the microenvironmental niche, which leads to an up-

regulation of the Bcl-2 family anti-apoptotic genes such as Bcl-X_L, Bfl-1 A1 and MCL-1[139,168]. Fludarabine and chlorambucil which cause cell death through the induction of apoptosis are consequently less active against CLL cells upon microenvironmental stimulation *in vitro*[141,190]. The Notch1 pathway has also been shown to be activated in CLL cells within the LN/BM, therefore these CLL cells may also be gaining further chemotherapeutic resistance against anti-CD20 MAbs in a Notch1 dependent manner[226-228,232]. Our results thus far from the four distinct cytogenetic subsets of CLL patients, indicate that the activity of anti-CD20 MAbs are associated with more than just expression of CD20 and complement inhibitory proteins. Therefore more detailed molecular analysis is required to determine the pathways involved in MAb therapy resistance.

Several important mechanisms are known to be involved in chemoresistance in cancer including alterations in the cell cycle, pathways involved in apoptosis and cell signalling. Indeed the poor prognostic cytogenetic aberrations 11q (*ATM*) and 17p (*TP53*) del both demonstrate different susceptibility to anti-CD20 MAbs. *TP53* encodes for p53, a key player in the regulation of uncontrolled cell cycle progression. p53 activity is crucial for preventing the replication of cells with DNA damage, by regulating the transition of dividing cells from G1 to S phase [367,373,374]. *ATM* is also involved in stopping DNA damage from entering into the genetic make-up of the cell, becoming activated in the presence of undesired double strand breaks caused by either an endogenous or DNA damaging agent, and halts the cell at either G1/S or G2/M phase by preventing Cdk activity[77,79,80]. Both these genetic aberrations contain genes involved in DNA damage repair, yet our research suggests that like $NOTCH1^{MUT}$, CLL patients with 17p del have reduced susceptibility to anti-CD20 MAbs through a down-regulation of CD20. Whereas 11q del CLL samples demonstrate enhanced susceptibility to RTX and OFA through low levels of complement exhaustion, high CD20 expression levels and high CDC levels which were further improved with NTL/CD154+IL-4 co-culture.

This demonstrates that although the role and function of CD20 is not fully elucidated in CLL there is clearly a complex interplay with other genetic pathways that may result in evasion of MAb therapy. This further highlights the importance for understanding the genetics of CLL cells that have evaded anti-CD20 MAbs tumour lysis, and for understanding the different responses of the

individual cytogenetic sub-sets to anti-CD20 MAbs. Identifying genes differentially regulated in CLL cells that have evaded OFA induced CDC may lead to the identification of a drugable target which could aid the activity of anti-CD20 MAbs.

6.2 Aim

The main focus was to determine the molecular profile of NOTCH1^{MUT} CLL cells compared to other cytogenetic subsets of CLL, to elucidate the potential mechanisms by which NOTCH1^{MUT} CLL cells evade anti-CD20 MAbs. To accomplish this we aimed to:

- Identify genes involved in cell cycle, apoptosis and cell signalling that are de-regulated in CLL cells that have evaded OFA induced CDC;
- Characterise differences in gene expression levels of key genes involved in the NOTCH1 pathway in the different CLL cytogenetic subsets;
- Identify a gene signature de-regulated in our NOTCH1^{MUT} CLL cohort compared to other CLL cohorts, and investigate this further using microenvironmental stimulation (NTL/CD154+IL-4 co-culture) with and without the presence of OFA treatment.

6.3 Results

Results from the previous chapters have highlighted that NOTCH1^{MUT} CLL cells are resistant to anti-CD20 MAbs, however the mechanisms surrounding this resistance are still unclear. Therefore we aim to elucidate the molecular profile of NOTCH1^{MUT} CLL cells to determine a potential cause for resistance.

6.3.1 Genomic mutations within CLL and NOTCH1^{MUT} CLL patients

CLL samples identified as being positive for *NOTCH1* mutation by ARMS PCR, together with CLL samples that were cytogenetically normal, were sequenced and analysed by Oxford BRC Molecular Diagnostic Laboratory in collaboration with Professor Anna Schuh (Figure 6.1). Mutations were observed in 18 different genes, the most frequently of which were within *ATM*, followed by *TP53*. *ATM* and *TP53* are associated with 11q and 17p del cytogenetic abnormalities respectively and result in a more aggressive poor prognostic disease. Of the samples assessed only 14% displayed no genomic mutation (Figure 6.1C). The NOTCH1^{MUT} status for two CLL samples was confirmed and two samples that were identified as being partially positive by ARMS PCR were determined to carry low frequency of mutation and were therefore excluded from the NOTCH1^{MUT} cohort. Two CLL patients (CLL90 and CLL125) had mutations in *FBXW7*. *FBXW7* targets ICN for ubiquitination, and mutations within this gene in CLL are thought to abrogate its function therefore this could result in a NOTCH1^{MUT} phenotype[95]. Consequently these samples were removed from the cytogenetically normal cohort of CLL samples.

6.3.2 Gene regulation changes following OFA induced CDC

Results from Chapter 5 demonstrated that there was an increase in OFA induced CDC for CLL cells co-cultured with NTL/CD154+IL-4. However despite this a substantial proportion of CLL cells escape OFA induced CDC. The evasion of CDC induction is most notable within our NOTCH1^{MUT} CLL cohort (Figure 5.15). Therefore it was important for us to establish whether the cells escaping OFA induced CDC were altering particular gene pathways to escape lysis. The experimental design is discussed in more detail in section 2.5.2 and shown in Figure 2.1. Briefly, CLL cells were cultured on NTL/CD154+IL-4 for 24 hr prior to

OFA treatment. OFA was present in culture for a further 24 hr, thereafter CLL cells underwent CDC (Figure 6.2), and surviving cells were placed back into co-culture with NTL/CD154+IL-4 for an additional 24 hr prior to RNA extraction. RNA was screened for 181 genes involved in different key pathways associated with CLL and tumourgenesis, using Fluidigm array analysis. In support of our previous analysis (Figure 5.15), NOTCH1^{MUT} CLL cells displayed significantly less CDC than both normal and 11q del CLL cells (Figure 6.2). CDC induction levels were used to provide a cut-off for RNA extraction, 30% or more CDC was deemed sufficient to establish a gene expression signature for CLL cells escaping OFA induced CDC. Therefore two NOTCH1^{MUT} and one 17p del CLL sample were excluded from gene analysis.

Following analysis of our CLL samples no distinct pattern was observable, genes that showed significant change in expression levels did not belong to any one particular pathway, or cellular process such as evading apoptosis. Of the genes analysed, three were consistently up-regulated in CLL cells evading OFA CDC (Figure 6.3). Interestingly one of the genes, *CD247* encodes for T cell receptor CD3ζ chain, which forms part of the TCR-CD3 complex. In particular the ζ chain is important for intracellular signal transduction in T cells[375]. MMPs are a large family of matrix metallopeptidase enzymes which have been linked with tumour growth and metastasis and are involved in different biological processes from cell migration to tissue repair. *MMP9* in particular is the principle MMP produced by lymphocytes associated with the digestion of the main component of basement membranes, type IV collagen, and plays an important role in CLL cell migration[376-378]. The third gene, *GATA3* is a transcription factor more commonly associated with T cell development[379]. When gene expression levels were compared against the percentage of CLL cells killed by CDC, *CD247* displayed a nearly significant positive linear correlation ($p=0.0571$, $r^2= 0.3456$) (Figure 6.4A). *GATA3* did not display a positive linear correlation with CDC (Figure 6.4Bi). However when expression levels were separated depending on the cytogenetic subset, 11q del subset showed a skew towards greater up-regulation of *GATA3* (Figure 6.4Bii), than cytogenetically normal CLL samples that had comparable induction of CDC (61.6 and 65.3% of dead cells respectively). *MMP9* expression displayed a strong positive linear correlation with CDC levels ($p=0.0057$, $r^2= 0.6876$) (Figure 6.4C). These data suggest that following OFA CDC induction

there was an up-regulation of genes involved in cross-talk to T cells, and tissue invasion, suggesting that the cells remaining following OFA CDC are those with the potential to migrate into either the LN or BM.

6.3.3 Gene Expression Profiling (GEP)

To assess the molecular profile of CLL patients, RNA was extracted from peripheral blood samples and Fluidigm analysis was performed for selected genes. Gene expression levels were determined relative to normal healthy B cells unless otherwise stated. The panel of genes selected were linked to CLL progression and poor prognosis phenotypes. Hierarchical clustering was performed based on the gene expression levels (Figure 6.5). Of the 44 genes analysed 10 were unchanged, 11 were up-regulated, 14 were down-regulated and 9 were differentially expressed between the different CLL patient samples examined. Several genes had similar expression between CLL cells and B cells, such as *NFATC3* and *MAX*. Whereas *AXIN2* displayed elevated expression in CLL cells compared to B cells as did *PRKCA* although expression varied from sample to sample. A cluster of 6 genes were identified as being consistently up-regulated in the CLL patients cells, some of which were associated with cell cycle progression such as *E2F3, CDK2 and CCND1* (Figure 6.5).

Several genes were not included in the heat map due to extremes in gene expression levels or loss of expression in the CLL cells, these are shown in Figure 6.6. *FOS* was down-regulated in CLL cells compared to B cells, with 17p del subset displaying a slightly elevated expression compared to the other CLL subsets (Figure 6.6A). Interestingly 11q del CLL cells had markedly reduced expression of *GATA3* compared to normal B cells, approximately 30 fold less. NOTCH1^{MUT} CLL cells displayed lower expression levels of *GATA3,* however this was only around a 2.5 fold reduction in expression (Figure 6.6B). Therefore it would appear that 11q del CLL cells display a bias towards up-regulating this gene within cells that have evaded OFA CDC in comparison to unstimulated CLL cells within the peripheral blood. Several CLL samples lacked *MMP9* expression, on average only 40% of normal CLL and NOTCH1^{MUT} CLL samples exhibited detectable *MMP9* expression (Figure 6.6C). However none of the 11q del CLL samples assessed had any detectable *MMP9* expression, whereas all 17p del CLL samples had some expression albeit very low in two samples. This suggests that

11q del CLL cells switch on and up-regulate *MMP9* expression following NTL/CD154+IL-4 stimulation and exposure to OFA induced CDC.

6.3.3.1 Cell cycle genes

Cell cycle genes are very important determinants for the aggressiveness of many different cancers, through their effect on cell cycle arrest and proliferation rates. Although heatmaps provide a valuable tool for observing global changes in gene expression levels, subtle differences in expression levels between the different cytogenetic subsets were not easily observed. A significant up-regulation of *CCND1* was detected in all of our CLL samples compared to B cells (Figure 6.7A), with normal cytogenetic CLL cells displaying significantly higher expression than NOTCH1^{MUT} CLL cells. Although not significant, *CCNE2* expression was also higher in cytogenetically normal CLL cells when compared against 11q del CLL cells, which displayed 2.5 fold lower mean expression levels (Figure 6.7B; p=0.0727). *CDK2* expression was elevated in all CLL subsets compared with normal B cells (Figure 6.7C). *CDKN1A,* which encodes the Cdk inhibitor p21$^{WAF1/CIP1}$, was expressed approximately 10 fold lower in CLL cells compared to normal B cells (Figure 6.7D). 17p del subset displayed significantly lower expression of *CDKN1A* than 11q del CLL samples. Our data demonstrates that genes involved in cell cycle progression are de-regulated in CLL, which may aid in the progression of the disease through altered proliferation rates and defects in cell cycle arrest. However, our findings indicate that the different cytogenetic sub-groups differentially regulate cell cycle genes in distinct ways, highlighting the heterogeneity of the disease. Some of these findings may relate to the loss of p53 and ATM observed in the 17p and 11q del patients.

In addition several genes were assessed which are associated with Ca^{2+} signalling, given the role of CD20 as a store-operated Ca^{2+} channel (Figure 6.8A-C). Expression of *NOXA1* in NOTCH1^{MUT} CLL cells was lower than that observed for cytogenetically normal CLL cells (p=0.109), whereas expression of *RRAD* and *JUN* displayed little difference between the cytogenetic subsets. *CD247,* which was identified as being up-regulated in CLL cells evading OFA CDC, demonstrated that 11q del CLL samples displayed significantly lower levels of *CD247* (p=0.0181), than normal B cells (Figure 6.8D). Of interest was the expression levels of *CD247, GATA3* and *MMP9* in 11q del CLL samples, as these

genes were all highly expressed in cells evading OFA CDC, despite having the lowest basal gene expression levels. Our results demonstrate that 11q del CLL patients respond well to anti-CD20 MAbs treatment, therefore part of this may be attributed to the lower levels of expression of *CD247, GATA3* and *MMP9* within circulating cells.

6.3.3.2 *NOTCH1* pathway

A panel of genes associated with the *NOTCH1* pathway were assessed in our CLL cells to determine if there were indications of de-regulation in our NOTCH1^{MUT} CLL cells (Figure 6.9). Interestingly several genes known to be modulated by the *NOTCH1* pathway, the *HES* family of genes and *HEY1* were down-regulated in our CLL patient cohort compared to normal B cells, even though *NOTCH1* was up-regulated in the majority of samples. *FBXW7* involved in ICN degradation was down-regulated, whereas *ADAM10* was up-regulated indicating that *NOTCH1* could potentially be more readily cleaved into ICN and expression may be prolonged due to loss of degradation. These findings suggest that there is a skew towards constitutively active *NOTCH1* signalling in CLL.

Comparing the expression levels of *NOTCH1* between our CLL subsets, the highest expression levels were observable in both our normal cytogenetic and NOTCH1^{MUT} CLL cells. Interestingly NOTCH1^{MUT} CLL cells only had approximately 0.2 fold higher gene expression levels than cytogenetically normal CLL cells (Figure 6.10A). 17p del CLL samples displayed the lowest levels of *NOTCH1* expression, with levels similar to that observed in the healthy B cells. In contrast *NOTCH2* was slightly down-regulated in our CLL samples, 17p del patients displayed the highest expression but this was similar to that observed in the normal B cells (Figure 6.10B). *NOTCH3* was not expressed in the normal B cell samples assessed, and therefore gene expression was shown relative to the CLL normal sample CLL57 (Figure 6.10C; ΔC_t values are shown in Supplementary Figure 6.1). Only one 11q del CLL patient displayed *NOTCH3* expression, cytogenetically normal and 17p del CLL cells had varied gene expression levels. *NOTCH4* expression was the highest within normal cytogenetic CLL cells, but again there was wide variation in expression from sample to sample (Figure 6.10D). These data suggest that 11q del CLL patients consistently had the lowest expression levels of all the *NOTCH* genes, however a larger cohort of patients

are required to confirm these observations. Given the link between constitutively active Notch1 signalling and resistance to anti-CD20 MAbs[108,109,233], it is noteworthy that the good responders 11q del CLL samples [346] displayed the lowest expression levels.

NOTCH1 downstream target genes *HES1* and *HEY1* expression levels, were down-regulated in our CLL patient cohort, even in NOTCH1^{MUT} CLL cells when compared against normal B cell samples (Figure 6.11A&B). *HES1* was significantly down-regulated compared to normal B cells, >100 fold lower, and as expected from our previous data 11q del CLL patients had the lowest expression levels. *DELTEX* a positive regulator of *NOTCH1* was significantly up-regulated in our NOTCH1^{MUT} samples compared to cytogenetically normal CLL cells (3 fold higher expression, p=0.0181; Figure 6.11C). 11q del CLL cells had significantly lower expression of the *NOTCH1* ligand gene *DLL1* (p=0.0181; Figure 6.11D). As expected our 17p del CLL patients displayed significantly lower expression of *TP53* than the other cytogenetic subsets. Interestingly the oncogene *MYC* expression levels were lower in CLL samples from peripheral blood compared with control B cells, but presumably *MYC* would be up-regulated compared to normal B cells in the LN and BM where there are stronger signals for cell division (Figure 6.12)[380].

Overall our data clearly demonstrate that normal B cells express components of the NOTCH pathway, and within CLL there is cytogenetic subset specific de-regulation of this pathway.

6.3.4 Gene expression and OFA NTL/CD154+IL-4 stimulation

To elucidate the mechanisms responsible for NOTCH1^{MUT} CLL cells resistance to anti-CD20 MAbs, gene expression analysis was performed on cytogenetically normal and NOTCH1^{MUT} CLL cells co-cultured on NTL/CD154+IL-4 with and without the presence of OFA. By comparing gene expression levels from freshly isolated CLL samples, several pathways appeared to be de-regulated in our NOTCH1^{MUT} CLL sample cohort. As expected this included the *NOTCH1* pathway but in addition genes associated with cell cycling and Ca^{2+} signalling were altered, prompting further investigation. Therefore, CLL cells were treated for 48 hr either on plastic (with and without OFA) or NTL/CD154+IL-4 (with and

without OFA) and then changes in gene expression levels were determined by Fluidigm array analysis. Unless otherwise stated all fold change in gene expression is relative to CLL70 cultured on plastic without the presence of OFA. CLL70 was used for calibration as it is a normal cytogenetic CLL sample which Oxford sequencing data identified as having no additional genomic mutations.

6.3.4.1 NOTCH1 signalling pathway

NOTCH1 pathway genes as well as several genes linked with *WNT* signalling were assessed, as the two pathways have been shown to interact in the presence of Ca^{2+} [224,368,381]. The *NOTCH1* pathway was up-regulated with NTL/CD154+IL-4 stimulation, with a clear up-regulation of *HEY1* in both our normal cytogenetic CLL and NOTCH1^{MUT} CLL samples (Figure 6.13). *DELTEX* expression, which was up-regulated in the freshly isolated NOTCH1^{MUT} samples when compared to normal CLL samples, was down-regulated following culture on plastic and further down-regulated with NTL/CD154+IL-4 stimulation in our NOTCH1^{MUT} CLL cells (Figure 6.14A; ΔC_t values are shown in Supplementary Figure 6.2A). The cytogenetically normal CLL samples displayed little change in *NOTCH1* gene expression levels until co-cultured with OFA and NTL/CD154+IL-4, whereby *NOTCH1* expression was increased. This is in contrast to NOTCH1^{MUT} CLL samples which upon NTL/CD154+IL-4 stimulation displayed down-regulation of *NOTCH1* which was further abrogated by the presence of OFA in culture, resulting in significantly lower *NOTCH1* expression between normal cytogenetic CLL cells and NOTCH1^{MUT} ($p=0.0405$; Figure 6.14B; ΔC_t values are shown in Supplementary Figure 6.2B). Interestingly the expression of *ROR2*, a tyrosine kinase receptor protein associated with the non-canonical *WNT* signalling pathway, was only present in two samples on plastic, CLL121 (CLL normal) and CLL133 (NOTCH1^{MUT}). Gene expression levels were made relative to CLL121 cultured on plastic without OFA (Un-calibrated ΔC_t values are shown in Supplementary Figure 6.2C). Upon stimulation with NTL/CD154+IL-4 there was an up-regulation of *ROR2* (over 1,500 fold increase; Figure 6.14Ci).Surprisingly NTL/CD154+IL-4 stimulation induced ROR2 expression in all the samples examined, which was more notable in our NOTCH1^{MUT} CLL cells ($n=3$; 40 fold higher; $p=0.2761$; Figure 6.14Cii).

6.3.4.2 Cell cycle

Previous reports have shown that upon stimulation with NTL/CD154+IL-4 or alternatively IL-21, B cells and CLL cells have the ability to start to proliferate[382,383]. Therefore it was not surprising that after 24 hr on NTL/CD154+IL-4 co-culture several genes involved in cell cycle progression such as *CCNE2* and *CDK1* were up-regulated in the CLL cells (Figure 6.15). NOTCH1^{MUT} CLL cells displayed a more pronounced de-regulation of genes involved in cell cycle progression in comparison to cytogenetically normal CLL cells. *CCND1* was more significantly up-regulated in NOTCH1^{MUT} CLL cells than cytogenetically normal CLL cells (Figure 6.16A; ΔC_t values are shown in Supplementary Figure 6.3A). NOTCH1^{MUT} *CDK1* expression was at least double that observed in normal cytogenetic CLL samples, when cultured on both plastic (0.91 vs 2.66 $\Delta\Delta C_t$ values respectively) and NTL/CD154+IL-4 (20.35 vs 46.90 $\Delta\Delta C_t$ values respectively; Figure 6.16B; ΔC_t values are shown in Supplementary Figure 6.3B). NOTCH1^{MUT} *CDK2* expression was two fold higher than that of cytogenetically normal CLL cells when cultured on NTL/CD154+IL-4 (7.39 vs 18.03 $\Delta\Delta C_t$ values respectively; Figure 6.16C; ΔC_t values are shown in Supplementary Figure 6.3C). Interestingly for *CCNE2* expression both NOTCH1^{MUT} and normal cytogenic CLL cells demonstrate marginal down-regulation when OFA was added to plastic culture, whereas when OFA was present in NTL/CD154+IL-4 co-culture NOTCH1^{MUT} CLL cells displayed a significant up-regulation of *CCNE2* (1.3 fold higher expression; p=0.0259). Normal cytogenetic CLL cells also displayed an up-regulation (1.6 fold increase; p=0.0731; Figure 6.16D; ΔC_t values are shown in Supplementary Figure 6.3D). This suggests that CLL normal cytogenetic and NOTCH1^{MUT} CLL cells both prepare for cell division when co-cultured with NTL/CD154+IL-4, however this appears more enhanced in NOTCH1^{MUT} CLL samples. The changes demonstrated in *CCNE2* expression in CLL cells, cultured with OFA on both plastic and NTL/CD154+IL-4 suggests that the binding of OFA to CD20 sends signals to the CLL cell to increase cell division in the presence of NTL/CD154+IL-4.

6.3.4.3 BCR and Ca^{2+} signalling

Analysis of genes linked with Ca^{2+} and BCR signalling provided a less clear differential in gene expression levels, following culture on either plastic or NTL/CD154+IL-4 (Figure 6.17). There was also much more patient variation

observed in gene expression levels within both normal cytogenetic and NOTCH1^{MUT} CLL subsets. However *JUN* was consistently up-regulated following NTL/CD154+IL-4 stimulation with expression more prominently up-regulated in the cytogenetically normal CLL cells compared to NOTCH1^{MUT} CLL (Figure 6.18A; ΔC_t values are shown in Supplementary Figure 6.4A). Whereas the oncogene *MYC* was largely down-regulated in NOTCH1^{MUT} CLL cells when cultured on plastic, upon co-culture with NTL/CD154+IL-4 expression increased 20 fold as opposed to 4 fold in the normal cytogenetic CLL sample cohort (Figure 6.18B; ΔC_t values are shown in Supplementary Figure 6.4B). This concurs with the data collected for the cell cycle genes and suggests that NOTCH1^{MUT} CLL cells are more primed towards cell division. *RRAD,* which is associated with regulation of voltage-dependent L-type calcium channel, was down-regulated on plastic, with expression in normal cytogenetic CLL cells further down-regulated when OFA was present in plastic (p=0.121; Figure 6.18C; ΔC_t values are shown in Supplementary Figure 6.4C). Interestingly in NOTCH1^{MUT} CLL cells, *RRAD* expression was up-regulated on plastic with OFA compared with untreated control (1.3 fold increase; p=0.0237). NTL/CD154+IL-4 stimulation caused further up-regulation of *RRAD* in NOTCH1^{MUT} CLL cells which was further increased with OFA stimulation, although this was not statistically significant. NOTCH1^{MUT} CLL cells displayed lower *SYK* expression levels than normal cytogenetic CLL, but for both cytogenetic sub-sets, expression was down-regulated approximately two fold on NTL/CD154+IL-4, significantly so for normal cytogenetic CLL cells with OFA (p=0.0456; Figure 6.18D; ΔC_t values are shown in Supplementary Figure 6.4D). This data suggests that constituently active *NOTCH* signalling may target several different genes linked with Ca^{2+} signalling in order to induce resistance to anti-CD20 MAbs.

6.3.4.4 Notch1 activation on NTL/CD154+IL-4

Protein expression levels were also determined for cytogenetically normal CLL samples (n=3) and NOTCH1^{MUT} CLL samples (n=3) cultured on plastic and NTL/CD154+IL-4 with and without the presence of OFA for 48 hr by Western blotting (Figure 6.19). Protein levels for Notch1, 2 and 4 all represent the active intracellular form of the protein. Incomplete transfer of proteins from gel to membrane occurred for sample CLL70/CLL108 cultured on plastic with and without OFA, therefore some immune-blotting data is missing for these samples

(Figure 6.19C). Corroborating our gene expression analysis, the Notch1 signalling pathway is activated by NTL/CD154+IL-4 stimulation in both cytogenetic subsets. Notch2 also appeared activated by NTL/CD154+IL-4 stimulation, while Notch3 expression was only detected in one out of six CLL samples analysed, NOTCH1^{MUT} CLL101 on plastic (Figure 6.19D). Notch4 expression remains consistently unchanged by stimulation. This suggests that NTL/CD154+IL-4 stimulation causes preferential activation of Notch1/2. Interestingly one CLL normal sample, CLL42, displayed continuous activation of Notch1/2, which remained unchanged by NTL/CD154+IL-4 stimulation indicating a potential mutation of a regulator of the Notch1/2 pathway for this patient (Figure 6.19B). ADAM-10 further highlights Notch1 activation by NTL/CD154+IL-4 stimulation as shown by the presence of the lower band, which represents the active form (~60 kDa) of the protein (Figure 6.19 A&B).

The up-regulation of phospho GSK3β (Ser9) and total GSK3β levels in the CLL samples assessed, suggests activation of the Akt and Wnt signalling pathways (Figure 6.19A&B). Expectedly the cell cycle protein CCNE1 was up-regulated with NTL/CD154+Il-4 stimulation in both NOTCH1^{MUT} and normal cytogenetic CLL cells (Figure 6.19A&B). CCNE2 expression however was only observed when cells were cultured with NTL/CD154+IL-4 in the presence of OFA. Therefore longer stimulation than 48 hr may be required to observe a more notable up-regulation. *CCNE2* expression was also up-regulated at the gene level following OFA stimulation which was most prominent in our NOTCH1^{MUT} CLL cells (Figure 6.16), CCNE2 protein expression levels also appear more up-regulated in NOTCH1^{MUT} CLL samples compared to cytogenetically normal CLL cells. Although a larger patient cohort would be required to determine if this is a statistically significant trend. CCNE2 results would suggest that CD20 bound with OFA could act to regulate CCNE2 expression presumably through the Ca^{2+} signalling cascade, or via the CD20/OFA complex stimulating another receptor/pathway to cause changes in CCNE2 expression.

6.3.5 NOTCH1^{MUT} CLL patients display calcium flux upon BCR stimulation

Differences in expression of genes associated with Ca^{2+} signalling between normal cytogenetic and NOTCH1^{MUT} CLL samples led us to analyse the Ca^{2+} flux

with BCR and OFA/RTX stimulation. Others have shown that Ca^{2+} flux only occurs when anti-CD20 MAb are combined with BCR stimulation. Soluble IgM fragments $F(ab')_2$ or IgM was used stimulate the BCR in combination with anti-CD20 MAb, and as a positive control Ca^{2+} ionophore Ionomycin (Iono) was used[334]. Ca^{2+} flux was measured using Fluo-4. A minimal Ca^{2+} response, determined by an increase in MFI, was observed in normal cytogenetic CLL cells following BCR crosslinking ($F(ab')_2$ + 89 MFI and IgM + 124 MFI; n=4; Figure 6.20). When the MFI signal produced over time was assessed there was very little change observed compared to NDC (Figure 6.21). However in $NOTCH1^{MUT}$ CLL samples upon BCR crosslinking there was an obvious flux in Ca^{2+} for three patients ($F(ab')_2$ + 507 MFI and IgM + 220 MFI; n=4; Figure 6.22). A Ca^{2+} flux was observed in $NOTCH1^{MUT}$ samples when CLL cells were incubated with either OFA or RTX but not quite so prominently, suggesting that Ca^{2+} signalling is possibly a contributing mechanism for the resistance of $NOTCH1^{MUT}$ CLL cells to anti-CD20 MAbs.

Investigating MFI changes over the 2 min period demonstrated that the response between $F(ab')_2$ and IgM BCR stimulation was different (Figure 6.23). $F(ab')_2$ stimulation appeared to cause an immediate Ca^{2+} flux which, due to the several second delay in our ability to record the data, meant we were only able to measure the end part of the flux when levels were returning back to normal. However IgM stimulation leads to a slower gradual increase in Ca^{2+} flux. Comparing the mean MFI levels for cytogenetically normal and $NOTCH1^{MUT}$ CLL cells confirmed that $NOTCH1^{MUT}$ cells demonstrate a large Ca^{2+} flux with BCR stimulation (Figure 6.24A). When CLL cells were stimulated with MAb, cytogenetically normal CLL cells demonstrated a slight flux in Ca^{2+} when pre-incubated with RTX or OFA, this flux increased further with BCR stimulation (Figure 6.24B&C). $NOTCH1^{MUT}$ CLL cells however did not demonstrate a notable flux with MAb co-culture; this may be attributed to the lower expression levels of CD20 on $NOTCH1^{MUT}$ CLL cells. Low CD20 expression levels could lead to insufficient MAb binding for the formation of CD20 into lipid rafts and subsequently reduced Ca^{2+} flux. Upon BCR stimulation there was an observable flux in Ca^{2+} within the $NOTCH1^{MUT}$ CLL samples, but this response was muted in comparison to BCR stimulation alone (Figure 6.24). Overall these findings indicate that alteration in Ca^{2+} flux may play a role in $NOTCH^{MUT}$ CLL resistance to anti-CD20 MAB therapies.

6.4 Discussion

6.4.1 Genetic instability in CLL cells

Whole genome sequencing revealed the extensive heterogeneity between different CLL patients. When the 13 CLL patients with mutations were compared no two CLL patients displayed the same set of mutated genes. *ATM* mutations were the most frequently reported with some patients having 2 or 3 mutations within *ATM*. This supports other studies which have also observed that *ATM* mutations are one of the most frequently occurring in CLL[80,384]. Although the NOTCH1^{MUT} CLL patient cohort we have is too small to draw any conclusions. It would be interesting to determine how frequently mutations within *ATM* are observed within NOTCH1^{MUT} CLL cells and how this impacts upon their response to anti-CD20 MAbs, as we and others found that 11q del patients respond well to anti-CD20 MAbs[346]. Of the two NOTCH1^{MUT} CLL patients screened for mutations, CLL67 displayed one mutation in the *ATM* gene, which did not improve its susceptibility to OFA induced CDC, with the percentage of dead cells observed being 14.4% compared to the mean average for NOTCH1^{MUT} CLL cells at 15.1%. Although this deletion may only affect one of the alleles, it would be interesting to determine if mutations of both *ATM* alleles in NOTCH1^{MUT} CLL cells results in any measurable improvement in susceptibility to anti-CD20 MAbs as observed with 11q del CLL patients. NOTCH1^{MUT} have been identified within CLL patients with 17p del however NOTCH1^{MUT} have not yet been observed in CLL patients with 11q del, suggesting they are mutually exclusive aberrations[88,108].

6.4.2 CLL cells escaping OFA induced CDC

Understanding the ability of malignant CLL cells to escape OFA CDC may lead to new targetable cancer therapies and help pinpoint the genes involved in NOTCH1^{MUT} resistance to anti-CD20 MAbs. Therefore we initiated OFA induced CDC on CLL cells cultured with NTL/CD154+IL-4, any surviving cells were then re-cultured with NTL/CD154+IL-4 overnight and cells harvested for gene expression analysis using Fluidigm array.

Analysis of the genes revealed that no specific common pathway was activated in the surviving CLL cells. The majority of genes that showed >2 fold change in

expression levels were specific to individual samples. After screening our CLL samples, three genes were identified as being consistently up-regulated in CLL cells escaping OFA CDC; *CD247*, *GATA-3* and *MMP9*. MMPs are a large family of enzymes linked with tumour growth and metastasis and are involved in different biological processes from cell migration to tissue repair. *MMP9* in particular is the principle MMP produced by lymphocytes associated with the digestion of the main component of basement membranes, type IV collagen. Increased *MMP9* expression has been associated with poor patient survival and advanced clinical stage in CLL[376,377]. High MMP9 expression has also been linked to extensive BM infiltration[377]. Infiltration of both the LN and BM by malignant CLL cells is associated with increased risk of morbidity and death via the suppression of normal haematopoiesis and immunity. Therefore it is possible that CLL cells that have successfully evaded OFA induced CDC are over expressing *MMP9* to enhance invasion of the LN or BM, thus enabling the aberrant CLL cells to be protected within these niches. Once in these niches the pro-survival signals provided will also help the surviving CLL cells to proliferate.

Possibly in support of this, the two other genes up-regulated are associated with T cell development and signalling, *GATA-3* and *CD247* respectively. *GATA-3* has been identified as a marker for the hormone response in breast cancer, but little is known about its role in CLL[385]. *GATA-3* is commonly understood to be an important transcription factor in T cell development, and is crucial for the transformation of naïve $CD4^+$ T cells in the presence of IL-4 and APC into T_H2 cells. *GATA-3* expression is specific to T_H2 lineage, and is not observed in T_H1 cells[379]. T_H2 are associated with expression of IL-4, which we have previously described as aiding the expansion of CLL cell clones and assisting survival[138,139,366,386]. *CD247* encodes for a TCR associated protein, the CD3ζ chain, CD3 is assembled with the TCR heterodimer in T cells. TCR signal activation can lead to several different cellular processes such as; proliferation, differentiation and also cytokine production[375]. TCR engagement with antigens results in the tyrosine phosphorylation of ITAMs located within the ζ subunit of CD3 (*CD247*), resulting in the sequential activation of Lck and Fyn and consequently orchestrates the activation of several different cellular pathways such as ERK, NFAT and NF-κB pathway[387]. Typically T cell associated proteins, ZAP-70 and Lck expression have been identified in CLL patients, with a propensity towards

unmutated *IGHV* patients. Within CLL, ZAP-70 and Lck expression leads to enhanced BCR signalling. BCR signalling results in an up-regulation in pro-survival pathways, which aids CLL cell survival[45,46,388]. Therefore our data suggests that CLL cells evading OFA induced CDC are those actively trying to migrate into the LN or BM with enhanced ability to cross-talk and tailoring their microenvironment to aid survival and expansion of the malignant clone.

Interestingly when gene expression levels for these three genes were compared within fresh CLL samples 11q del CLL patients demonstrated significantly lower expression levels of *GATA-3* and *CD247* than cytogenetically normal CLL cells, whilst expression of *MMP9* was undetectable. Throughout this body of research we have demonstrated the susceptibility of 11q del CLL samples to anti-CD20 MAbs. In particular we have highlighted their enhanced levels of OFA induced CDC with and without stromal co-culture, supporting our findings which suggest that higher expression of these genes results in reduced MAb activity. NOTCH1^{MUT} CLL sample expression levels for these genes revealed no significant differences other than lower levels of *GATA-3*, which if our findings are correct should aid CDC. Therefore this would indicate that NOTCH1^{MUT} CLL cells have a novel mechanism for evading MAb CDC, which requires further investigation.

6.4.3 GEP of unstimulated NOTCH1^{MUT} CLL cells displays a similar pattern of expression to cytogenetically normal CLL cells

No particular gene or pathway was highlighted as being deregulated between each of the four cytogenetic sub-groups, despite having different mutations. However. closer examination revealed subtle differences in the expression of several genes. Previous findings have identified that Notch1 expression results in both cell cycle progression and arrest depending on the tissue type. Within pancreatic cancer and T-ALL *NOTCH* expression results in increased passage to the G_1/S phase. However within the RNA of NOTCH1^{MUT} fresh CLL samples, we identified significantly lower expression levels of the cell cycle regulatory genes *CCND1* and nearly significant levels of reduced *CCNE2* expression ($p=0.0727$)[389,390]. This may be due to a lack of *NOTCH* stimulation for CLL cells within the peripheral blood. Investigating *NOTCH1* expression levels identified marginally elevated levels in our NOTCH1^{MUT} subset compared to cytogenetically

normal CLL cells. *HES1* expression was also slightly higher but there was little difference within the other *NOTCH1* downstream genes *HES5* and *HEY1*. This suggests similar expression of NOTCH1 pathway genes between cytogenetically normal and NOTCH1^{MUT} CLL cells located within the circulating compartment. Interestingly in the NOTCH1^{MUT} CLL subset, there was significantly higher expression of *DELTEX1* a positive regulator of *NOTCH1*, suggesting that NOTCH1^{MUT} are more readily primed towards constitutively active *NOTCH1* signalling[391]. Pozzo *et al.,* established that in NOTCH1^{MUT} CLL cells, those with lowest levels of CD20 expression were enriched for *NOTCH1* expression, concurrent with an up-regulation of both *HDAC1/2* at the transcriptional and protein level[233]. By performing co-immunoprecipitation assay they determined that the reduced CD20 expression levels was due to competition between HDAC1/2 and Notch1 binding to CBF1[233]. CBF1 in combination with suppressor of hairless and Lag-1 make up the transcription factor complex CSL. CSL is the principle transcription factor responsible for activating gene transcription downstream of Notch1, and also binds HDAC1 and HDAC2. However Notch1 is able to outcompete HDAC1/2 to bind to CSL[392,393]. Presumably this then leaves the elevated levels of HDAC1/2 to bind to and repress the activity of the transcription factor Sp1, a CD20 specific transcription factor[394]. Pozzo *et al.,* further identified an increase in the expression of CD20 in NOTCH1^{MUT} CLL cells upon the treatment with the HDAC inhibitor VPA, although they do not report whether this resulted in increased lysis by CDC and ADCC following Mab treatment. Our investigation was carried out prior to this research therefore *HDAC1* or *HDAC2* genes were not investigated in our panel of genes, however *HDAC4* was included. *HDAC4* was down-regulated in our NOTCH1^{MUT} CLL cells compared to cytogenetically normal CLL cells, however *HDAC4* is a type IIa HDAC, whereas HDAC1/ 2 are type I, which subsequently have different binding sites and repress different pathways[359-361,395].

6.4.4 Microenvironmental stimulation and NOTCH1^{MUT} CLL cells

6.4.4.1 NOTCH1 pathway

To further understand the molecular mechanisms behind NOTCH1^{MUT} CLL cell resistance to OFA we incubated CLL cells with and without OFA in co-culture for 48 hr on plastic and NTL/CD154+IL-4. Downstream activation of the *NOTCH1*

pathway was observed at the transcriptional level via elevated *HEY1* expression following culture with NTL/CD154+IL-4. Interestingly in our freshly isolated NOTCH1^{MUT} CLL cells which displayed high *DELTEX* expression, upon culture on plastic expression is lowered compared to cytogenetically normal CLL cells. Following activation of *NOTCH1* on NTL/CD154+IL-4 *DELTEX* is further down-regulated in the NOTCH1^{MUT} CLL cells. Although *NOTCH1* levels are down-regulated upon stimulation with NTL/CD154+IL-4, this may be due to the transcript being rapidly made into protein to activate the Notch1 pathway. This is corroborated by our immunoblotting results where overexpression of Notch1 was observed at the protein level on NTL/CD154+IL-4 in both our normal and NOTCH1^{MUT} CLL cells. Intracellular Notch1 and Notch2 also appear to be up-regulated at the protein level following stimulation with NTL/CD154+IL-4, indicating Notch activation. However Notch3 and Notch4 were not well expressed at the transcriptional level and remained relatively unchanged at the protein level suggesting differential activation of the Notch receptors. It has previously been reported that the activation of Notch is due to the up-regulation of NF-κB on NTL/CD154+IL-4, which was able to induce expression of the Notch receptor ligand Jagged1[230]. This would support our findings, as Jagged1 preferential activates Notch1 and Notch2. Activation of the Notch1 pathway at the protein level is further supported by the presence of the active form of ADAM10 on NTL/CD154+IL-4[396]. One of the normal CLL samples, CLL42, displayed Notch1 and Notch2 activation on plastic and NTL/CD154+IL-4, suggesting a potential downstream mutation causing constitutive signalling; therefore it would be interesting to analyse this sample for a *NOTCH* pathway related mutation. CLL42 however, unlike the other CLL samples assessed, appeared to be insensitive to further Notch1 or Notch2 activation by NTL/CD154+IL-4, which may be due to this sample already having constitutively active signalling.

An up-regulation of phospho GSK3β and total GSK3β was observed at the protein level on NTL/CD154+IL-4, in both NOTCH1^{MUT} and cytogenetically normal CLL cells, suggesting activation of the Akt and Wnt signalling pathways, although some genes in the Wnt pathway did not show an up-regulation such as *AXIN1/2* and *DV1*. Further cross-talk between these two pathways could explain this, reports have shown that GSK3β is able to bind and phosphorylate the intracytoplasmic region of Notch following cleavage. GSK3β phosphorylation of

Notch then effects its transcriptional activity by modulating *HES1* expression[397]. *APC*, a negative regulator of the Wnt signalling pathway had higher expression in our cytogenetically normal CLL cells[224,398]. Lef1 which forms the transcriptional complex with ß-catenin, the transcriptional regulator of canonical Wnt signalling, was more strongly up-regulated at the transcriptional level upon NTL/CD154+IL-4 stimulation in our NOTCH1^{MUT} CLL cells suggesting that NOTCH1^{MUT} CLL samples also have increased Wnt signalling. *ROR2* encodes for a membrane bound receptor tyrosine kinase which when bound by WNT5A activates the non-canonical ß-catenin independent Wnt signalling pathway[399,400]. Non-canonical WNT5A signalling has been described as both a tumour suppressor and tumour enhancing pathway. When acting as a tumour suppressor, the protein displays an association with degrading ß-catenin and therefore suppressing the tumour activity of canonical Wnt signalling causing a down-regulation of c-MYC[401]. However our results demonstrated an increase in *MYC* expression at the transcriptional level following NTL/CD154+IL-4 stimulation, therefore it would appear more likely that WNT5A expression in our cytogenetically normal and NOTCH1^{MUT} CLL cells is oncogenic. Increased levels of $Ca^{2+}$are involved in this process, activating Ca^{2+} sensitive receptors initiates WNT5A expression [399,400]. Jak *et al.*, have reported increased Ca^{2+} within CLL cells when stimulated with CD40[176]. When WNT5A is active it functions in concert with the canonical Wnt pathway to cause an up-regulation of genes involved in the invasive nature of malignant cancer cells, such as MMP expression which as previously described displays a correlation with CLL cells evading OFA induced CDC.

Interestingly previous gene expression profiling experiments had identified *ROR1* as a signature gene of CLL cells and consequently as a target for MAb therapy[118,402,403]. Within these two independent studies *ROR1* was identified as being highly expressed in CLL cells, whilst *ROR2* was not. *ROR1* and *ROR2* share 97% sequence homology to each other[402]. The two CLL samples that had *ROR2* expression when unstimulated on plastic (CLL121 &CLL133) both up-regulated *ROR2* expression to a similar extent when stimulated with NTL/CD154+IL-4. In the remaining CLL samples NTL/CD154+IL-4 stimulation resulted in an activation of *ROR2* expression in all the samples. This suggests another mechanism by which CLL cells maintain non-canonical Wnt signalling to aid their survival in the

LN microenvironment. NOTCH1^{MUT} CLL samples demonstrated more enhanced *ROR2* activation in comparison to cytogenetically normal CLL cells suggesting they are primed towards non-canonical Wnt signalling to aid survival/proliferation resulting in their more aggressive phenotype.

6.4.4.2 Cell cycle

It has previously been characterised by carboxyfluorescein diacetate succinimidyl ester (CFSE) assay that resting B cells upon stimulation with CD154/IL-4 will proliferate, and the same has been observed for CLL cells[382,383,404]. Therefore it was not surprising that many of the genes involved in cell cycle were largely up-regulated upon NTL/CD154+IL-4 stimulation in our CLL samples, CCNE1 and CCNE2 at the protein level also displayed up-regulation in expression upon NTL/CD154+IL-4 stimulation. Freshly isolate NOTCH1^{MUT} CLL cells were characterised by GEP as having lower expression levels of cell cycle genes indicating slow cycling. However upon stimulation with NTL/CD154+IL-4 they demonstrated a much higher up-regulation of cell cycle genes; such as *CDK1, CDK2* and *CCNE2,* which indicates rapid cycling. This further highlights the more aggressive nature of NOTCH1^{MUT} CLL than normal CLL cells. Unexpectedly *CCNE2* expression in CLL cells was further up-regulated by the presence of OFA, when stimulated with NTL/CD154+IL-4. For two of the three samples, this was more prominent in our NOTCH1^{MUT} CLL samples. G1 to S phase transition is dependent on a reduction in intracellular Ca^{2+} levels. It has previously been established that CD20 activity is associated with B cell activation and proliferation and that different CD20 MAb's are able to either inhibit or enhance cell cycle progression through binding to CD20 and changing intracellular Ca^{2+} homeostasis [291]. Therefore our data would suggest that OFA binding to CD20 potentially reduces Ca^{2+} influx lowering intracellular levels so that CLL cells are activated towards proliferation[291].

6.4.4.3 Calcium signalling

In order to clarify how different CLL cytogenetic cohorts alter Ca^{2+} signalling following MAb binding we investigated this pathway further. When NOTCH1^{MUT} and cytogenetically normal CLL cells were stimulated with NTL/CD154+IL-4 several genes related to Ca^{2+} signalling were identified as being deregulated in

our NOTCH1^{MUT} CLL cells. These genes included *ROR2*, *RRAD* a suppressor of voltage-gated L-type Ca^{2+} currents and *SYK* upstream of BCR induced Ca^{2+} signalling. Notch has been implicated in different tissue types as utilising Ca^{2+} signalling, within pulmonary arterial smooth muscle cells Notch stimulation with soluble Jagged 1 caused a release in store-operated Ca^{2+} entry which subsequently caused a release of Ca^{2+} from intracellular stores[405]. Within glioblastoma Notch expression has been identified as causing hypoxia induced up-regulation of the TCRPC6 cation channel from the transient receptor potential subfamily[406]. TCRP6 expression results in elevated intracellular Ca^{2+} levels which causes NFAT pathway activation. Within glioblastoma Notch expression through Ca^{2+} signalling results in a malignant phenotype with enhanced proliferation and migration capabilities[406]. In conjunction with our findings of aberrant Ca^{2+} signalling in NOTCH1^{MUT} CLL cells, others also identified that NOTCH1^{MUT} down-regulate CD20 a Ca^{2+} channel, due to increased HDAC1 and HDAC2 expression as previously described. Although only preliminary, our data investigating Ca^{2+} signalling would suggest that NOTCH1^{MUT} CLL cells have enhanced BCR signalling as they respond to BCR stimulation with a prominent flux in Ca^{2+}. Within BCR signalling an increase in cytosolic Ca^{2+} levels causes a further cascade of Ca^{2+} release from store-operated calcium channels, which activate both NFAT and classical PKCs [17,20,22]. PKCβ in turn then causes the activation of the pro-survival NF-κB pathway[14,15]. In support of enhanced BCR signalling through NOTCH1^{MUT}, CLL42 a cytogenetically normal patient which displayed by immunoblotting constitutively active Notch1/2 demonstrated the strongest Ca^{2+} flux with BCR stimulation, $F(ab')_2$ stimulation compared with other cytogenetically normal CLL samples.

In conclusion this study has implications for the use of anti-CD20 MAbs in the treatment of NOTCH1^{MUT} CLL cases. We provide evidence to suggest NOTCH1^{MUT} CLL cells have tailored de-regulated Ca^{2+} signalling to aid their resistance to anti-CD20 MAbs and produce a more aggressive phenotype. Development of an effective Notch1 blocking or γ secretase inhibitor for the treatment of CLL may prove beneficial not only for increased susceptibility to anti-CD20 MAbs but to also reduce BCR signalling within CLL cells. In order to treat NOTCH1^{MUT} CLL patients effectively, a dual targeting approach may be required, which includes using a Notch1 inhibitor capable of abrogating the complex de-regulation of Ca^{2+}

signalling in NOTCH1^{MUT} CLL alongside an anti-CD20 MAb. Without this, the ineffective clearance of NOTCH1^{MUT} cells with the current treatment regimens could result in the accumulation of resistant cells within the BM and LN resulting in clonal take over by the malignant NOTCH1^{MUT} clone. Overall these data suggest that NOTCH1^{MUT} CLL patients require more tailored treatment strategies.

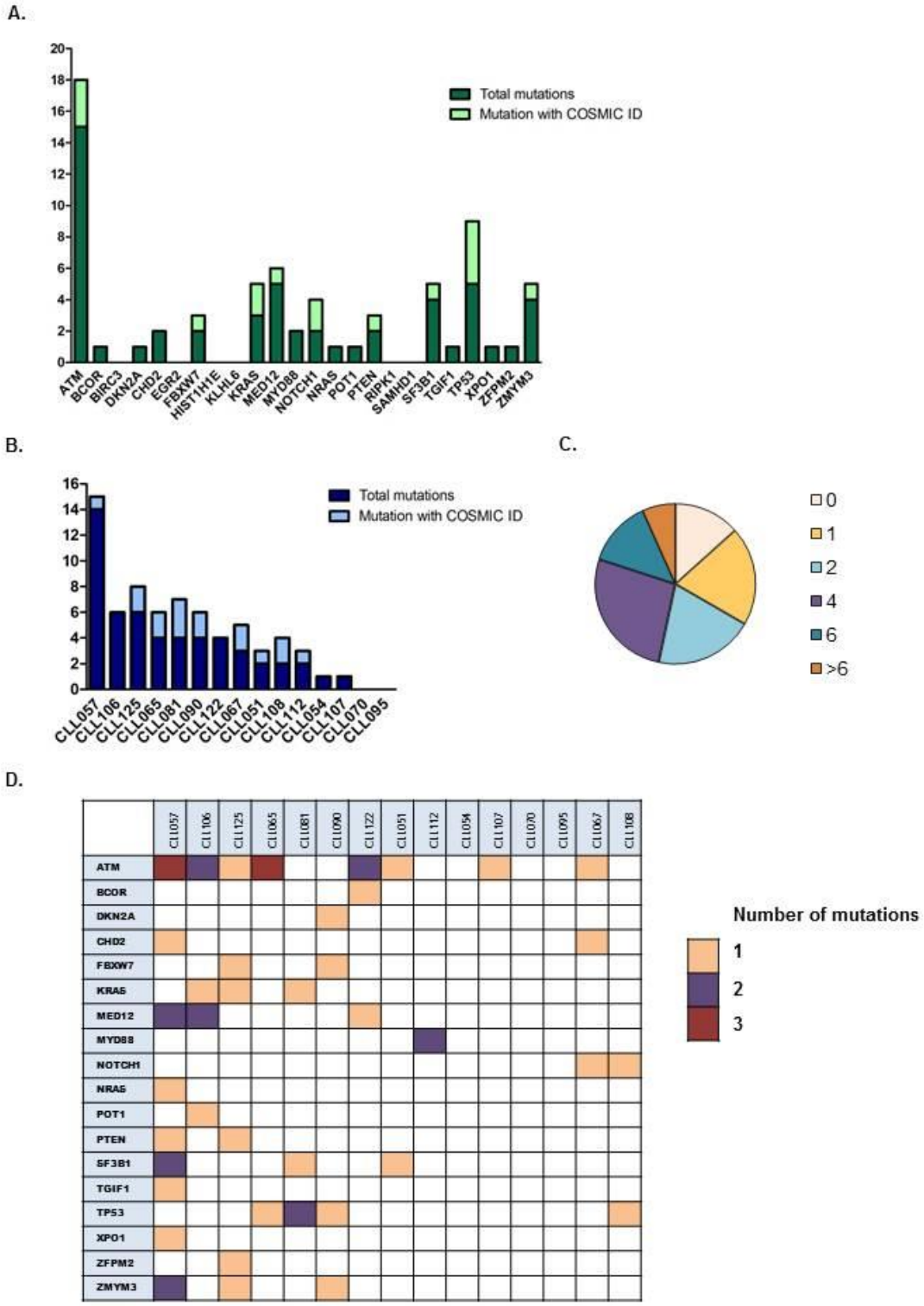

Figure 6.1 CLL patients are susceptible to the acquisition of multiple different genomic mutations

The genomes of fifteen CLL patients were sequenced on Miseq (Illumina, Inc) by Oxford MRC Molecular Diagnostic Laboratory, and the analysis provided was also performed by Oxford University. A. Total number of mutations observed per gene. B. Total number of mutations per CLL patient. C. Pie chart showing the number of mutations observed per CLL patient. D. Association between CLL patients and the specific gene mutation observed.

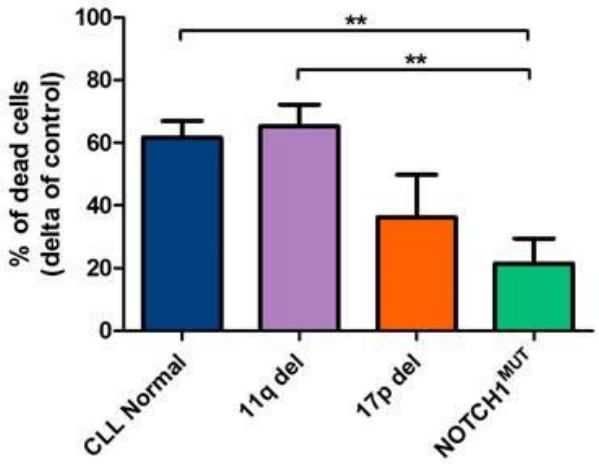

Figure 6.2 NOTCH1^{MUT} CLL cells display significantly less OFA-CDC than normal and 11q del CLL cells

Primary CLL cells (n=16) were cultured on NTL/CD154+IL-4 for 24 hr before 20 μg/ml OFA was added. CLL cells were then cultured with OFA for an additional 24 hr before undergoing CDC. The mean ± SEM percentage of dead cells are shown from cytogenetically normal CLL samples (n=5), 11q del (n=4), 17p del (n=4). NOTCH1^{MUT} (n=3). The percentage of dead cells is relative to untreated control. p values were determined by an un-paired t-test (**, $p<0.01$).

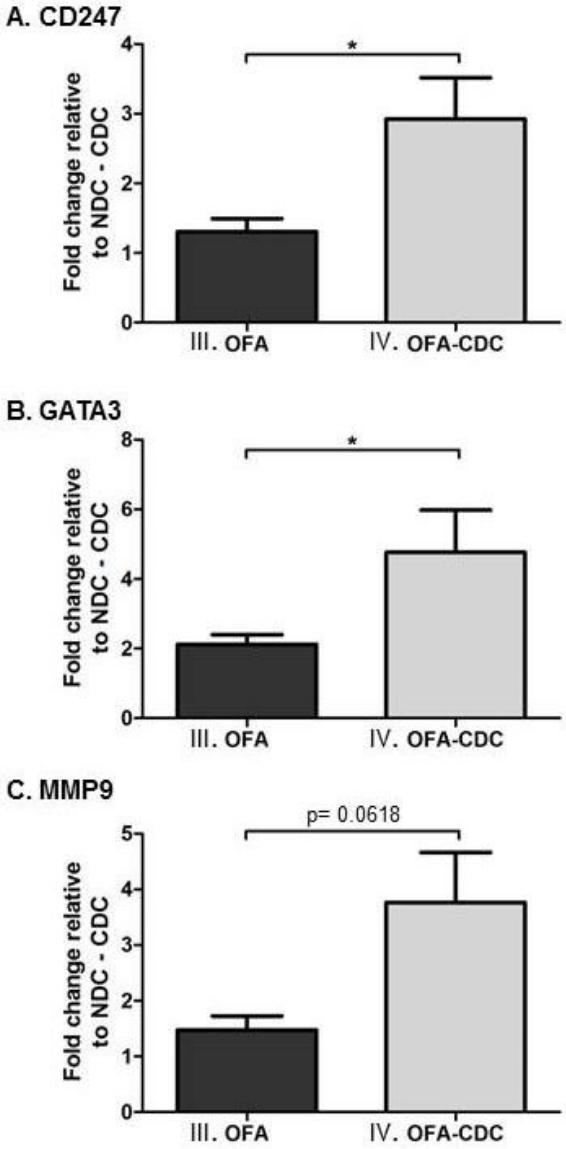

Figure 6.3 Genes linked with migration, T-cell development and signalling are up-regulated in CLL cells escaping OFA CDC

Primary CLL cells (n=13) were cultured on NTL/CD154+IL-4 for 24 hr before 20 μg/ml OFA was added. CLL cells were cultured with OFA for a further 24 hr before undergoing CDC. After CDC surviving CLL cells were then cultured with NTL/CD154+IL-4 for an additional 24 hr, after which RNA was extracted and gene expression levels were then determined by Fluidigm array analysis[a]. Gene expression levels are shown relative to NDC cells that underwent CDC without MAb (Figure 2.1 samples II.). GEP were calculated using $\Delta\Delta C_t$ method with the average of four housekeeping genes as reference. A. CD247 (n=11). B. GATA-3 (n=13). C. MMP9 (n=10). The mean $\pm$ SEM are shown. p values were determined by an unpaired t-test (*, $p<0.05$).

[a] Experimental design is described in section 2.5.2 and shown in Figure 2.1.

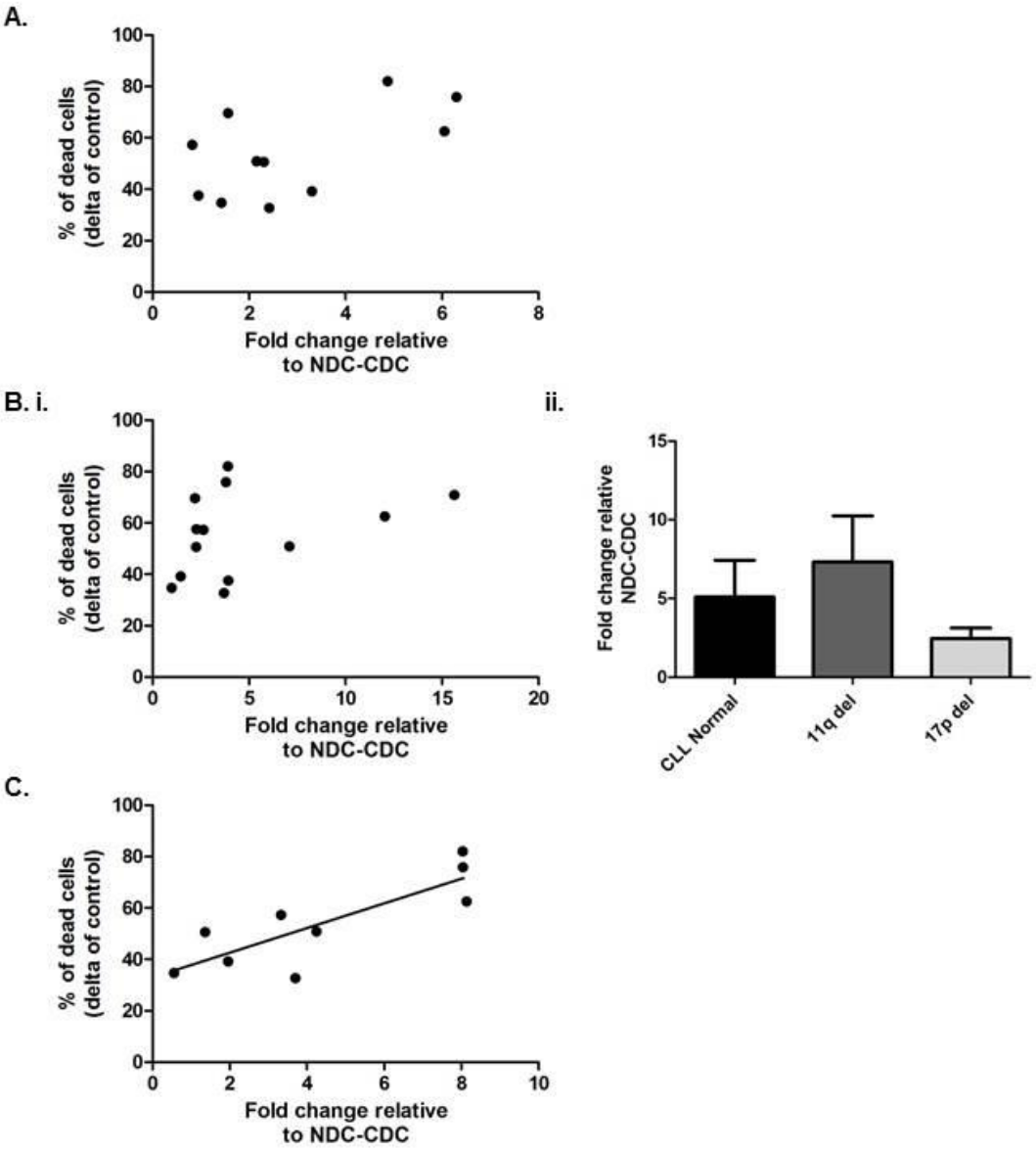

Figure 6.4 Genes associated with surviving OFA induced CDC show a positive correlation in expression and the level of CDC observed

Primary CLL cells were cultured on NTL/CD154+IL-4 for 24 hr before 20 µg/ml OFA was added. CLL cells were cultured with OFA for a further 24 hr before undergoing CDC (Figure 2.1 samples IV.). After CDC surviving CLL cells were cultured with NTL/CD154+IL-4 for an additional 24 hr, after which RNA was extracted and gene expression levels were determined by Fluidigm array analysis. Gene expression levels are shown relative to NDC cells that underwent CDC without MAb (Figure 2.1 samples II.). GEP were calculated using $\Delta\Delta C_t$ method with the average of four housekeeping genes as reference. Gene expression levels were plotted against the percentage of CDC observed. A. CD247 (n=11), r^2, 0.3456, p value, <0.0571. B.i. GATA-3 expression vs. CDC (n=13), r^2, 0.1263, p value, 0.2334. ii. Gene expression vs. CDC based on cytogenetic subset; CLL normal (n=4), 11q del (n=4) and 17p del (n=3). mean $\pm$ SEM is shown. C. MMP9 expression vs. CDC (n=10), r^2, 0.6876 and p value, 0.0057 (statistically significant).

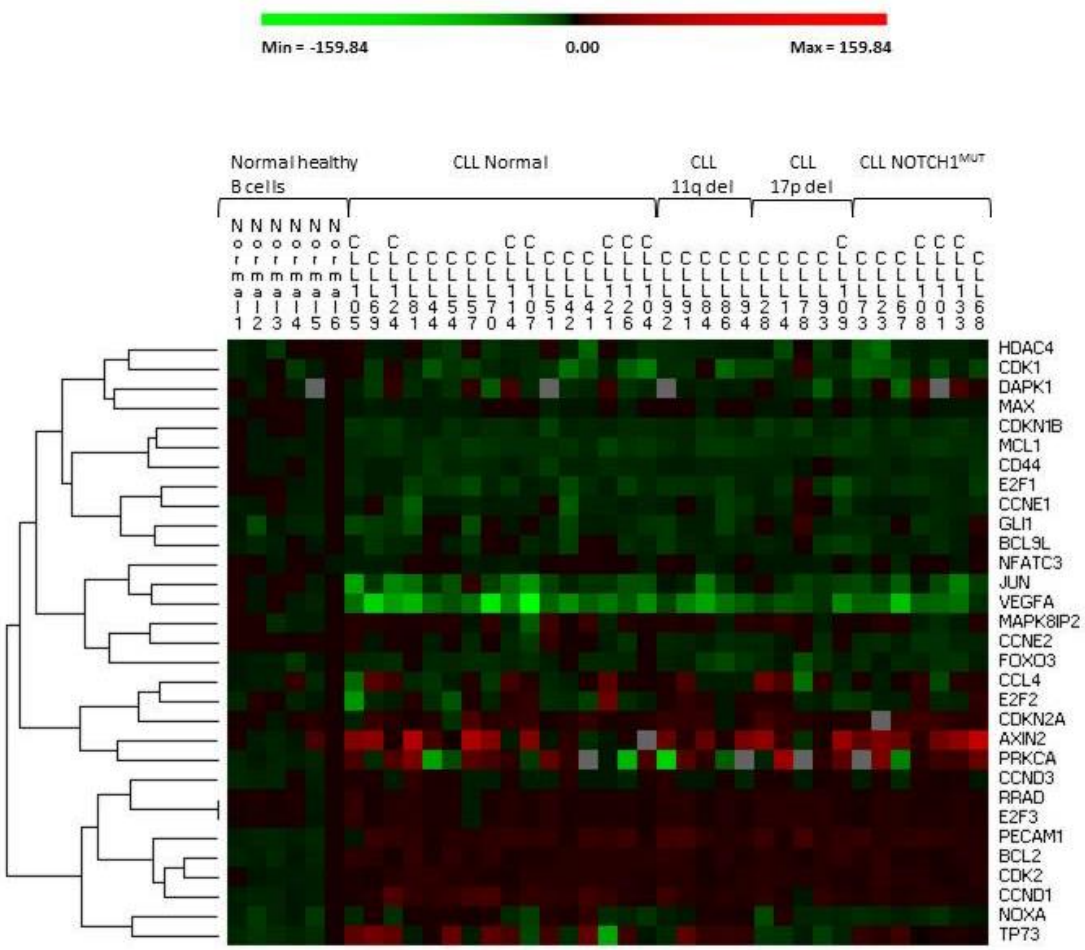

Figure 6.5 GEP between CLL samples are similar between the different cytogenetic sub-groups

GEP of genes previously identified as being deregulated in CLL cells surviving OFA induced CDC were performed. GEPs were determined from normal healthy B cells (n=6), and CLL cells after purification from peripheral blood. GEP levels were determined by Fluidigm array analysis. Relative gene expression levels were determined using the average normal B cell value as calibrator calculated using the $\Delta\Delta C_t$ method using an average of four housekeeping genes as reference. GEPs were determined for CLL samples that had no 11q or 17p del (CLL normal) (n=16), 11q del (n=5), 17p del (n=5), and NOTCH1^{MUT} CLL patients (n=7). Heat maps were produced using PermutMatrix software.

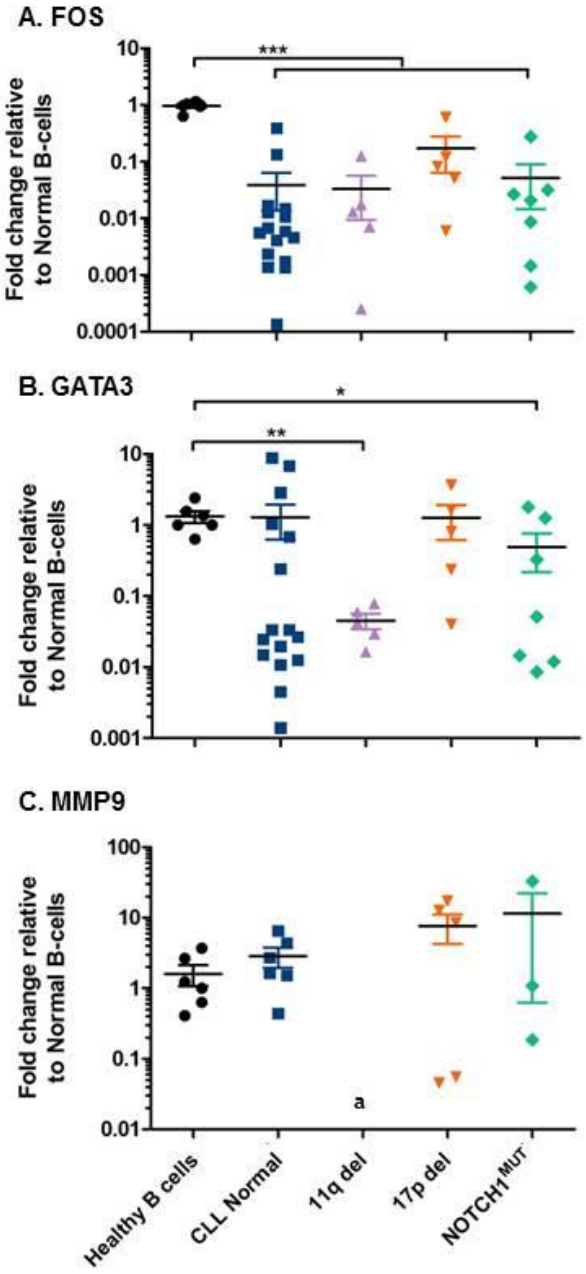

Figure 6.6 Focused gene analysis identifies differences between gene regulation and the different cytogenetic CLL subsets

Gene expression was determined from normal healthy B cells and CLL cells after purification from peripheral blood. Gene expression levels were determined by Fluidigm array analysis. Relative gene expression levels were determined against the average normal B cell values calculated using the $\Delta\Delta C_t$ method with an average of four housekeeping genes as reference. A. FOS expression from healthy B cells (n=6), CLL normal (n=16), 11q del (n=5), 17p del (n=5), and NOTCH1^{MUT} (n=7). B. GATA-3 expression from healthy B cells (n=6), CLL normal (n=16), 11q del (n=5), 17p del (n=5), and NOTCH1^{MUT} (n=7). C. MMP9 expression from healthy B cells (n=6), CLL normal (n=6), 11q del (n=0)[a], 17p del (n=5), and NOTCH1^{MUT} (n=3). p values were determined by an unpaired t-test (*, p<0.05, ** p<0.01, *** p<0.001).

[a] MMP9 gene expression levels were undetectable for all 11q del CLL samples (n=5) assessed.

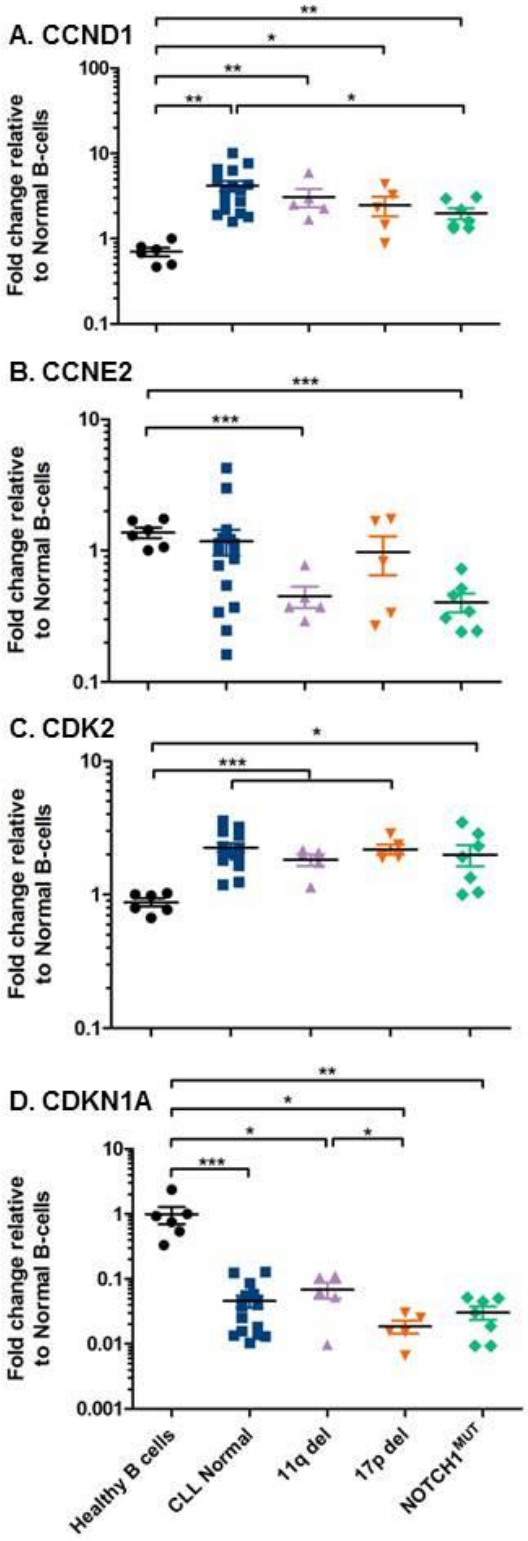

Figure 6.7 Cell cycle genes are de-regulated in CLL cells

Gene expression was determined from normal healthy B cells (n=6), and CLL cells after purification from peripheral blood. Gene expression levels was determined by Fluidigm array analysis using the $\Delta\Delta C_t$ method with an average of four housekeeping genes as reference, fold change is relative to the average normal healthy B cell value. Gene expression levels were determined for CLL Normal (n=16), 11q del (n=5), 17p del (n=5), and NOTCH1^{MUT} (n=7) unless otherwise stated. A. CCND1 expression. B. CCNE2 expression C. CDK2 expression. D. CDKN1A expression levels for CLL Normal (n=15), 11q del (n=5), 17p del (n=5), and NOTCH1^{MUT} (n=7), p values were determined by an unpaired t-test (*, p<0.05, ** p<0.01, *** p<0.001).

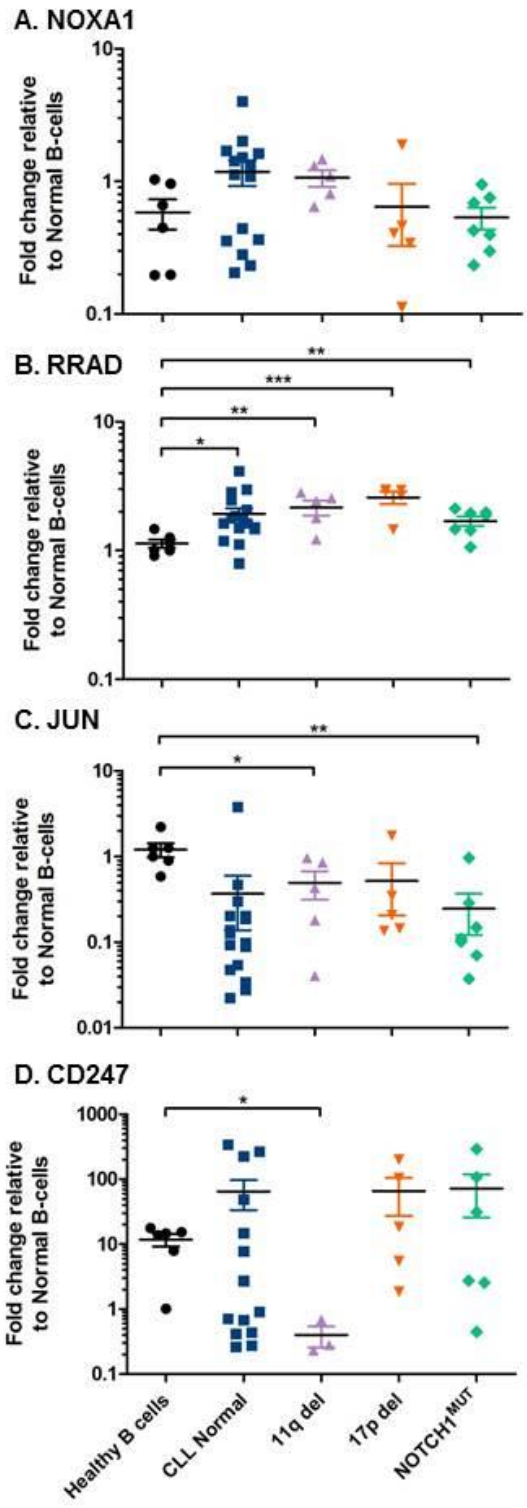

Figure 6.8 CD247, a gene of interest in CLL cells escaping OFA induced CDC, is significantly down-regulated in 11q del CLL samples

Gene expression was determined from normal healthy B cells (n=6), and CLL cells after purification from peripheral blood. Gene expression levels was determined by Fluidigm array analysis using the $\Delta\Delta C_t$ method with an average of four housekeeping genes as reference, fold change is relative to normal healthy B cells. Gene expression levels were determined for CLL Normal (n=16), 11q del (n=5), 17p del (n=5), and NOTCH1^{MUT} (n=7) unless otherwise stated. A. NOXA1 expression levels for CLL Normal (n=15), 11q del (n=5), 17p del (n=5), and NOTCH1^{MUT} (n=7). B. RRAD expression C. JUN expression. D. CD247 expression levels for CLL Normal (n=14), 11q del (n=3), 17p del (n=5), and NOTCH1^{MUT} (n=6). p values were determined by an unpaired t-test (*, $p<0.05$, ** $p<0.01$, *** $p<0.001$).

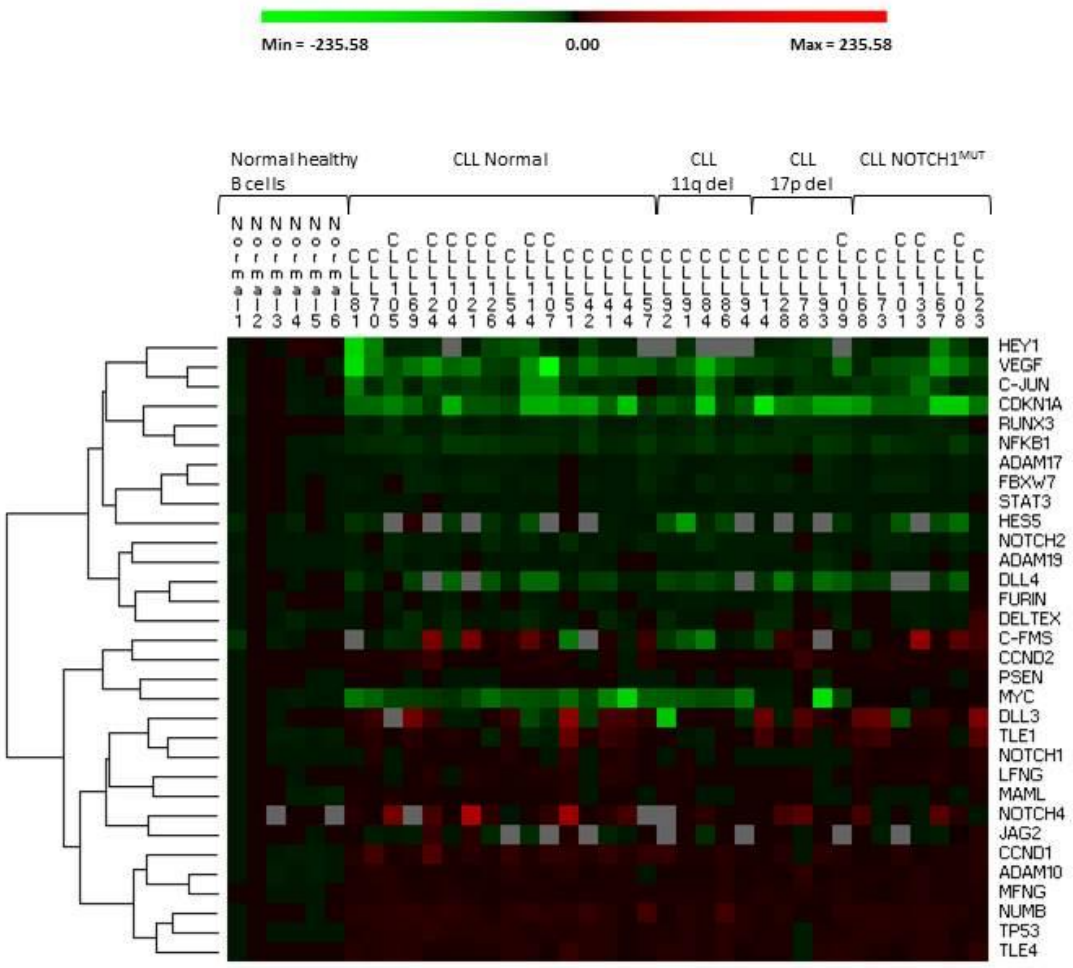

Figure 6.9 NOTCH signalling pathway is de-regulated in all CLL subsets compared to normal healthy B cells

GEPs were determined from normal healthy B cells (n=6), and CLL cells after purification from peripheral blood. GEP levels were determined by Fluidigm array analysis. Relative gene expression levels were determined by $\Delta\Delta C_t$ method using an average of four housekeeping genes as reference and the average normal B cell value as the calibrator. GEP's were determined for CLL patients that are CLL Normal with no 11q or 17p del (n=16), 11q del (n=5), 17p del (n=5), and NOTCH1^{MUT} CLL patients (n=7). Heat maps were produced using PermutMatrix software. GEP of genes associated with the NOTCH1 signalling pathway.

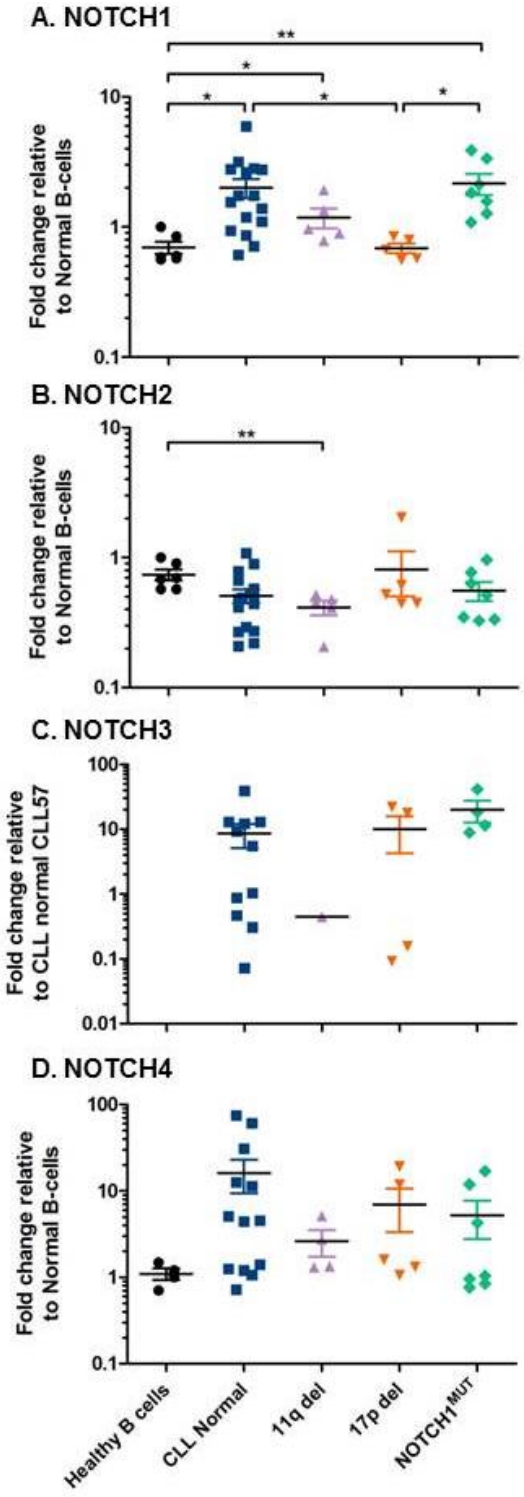

Figure 6.10 All NOTCH receptors apart from NOTCH2 are up-regulated in our CLL samples

Gene expression was determined from normal healthy B cells, and CLL cells after purification from peripheral blood. Gene expression levels was determined by Fluidigm array analysis. Relative gene expression levels were determined by $\Delta\Delta C_t$ method using an average of four housekeeping genes as reference, fold change is relative to normal healthy B cells unless stated otherwise. A. NOTCH1 expression for normal healthy B cells (n=6), CLL Normal (n=16), 11q del (n=5), 17p del (n=5), and NOTCH1^{MUT} (n=7). B. NOTCH2 expression for normal healthy B cells (n=6), CLL Normal (n=15), 11q del (n=5), 17p del (n=5), and NOTCH1^{MUT} (n=7). C. NOTCH3 expression, fold change relative to CLL normal sample CLL57. Expression was determined for CLL Normal (n=11), 11q del (n=1), 17p del (n=4), and NOTCH1^{MUT} (n=4). D. NOTCH4 expression levels for normal healthy B cells (n=4), CLL Normal (n=13), 11q del (n=4), 17p del (n=5), and NOTCH1^{MUT} (n=7). p values were determined by an unpaired t-test (*, $p<0.05$, ** $p<0.01$).

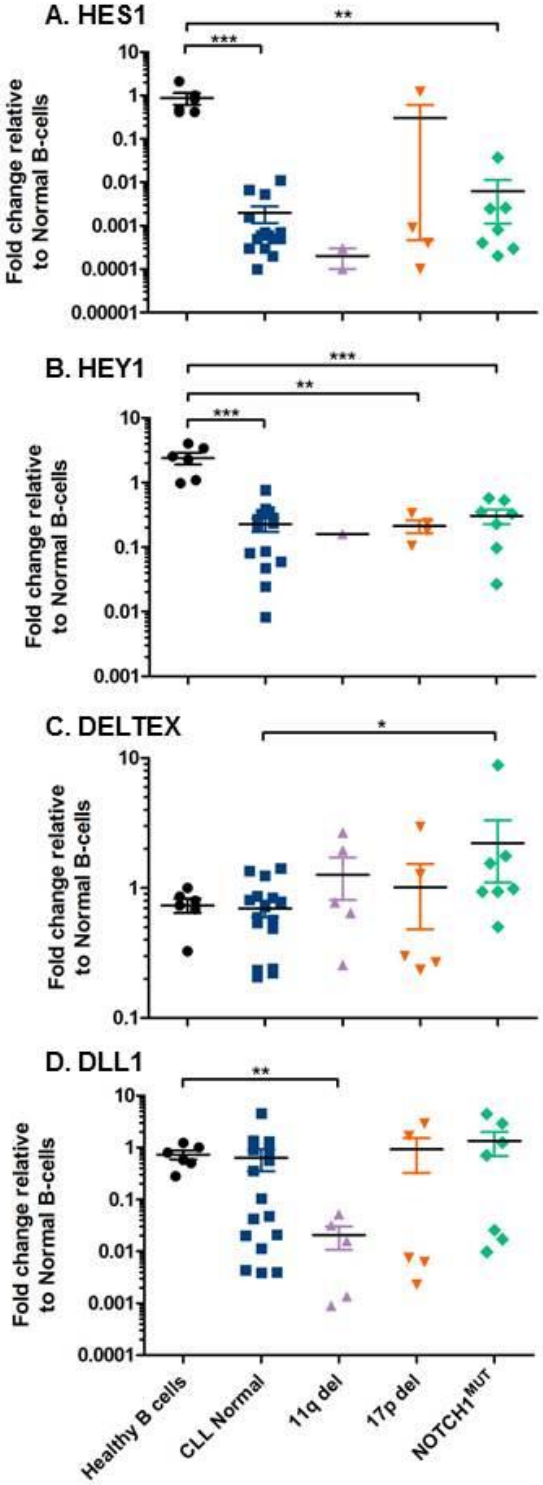

Figure 6.11 Target genes downstream of NOTCH1 are down-regulated in CLL compared to normal healthy B cells

Gene expression was determined from normal healthy B cells (n=6), and CLL cells after purification from peripheral blood. Gene expression levels was determined by Fluidigm array analysis. Relative gene expression levels were determined by $\Delta\Delta C_t$ method using an average of four housekeeping genes as reference, fold change is relative to normal healthy B cells. Gene expression levels were determined for CLL Normal (n=16), 11q del (n=5), 17p del (n=5), and $NOTCH1^{MUT}$ (n=7) unless otherwise stated A. HES1 expression levels for CLL Normal (n=15), 11q del (n=2), 17p del (n=4), and $NOTCH1^{MUT}$ (n=7). B. HEY1 expression for CLL Normal (n=14), 11q del (n=1), 17p del (n=4), and $NOTCH1^{MUT}$ (n=7). C. DELTEX expression. D. DLL1 expression levels. p values were determined by an unpaired t-test (*, $p<0.05$, ** $p<0.01$, *** $p<0.001$).

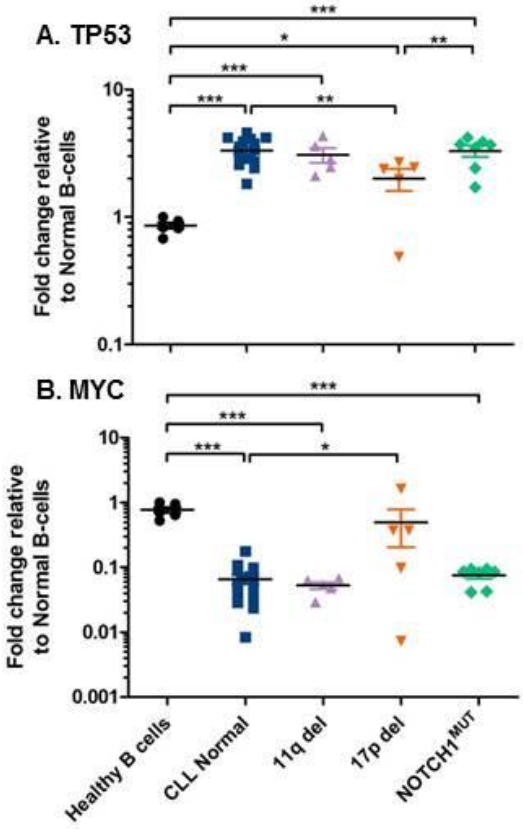

Figure 6.12 CLL samples display significantly different TP53 and MYC gene expression patterns compared to normal B cells

Gene expression was determined from normal healthy B cells (n=6), and CLL cells after purification from peripheral blood. Gene expression levels was determined by Fluidigm array analysis. Relative gene expression levels were determined by $\Delta\Delta C_t$ method using an average of four housekeeping genes as reference, fold change is relative to normal healthy B cells. Gene expression levels were determined for CLL Normal (n=16), 11q del (n=5), 17p del (n=5), and $NOTCH1^{MUT}$ (n=7). A. TP53 expression. B. MYC expression. p values were determined by an unpaired t-test. (*, $p<0.05$, ** $p<0.01$, *** $p<0.001$).

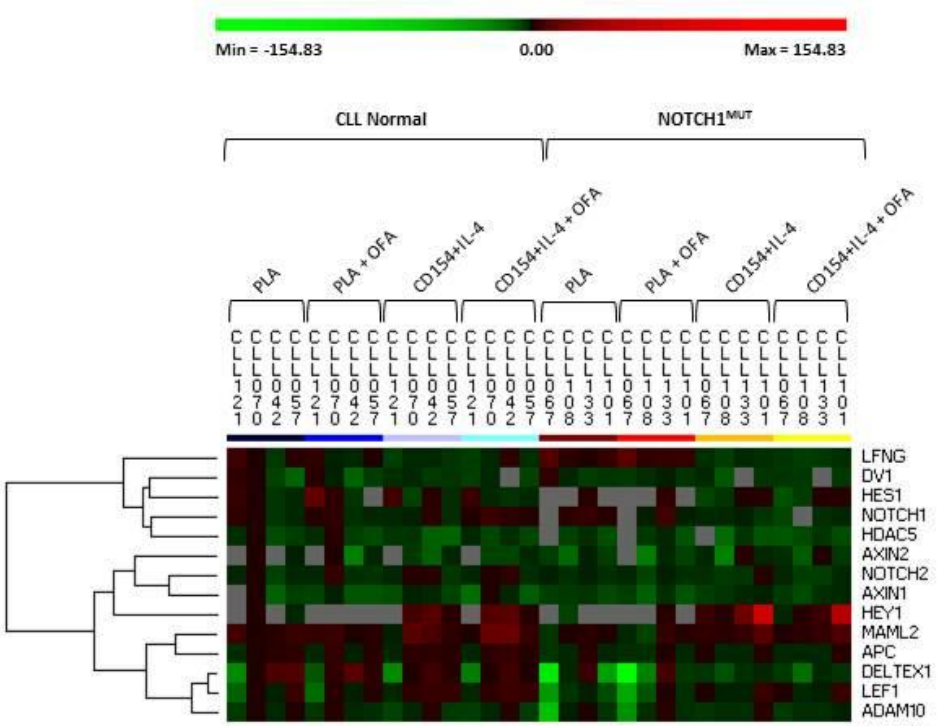

Figure 6.13 NOTCH1 signalling pathway is stimulated by NTL/CD154+IL-4 for both cytogenetically normal and NOTCH1^{MUT} CLL cells

CLL normal (n=4) and NOTCH1^{MUT} (n=4) were cultured on plastic and NTL/CD154+IL-4 with and without 20 μg/ml OFA for 48 hr. CLL cells were then isolated and RNA extracted and GEP levels determined by Fluidigm array analysis. Relative gene expression levels were determined by $\Delta\Delta C_t$ method using an average of four housekeeping genes as reference, fold change is relative to a CLL normal sample (CLL70) cultured on plastic without the presence of OFA. Heat maps were produced using PermutMatrix software. GEP of genes associated with the NOTCH1 and WNT signalling pathways.

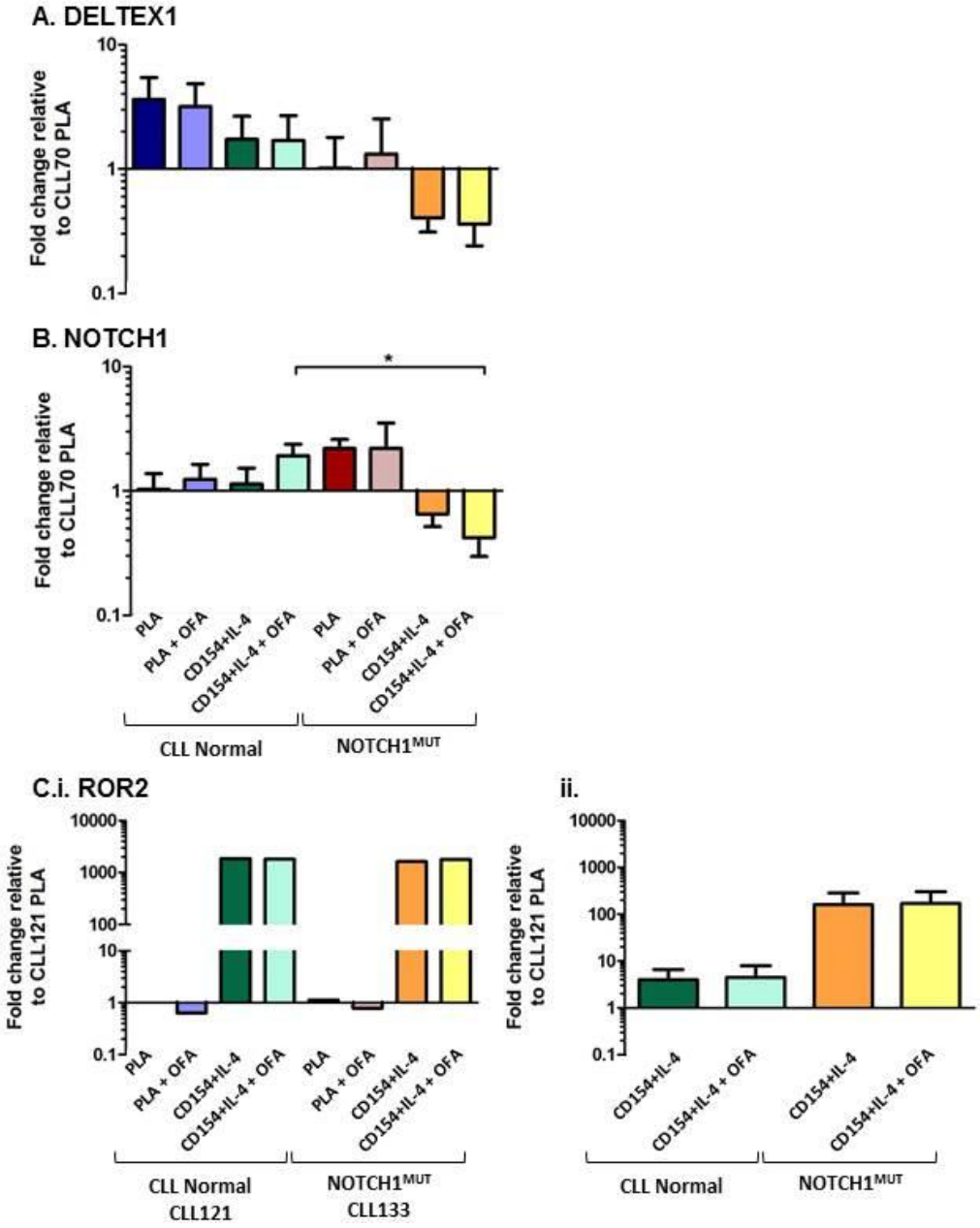

Figure 6.14 Genes associated with NOTCH1 and WNT signalling are de-regulated between CLL normal and NOTCH1^{MUT} CLL cells following stimulation with NTL/CD154+IL-4

CLL normal (n=4) and NOTCH1^{MUT} (n=4) were cultured on plastic and NTL/CD154+IL-4 with and without 20 µg/ml OFA for 48 hr. CLL cells were then isolated and RNA extracted and GEP levels determined by Fluidigm array analysis. Relative gene expression levels were determined by $\Delta\Delta C_t$ method using an average of four housekeeping genes as reference, fold change is relative to a CLL normal sample (CLL70) cultured on plastic without the presence of OFA, unless stated otherwise. A. DELTEX1 expression. B. NOTCH1 expression. C. ROR2 fold change expression levels are relative to CLL normal sample (CLL121) cultured on plastic without OFA. i. Expression levels for the CLL normal sample CLL121 and NOTCH1^{MUT} CLL 133. i. The mean ROR2 expression levels for CLL normal (n=3) and NOTCH1^{MUT} (n=3) CLL samples cultured on CD154/IL-4 with and without OFA. The mean $\pm$ SEM is shown. p values were determined by an unpaired t-test. (*, $p<0.05$).

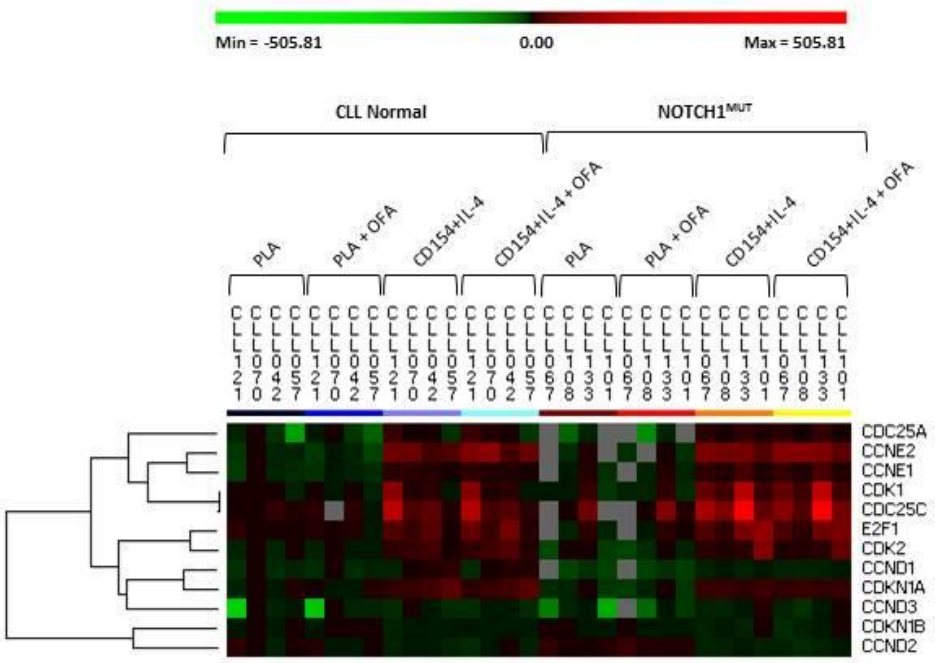

Figure 6.15 Cell cycle genes are up-regulated in CLL cells co-cultured with NTL/CD154+IL-4

CLL normal (n=4) and NOTCH1^{MUT} (n=4) were cultured on plastic and NTL/CD154+IL-4 with and without 20 μg/ml OFA for 48 hr. CLL cells were then isolated and RNA extracted and GEP levels determined by Fluidigm array analysis. Relative gene expression levels were determined by $\Delta\Delta C_t$ method using an average of four housekeeping genes as reference, fold change is relative to a CLL normal sample (CLL70) cultured on plastic without the presence of OFA. Heat maps were produced using PermutMatrix software. GEP of genes associated with the cell cycle regulation.

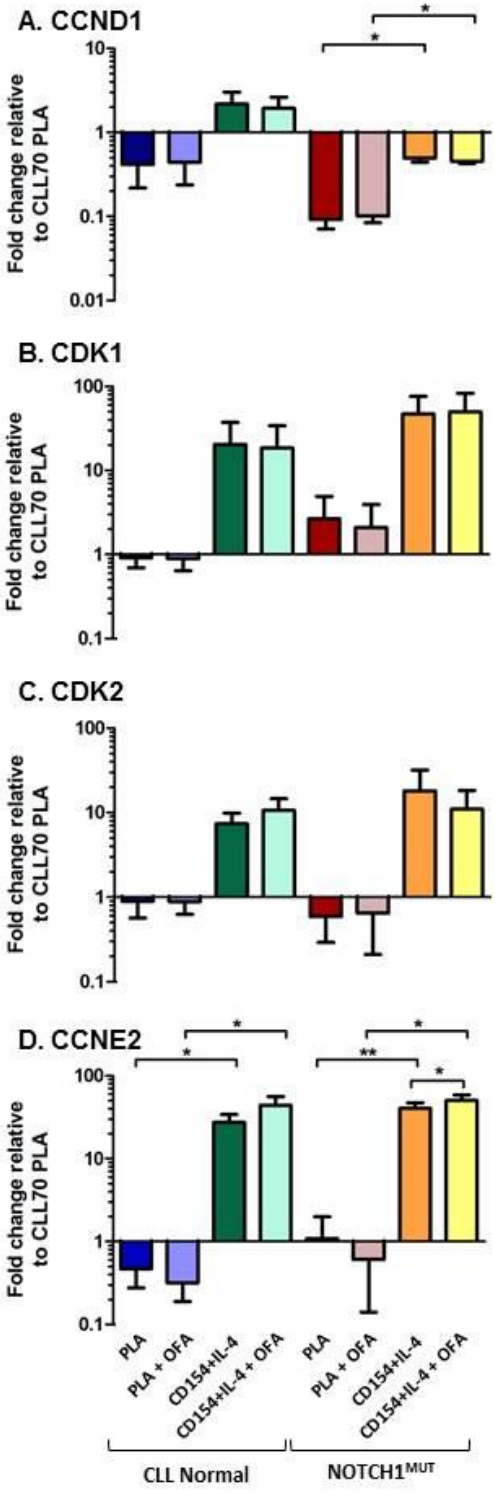

Figure 6.16 NOTCH1^{MUT} CLL cells activate cell cycle genes to a greater extent than normal CLL cells when co-cultured with NTL/CD154+IL-4

CLL normal (n=4) and NOTCH1^{MUT} (n=4) were cultured on plastic and NTL/CD154+IL-4 with and without 20 μg/ml OFA for 48 hr. CLL cells were then isolated and RNA extracted and GEP levels determined by Fluidigm array analysis. Relative gene expression levels were determined by $\Delta\Delta C_t$ method using an average of four housekeeping genes as reference, fold change is relative to a CLL normal sample (CLL70) cultured on plastic without the presence of OFA. A. CCND1 expression. B. CDK1 expression. C. CDK2 expression. D. CCNE2 expression. The mean ± SEM is shown. p values were determined by a paired t-test (*, p<0.05, ** p<0.01, *** p<0.001).

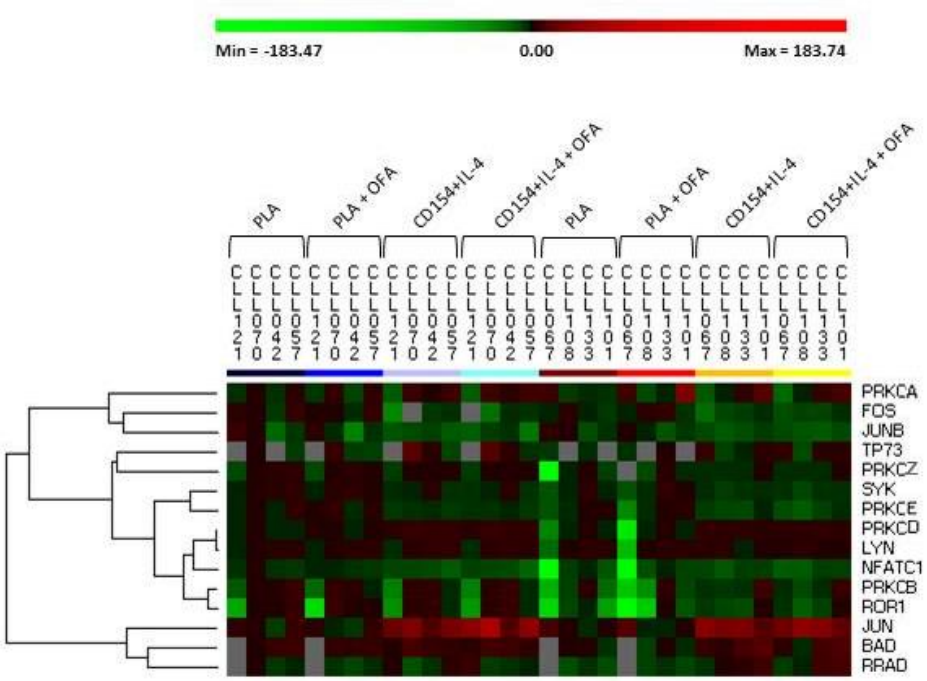

Figure 6.17 CLL cells differentially regulate genes associated with Ca^{2+} and BCR signalling upon stimulation with NTL/CD154+IL-4

CLL normal (n=4) and $NOTCH1^{MUT}$ (n=4) were cultured on plastic and NTL/CD154+IL-4 with and without 20 μg/ml OFA for 48 hr. CLL cells were then isolated and RNA extracted and GEP levels determined by Fluidigm array analysis. Relative gene expression levels were determined by $\Delta\Delta C_t$ method using an average of four housekeeping genes as reference, fold change is relative to a CLL normal sample (CLL70) cultured on plastic without the presence of OFA. Heat maps were produced using PermutMatrix software. GEP of genes associated with Ca^{2+} and BCR signalling.

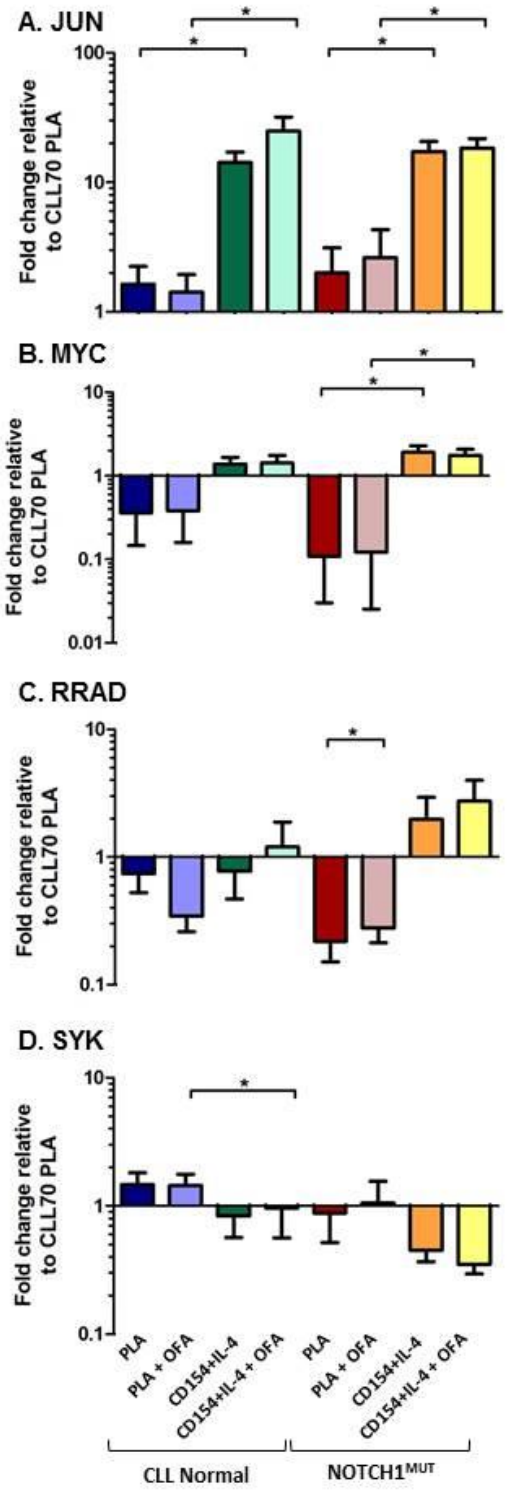

Figure 6.18 NOTCH1^{MUT} CLL cells display an elevated response in genes associated with Ca^{2+} and BCR signalling upon NTL/CD154+IL-4 stimulation

CLL normal (n=4) and NOTCH1^{MUT} (n=4) were cultured on plastic and NTL/CD154+IL-4 with and without 20 μg/ml OFA for 48 hr. CLL cells were then isolated and RNA extracted and GEP levels determined by Fluidigm array analysis. Relative gene expression levels were determined by $\Delta\Delta C_t$ method using an average of four housekeeping genes as reference, fold change is relative to a CLL normal sample (CLL70) cultured on plastic without the presence of OFA. A. JUN expression. B. MYC expression. C. RRAD expression. D. SYK expression. The mean $\pm$ SEM is shown. p values were determined by a paired t-test (*, $p<0.05$).

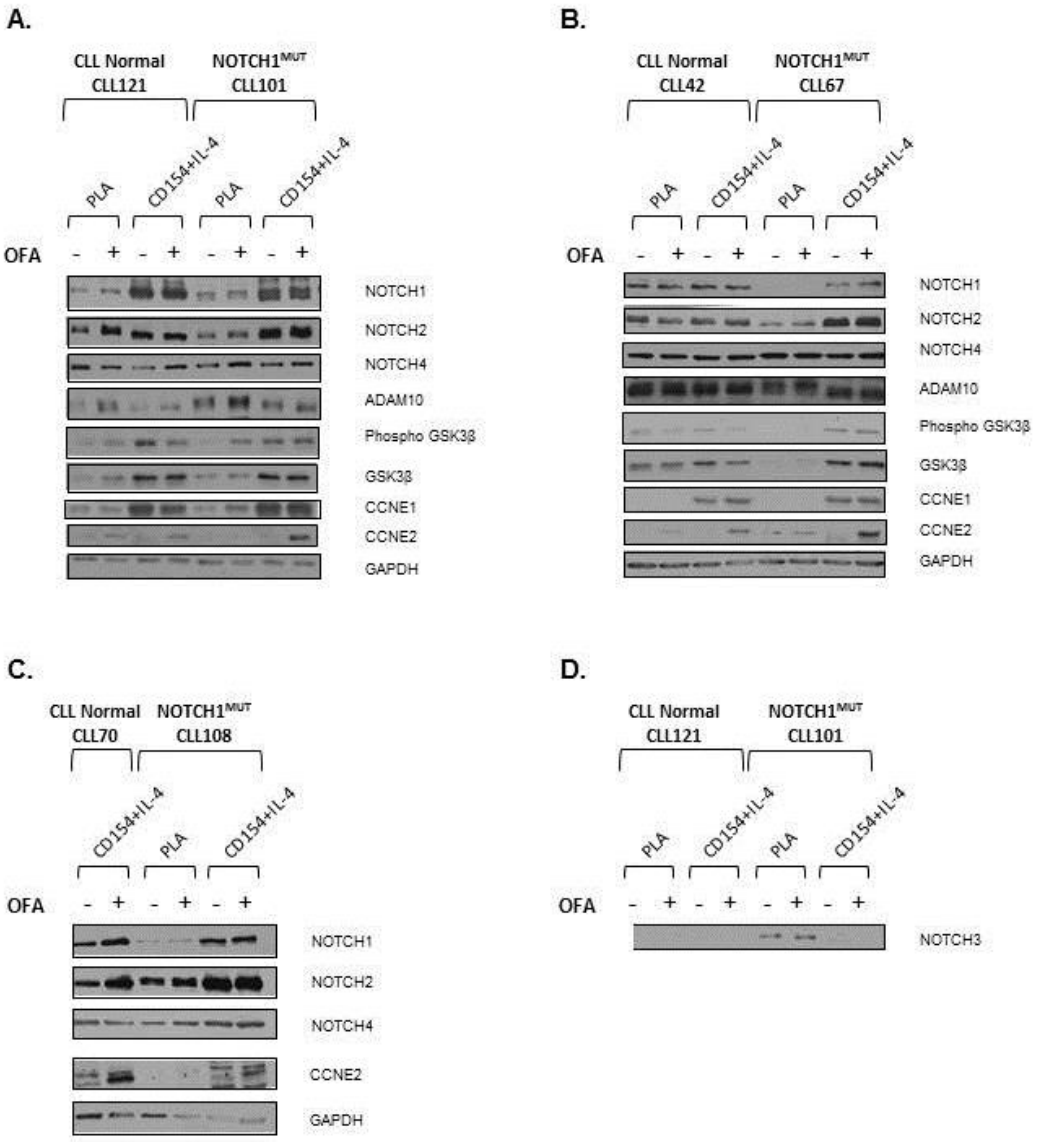

Figure 6.19 Notch1 and Notch2 appear activated at the protein level upon stimulation with NTL/CD154+IL-4 for both CLL normal and NOTCH1^{MUT} CLL cells

CLL normal (n=3) and NOTCH1^{MUT} (n=3) were cultured on plastic and NTL/CD154+IL-4 with and without 20 μg/ml OFA for 48 hr. CLL cells were then isolated and protein extracted and expression levels determined by western blot analysis. Expression levels for Notch1-4 all represent the active intracellular forms of the protein. A. CLL normal, CLL121, and NOTCH1^{MUT}, CLL101. B. CLL normal, CLL42, and NOTCH1^{MUT}, CLL67. C. CLL normal, CLL70, and NOTCH1^{MUT}, CLL108. D. CLL normal, CLL121, and NOTCH1^{MUT}, CLL101 intracellular Notch3 expression.

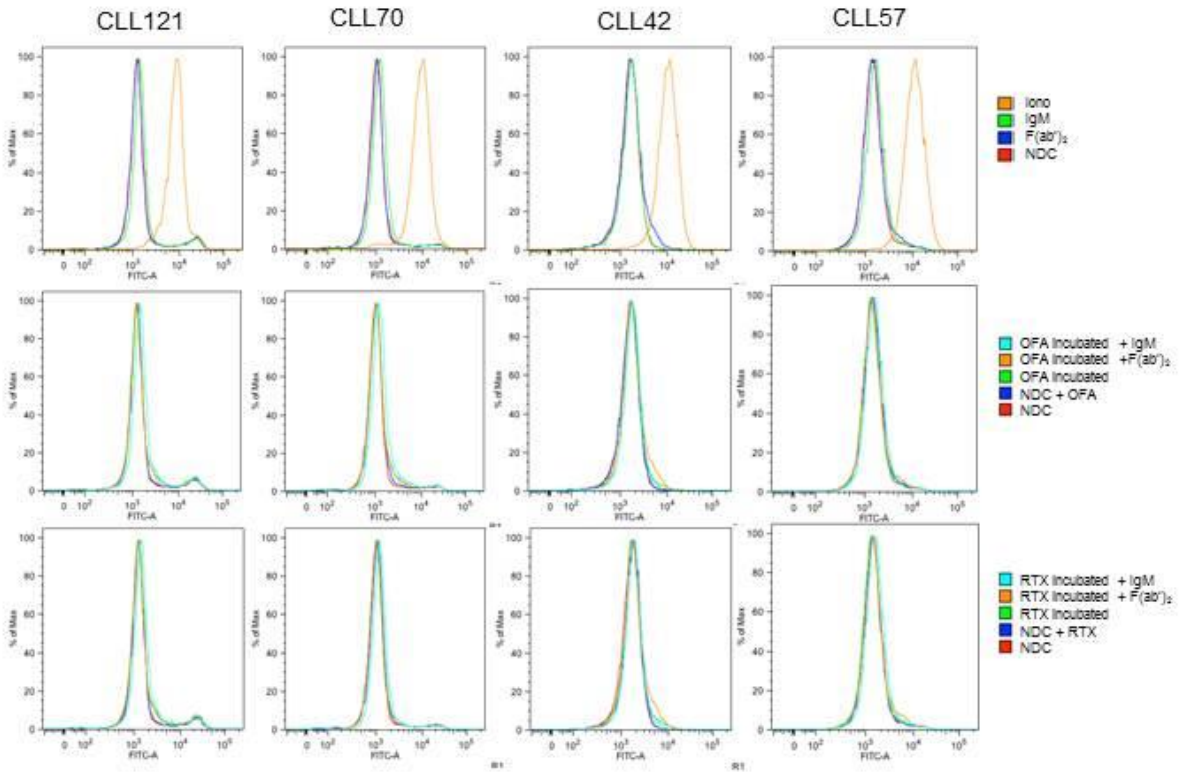

Figure 6.20 Cytogenetically normal CLL samples display no Ca^{2+} flux upon BCR stimulation

Fluo-4 (2 μM) calcium indicator was used to determine calcium flux in CLL patients by flow cytometry. CLL patients were incubated with fluo-4 for 45 min, CLL cells were then washed and left to incubate for a further 30 min. CLL cells were either not treated (NDC) or incubated with 20 μg/ml OFA or RTX for 15 min prior to reading fluo-4 signal in the FITC channel on the FACS Canto II. NDC or OFA/RTX incubated CLL cells, calcium signal was measured immediately following either 10 μg/ml $F(ab')_2$, 10 μg/ml IgM, 20 μg/ml OFA, 20 μg/ml RTX or 500 nM Ionomycin (Iono) addition (+). Fluo-4 signal was recorded for 2 min and the MFI is shown. Normal CLL samples (n=4).

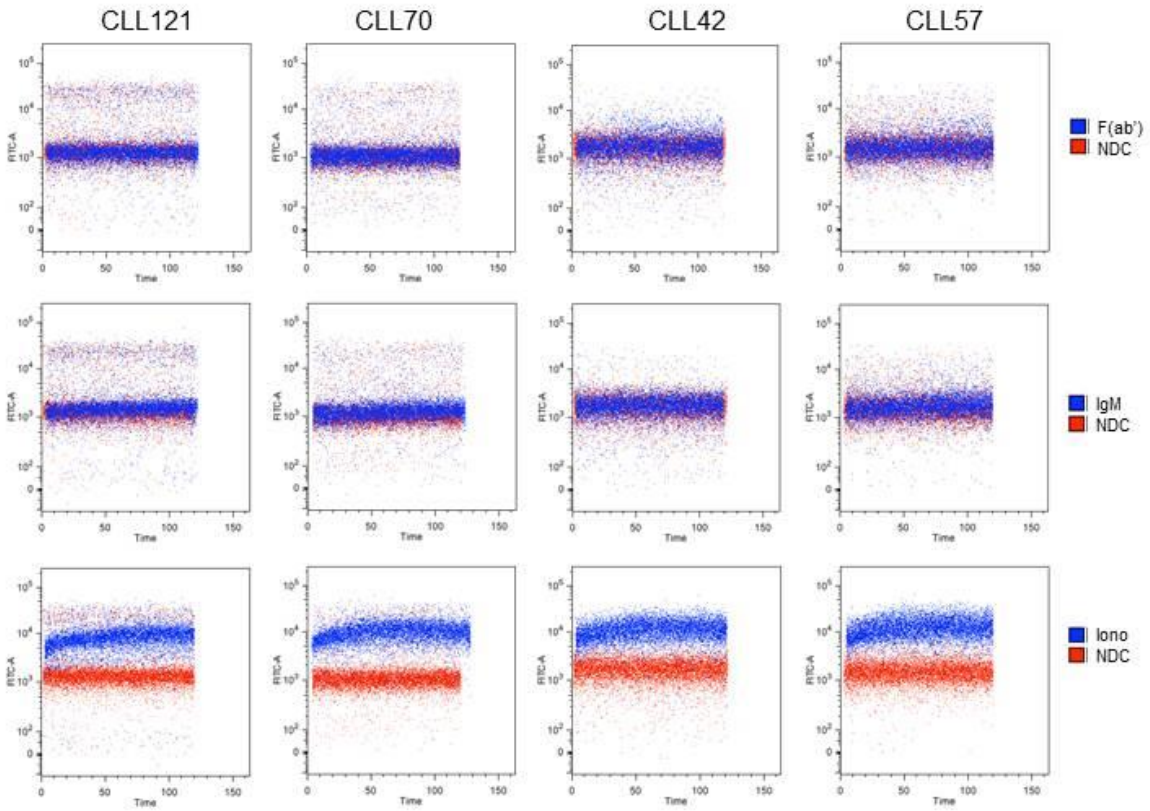

Figure 6.21 Cytogenetically normal CLL samples display no Ca^{2+} flux over time upon BCR stimulation

Fluo-4 (2 μM) calcium indicator was used to determine calcium flux in CLL patients by flow cytometry. CLL patients were incubated with fluo-4 for 45 min, CLL cells were then washed and left to incubate for a further 30 min. CLL cells were either not treated (NDC) or incubated with 20 μg/ml OFA or RTX for 15 min prior to reading fluo-4 signal in the FITC channel on the FACS Canto II. NDC or OFA/RTX incubated CLL cells, calcium signal was measured immediately following either 10 μg/ml $F(ab')_2$, 10 μg/ml IgM, 20 μg/ml OFA, 20 μg/ml RTX or 500 nM Ionomycin (Iono) addition (+). Fluo-4 signal was recorded for 2 min and FITC signal vs. time is shown. Cytogenetically normal CLL samples (n=4).

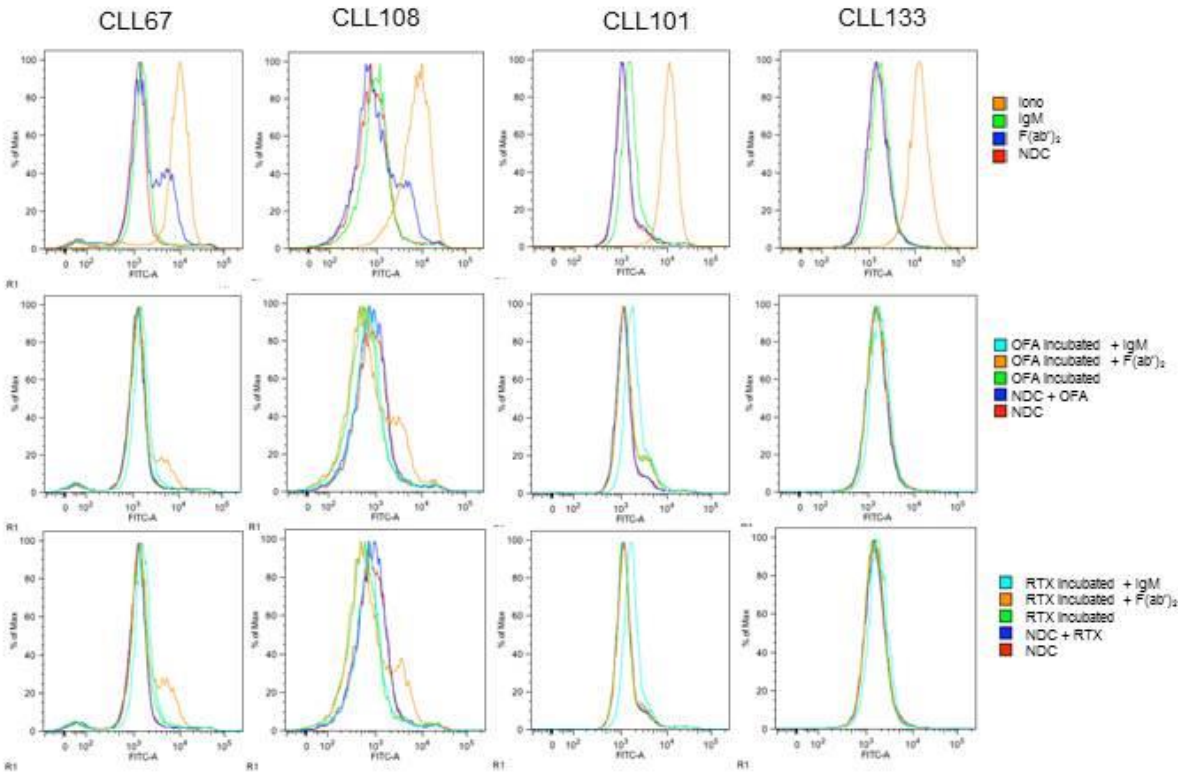

Figure 6.22. CLL samples with NOTCH1^{MUT} display differential Ca^{2+}signalling with BCR stimulation compared to cytogenetically normal CLL samples

Fluo-4 (2 μM) calcium indicator was used to determine calcium flux in CLL patients by flow cytometry. CLL patients were incubated with fluo-4 for 45 min, CLL cells were then washed and left to incubate for a further 30 min. CLL cells were either not treated (NDC) or incubated with 20 μg/ml OFA or RTX for 15 min prior to reading fluo-4 signal in the FITC channel on the FACS Canto II. NDC or OFA/RTX incubated CLL cells, calcium signal was measured immediately following either 10 μg/ml F(ab')$_2$, 10 μg/ml IgM, 20 μg/ml OFA, 20 μg/ml RTX or 500 nM Ionomycin (Iono) addition (+).Fluo-4 signal was recorded for 2 min and the MFI is shown. NOTCH1^{MUT} CLL samples (n=4).

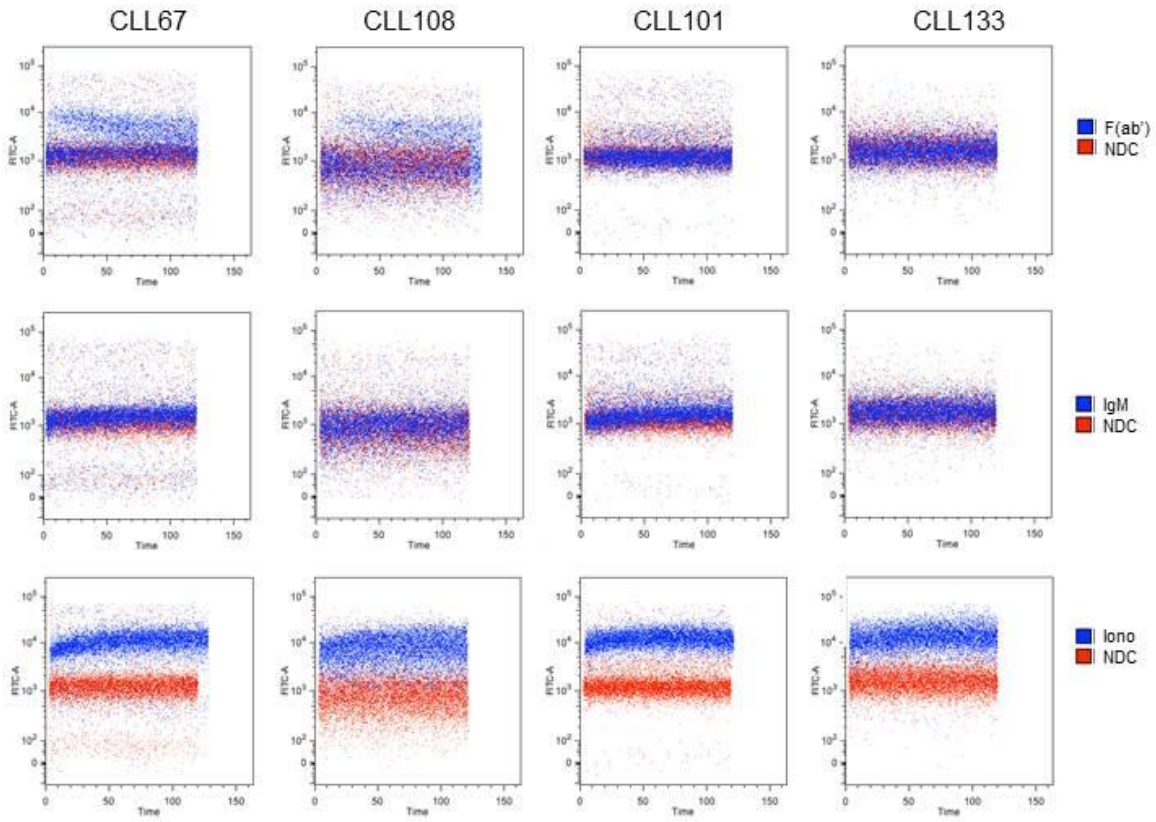

Figure 6.23 CLL samples with NOTCH1^{MUT} display differential Ca^{2+} signalling with different BCR stimulation over time

Fluo-4 (2 μM) calcium indicator was used to determine calcium flux in CLL patients by flow cytometry. CLL patients were incubated with fluo-4 for 45 min, CLL cells were then washed and left to incubate for a further 30 min. CLL cells were either not treated (NDC) or incubated with 20 μg/ml OFA or RTX for 15 min prior to reading fluo-4 signal in the FITC channel on the FACS Canto II. NDC or OFA/RTX incubated CLL cells, calcium signal was measured immediately following either 10 μg/ml F(ab')$_2$, 10 μg/ml IgM, 20 μg/ml OFA, 20 μg/ml RTX or 500 nM Ionomycin (Iono) addition (+).Fluo-4 signal was recorded for 2 min and the FITC signal vs. time is shown. NOTCH1^{MUT} CLL samples (n=4).

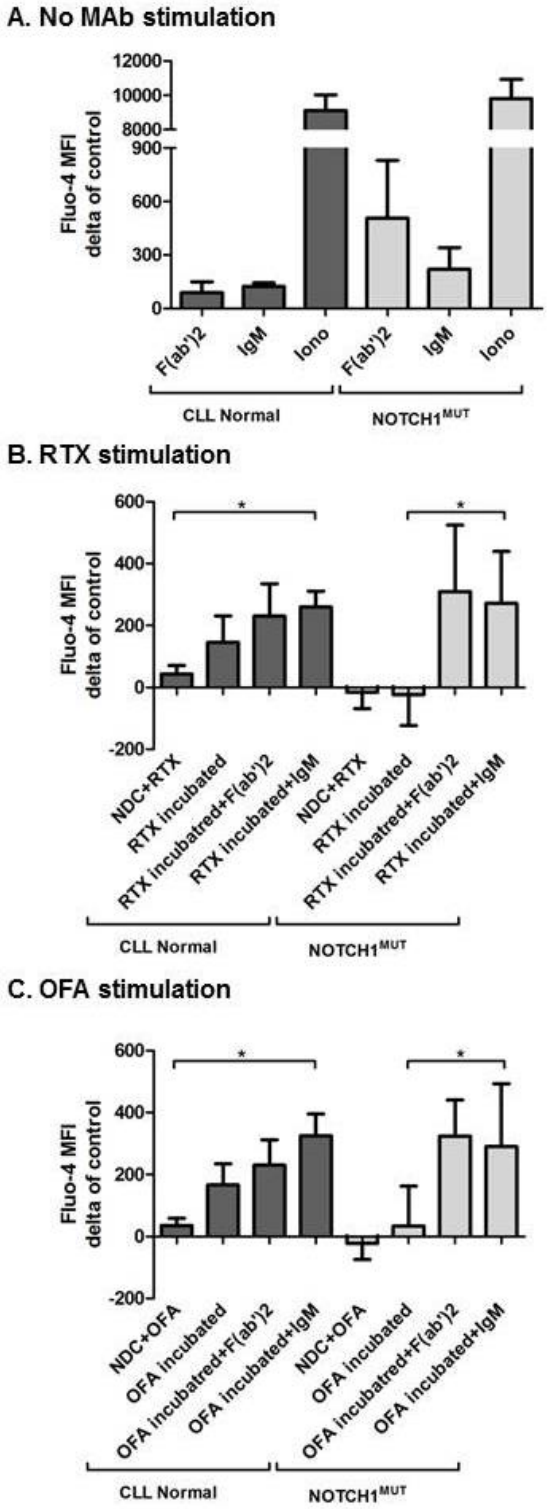

Figure 6.24 CLL samples with NOTCH1^{MUT} display muted Ca^{2+} signalling with OFA/RTX treatment

Fluo-4 (2 μM) calcium indicator was used to determine calcium flux in CLL patients by flow cytometry. CLL patients were incubated with fluo-4 for 45 min, CLL cells were then washed and left to incubate for a further 30 min. CLL cells were either not treated (NDC) or incubated with 20 μg/ml OFA or RTX for 15 min prior to reading fluo-4 signal in the FITC channel on the FACS Canto II. NDC or OFA/RTX incubated CLL cells, calcium signal was measured immediately following either 10 μg/ml F(ab')$_2$, 10 μg/ml IgM, 20 μg/ml OFA, 20 μg/ml RTX or 500 nM Ionomycin (Iono) addition (+).Fluo-4 signal was recorded for 2 min and the MFI is shown for cytogenetically normal (n=4) and NOTCH1^{MUT} (n=4) CLL cells. A. Stimulation response without RTX or OFA treatment. B. RTX stimulation. C. OFA stimulation. The mean $\pm$ SEM is shown. p values were determined by a paired t-test (*, $p<0.05$).

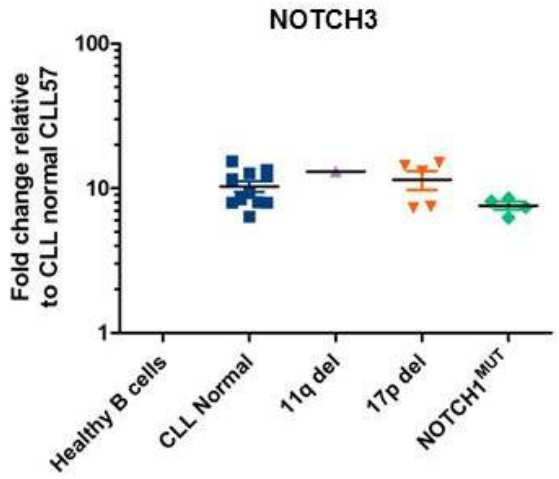

Supplementary Figure 6.1 ΔC_t levels for NOTCH3 expression

NOTCH3 gene expression was determined from CLL cells after purification from peripheral blood. Gene expression levels were determined by Fluidigm array analysis. ΔC_t gene expression levels were determined using an average of four housekeeping genes as reference NOTCH3 expression, fold change relative to CLL normal sample CLL57. Expression was determined for CLL Normal (n=11), 11q del (n=1), 17p del (n=4), and $NOTCH1^{MUT}$ (n=4).

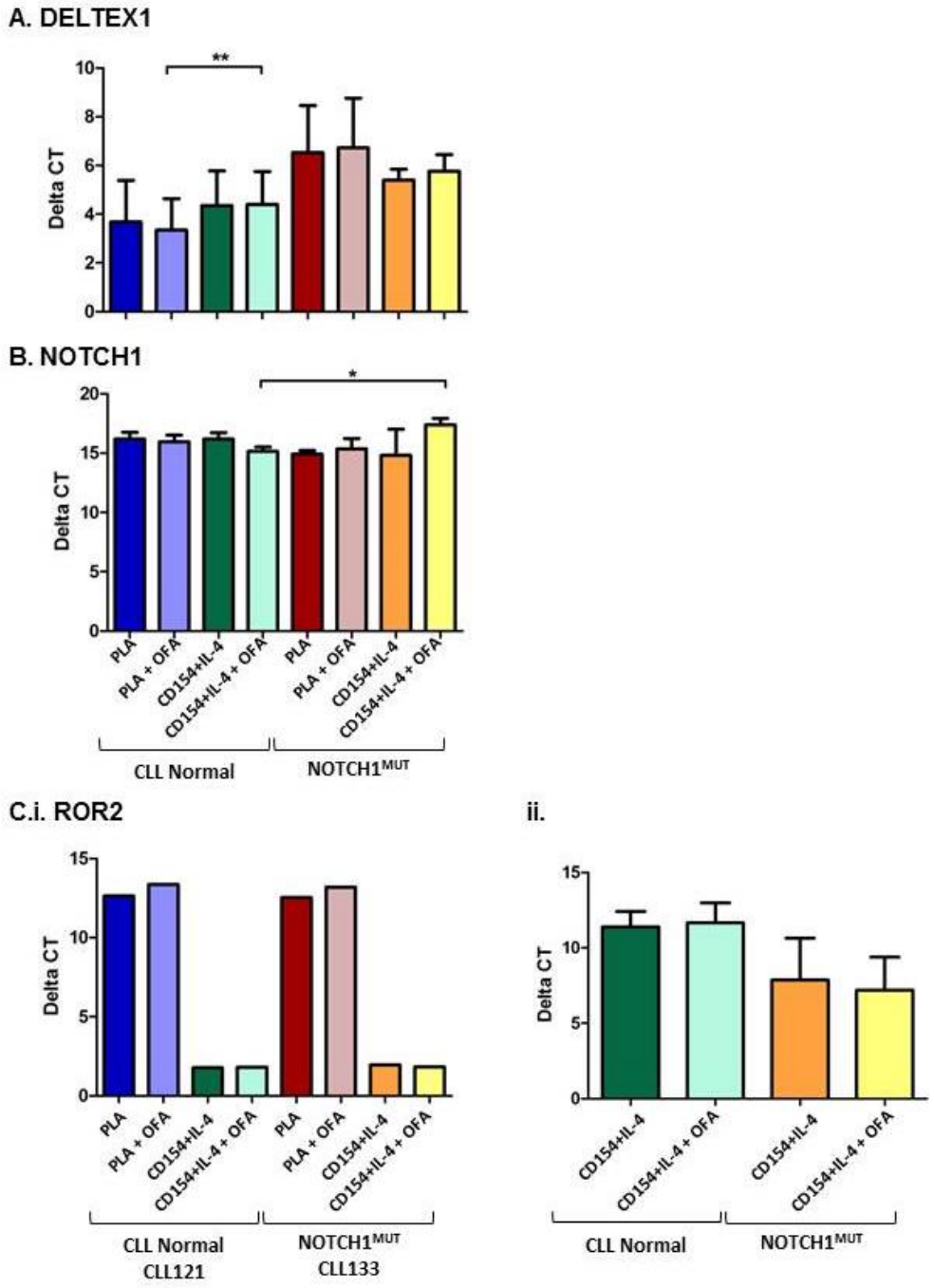

Supplementary Figure 6.2 ΔC_t levels for genes associated with NOTCH1 and WNT signalling

CLL normal (n=4) and NOTCH1^{MUT} (n=4) CLL cells were cultured on plastic and NTL/CD154+IL-4 with and without 20 µg/ml OFA for 48 hr. CLL cells were then isolated and RNA extracted and GEP levels determined by Fluidigm array analysis. ΔC_t gene expression levels were determined using an average of four housekeeping genes as reference. A. DELTEX1 expression. B. NOTCH1 expression. C. ROR2 fold change expression levels are relative to CLL normal sample (CLL121) cultured on plastic without OFA. i. Expression levels for the CLL normal sample CLL121 and NOTCH1^{MUT} CLL 133. i. The mean ROR2 expression levels for CLL normal (n=3) and NOTCH1^{MUT} (n=3) CLL samples cultured on CD154/IL-4 with and without OFA. p values between different cytogenetic subsets were determined by an unpaired t-test, and p values within a cytogenetic subset were determined by a paired t test (*, $p<0.05$, ** $p<0.01$).

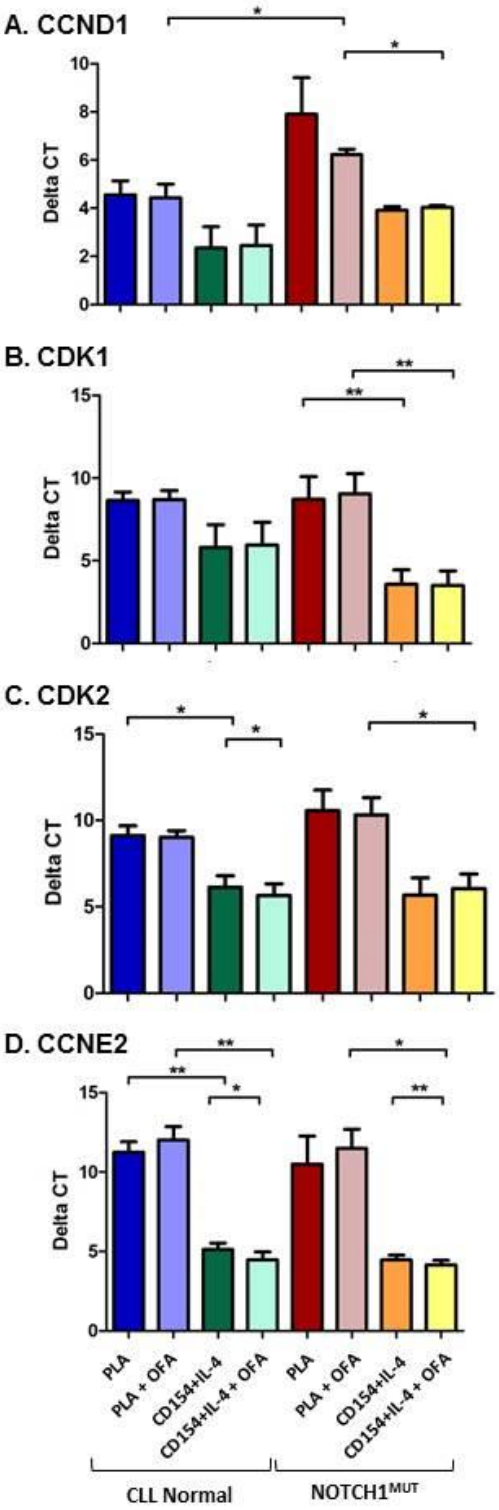

Supplementary Figure 6.3 ΔC_t levels for genes associated with cell cycle progression

CLL normal (n=4) and NOTCH1^{MUT} (n=4) CLL cells were cultured on plastic and NTL/CD154+IL-4 with and without 20 µg/ml OFA for 48 hr. CLL cells were then isolated and RNA extracted and GEP levels determined by Fluidigm array analysis. ΔC_t gene expression levels were determined using an average of four housekeeping genes as reference. A. CCND1 expression. B. CDK1 expression. C. CDK2 expression. D. CCNE2 expression. p values were determined by a paired t-test (*, $p<0.05$, ** $p<0.01$).

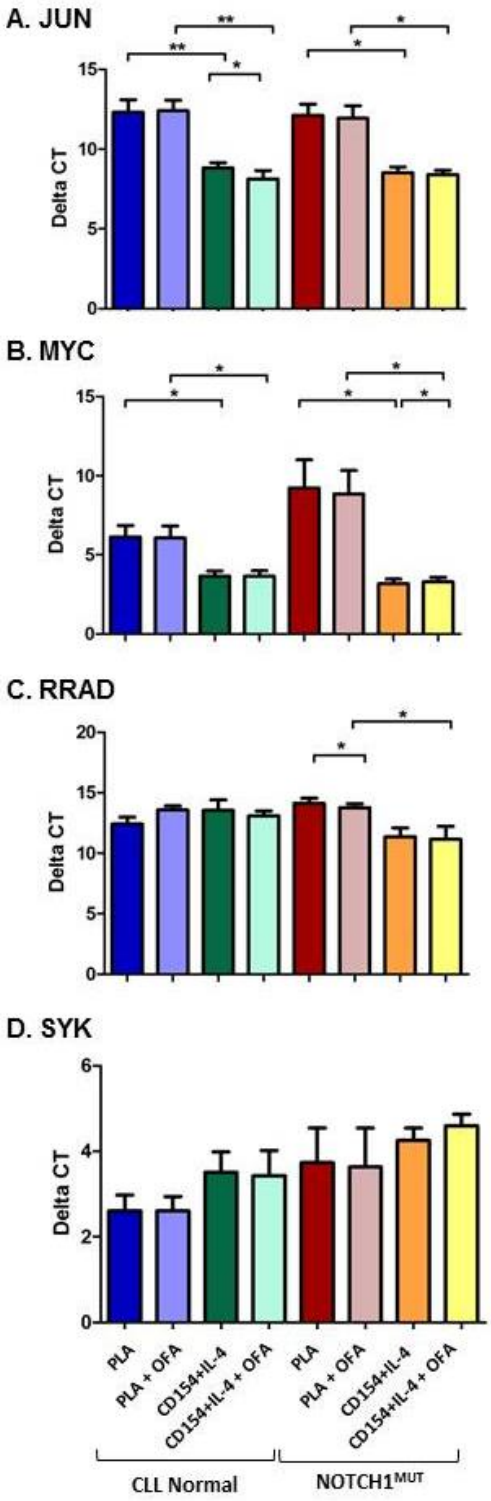

Supplementary Figure 6.4 ΔC_t levels for genes associated with Ca^{2+} and BCR signalling

CLL normal (n=4) and NOTCH1^{MUT} (n=4) CLL cells were cultured on plastic and NTL/CD154+IL-4 with and without 20 µg/ml OFA for 48 hr. CLL cells were then isolated and RNA extracted and GEP levels determined by Fluidigm array analysis. ΔC_t gene expression levels were determined using an average of four housekeeping genes as reference. A. JUN expression. B. MYC expression. C. RRAD expression. D. SYK expression. p values between different cytogenetic subsets were determined by an unpaired t-test, and p values within a cytogenetic subset were determined by a paired t test (*, $p<0.05$, ** $p<0.01$).

7 General discussion

Anti-CD20 MAbs are an integral part of the first line treatment of CLL. OFA, a next generation type I anti-CD20 MAb, has recently been given FDA approval for the treatment of CLL patients in combination with chlorambucil for previously untreated CLL patients, and as a single agent for CLL patients that are double refractory. We, and others, have shown OFA to be a far superior inducer of CDC than RTX[315,344]. The ability of OFA to elicit a CDC response is an important part of its efficacy. We have demonstrated that OFA activity is limited in the treatment of CLL by several different factors including; complement levels, CD20 expression, microenvironmental stimulation and CLL genetic mutations.

7.1 Clinical efficacy of OFA

Within clinical trials, OFA demonstrated great promise for the treatment of CLL. For 59 CLL patients that were double refractory to both fludarabine and alemtuzumab, OFA infusion resulted in ORR of 58%, CR in 57% of patients, PFS of 5.7 months and OS 13.7 months[257]. Despite superior results as a single agent in comparison to RTX, OFA is not licenced as a first line therapy for CLL patients. While improved treatment options are now available, CLL is currently incurable and most CLL patients with aggressive disease will relapse. Ineffective clearance can result in the appearance of MRD, which has been associated with reduced OS[281]. The presence of MRD can be assessed by either allele specific oligonucleotide PCR or four/six colour flow cytometry, which is able to detect 1 CLL cell in 10^4 leukocytes. MRD negativity is considered to be less than 1 CLL cell present in 10^4 cells/μl[280,282,407]. OFA demonstrates improved efficacy in combination with chlorambucil and bendamustine chemotherapy. GIMEMA multicentre Phase II trial of bendamustine with OFA in relapsed or refractory CLL patients (n=47) observed at a median follow up of 24.2 months 83.6% OS, PFS 49.6% and median PFS of 23.6 months[408]. COMPLEMENT I phase III trial investigated the efficacy of chlorambucil alone (n=227) or chlorambucil plus OFA (n=217). Trial results demonstrated superior efficacy of chlorambucil plus OFA compared to chlorambucil alone, PFS was 22.4 and 13.1 months respectively, and objective response occurred in 82.4% and 68.6% respectively[279].

When comparing the responses of OFA in a phase III clinical trial with the BCR antagonist ibrutinib within 391 relapsed refractory CLL and small cell lymphoma (SLL) patients, ibrutinb had superior responses. After 12 months, median survival for patients receiving ibrutininb vs. OFA was 90% vs. 81% and ORR was 42.6% with ibrutinib and 4.1% for those receiving OFA ($p<0.001$)[409]. It would appear that OFA and other type I anti-CD20 MAbs function most efficiently when used in combination therapy. A phase I trial of idelalisib in 54 relapsed or refractory CLL patients ORR was 72% and 15.8 months PFS[268]. A phase I trial of 21 relapsed or refractory CLL patients found a combination of idelalisib and OFA produced 76% ORR and 17.8 months PFS[410]. However recent publications suggest that there may be some antagonistic activity between BCR inhibitors and anti-CD20 MAbs and more research is required[411]. Type I anti-CD20 MAbs are thought to trigger direct cell death through coupling with the BCR to hijack the Ca^{2+} flux resulting in activation ROS and cell death[176]. However, cross-linking of antibodies is required for this to occur *in vitro* and therefore may not be clinically relevant. BCR inhibitors may cause down modulation of CD20, one recent publication found that co-culture with ibruitinib or idelalisib caused down-regulation of CD20 which then negatively impacted upon the ability of OFA or RTX to induce CDC. This reduced efficacy was more prominent with ibrutinib[411]. Another recent study also found that ibrutinib and to a lesser extent idelalisib caused NK cell degranulation abrogating ADCC function as well as phagocyte activation[412]. ADCC is an important pathway for anti-CD20 MAb efficacy[413]. However BCR signalling inhibitors have been shown to cause egress of CLL cells into the peripheral blood, this may provide an opportunity for a potent inducer of CDC, such as OFA to eradicate the cells[414,415]. Therefore any dosing schedules in BCR/anti-CD20 MAb combination therapies will have to be carefully considered to avoid antagonistic activity.

7.2 Limitations of complement

The identification that a large proportion of CLL patients harbour complement deficiencies, 37.5% in our CLL patient cohort, has important implications not only for anti-CD20 MAbs but also other MAbs, such as alemtuzumab, which utilise the CDC pathway. We identified that an even larger proportion (42.3%) of CLL patient sera became exhausted of complement when used for a second time *in vitro*. Complement exhaustion was also observed *in vivo* following OFA and RTX

immunotherapy, with preliminary results suggesting that complement levels took longer than 7 days to be regenerated. Our *in vitro* studies with primary CLL cells and different tumour burdens also provided important implications for complement consumption *in vivo*. The concentrations of CLL cells that we used were modest and do not represent the high lymphocyte counts typical of CLL patients that are eligible for OFA treatment. Impaired innate immunity through complement dysregulation further highlights the wide spread pathogenesis of CLL. CLL patient's immunity is further compromised through T cells involved in both adaptive and immune function displaying dysregulation, as well as NK cells which are important for the induction of ADCC [137,162-164,416]. Therefore, adding to complement deficiencies, there appears to be widespread CLL related immune suppression.

Our results suggest that the dosing schedule for OFA is inappropriate for maximal efficacy. The recommended treatment schedule for OFA infusion involves an initial low dose of 300 mg followed by weekly doses of 2000 mg for 7 weeks, after this time 2000 mg is administered monthly. RTX treatment on the other hand is administered every 4 weeks for at least 5 cycles of 375 mg/m^2. For comparison the average male is 1.9 m^2 whilst females are 1.7 m^2 therefore this would make the monthly doses 712.5 mg and 637.5 mg respectively[417]. Our results indicate that at the high doses of OFA, complement levels require longer than 7 days to recover. Whereas the monthly doses of RTX were long enough apart for complement levels to be restored in all CLL patients excluding the patient with complement deficiencies. It would appear therefore that the high doses of OFA may do more harm than good. A way of restoring the efficacy of OFA and RTX treatment is the inclusion of FFP with chemoimmunotherapy. Although our results would suggest that the most benefit would be from receiving C2 complement. However individual complement components are not currently clinically achievable, whereas FFP is readily available within the clinic. The side effects associated with adding FFP to treatment could include transfusion related lung injury, transfusion related circulatory overload and allergic reaction to transfusion[418], with the most common resulting from a lack of regulation when administering FFP. Apart from transfusion related risks there is also an elevated risk of infection as FFP is a human product, which is a particularly important consideration when administering FFP as many CLL

patients are immunosuppressed. Therefore with strict regulations for administering FFP the potential increase in OFA efficacy could be high. Two small clinical studies have already shown that the effect of adding FFP to RTX produced superior results than without FFP[347,348]. Adding FFP may also prove valuable in preventing the risk of serious infection within CLL patients.

One of the major causes of morbidity and mortality within CLL patients is not disease related but rather due to infections[338,345]. Disorders with complement deficiencies are associated with reduced efficiency of immune clearance and susceptibility to re-occurring infections[322-324]. It has also been identified that within CLL trogocytosis occurs, which causes rapid depletion of CD20 levels. Trogocytosis occurs when effector cells cleave the CD20/anti-CD20 MAb complex. Effector cells which include monocytes, macrophages, neutrophils and NK cells recognise the Fcγ portion of the MAb and instead of destroying the target cell cleave off the MAb with its target instead. This has been observed both *in vivo* and *in vitro* for both OFA and RTX, and severely compromises their activity[317,319,329,419]. CDC is incredibly fast acting; we observed maximal CDC activity after only 1 hour incubation of serum with HG3 cells. Sera from CLL patients undergoing RTX immunotherapy also demonstrate fast complement exhaustion, which occurs 24 hours post infusion. If, as predicted by our findings, it takes longer than 7 days to restore complement levels this provides a window of opportunity for the effector cells to perform trogocytosis. Ineffective clearance and subsequent loss of CD20 from the surface of the CLL cell can lead to anti-CD20 MAb resistance. Further to this, our CLL and NTL co-culture experiment, which mimics the circulating compartment of CLL cells, suggest that when OFA was present in culture there was a dramatic reduction in CDC activity even after only 24 hr of co-culture. This highlights that even in the absence of effector cells to perform trogocytosis CLL cells are effective at removing the anti-CD20 MAb/CD20 complex from the surface of the cell either from loss or internalisation. Trials using low dose RTX are promising and limit the loss of CD20 from the surface of CLL cells, so perhaps the same strategy can be applied to OFA dosing[420,421]. In support of low dosing for OFA and RTX our *in vitro* ADCC assay indicated that optimal efficacy was achieved at 100 ng/ml and 1 μg/ml respectively, concentrations above this then resulted in reduced ADCC induction. A 2000 mg dose of OFA equates to 400 μg/ml within the circulating

blood supply, therefore it may be possible that there is reduced ADCC efficacy at this concentration.

7.3 Microenvironmental stimulation and anti-CD20 MAb efficacy

A significant part of CLL pathogenesis is due to resistance to apoptosis and subsequent chemoresistance. These factors are enhanced through signals derived from their microenvironmental niche[136]. The microenvironment provides important protective signals to CLL cells that assist in cell survival and chemoresistance. *In vitro* experiments have demonstrated that co-culture with BM cells gives rise to resistance to fludarabine and chlorambucil[141,190]. Therefore we aimed to establish the impact microenvironmental stimulation had on the efficacy of anti-CD20 MAbs. Others have shown that CD40 stimulation sensitised CLL cells to RTX induced direct cell death due to increased cytosolic Ca^{2+} levels and ROS induced cell death. Our results demonstrate that there is also an increase in the induction of CDC with both RTX and more notably with OFA when CLL cells were stimulated with CD154 and IL-4. This increase in CDC was independent of any notable changes in CD20 expression levels or complement inhibitory proteins CD55 or CD59. A recent study demonstrated that CD20 expression levels were reduced after 2 weeks of co-culture with BM stromal cells, which conferred reduced susceptibility to RTX induced CDC[144]. CDC levels are critically dependent on the expression levels of the target antigen[311]. CLL cells have reduced CD20 expression compared to normal healthy B cells and other B cell malignancies and any further drop in CD20 expression limits MAb efficacy. Our experiments were only carried out over a 72 hour time period; however it does appear that after the peak in CDC at 48 hours CDC levels started to drop after this point. This suggests that microenvironmental stimulation could potentially provide resistance to anti-CD20 MAbs in the long term.

BM stromal cells also display expression of Notch1 ligands, enhancing the induction of Notch1 within the LN[226-228]. Notch1 expression can also be induced by the presence of NF-κB signalling which leads to Jagged 1 expression. An enrichment of $NOTCH1^{MUT}$ CLL cells[230] has been observed *in vivo* within the LN as well as higher expression levels of ICN *in vitro* following co-culture with stromal cells observed by us and others[101,232]. Notch1 signalling also leads to an increase

in expression of the anti-apoptotic protein MCL-1[200]. MCL-1 is a key protein down-stream of BCR signalling associated with the resistance of CLL cells to apoptosis[175]. Further to this, Notch1 downstream target is c-MYC, a well-known oncogene, and the expression of both has been identified as producing glycolytic switch within CLL cells co-cultured with BM stromal cells[422]. Glucose metabolism has been identified as a key pathway cancer cells utilise when developing drug resistance. A study of CLL patients (n=692) identified that NOTCH1^{MUT} CLL patients had lower expression levels of CD20. This was due to HDAC being displaced from the CSL transcriptional complex by ICN, subsequently HDAC then bound to the promoter of CD20 resulting in epigenetic silencing of the gene[233]. Presumably within the LN where there is enhanced activation of Notch1 this mechanism will be exacerbated. Notch1 and Notch2 inhibitors, after 3 days in co-culture with CLL cells and BM stromal cells, resulted in increased susceptibility to chemotherapeutic agents. This suggests that Notch1 inhibitors are a possible therapeutic avenue for CLL treatment. Notch1 inhibitors include Abs which target the Notch1 receptor so that it no longer can be activated by ligand binding [232]and γ-secretase inhibitors which block the activation of ICN [423]. Overexpression of Notch1 is observed within our *NOTCH1* wild-type CLL samples as well as NOTCH1^{MUT} when co-cultured with NTL/CD154+IL-4. Therefore an inhibitor of Notch1 may prove to be an important therapeutic target for disrupting the pro-survival signals gained from CLL cells interacting with the microenvironment.

Although very preliminary our genetic and Ca^{2+} signalling data provide an interesting and novel way in which NOTCH1 display resistance to anti-CD20 MAbs and potentially other chemotherapeutic agents. Upon BCR stimulation our NOTCH1^{MUT} CLL samples displayed an immediate flux in Ca^{2+}, although this will have to be corroborated with more thorough experimentation. This suggests that NOTCH1^{MUT} CLL samples have enhanced BCR signalling, which may lead to the up-regulation of Bcl-2 related anti-apoptotic proteins aiding survival. Therefore an appropriate treatment regime for NOTCH1^{MUT} CLL patients may be the use of BCR inhibitors, idelalisib or ibrutinib. Although NOTCH1^{MUT} CLL patients displayed improvements in PFS with the addition of OFA plus chlorambucil this only lasted 18 months[109]. Our data would suggest that the initial benefit is likely through CDC eradication of CLL cells not expressing NOTCH1^{MUT}. The remaining

CLL cells are then only those with higher ICN expression. It appears that NOTCH1^{MUT} CLL cells favour localising within the LN, as observed *in vivo*[228]. Within the LN NOTCH1^{MUT} CLL cells have chronic Notch1 activation which presumably leads to further reduced efficacy of anti-CD20 MAb therapies[101]. This is corroborated by our *in vitro* co-culture of NOTCH1^{MUT} CLL cells with NTL/CD154+IL-4 which displayed lower OFA-CDC levels than our cytogenetically normal patient cohort. The ineffective clearance of NOTCH1^{MUT} CLL cells by anti-CD20 MAbs could lead to an enhanced level of MRD after treatment, and allow clonal evolution of the malignant cells. This suggests that anti-CD20 MAbs should not be used for the treatment of CLL patients with a high proportion of NOTCH1^{MUT} CLL cells. CLL patients with low clonal levels of NOTCH1^{MUT} CLL cells may benefit from a dual strategy of anti-CD20 MAb in combination with a Notch inhibitor and BCR inhibitor. Although some antagonistic activity between BCR inhibitors and anti-CD20 MAbs have been identified, through the down modulation of CD20[412] and NK cell granulation causing reduced ADCC[411], these factors will have to be considered against the potential benefit. Benefits could be observed through BCR inhibitors causing egress of CLL cells from the BM[414,415], long term co-culture of CLL cells with BM stromal cells have been shown to cause significant down modulation of CD20[144] and without BM stimulation there will be less stimulation of the Notch1 pathway[232], highlighting the potential synergistic activity of these two chemotherapies. A proposed mechanism by which NOTCH1^{MUT} CLL cells evade OFA CDC is shown in Figure 7.1. We hypothesise that high OFA dosing and complement deficiencies result in high rates of complement exhaustion within CLL patients. Complement exhaustion in conjunction with ADCC effector cell exhaustion would result in ineffective clearance of the CLL cell. NOTCH1^{MUT} CLL cells with low CD20 expression will likely escape OFA induced CDC.

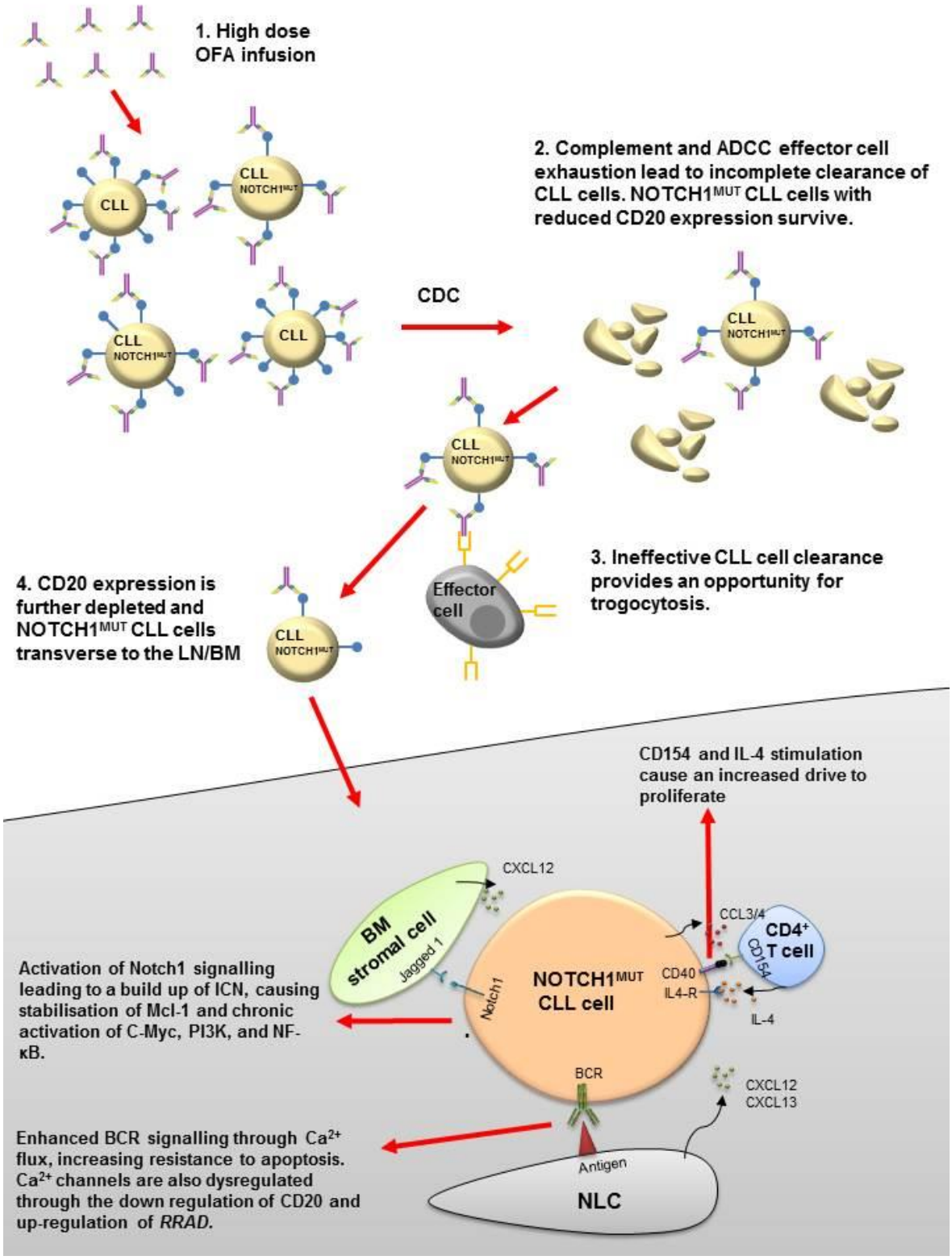

Figure 7.1 Hypothetical response of NOTCH1^{MUT} CLL cells to OFA

OFA demonstrates stronger binding and slower dissociation rates than RTX and our experiments suggest it is still stable and active 7 days after infusion. ADCC effector cells have also demonstrated exhaustion following anti-CD20 MAb infusion in CLL patients with high tumour burdens[371,424]. Exhausted complement

and ADCC cells allows time for trogocytosis effector cells to remove any bound OFA and CD20 leading to a further reduction in the expression of CD20 on the surface of the cell. The NOTCH1^{MUT} CLL cell can then travel to the LN/BM to gain further pro-survival signals. BM cells express Notch1 ligands and therefore lead to activation of ICN[232]. BM cells also provide stimulation for BCR signalling[137]. Downstream targets of Notch1 include oncogene c-Myc. Our results corroborate this as *MYC* expression was more actively up-regulated in NOTCH1^{MUT} CLL cells than *NOTCH1* wild-type cells. Our results also suggest that NOTCH1^{MUT} CLL cells are more primed towards proliferation upon NTL/CD154+IL-4 stimulation than our normal cytogenetic CLL subset, possibly enhancing clonal expansion. NOTCH1^{MUT} CLL cells also demonstrated sensitivity to BCR stimulation and displayed de-regulation of genes identified to be involved in Ca^{2+} signalling, including *ROR2* and *RRAD*. Pro-apoptotic gene *NOXA* was also down-regulated in our NOTCH1^{MUT} CLL patients. Together the microenvironmental signals provide enhanced survival and chemoresistance signals for NOTCH1^{MUT} CLL cells, allowing the clonal evolution of NOTCH1^{MUT} CLL cells.

In conclusion anti-CD20 MAbs are an important treatment strategy for CLL patients. However our data would suggest that the clinical efficacy of OFA is reduced by complement deficiencies within a large proportion of CLL patients. The dosing schedule of OFA does not allow suitable time for complement levels to be restored and therefore any subsequent dosing will have reduced efficacy. Although OFA is superior to RTX in the induction of CDC, like RTX OFA is most effective when used in combination therapy. This body of research provides additional evidence for the inclusion of FFP with MAb infusion to further improve clinical response. As the role of NOTCH1^{MUT} in the pathogenesis of CLL continues to be further elucidated it would appear that due to the complex network of Notch1 signalling, type I anti-CD20 MAbs are rendered ineffective treatments in this patient cohort. Therefore to avoid poor CLL cell clearance, type I anti-CD20 MAbs should not be considered a suitable therapy for NOTCH1^{MUT} CLL patients, a more appropriate treatment regime would be the use of novel BCR-targeting therapies which may then provide a successful clinical outcome for this poor prognostic subset of CLL patients.

List of References

1. Murphy K. Janeway's immunobiology. 8th ed. New York: Garland Science, Taylor & Francis Group, LLC.; 2012.
2. Nagasawa T. Microenvironmental niches in the bone marrow required for B-cell development. Nat Rev Immunol 2006;6:107-16.
3. Milne CD, Paige CJ. IL-7: a key regulator of B lymphopoiesis. Semin Immunol 2006;18:20-30.
4. Busslinger M. Transcriptional control of early B cell development. Annu Rev Immunol 2004;22:55-79.
5. Miga A, Masters S, Gonzalez M, Noelle RJ. The role of CD40-CD154 interactions in the regulation of cell mediated immunity. Immunol Invest 2000;29:111-4.
6. Grewal IS, Flavell RA. CD40 and CD154 in cell-mediated immunity. Annu Rev Immunol 1998;16:111-35.
7. McHeyzer-Williams LJ, Malherbe LP, McHeyzer-Williams MG. Helper T cell-regulated B cell immunity. Curr Top Microbiol Immunol 2006;311:59-83.
8. Heesters BA, Myers RC, Carroll MC. Follicular dendritic cells: dynamic antigen libraries. Nat Rev Immunol 2014;14:495-504.
9. Allen CD, Okada T, Cyster JG. Germinal-center organization and cellular dynamics. Immunity 2007;27:190-202.
10. Klein U, Dalla-Favera R. Germinal centres: role in B-cell physiology and malignancy. Nat Rev Immunol 2008;8:22-33.
11. Victora GD, Nussenzweig MC. Germinal centers. Annu Rev Immunol 2012;30:429-57.
12. Vinuesa CG, Sanz I, Cook MC. Dysregulation of germinal centres in autoimmune disease. Nat Rev Immunol 2009;9:845-57.
13. Victora GD, Dominguez-Sola D, Holmes AB, Deroubaix S, Dalla-Favera R, Nussenzweig MC. Identification of human germinal center light and dark zone cells and their relationship to human B-cell lymphomas. Blood 2012;120:2240-8.
14. Burger JA. Inhibiting B-cell receptor signaling pathways in chronic lymphocytic leukemia. Curr Hematol Malig Rep 2012;7:26-33.
15. Burger JA, Chiorazzi N. B cell receptor signaling in chronic lymphocytic leukemia. Trends Immunol 2013;34:592-601.
16. Choi MY, Kipps TJ. Inhibitors of B-cell receptor signaling for patients with B-cell malignancies. Cancer J 2012;18:404-10.
17. Avalos AM, Meyer-Wentrup F, Ploegh HL. B-cell receptor signaling in lymphoid malignancies and autoimmunity. Adv Immunol 2014;123:1-49.
18. O'Rourke L, Tooze R, Fearon DT. Co-receptors of B lymphocytes. Curr Opin Immunol 1997;9:324-9.
19. Dal Porto JM, Gauld SB, Merrell KT, Mills D, Pugh-Bernard AE, Cambier J. B cell antigen receptor signaling 101. Mol Immunol 2004;41:599-613.
20. Chiorazzi N, Ferrarini M. B cell chronic lymphocytic leukemia: lessons learned from studies of the B cell antigen receptor. Annu Rev Immunol 2003;21:841-94.
21. Stevenson FK, Krysov S, Davies AJ, Steele AJ, Packham G. B-cell receptor signaling in chronic lymphocytic leukemia. Blood 2011;118:4313-20.
22. Davis RE, Ngo VN, Lenz G, et al. Chronic active B-cell-receptor signalling in diffuse large B-cell lymphoma. Nature 2010;463:88-92.
23. Hashimoto A, Okada H, Jiang A, et al. Involvement of guanosine triphosphatases and phospholipase C-gamma2 in extracellular signal-regulated kinase, c-Jun NH2-terminal kinase, and p38 mitogen-activated protein kinase activation by the B cell antigen receptor. J Exp Med 1998;188:1287-95.
24. Chiorazzi N, Rai KR, Ferrarini M. Chronic lymphocytic leukemia. N Engl J Med 2005;352:804-15.
25. Hallek M. Chronic lymphocytic leukemia: 2015 Update on diagnosis, risk stratification, and treatment. Am J Hematol 2015;90:446-60.
26. Dighiero G. Unsolved issues in CLL biology and management. Leukemia 2003;17:2385-91.

27. Dighiero G, Hamblin TJ. Chronic lymphocytic leukaemia. Lancet 2008;371:1017-29.
28. Messmer BT, Messmer D, Allen SL, et al. In vivo measurements document the dynamic cellular kinetics of chronic lymphocytic leukemia B cells. J Clin Invest 2005;115:755-64.
29. Rai KR, Sawitsky A, Cronkite EP, Chanana AD, Levy RN, Pasternack BS. Clinical staging of chronic lymphocytic leukemia. Blood 1975;46:219-34.
30. Rai KR, Sawitsky A. A review of the prognostic role of cytogenetic, phenotypic, morphologic, and immune function characteristics in chronic lymphocytic leukemia. Blood Cells 1987;12:327-38.
31. Binet JL, Auquier A, Dighiero G, et al. A new prognostic classification of chronic lymphocytic leukemia derived from a multivariate survival analysis. Cancer 1981;48:198-206.
32. Hallek M, Cheson BD, Catovsky D, et al. Guidelines for the diagnosis and treatment of chronic lymphocytic leukemia: a report from the International Workshop on Chronic Lymphocytic Leukemia updating the National Cancer Institute-Working Group 1996 guidelines. Blood 2008;111:5446-56.
33. Hallek M, Cheson BD, Catovsky D, et al. Guidelines for the diagnosis and treatment of chronic lymphocytic leukemia: a report from the International Workshop on Chronic Lymphocytic Leukemia updating the National Cancer Institute-Working Group 1996 guidelines. Blood 2008;111:5446-56.
34. Cramer P, Hallek M. Prognostic factors in chronic lymphocytic leukemia-what do we need to know? Nat Rev Clin Oncol 2011;8:38-47.
35. Späti B, Child JA, Kerruish SM, Cooper EH. Behaviour of serum beta 2-microglobulin and acute phase reactant proteins in chronic lymphocytic leukaemia. A multicentre study. Acta Haematol 1980;64:79-86.
36. Molica S, Levato D, Cascavilla N, Levato L, Musto P. Clinico-prognostic implications of simultaneous increased serum levels of soluble CD23 and beta2-microglobulin in B-cell chronic lymphocytic leukemia. Eur J Haematol 1999;62:117-22.
37. Schroeder HW, Dighiero G. The pathogenesis of chronic lymphocytic leukemia: analysis of the antibody repertoire. Immunol Today 1994;15:288-94.
38. Oscier DG, Gardiner AC, Mould SJ, et al. Multivariate analysis of prognostic factors in CLL: clinical stage, IGVH gene mutational status, and loss or mutation of the p53 gene are independent prognostic factors. Blood 2002;100:1177-84.
39. Hamblin TJ, Davis Z, Gardiner A, Oscier DG, Stevenson FK. Unmutated Ig V(H) genes are associated with a more aggressive form of chronic lymphocytic leukemia. Blood 1999;94:1848-54.
40. Jelinek DF, Tschumper RC, Geyer SM, et al. Analysis of clonal B-cell CD38 and immunoglobulin variable region sequence status in relation to clinical outcome for B-chronic lymphocytic leukaemia. Br J Haematol 2001;115:854-61.
41. Tobin G, Thunberg U, Johnson A, et al. Somatically mutated Ig V(H)3-21 genes characterize a new subset of chronic lymphocytic leukemia. Blood 2002;99:2262-4.
42. Ghia EM, Jain S, Widhopf GF, 2nd, et al. Use of IGHV3-21 in chronic lymphocytic leukemia is associated with high-risk disease and reflects antigen-driven, post-germinal center leukemogenic selection. Blood 2008;111:5101-8.
43. Montserrat E. New prognostic markers in CLL. Hematology Am Soc Hematol Educ Program 2006:279-84.
44. Damle RN, Wasil T, Fais F, et al. Ig V gene mutation status and CD38 expression as novel prognostic indicators in chronic lymphocytic leukemia. Blood 1999;94:1840-7.
45. Orchard JA, Ibbotson RE, Davis Z, et al. ZAP-70 expression and prognosis in chronic lymphocytic leukaemia. Lancet 2004;363:105-11.
46. Chen L, Widhopf G, Huynh L, et al. Expression of ZAP-70 is associated with increased B-cell receptor signaling in chronic lymphocytic leukemia. Blood 2002;100:4609-14.
47. Crespo M, Bosch F, Villamor N, et al. ZAP-70 expression as a surrogate for immunoglobulin-variable-region mutations in chronic lymphocytic leukemia. N Engl J Med 2003;348:1764-75.
48. Wiestner A, Rosenwald A, Barry TS, et al. ZAP-70 expression identifies a chronic lymphocytic leukemia subtype with unmutated immunoglobulin genes, inferior clinical outcome, and distinct gene expression profile. Blood 2003;101:4944-51.

49. Schroers R, Griesinger F, Trümper L, et al. Combined analysis of ZAP-70 and CD38 expression as a predictor of disease progression in B-cell chronic lymphocytic leukemia. Leukemia 2005;19:750-8.
50. Patten PE, Buggins AG, Richards J, et al. CD38 expression in chronic lymphocytic leukemia is regulated by the tumor microenvironment. Blood 2008;111:5173-81.
51. Kröber A, Seiler T, Benner A, et al. V(H) mutation status, CD38 expression level, genomic aberrations, and survival in chronic lymphocytic leukemia. Blood 2002;100:1410-6.
52. Deaglio S, Vaisitti T, Bergui L, et al. CD38 and CD100 lead a network of surface receptors relaying positive signals for B-CLL growth and survival. Blood 2005;105:3042-50.
53. Jønsson V, Houlston RS, Catovsky D, et al. CLL family 'Pedigree 14' revisited: 1947-2004. Leukemia 2005;19:1025-8.
54. Landgren O, Albitar M, Ma W, et al. B-cell clones as early markers for chronic lymphocytic leukemia. N Engl J Med 2009;360:659-67.
55. Goldin LR, Slager SL, Caporaso NE. Familial chronic lymphocytic leukemia. Curr Opin Hematol 2010;17:350-5.
56. Chiorazzi N, Ferrarini M. Cellular origin(s) of chronic lymphocytic leukemia: cautionary notes and additional considerations and possibilities. Blood 2011;117:1781-91.
57. Marti GE, Rawstron AC, Ghia P, et al. Diagnostic criteria for monoclonal B-cell lymphocytosis. Br J Haematol 2005;130:325-32.
58. Ghia P, Prato G, Scielzo C, et al. Monoclonal CD5+ and CD5- B-lymphocyte expansions are frequent in the peripheral blood of the elderly. Blood 2004;103:2337-42.
59. Rawstron AC, Yuille MR, Fuller J, et al. Inherited predisposition to CLL is detectable as subclinical monoclonal B-lymphocyte expansion. Blood 2002;100:2289-90.
60. Shanafelt TD, Ghia P, Lanasa MC, Landgren O, Rawstron AC. Monoclonal B-cell lymphocytosis (MBL): biology, natural history and clinical management. Leukemia 2010;24:512-20.
61. Raval A, Tanner SM, Byrd JC, et al. Downregulation of death-associated protein kinase 1 (DAPK1) in chronic lymphocytic leukemia. Cell 2007;129:879-90.
62. Döhner H, Stilgenbauer S, Benner A, et al. Genomic aberrations and survival in chronic lymphocytic leukemia. N Engl J Med 2000;343:1910-6.
63. Dohner H, Stilgenbauer S, Benner A, et al. Genomic aberrations and survival in chronic lymphocytic leukemia. N Engl J Med 2000;343:1910-6.
64. Dewald GW, Brockman SR, Paternoster SF, et al. Chromosome anomalies detected by interphase fluorescence in situ hybridization: correlation with significant biological features of B-cell chronic lymphocytic leukaemia. Br J Haematol 2003;121:287-95.
65. Cuneo A, Rigolin GM, Bigoni R, et al. Chronic lymphocytic leukemia with 6q- shows distinct hematological features and intermediate prognosis. Leukemia 2004;18:476-83.
66. Wang DM, Miao KR, Fan L, et al. Intermediate prognosis of 6q deletion in chronic lymphocytic leukemia. Leuk Lymphoma 2011;52:230-7.
67. Furman RR. Prognostic markers and stratification of chronic lymphocytic leukemia. Hematology Am Soc Hematol Educ Program 2010;2010:77-81.
68. Degheidy HA, Gadalla SM, Farooqui MZ, et al. Bcl-2 level as a biomarker for 13q14 deletion in CLL. Cytometry B Clin Cytom 2013;84:237-47.
69. Cimmino A, Calin GA, Fabbri M, et al. miR-15 and miR-16 induce apoptosis by targeting BCL2. Proc Natl Acad Sci U S A 2005;102:13944-9.
70. Klein U, Lia M, Crespo M, et al. The DLEU2/miR-15a/16-1 cluster controls B cell proliferation and its deletion leads to chronic lymphocytic leukemia. Cancer Cell 2010;17:28-40.
71. Grever MR, Lucas DM, Dewald GW, et al. Comprehensive assessment of genetic and molecular features predicting outcome in patients with chronic lymphocytic leukemia: results from the US Intergroup Phase III Trial E2997. J Clin Oncol 2007;25:799-804.
72. Zenz T, Döhner H, Stilgenbauer S. Genetics and risk-stratified approach to therapy in chronic lymphocytic leukemia. Best Pract Res Clin Haematol 2007;20:439-53.
73. Ganghammer S, Hutterer E, Hinterseer E, et al. CXCL12-induced VLA-4 activation is impaired in trisomy 12 chronic lymphocytic leukemia cells: a role for CCL21. Oncotarget 2015;6:12048-60.

74. Döhner H, Stilgenbauer S, James MR, et al. 11q deletions identify a new subset of B-cell chronic lymphocytic leukemia characterized by extensive nodal involvement and inferior prognosis. Blood 1997;89:2516-22.
75. Lavin MF. Ataxia-telangiectasia: from a rare disorder to a paradigm for cell signalling and cancer. Nat Rev Mol Cell Biol 2008;9:759-69.
76. Stilgenbauer S, Liebisch P, James MR, et al. Molecular cytogenetic delineation of a novel critical genomic region in chromosome bands 11q22.3-923.1 in lymphoproliferative disorders. Proc Natl Acad Sci U S A 1996;93:11837-41.
77. Austen B, Powell JE, Alvi A, et al. Mutations in the ATM gene lead to impaired overall and treatment-free survival that is independent of IGVH mutation status in patients with B-CLL. Blood 2005;106:3175-82.
78. Austen B, Skowronska A, Baker C, et al. Mutation status of the residual ATM allele is an important determinant of the cellular response to chemotherapy and survival in patients with chronic lymphocytic leukemia containing an 11q deletion. J Clin Oncol 2007;25:5448-57.
79. Eclache V, Caulet-Maugendre S, Poirel HA, et al. Cryptic deletion involving the ATM locus at 11q22.3 approximately q23.1 in B-cell chronic lymphocytic leukemia and related disorders. Cancer Genet Cytogenet 2004;152:72-6.
80. Guarini A, Marinelli M, Tavolaro S, et al. ATM gene alterations in chronic lymphocytic leukemia patients induce a distinct gene expression profile and predict disease progression. Haematologica 2012;97:47-55.
81. Byrd JC, Gribben JG, Peterson BL, et al. Select high-risk genetic features predict earlier progression following chemoimmunotherapy with fludarabine and rituximab in chronic lymphocytic leukemia: justification for risk-adapted therapy. J Clin Oncol 2006;24:437-43.
82. Zenz T, Kröber A, Scherer K, et al. Monoallelic TP53 inactivation is associated with poor prognosis in chronic lymphocytic leukemia: results from a detailed genetic characterization with long-term follow-up. Blood 2008;112:3322-9.
83. Strachan T, Read A. Human Molecular Genetics 4th Edition. New York, USA.: Garland Science, Taylor & Francis Group, LLC.; 2011.
84. Rosenwald A, Chuang EY, Davis RE, et al. Fludarabine treatment of patients with chronic lymphocytic leukemia induces a p53-dependent gene expression response. Blood 2004;104:1428-34.
85. Dreger P, Döhner H, Ritgen M, et al. Allogeneic stem cell transplantation provides durable disease control in poor-risk chronic lymphocytic leukemia: long-term clinical and MRD results of the German CLL Study Group CLL3X trial. Blood 2010;116:2438-47.
86. Lozanski G, Heerema NA, Flinn IW, et al. Alemtuzumab is an effective therapy for chronic lymphocytic leukemia with p53 mutations and deletions. Blood 2004;103:3278-81.
87. Zenz T, Benner A, Döhner H, Stilgenbauer S. Chronic lymphocytic leukemia and treatment resistance in cancer: the role of the p53 pathway. Cell Cycle 2008;7:3810-4.
88. Puente XS, Pinyol M, Quesada V, et al. Whole-genome sequencing identifies recurrent mutations in chronic lymphocytic leukaemia. Nature 2011;475:101-5.
89. Quesada V, Conde L, Villamor N, et al. Exome sequencing identifies recurrent mutations of the splicing factor SF3B1 gene in chronic lymphocytic leukemia. Nat Genet 2012;44:47-52.
90. Mansouri L, Sutton LA, Ljungström V, et al. Functional loss of IκBε leads to NF-κB deregulation in aggressive chronic lymphocytic leukemia. J Exp Med 2015;212:833-43.
91. Wang L, Lawrence MS, Wan Y, et al. SF3B1 and other novel cancer genes in chronic lymphocytic leukemia. N Engl J Med 2011;365:2497-506.
92. Ojha J, Secreto CR, Rabe KG, et al. Identification of recurrent truncated DDX3X mutations in chronic lymphocytic leukaemia. Br J Haematol 2015;169:445-8.
93. Lapalombella R, Sun Q, Williams K, et al. Selective inhibitors of nuclear export show that CRM1/XPO1 is a target in chronic lymphocytic leukemia. Blood 2012;120:4621-34.
94. Jeromin S, Weissmann S, Haferlach C, et al. SF3B1 mutations correlated to cytogenetics and mutations in NOTCH1, FBXW7, MYD88, XPO1 and TP53 in 1160 untreated CLL patients. Leukemia 2014;28:108-17.
95. O'Neil J, Grim J, Strack P, et al. FBW7 mutations in leukemic cells mediate NOTCH pathway activation and resistance to gamma-secretase inhibitors. J Exp Med 2007;204:1813-24.

96. Weissmann S, Roller A, Jeromin S, et al. Prognostic impact and landscape of NOTCH1 mutations in chronic lymphocytic leukemia (CLL): a study on 852 patients. Leukemia 2013;27:2393-6.
97. Fabbri G, Rasi S, Rossi D, et al. Analysis of the chronic lymphocytic leukemia coding genome: role of NOTCH1 mutational activation. J Exp Med 2011;208:1389-401.
98. Rossi D, Rasi S, Fabbri G, et al. Mutations of NOTCH1 are an independent predictor of survival in chronic lymphocytic leukemia. Blood 2012;119:521-9.
99. Sportoletti P, Baldoni S, Cavalli L, et al. NOTCH1 PEST domain mutation is an adverse prognostic factor in B-CLL. Br J Haematol 2010;151:404-6.
100. Balatti V, Bottoni A, Palamarchuk A, et al. NOTCH1 mutations in CLL associated with trisomy 12. Blood 2012;119:329-31.
101. Arruga F, Gizdic B, Serra S, et al. Functional impact of NOTCH1 mutations in chronic lymphocytic leukemia. Leukemia 2014;28:1060-70.
102. Oscier DG, Rose-Zerilli MJ, Winkelmann N, et al. The clinical significance of NOTCH1 and SF3B1 mutations in the UK LRF CLL4 trial. Blood 2013;121:468-75.
103. Mansouri L, Cahill N, Gunnarsson R, et al. NOTCH1 and SF3B1 mutations can be added to the hierarchical prognostic classification in chronic lymphocytic leukemia. Leukemia 2013;27:512-4.
104. Foà R, Del Giudice I, Guarini A, Rossi D, Gaidano G. Clinical implications of the molecular genetics of chronic lymphocytic leukemia. Haematologica 2013;98:675-85.
105. Rossi D, Spina V, Deambrogi C, et al. The genetics of Richter syndrome reveals disease heterogeneity and predicts survival after transformation. Blood 2011;117:3391-401.
106. Tsimberidou AM, Keating MJ. Richter syndrome: biology, incidence, and therapeutic strategies. Cancer 2005;103:216-28.
107. Gaidano G, Foà R, Dalla-Favera R. Molecular pathogenesis of chronic lymphocytic leukemia. J Clin Invest 2012;122:3432-8.
108. Stilgenbauer S, Schnaiter A, Paschka P, et al. Gene mutations and treatment outcome in chronic lymphocytic leukemia: results from the CLL8 trial. Blood 2014;123:3247-54.
109. Tausch E, Beck P, Schlenk R, Kless S, Galler C, Stilgenbauer S. *NOTCH1* Mutation and Treatment Outcome In CLL Patients Treated With Chlorambucil (Chl) Or Ofatumumab-Chl (O-Chl): Results From The Phase III Study Complement 1 (OMB110911). American Society of Hematology2013.
110. Rossi D, Bruscaggin A, Spina V, et al. Mutations of the SF3B1 splicing factor in chronic lymphocytic leukemia: association with progression and fludarabine-refractoriness. Blood 2011;118:6904-8.
111. Will CL, Lührmann R. Spliceosome structure and function. Cold Spring Harb Perspect Biol 2011;3.
112. Rossi D, Rasi S, Spina V, et al. Integrated mutational and cytogenetic analysis identifies new prognostic subgroups in chronic lymphocytic leukemia. Blood 2013;121:1403-12.
113. Rossi D, Fangazio M, Rasi S, et al. Disruption of BIRC3 associates with fludarabine chemorefractoriness in TP53 wild-type chronic lymphocytic leukemia. Blood 2012;119:2854-62.
114. Lau R, Niu MY, Pratt MA. cIAP2 represses IKKα/β-mediated activation of MDM2 to prevent p53 degradation. Cell Cycle 2012;11:4009-19.
115. Zarnegar BJ, Wang Y, Mahoney DJ, et al. Noncanonical NF-kappaB activation requires coordinated assembly of a regulatory complex of the adaptors cIAP1, cIAP2, TRAF2 and TRAF3 and the kinase NIK. Nat Immunol 2008;9:1371-8.
116. Martínez-Trillos A, Pinyol M, Navarro A, et al. Mutations in TLR/MYD88 pathway identify a subset of young chronic lymphocytic leukemia patients with favorable outcome. Blood 2014;123:3790-6.
117. Cortese D, Sutton LA, Cahill N, et al. On the way towards a 'CLL prognostic index': focus on TP53, BIRC3, SF3B1, NOTCH1 and MYD88 in a population-based cohort. Leukemia 2014;28:710-3.
118. Klein U, Tu Y, Stolovitzky GA, et al. Gene expression profiling of B cell chronic lymphocytic leukemia reveals a homogeneous phenotype related to memory B cells. J Exp Med 2001;194:1625-38.

119. Weill JC, Weller S, Reynaud CA. Human marginal zone B cells. Annu Rev Immunol 2009;27:267-85.
120. Weller S, Mamani-Matsuda M, Picard C, et al. Somatic diversification in the absence of antigen-driven responses is the hallmark of the IgM+ IgD+ CD27+ B cell repertoire in infants. J Exp Med 2008;205:1331-42.
121. William J, Euler C, Christensen S, Shlomchik MJ. Evolution of autoantibody responses via somatic hypermutation outside of germinal centers. Science 2002;297:2066-70.
122. Stamatopoulos K, Belessi C, Moreno C, et al. Over 20% of patients with chronic lymphocytic leukemia carry stereotyped receptors: Pathogenetic implications and clinical correlations. Blood 2007;109:259-70.
123. Murray F, Darzentas N, Hadzidimitriou A, et al. Stereotyped patterns of somatic hypermutation in subsets of patients with chronic lymphocytic leukemia: implications for the role of antigen selection in leukemogenesis. Blood 2008;111:1524-33.
124. Tobin G, Thunberg U, Johnson A, et al. Chronic lymphocytic leukemias utilizing the VH3-21 gene display highly restricted Vlambda2-14 gene use and homologous CDR3s: implicating recognition of a common antigen epitope. Blood 2003;101:4952-7.
125. Ghiotto F, Fais F, Valetto A, et al. Remarkably similar antigen receptors among a subset of patients with chronic lymphocytic leukemia. J Clin Invest 2004;113:1008-16.
126. Widhopf GF, Rassenti LZ, Toy TL, Gribben JG, Wierda WG, Kipps TJ. Chronic lymphocytic leukemia B cells of more than 1% of patients express virtually identical immunoglobulins. Blood 2004;104:2499-504.
127. Chu CC, Catera R, Zhang L, et al. Many chronic lymphocytic leukemia antibodies recognize apoptotic cells with exposed nonmuscle myosin heavy chain IIA: implications for patient outcome and cell of origin. Blood 2010;115:3907-15.
128. Zupo S, Dono M, Massara R, Taborelli G, Chiorazzi N, Ferrarini M. Expression of CD5 and CD38 by human CD5- B cells: requirement for special stimuli. Eur J Immunol 1994;24:1426-33.
129. Dorshkind K, Montecino-Rodriguez E. Fetal B-cell lymphopoiesis and the emergence of B-1-cell potential. Nat Rev Immunol 2007;7:213-9.
130. Martin F, Kearney JF. B1 cells: similarities and differences with other B cell subsets. Curr Opin Immunol 2001;13:195-201.
131. Caligaris-Cappio F, Gobbi M, Bofill M, Janossy G. Infrequent normal B lymphocytes express features of B-chronic lymphocytic leukemia. J Exp Med 1982;155:623-8.
132. Brezinschek HP, Foster SJ, Brezinschek RI, Dörner T, Domiati-Saad R, Lipsky PE. Analysis of the human VH gene repertoire. Differential effects of selection and somatic hypermutation on human peripheral CD5(+)/IgM+ and CD5(-)/IgM+ B cells. J Clin Invest 1997;99:2488-501.
133. Seifert M, Sellmann L, Bloehdorn J, et al. Cellular origin and pathophysiology of chronic lymphocytic leukemia. J Exp Med 2012;209:2183-98.
134. Seifert M, Scholtysik R, Küppers R. Origin and pathogenesis of B cell lymphomas. Methods Mol Biol 2013;971:1-25.
135. Kikushige Y, Ishikawa F, Miyamoto T, et al. Self-renewing hematopoietic stem cell is the primary target in pathogenesis of human chronic lymphocytic leukemia. Cancer Cell 2011;20:246-59.
136. Panayiotidis P, Jones D, Ganeshaguru K, Foroni L, Hoffbrand AV. Human bone marrow stromal cells prevent apoptosis and support the survival of chronic lymphocytic leukaemia cells in vitro. Br J Haematol 1996;92:97-103.
137. Ten Hacken E, Burger JA. Microenvironment interactions and B-cell receptor signaling in Chronic Lymphocytic Leukemia: Implications for disease pathogenesis and treatment. Biochim Biophys Acta 2015.
138. Ten Hacken E, Burger JA. Microenvironment dependency in Chronic Lymphocytic Leukemia: The basis for new targeted therapies. Pharmacol Ther 2014.
139. Burger JA, Ghia P, Rosenwald A, Caligaris-Cappio F. The microenvironment in mature B-cell malignancies: a target for new treatment strategies. Blood 2009;114:3367-75.
140. McCaig AM, Cosimo E, Leach MT, Michie AM. Dasatinib inhibits B cell receptor signalling in chronic lymphocytic leukaemia but novel combination approaches are required to overcome additional pro-survival microenvironmental signals. Br J Haematol 2011;153:199-211.

141. Kurtova AV, Balakrishnan K, Chen R, et al. Diverse marrow stromal cells protect CLL cells from spontaneous and drug-induced apoptosis: development of a reliable and reproducible system to assess stromal cell adhesion-mediated drug resistance. Blood 2009;114:4441-50.
142. Sivina M, Hartmann E, Vasyutina E, et al. Stromal cells modulate TCL1 expression, interacting AP-1 components and TCL1-targeting micro-RNAs in chronic lymphocytic leukemia. Leukemia 2012;26:1812-20.
143. Burger JA, Burger M, Kipps TJ. Chronic lymphocytic leukemia B cells express functional CXCR4 chemokine receptors that mediate spontaneous migration beneath bone marrow stromal cells. Blood 1999;94:3658-67.
144. Marquez ME, Hernández-Uzcátegui O, Cornejo A, Vargas P, Da Costa O. Bone marrow stromal mesenchymal cells induce down regulation of CD20 expression on B-CLL: implications for rituximab resistance in CLL. Br J Haematol 2015;169:211-8.
145. Bürkle A, Niedermeier M, Schmitt-Gräff A, Wierda WG, Keating MJ, Burger JA. Overexpression of the CXCR5 chemokine receptor, and its ligand, CXCL13 in B-cell chronic lymphocytic leukemia. Blood 2007;110:3316-25.
146. Jia L, Clear A, Liu FT, et al. Extracellular HMGB1 promotes differentiation of nurse-like cells in chronic lymphocytic leukemia. Blood 2014;123:1709-19.
147. Burger JA, Tsukada N, Burger M, Zvaifler NJ, Dell'Aquila M, Kipps TJ. Blood-derived nurse-like cells protect chronic lymphocytic leukemia B cells from spontaneous apoptosis through stromal cell-derived factor-1. Blood 2000;96:2655-63.
148. Nishio M, Endo T, Tsukada N, et al. Nurselike cells express BAFF and APRIL, which can promote survival of chronic lymphocytic leukemia cells via a paracrine pathway distinct from that of SDF-1alpha. Blood 2005;106:1012-20.
149. Burger M, Hartmann T, Krome M, et al. Small peptide inhibitors of the CXCR4 chemokine receptor (CD184) antagonize the activation, migration, and antiapoptotic responses of CXCL12 in chronic lymphocytic leukemia B cells. Blood 2005;106:1824-30.
150. O'Hayre M, Salanga CL, Kipps TJ, Messmer D, Dorrestein PC, Handel TM. Elucidating the CXCL12/CXCR4 signaling network in chronic lymphocytic leukemia through phosphoproteomics analysis. PLoS One 2010;5:e11716.
151. Calissano C, Damle RN, Hayes G, et al. In vivo intraclonal and interclonal kinetic heterogeneity in B-cell chronic lymphocytic leukemia. Blood 2009;114:4832-42.
152. Brachtl G, Sahakyan K, Denk U, et al. Differential bone marrow homing capacity of VLA-4 and CD38 high expressing chronic lymphocytic leukemia cells. PLoS One 2011;6:e23758.
153. Gattei V, Bulian P, Del Principe MI, et al. Relevance of CD49d protein expression as overall survival and progressive disease prognosticator in chronic lymphocytic leukemia. Blood 2008;111:865-73.
154. Burger JA, Quiroga MP, Hartmann E, et al. High-level expression of the T-cell chemokines CCL3 and CCL4 by chronic lymphocytic leukemia B cells in nurselike cell cocultures and after BCR stimulation. Blood 2009;113:3050-8.
155. Zucchetto A, Benedetti D, Tripodo C, et al. CD38/CD31, the CCL3 and CCL4 chemokines, and CD49d/vascular cell adhesion molecule-1 are interchained by sequential events sustaining chronic lymphocytic leukemia cell survival. Cancer Res 2009;69:4001-9.
156. Shaffer AL, Yu X, He Y, Boldrick J, Chan EP, Staudt LM. BCL-6 represses genes that function in lymphocyte differentiation, inflammation, and cell cycle control. Immunity 2000;13:199-212.
157. Sivina M, Hartmann E, Kipps TJ, et al. CCL3 (MIP-1α) plasma levels and the risk for disease progression in chronic lymphocytic leukemia. Blood 2011;117:1662-9.
158. Kitada S, Zapata JM, Andreeff M, Reed JC. Bryostatin and CD40-ligand enhance apoptosis resistance and induce expression of cell survival genes in B-cell chronic lymphocytic leukaemia. Br J Haematol 1999;106:995-1004.
159. Mainou-Fowler T, Copplestone JA, Prentice AG. Effect of interleukins on the proliferation and survival of B cell chronic lymphocytic leukaemia cells. J Clin Pathol 1995;48:482-7.
160. Levesque MC, Misukonis MA, O'Loughlin CW, et al. IL-4 and interferon gamma regulate expression of inducible nitric oxide synthase in chronic lymphocytic leukemia cells. Leukemia 2003;17:442-50.

161. Gribben JG, O'Brien S. Update on therapy of chronic lymphocytic leukemia. J Clin Oncol 2011;29:544-50.
162. Ramsay AG, Johnson AJ, Lee AM, et al. Chronic lymphocytic leukemia T cells show impaired immunological synapse formation that can be reversed with an immunomodulating drug. J Clin Invest 2008;118:2427-37.
163. Ramsay AG, Clear AJ, Fatah R, Gribben JG. Multiple inhibitory ligands induce impaired T-cell immunologic synapse function in chronic lymphocytic leukemia that can be blocked with lenalidomide: establishing a reversible immune evasion mechanism in human cancer. Blood 2012;120:1412-21.
164. Ramsay AG, Evans R, Kiaii S, Svensson L, Hogg N, Gribben JG. Chronic lymphocytic leukemia cells induce defective LFA-1-directed T-cell motility by altering Rho GTPase signaling that is reversible with lenalidomide. Blood 2013;121:2704-14.
165. Riches JC, Gribben JG. Understanding the immunodeficiency in chronic lymphocytic leukemia: potential clinical implications. Hematol Oncol Clin North Am 2013;27:207-35.
166. Coscia M, Vitale C, Peola S, et al. Dysfunctional Vγ9Vδ2 T cells are negative prognosticators and markers of dysregulated mevalonate pathway activity in chronic lymphocytic leukemia cells. Blood 2012;120:3271-9.
167. Motta M, Rassenti L, Shelvin BJ, et al. Increased expression of CD152 (CTLA-4) by normal T lymphocytes in untreated patients with B-cell chronic lymphocytic leukemia. Leukemia 2005;19:1788-93.
168. Harnett MM. CD40: a growing cytoplasmic tale. Sci STKE 2004;2004:pe25.
169. Bishop GA, Hostager BS. The CD40-CD154 interaction in B cell-T cell liaisons. Cytokine Growth Factor Rev 2003;14:297-309.
170. Schattner EJ. CD40 ligand in CLL pathogenesis and therapy. Leuk Lymphoma 2000;37:461-72.
171. Dallman C, Johnson PW, Packham G. Differential regulation of cell survival by CD40. Apoptosis 2003;8:45-53.
172. Janumyan YM, Sansam CG, Chattopadhyay A, et al. Bcl-xL/Bcl-2 coordinately regulates apoptosis, cell cycle arrest and cell cycle entry. EMBO J 2003;22:5459-70.
173. Hirai H, Adachi T, Tsubata T. Involvement of cell cycle progression in survival signaling through CD40 in the B-lymphocyte line WEHI-231. Cell Death Differ 2004;11:261-9.
174. Schattner EJ, Mascarenhas J, Reyfman I, et al. Chronic lymphocytic leukemia B cells can express CD40 ligand and demonstrate T-cell type costimulatory capacity. Blood 1998;91:2689-97.
175. Smit LA, Hallaert DY, Spijker R, et al. Differential Noxa/Mcl-1 balance in peripheral versus lymph node chronic lymphocytic leukemia cells correlates with survival capacity. Blood 2007;109:1660-8.
176. Jak M, van Bochove GG, van Lier RA, Eldering E, van Oers MH. CD40 stimulation sensitizes CLL cells to rituximab-induced cell death. Leukemia 2011;25:968-78.
177. Kay NE, Pittner BT. IL-4 biology: impact on normal and leukemic CLL B cells. Leuk Lymphoma 2003;44:897-903.
178. Nelms K, Keegan AD, Zamorano J, Ryan JJ, Paul WE. The IL-4 receptor: signaling mechanisms and biologic functions. Annu Rev Immunol 1999;17:701-38.
179. Wang LM, Myers MG, Sun XJ, Aaronson SA, White M, Pierce JH. IRS-1: essential for insulin- and IL-4-stimulated mitogenesis in hematopoietic cells. Science 1993;261:1591-4.
180. Sun XJ, Wang LM, Zhang Y, et al. Role of IRS-2 in insulin and cytokine signalling. Nature 1995;377:173-7.
181. Jewell AP, Worman CP, Lydyard PM, Yong KL, Giles FJ, Goldstone AH. Interferon-alpha up-regulates bcl-2 expression and protects B-CLL cells from apoptosis in vitro and in vivo. Br J Haematol 1994;88:268-74.
182. Kaplan MH, Schindler U, Smiley ST, Grusby MJ. Stat6 is required for mediating responses to IL-4 and for development of Th2 cells. Immunity 1996;4:313-9.
183. Patel BK, Pierce JH, LaRochelle WJ. Regulation of interleukin 4-mediated signaling by naturally occurring dominant negative and attenuated forms of human Stat6. Proc Natl Acad Sci U S A 1998;95:172-7.

184. Kay NE, Han L, Bone N, Williams G. Interleukin 4 content in chronic lymphocytic leukaemia (CLL) B cells and blood CD8+ T cells from B-CLL patients: impact on clonal B-cell apoptosis. Br J Haematol 2001;112:760-7.
185. Mainou-Fowler T, Proctor SJ, Miller S, Dickinson AM. Expression and production of interleukin 4 in B-cell chronic lymphocytic leukaemia. Leuk Lymphoma 2001;42:689-98.
186. Mainou-Fowler T, Miller S, Proctor SJ, Dickinson AM. The levels of TNF alpha, IL4 and IL10 production by T-cells in B-cell chronic lymphocytic leukaemia (B-CLL). Leuk Res 2001;25:157-63.
187. Douglas RS, Capocasale RJ, Lamb RJ, Nowell PC, Moore JS. Chronic lymphocytic leukemia B cells are resistant to the apoptotic effects of transforming growth factor-beta. Blood 1997;89:941-7.
188. Rizzo R, Audrito V, Vacca P, et al. HLA-G is a component of the chronic lymphocytic leukemia escape repertoire to generate immune suppression: impact of the HLA-G 14 base pair (rs66554220) polymorphism. Haematologica 2014;99:888-96.
189. Ghosh AK, Secreto CR, Knox TR, Ding W, Mukhopadhyay D, Kay NE. Circulating microvesicles in B-cell chronic lymphocytic leukemia can stimulate marrow stromal cells: implications for disease progression. Blood 2010;115:1755-64.
190. Kay NE, Shanafelt TD, Strege AK, Lee YK, Bone ND, Raza A. Bone biopsy derived marrow stromal elements rescue chronic lymphocytic leukemia B-cells from spontaneous and drug induced cell death and facilitates an "angiogenic switch". Leuk Res 2007;31:899-906.
191. Rawstron AC, Kennedy B, Evans PA, et al. Quantitation of minimal disease levels in chronic lymphocytic leukemia using a sensitive flow cytometric assay improves the prediction of outcome and can be used to optimize therapy. Blood 2001;98:29-35.
192. Mockridge CI, Potter KN, Wheatley I, Neville LA, Packham G, Stevenson FK. Reversible anergy of sIgM-mediated signaling in the two subsets of CLL defined by VH-gene mutational status. Blood 2007;109:4424-31.
193. Zonta F, Pagano MA, Trentin L, et al. Lyn-mediated procaspase 8 dimerization blocks apoptotic signaling in B-cell chronic lymphocytic leukemia. Blood 2014;123:875-83.
194. Hoogeboom R, van Kessel KP, Hochstenbach F, et al. A mutated B cell chronic lymphocytic leukemia subset that recognizes and responds to fungi. J Exp Med 2013;210:59-70.
195. Dühren-von Minden M, Übelhart R, Schneider D, et al. Chronic lymphocytic leukaemia is driven by antigen-independent cell-autonomous signalling. Nature 2012;489:309-12.
196. Binder M, Müller F, Frick M, et al. CLL B-cell receptors can recognize themselves: alternative epitopes and structural clues for autostimulatory mechanisms in CLL. Blood 2013;121:239-41.
197. Young RM, Staudt LM. Targeting pathological B cell receptor signalling in lymphoid malignancies. Nat Rev Drug Discov 2013;12:229-43.
198. Lobry C, Oh P, Mansour MR, Look AT, Aifantis I. Notch signaling: switching an oncogene to a tumor suppressor. Blood 2014;123:2451-9.
199. Radtke F, Wilson A, Mancini SJ, MacDonald HR. Notch regulation of lymphocyte development and function. Nat Immunol 2004;5:247-53.
200. De Falco F, Sabatini R, Del Papa B, et al. Notch signaling sustains the expression of Mcl-1 and the activity of eIF4E to promote cell survival in CLL. Oncotarget 2015;6:16559-72.
201. Beverly LJ, Felsher DW, Capobianco AJ. Suppression of p53 by Notch in lymphomagenesis: implications for initiation and regression. Cancer Res 2005;65:7159-68.
202. Rizzo P, Miao H, D'Souza G, et al. Cross-talk between notch and the estrogen receptor in breast cancer suggests novel therapeutic approaches. Cancer Res 2008;68:5226-35.
203. Palomero T, Lim WK, Odom DT, et al. NOTCH1 directly regulates c-MYC and activates a feed-forward-loop transcriptional network promoting leukemic cell growth. Proc Natl Acad Sci U S A 2006;103:18261-6.
204. Blaumueller CM, Qi H, Zagouras P, Artavanis-Tsakonas S. Intracellular cleavage of Notch leads to a heterodimeric receptor on the plasma membrane. Cell 1997;90:281-91.
205. Okajima T, Xu A, Irvine KD. Modulation of notch-ligand binding by protein O-fucosyltransferase 1 and fringe. J Biol Chem 2003;278:42340-5.
206. Okajima T, Irvine KD. Regulation of notch signaling by o-linked fucose. Cell 2002;111:893-904.

207. Moloney DJ, Panin VM, Johnston SH, et al. Fringe is a glycosyltransferase that modifies Notch. Nature 2000;406:369-75.
208. Haines N, Irvine KD. Glycosylation regulates Notch signalling. Nat Rev Mol Cell Biol 2003;4:786-97.
209. Brückner K, Perez L, Clausen H, Cohen S. Glycosyltransferase activity of Fringe modulates Notch-Delta interactions. Nature 2000;406:411-5.
210. Bray SJ. Notch signalling: a simple pathway becomes complex. Nat Rev Mol Cell Biol 2006;7:678-89.
211. Andersson ER, Lendahl U. Therapeutic modulation of Notch signalling--are we there yet? Nat Rev Drug Discov 2014;13:357-78.
212. Shah S, Lee SF, Tabuchi K, et al. Nicastrin functions as a gamma-secretase-substrate receptor. Cell 2005;122:435-47.
213. Kao HY, Ordentlich P, Koyano-Nakagawa N, et al. A histone deacetylase corepressor complex regulates the Notch signal transduction pathway. Genes Dev 1998;12:2269-77.
214. Yatim A, Benne C, Sobhian B, et al. NOTCH1 nuclear interactome reveals key regulators of its transcriptional activity and oncogenic function. Mol Cell 2012;48:445-58.
215. Nakayama KI, Nakayama K. Ubiquitin ligases: cell-cycle control and cancer. Nat Rev Cancer 2006;6:369-81.
216. Fryer CJ, White JB, Jones KA. Mastermind recruits CycC:CDK8 to phosphorylate the Notch ICD and coordinate activation with turnover. Mol Cell 2004;16:509-20.
217. Baldoni S, Sportoletti P, Del Papa B, et al. NOTCH and NF-κB interplay in chronic lymphocytic leukemia is independent of genetic lesion. Int J Hematol 2013;98:153-7.
218. Andersen P, Uosaki H, Shenje LT, Kwon C. Non-canonical Notch signaling: emerging role and mechanism. Trends Cell Biol 2012;22:257-65.
219. Ayaz F, Osborne BA. Non-canonical notch signaling in cancer and immunity. Front Oncol 2014;4:345.
220. D'Souza B, Meloty-Kapella L, Weinmaster G. Canonical and non-canonical Notch ligands. Curr Top Dev Biol 2010;92:73-129.
221. Fodde R, Brabletz T. Wnt/beta-catenin signaling in cancer stemness and malignant behavior. Curr Opin Cell Biol 2007;19:150-8.
222. Reya T, Clevers H. Wnt signalling in stem cells and cancer. Nature 2005;434:843-50.
223. Kwon C, Cheng P, King IN, et al. Notch post-translationally regulates β-catenin protein in stem and progenitor cells. Nat Cell Biol 2011;13:1244-51.
224. Komiya Y, Habas R. Wnt signal transduction pathways. Organogenesis 2008;4:68-75.
225. Lu D, Zhao Y, Tawatao R, et al. Activation of the Wnt signaling pathway in chronic lymphocytic leukemia. Proc Natl Acad Sci U S A 2004;101:3118-23.
226. Liotta F, Angeli R, Cosmi L, et al. Toll-like receptors 3 and 4 are expressed by human bone marrow-derived mesenchymal stem cells and can inhibit their T-cell modulatory activity by impairing Notch signaling. Stem Cells 2008;26:279-89.
227. Calvi LM, Adams GB, Weibrecht KW, et al. Osteoblastic cells regulate the haematopoietic stem cell niche. Nature 2003;425:841-6.
228. Onaindia A, Gómez S, Piris-Villaespesa M, et al. Chronic lymphocytic leukemia cells in lymph nodes show frequent NOTCH1 activation. Haematologica 2015;100:e200-3.
229. Rosati E, Sabatini R, Rampino G, et al. Constitutively activated Notch signaling is involved in survival and apoptosis resistance of B-CLL cells. Blood 2009;113:856-65.
230. Bash J, Zong WX, Banga S, et al. Rel/NF-kappaB can trigger the Notch signaling pathway by inducing the expression of Jagged1, a ligand for Notch receptors. EMBO J 1999;18:2803-11.
231. Jitschin R, Braun M, Qorraj M, et al. Stromal cell-mediated glycolytic switch in CLL-cells involves Notch-c-Myc signaling. Blood 2015. 125:3423-3426
232. Nwabo Kamdje AH, Bassi G, Pacelli L, et al. Role of stromal cell-mediated Notch signaling in CLL resistance to chemotherapy. Blood Cancer J 2012;2:e73.
233. Pozzo F, Bittolo T, Arruga F, et al. NOTCH1 mutations associate with low CD20 level in chronic lymphocytic leukemia: evidence for a NOTCH1 mutation-driven epigenetic dysregulation. Leukemia 2016. 30:182-189
234. Malumbres M, Barbacid M. Cell cycle, CDKs and cancer: a changing paradigm. Nat Rev Cancer 2009;9:153-66.

235. Hartwell LH, Kastan MB. Cell cycle control and cancer. Science 1994;266:1821-8.
236. Kastan MB, Bartek J. Cell-cycle checkpoints and cancer. Nature 2004;432:316-23.
237. O'Brien S, del Giglio A, Keating M. Advances in the biology and treatment of B-cell chronic lymphocytic leukemia. Blood 1995;85:307-18.
238. Decker T, Schneller F, Hipp S, et al. Cell cycle progression of chronic lymphocytic leukemia cells is controlled by cyclin D2, cyclin D3, cyclin-dependent kinase (cdk) 4 and the cdk inhibitor p27. Leukemia 2002;16:327-34.
239. Vrhovac R, Delmer A, Tang R, Marie JP, Zittoun R, Ajchenbaum-Cymbalista F. Prognostic significance of the cell cycle inhibitor p27Kip1 in chronic B-cell lymphocytic leukemia. Blood 1998;91:4694-700.
240. Wagner EF, Hleb M, Hanna N, Sharma S. A pivotal role of cyclin D3 and cyclin-dependent kinase inhibitor p27 in the regulation of IL-2-, IL-4-, or IL-10-mediated human B cell proliferation. J Immunol 1998;161:1123-31.
241. Wang Z, Zhang Y, Li Y, Banerjee S, Liao J, Sarkar FH. Down-regulation of Notch-1 contributes to cell growth inhibition and apoptosis in pancreatic cancer cells. Mol Cancer Ther 2006;5:483-93.
242. Sriuranpong V, Borges MW, Ravi RK, et al. Notch signaling induces cell cycle arrest in small cell lung cancer cells. Cancer Res 2001;61:3200-5.
243. Joshi I, Minter LM, Telfer J, et al. Notch signaling mediates G1/S cell-cycle progression in T cells via cyclin D3 and its dependent kinases. Blood 2009;113:1689-98.
244. Del Giudice I, Rossi D, Chiaretti S, et al. NOTCH1 mutations in +12 chronic lymphocytic leukemia (CLL) confer an unfavorable prognosis, induce a distinctive transcriptional profiling and refine the intermediate prognosis of +12 CLL. Haematologica 2012;97:437-41.
245. Demetrick DJ, Zhang H, Beach DH. Chromosomal mapping of human CDK2, CDK4, and CDK5 cell cycle kinase genes. Cytogenet Cell Genet 1994;66:72-4.
246. Robak T, Kasznicki M. Alkylating agents and nucleoside analogues in the treatment of B cell chronic lymphocytic leukemia. Leukemia 2002;16:1015-27.
247. Chemotherapeutic options in chronic lymphocytic leukemia: a meta-analysis of the randomized trials. CLL Trialists' Collaborative Group. J Natl Cancer Inst 1999;91:861-8.
248. Robak T, Korycka A, Lech-Maranda E, Robak P. Current status of older and new purine nucleoside analogues in the treatment of lymphoproliferative diseases. Molecules 2009;14:1183-226.
249. Rai KR, Peterson BL, Appelbaum FR, et al. Fludarabine compared with chlorambucil as primary therapy for chronic lymphocytic leukemia. N Engl J Med 2000;343:1750-7.
250. Plunkett W, Gandhi V, Huang P, et al. Fludarabine: pharmacokinetics, mechanisms of action, and rationales for combination therapies. Semin Oncol 1993;20:2-12.
251. Desai S, Pinilla-Ibarz J. Front-line therapy for chronic lymphocytic leukemia. Cancer Control 2012;19:26-36.
252. Knauf WU, Lissitchkov T, Aldaoud A, et al. Bendamustine compared with chlorambucil in previously untreated patients with chronic lymphocytic leukaemia: updated results of a randomized phase III trial. Br J Haematol 2012;159:67-77.
253. Keating GM. Rituximab: a review of its use in chronic lymphocytic leukaemia, low-grade or follicular lymphoma and diffuse large B-cell lymphoma. Drugs 2010;70:1445-76.
254. Teeling JL, Mackus WJ, Wiegman LJ, et al. The biological activity of human CD20 monoclonal antibodies is linked to unique epitopes on CD20. J Immunol 2006;177:362-71.
255. Teeling JL, French RR, Cragg MS, et al. Characterization of new human CD20 monoclonal antibodies with potent cytolytic activity against non-Hodgkin lymphomas. Blood 2004;104:1793-800.
256. Wierda WG, Kipps TJ, Mayer J, et al. Ofatumumab as single-agent CD20 immunotherapy in fludarabine-refractory chronic lymphocytic leukemia. J Clin Oncol 2010;28:1749-55.
257. Wierda WG, Padmanabhan S, Chan GW, et al. Ofatumumab is active in patients with fludarabine-refractory CLL irrespective of prior rituximab: results from the phase 2 international study. Blood 2011;118:5126-9.
258. Mössner E, Brünker P, Moser S, et al. Increasing the efficacy of CD20 antibody therapy through the engineering of a new type II anti-CD20 antibody with enhanced direct and immune effector cell-mediated B-cell cytotoxicity. Blood 2010;115:4393-402.

259. Cartron G, de Guibert S, Dilhuydy MS, et al. Obinutuzumab (GA101) in relapsed/refractory chronic lymphocytic leukemia: final data from the phase 1/2 GAUGUIN study. Blood 2014;124:2196-202.
260. Lundin J, Kimby E, Björkholm M, et al. Phase II trial of subcutaneous anti-CD52 monoclonal antibody alemtuzumab (Campath-1H) as first-line treatment for patients with B-cell chronic lymphocytic leukemia (B-CLL). Blood 2002;100:768-73.
261. Hillmen P, Skotnicki AB, Robak T, et al. Alemtuzumab compared with chlorambucil as first-line therapy for chronic lymphocytic leukemia. J Clin Oncol 2007;25:5616-23.
262. Glennie MJ, French RR, Cragg MS, Taylor RP. Mechanisms of killing by anti-CD20 monoclonal antibodies. Mol Immunol 2007;44:3823-37.
263. Byrd JC, Kipps TJ, Flinn IW, et al. Phase I study of the anti-CD40 humanized monoclonal antibody lucatumumab (HCD122) in relapsed chronic lymphocytic leukemia. Leuk Lymphoma 2012;53:2136-42.
264. Zhang S, Wu CC, Fecteau JF, et al. Targeting chronic lymphocytic leukemia cells with a humanized monoclonal antibody specific for CD44. Proc Natl Acad Sci U S A 2013;110:6127-32.
265. Pogue SL, Kurosaki T, Bolen J, Herbst R. B cell antigen receptor-induced activation of Akt promotes B cell survival and is dependent on Syk kinase. J Immunol 2000;165:1300-6.
266. Friedberg JW, Sharman J, Sweetenham J, et al. Inhibition of Syk with fostamatinib disodium has significant clinical activity in non-Hodgkin lymphoma and chronic lymphocytic leukemia. Blood 2010;115:2578-85.
267. Hoellenriegel J, Meadows SA, Sivina M, et al. The phosphoinositide 3'-kinase delta inhibitor, CAL-101, inhibits B-cell receptor signaling and chemokine networks in chronic lymphocytic leukemia. Blood 2011;118:3603-12.
268. Brown JR, Byrd JC, Coutre SE, et al. Idelalisib, an inhibitor of phosphatidylinositol 3-kinase p110δ, for relapsed/refractory chronic lymphocytic leukemia. Blood 2014;123:3390-7.
269. Herman SE, Gordon AL, Hertlein E, et al. Bruton tyrosine kinase represents a promising therapeutic target for treatment of chronic lymphocytic leukemia and is effectively targeted by PCI-32765. Blood 2011;117:6287-96.
270. Byrd JC, Furman RR, Coutre SE, et al. Targeting BTK with ibrutinib in relapsed chronic lymphocytic leukemia. N Engl J Med 2013;369:32-42.
271. Sher T, Miller KC, Lawrence D, et al. Efficacy of lenalidomide in patients with chronic lymphocytic leukemia with high-risk cytogenetics. Leuk Lymphoma 2010;51:85-8.
272. Figueroa JA, Reidy A, Mirandola L, et al. Chimeric antigen receptor engineering: a right step in the evolution of adoptive cellular immunotherapy. Int Rev Immunol 2015;34:154-87.
273. Porter DL, Levine BL, Kalos M, Bagg A, June CH. Chimeric antigen receptor-modified T cells in chronic lymphoid leukemia. N Engl J Med 2011;365:725-33.
274. Catovsky D, Richards S, Matutes E, et al. Assessment of fludarabine plus cyclophosphamide for patients with chronic lymphocytic leukaemia (the LRF CLL4 Trial): a randomised controlled trial. Lancet 2007;370:230-9.
275. Hallek M, Eichhorst BF. Chemotherapy combination treatment regimens with fludarabine in chronic lymphocytic leukemia. Hematol J 2004;5 Suppl 1:S20-30.
276. Hallek M, Fischer K, Fingerle-Rowson G, et al. Addition of rituximab to fludarabine and cyclophosphamide in patients with chronic lymphocytic leukaemia: a randomised, open-label, phase 3 trial. Lancet 2010;376:1164-74.
277. Parikh SA, Keating MJ, O'Brien S, et al. Frontline chemoimmunotherapy with fludarabine, cyclophosphamide, alemtuzumab, and rituximab for high-risk chronic lymphocytic leukemia. Blood 2011;118:2062-8.
278. Fischer K, Cramer P, Busch R, et al. Bendamustine combined with rituximab in patients with relapsed and/or refractory chronic lymphocytic leukemia: a multicenter phase II trial of the German Chronic Lymphocytic Leukemia Study Group. J Clin Oncol 2011;29:3559-66.
279. Hillmen P, Robak T, Janssens A, et al. Chlorambucil plus ofatumumab versus chlorambucil alone in previously untreated patients with chronic lymphocytic leukaemia (COMPLEMENT 1): a randomised, multicentre, open-label phase 3 trial. Lancet 2015;385:1873-83.
280. Nabhan C, Coutre S, Hillmen P. Minimal residual disease in chronic lymphocytic leukaemia: is it ready for primetime? Br J Haematol 2007;136:379-92.

281. Böttcher S, Ritgen M, Fischer K, et al. Minimal residual disease quantification is an independent predictor of progression-free and overall survival in chronic lymphocytic leukemia: a multivariate analysis from the randomized GCLLSG CLL8 trial. J Clin Oncol 2012;30:980-8.
282. Sayala HA, Rawstron AC, Hillmen P. Minimal residual disease assessment in chronic lymphocytic leukaemia. Best Pract Res Clin Haematol 2007;20:499-512.
283. Tam CS, O'Brien S, Lerner S, et al. The natural history of fludarabine-refractory chronic lymphocytic leukemia patients who fail alemtuzumab or have bulky lymphadenopathy. Leuk Lymphoma 2007;48:1931-9.
284. Walport MJ. Complement. First of two parts. N Engl J Med 2001;344:1058-66.
285. Cragg MS, Glennie MJ. Antibody specificity controls in vivo effector mechanisms of anti-CD20 reagents. Blood 2004;103:2738-43.
286. Polyak MJ, Deans JP. Alanine-170 and proline-172 are critical determinants for extracellular CD20 epitopes; heterogeneity in the fine specificity of CD20 monoclonal antibodies is defined by additional requirements imposed by both amino acid sequence and quaternary structure. Blood 2002;99:3256-62.
287. Ruuls SR, Lammerts van Bueren JJ, van de Winkel JG, Parren PW. Novel human antibody therapeutics: the age of the Umabs. Biotechnol J 2008;3:1157-71.
288. Cragg MS. CD20 antibodies: doing the time warp. Blood 2011;118:219-20.
289. O'Keefe TL, Williams GT, Davies SL, Neuberger MS. Mice carrying a CD20 gene disruption. Immunogenetics 1998;48:125-32.
290. Li H, Ayer LM, Lytton J, Deans JP. Store-operated cation entry mediated by CD20 in membrane rafts. J Biol Chem 2003;278:42427-34.
291. Tedder TF, Engel P. CD20: a regulator of cell-cycle progression of B lymphocytes. Immunol Today 1994;15:450-4.
292. Reff ME, Carner K, Chambers KS, et al. Depletion of B cells in vivo by a chimeric mouse human monoclonal antibody to CD20. Blood 1994;83:435-45.
293. Pescovitz MD. Rituximab, an anti-cd20 monoclonal antibody: history and mechanism of action. Am J Transplant 2006;6:859-66.
294. Zhang B. Ofatumumab. MAbs 2009;1:326-31.
295. Chan HT, Hughes D, French RR, et al. CD20-induced lymphoma cell death is independent of both caspases and its redistribution into triton X-100 insoluble membrane rafts. Cancer Res 2003;63:5480-9.
296. Cragg MS, Morgan SM, Chan HT, et al. Complement-mediated lysis by anti-CD20 mAb correlates with segregation into lipid rafts. Blood 2003;101:1045-52.
297. Merle NS, Church SE, Fremeaux-Bacchi V, Roumenina LT. Complement System Part I - Molecular Mechanisms of Activation and Regulation. Front Immunol 2015;6:262.
298. Merle NS, Noe R, Halbwachs-Mecarelli L, Fremeaux-Bacchi V, Roumenina LT. Complement System Part II: Role in Immunity. Front Immunol 2015;6:257.
299. Rochowiak A, Niemir ZI. [The role of CR1 complement receptor in pathology]. Pol Merkur Lekarski 2010;28:84-8.
300. Sjöholm AG, Jönsson G, Braconier JH, Sturfelt G, Truedsson L. Complement deficiency and disease: an update. Mol Immunol 2006;43:78-85.
301. Cicardi M, Bergamaschini L, Cugno M, et al. Pathogenetic and clinical aspects of C1 inhibitor deficiency. Immunobiology 1998;199:366-76.
302. Rawal N, Pangburn MK. Structure/function of C5 convertases of complement. Int Immunopharmacol 2001;1:415-22.
303. Sonnen AF, Henneke P. Structural biology of the membrane attack complex. Subcell Biochem 2014;80:83-116.
304. Young JD, Cohn ZA, Podack ER. The ninth component of complement and the pore-forming protein (perforin 1) from cytotoxic T cells: structural, immunological, and functional similarities. Science 1986;233:184-90.
305. Charchaflieh J, Wei J, Labaze G, et al. The role of complement system in septic shock. Clin Dev Immunol 2012;2012:407324.
306. Zipfel PF, Skerka C. Complement regulators and inhibitory proteins. Nat Rev Immunol 2009;9:729-40.

307. Spiller OB, Criado-García O, Rodríguez De Córdoba S, Morgan BP. Cytokine-mediated up-regulation of CD55 and CD59 protects human hepatoma cells from complement attack. Clin Exp Immunol 2000;121:234-41.
308. Weng WK, Levy R. Expression of complement inhibitors CD46, CD55, and CD59 on tumor cells does not predict clinical outcome after rituximab treatment in follicular non-Hodgkin lymphoma. Blood 2001;98:1352-7.
309. Wang SY, Weiner G. Complement and cellular cytotoxicity in antibody therapy of cancer. Expert Opin Biol Ther 2008;8:759-68.
310. Golay J, Zaffaroni L, Vaccari T, et al. Biologic response of B lymphoma cells to anti-CD20 monoclonal antibody rituximab in vitro: CD55 and CD59 regulate complement-mediated cell lysis. Blood 2000;95:3900-8.
311. Golay J, Lazzari M, Facchinetti V, et al. CD20 levels determine the in vitro susceptibility to rituximab and complement of B-cell chronic lymphocytic leukemia: further regulation by CD55 and CD59. Blood 2001;98:3383-9.
312. Macor P, Tripodo C, Zorzet S, et al. In vivo targeting of human neutralizing antibodies against CD55 and CD59 to lymphoma cells increases the antitumor activity of rituximab. Cancer Res 2007;67:10556-63.
313. Nightingale G. Ofatumumab: a novel anti-CD20 monoclonal antibody for treatment of refractory chronic lymphocytic leukemia. Ann Pharmacother 2011;45:1248-55.
314. Osterborg A. Ofatumumab, a human anti-CD20 monoclonal antibody. Expert Opin Biol Ther 2010;10:439-49.
315. Beum PV, Lindorfer MA, Beurskens F, et al. Complement activation on B lymphocytes opsonized with rituximab or ofatumumab produces substantial changes in membrane structure preceding cell lysis. J Immunol 2008;181:822-32.
316. Pawluczkowycz AW, Beurskens FJ, Beum PV, et al. Binding of submaximal C1q promotes complement-dependent cytotoxicity (CDC) of B cells opsonized with anti-CD20 mAbs ofatumumab (OFA) or rituximab (RTX): considerably higher levels of CDC are induced by OFA than by RTX. J Immunol 2009;183:749-58.
317. Taylor RP, Lindorfer MA. Fcγ-receptor-mediated trogocytosis impacts mAb-based therapies: historical precedence and recent developments. Blood 2015;125:762-6.
318. Taylor RP, Lindorfer MA. Immunotherapeutic mechanisms of anti-CD20 monoclonal antibodies. Curr Opin Immunol 2008;20:444-9.
319. Kennedy AD, Beum PV, Solga MD, et al. Rituximab infusion promotes rapid complement depletion and acute CD20 loss in chronic lymphocytic leukemia. J Immunol 2004;172:3280-8.
320. Lim SH, Vaughan AT, Ashton-Key M, et al. Fc gamma receptor IIb on target B cells promotes rituximab internalization and reduces clinical efficacy. Blood 2011;118:2530-40.
321. Cooper MD, Lanier LL, Conley ME, Puck JM. Immunodeficiency disorders. Hematology Am Soc Hematol Educ Program 2003:314-30.
322. Bryan AR, Wu EY. Complement deficiencies in systemic lupus erythematosus. Curr Allergy Asthma Rep 2014;14:448.
323. Jönsson G, Truedsson L, Sturfelt G, Oxelius VA, Braconier JH, Sjöholm AG. Hereditary C2 deficiency in Sweden: frequent occurrence of invasive infection, atherosclerosis, and rheumatic disease. Medicine (Baltimore) 2005;84:23-34.
324. Drogari-Apiranthitou M, Kuijper EJ, Dekker N, Dankert J. Complement activation and formation of the membrane attack complex on serogroup B Neisseria meningitidis in the presence or absence of serum bactericidal activity. Infect Immun 2002;70:3752-8.
325. Fust G, Czink E, Minh D, Miszlay Z, Varga L, Hollan SR. Depressed classical complement pathway activities in chronic lymphocytic leukaemia. Clin Exp Immunol 1985;60:489-95.
326. Fust G, Miszlay Z, Czink E, et al. C1 and C4 abnormalities in chronic lymphocytic leukaemia and their significance. Immunol Lett 1987;14:255-9.
327. Heath ME, Cheson BD. Defective complement activity in chronic lymphocytic leukemia. Am J Hematol 1985;19:63-73.
328. Varga L, Czink E, Miszlai Z, et al. Low activity of the classical complement pathway predicts short survival of patients with chronic lymphocytic leukaemia. Clin Exp Immunol 1995;99:112-6.

329. Beurskens FJ, Lindorfer MA, Farooqui M, et al. Exhaustion of cytotoxic effector systems may limit monoclonal antibody-based immunotherapy in cancer patients. J Immunol 2012;188:3532-41.
330. Manches O, Lui G, Chaperot L, et al. In vitro mechanisms of action of rituximab on primary non-Hodgkin lymphomas. Blood 2003;101:949-54.
331. Nimmerjahn F, Ravetch JV. Fc-receptors as regulators of immunity. Adv Immunol 2007;96:179-204.
332. Nimmerjahn F, Ravetch JV. Fcgamma receptors as regulators of immune responses. Nat Rev Immunol 2008;8:34-47.
333. Jak M, van Bochove GG, Reits EA, et al. CD40 stimulation sensitizes CLL cells to lysosomal cell death induction by type II anti-CD20 mAb GA101. Blood 2011;118:5178-88.
334. Walshe CA, Beers SA, French RR, et al. Induction of cytosolic calcium flux by CD20 is dependent upon B Cell antigen receptor signaling. J Biol Chem 2008;283:16971-84.
335. Petrie RJ, Deans JP. Colocalization of the B cell receptor and CD20 followed by activation-dependent dissociation in distinct lipid rafts. J Immunol 2002;169:2886-91.
336. Meijer AJ, Codogno P. Autophagy: regulation and role in disease. Crit Rev Clin Lab Sci 2009;46:210-40.
337. Coiffier B, Lepretre S, Pedersen LM, et al. Safety and efficacy of ofatumumab, a fully human monoclonal anti-CD20 antibody, in patients with relapsed or refractory B-cell chronic lymphocytic leukemia: a phase 1-2 study. Blood 2008;111:1094-100.
338. Molica S. Infections in chronic lymphocytic leukemia: risk factors, and impact on survival, and treatment. Leuk Lymphoma 1994;13:203-14.
339. Rosén A, Bergh AC, Gogok P, et al. Lymphoblastoid cell line with B1 cell characteristics established from a chronic lymphocytic leukemia clone by in vitro EBV infection. Oncoimmunology 2012;1:18-27.
340. Wendel-Hansen V, Sällström J, De Campos-Lima PO, et al. Epstein-Barr virus (EBV) can immortalize B-cll cells activated by cytokines. Leukemia 1994;8:476-84.
341. Nilsson K, Giovanella BC, Stehlin JS, Klein G. Tumorigenicity of human hematopoietic cell lines in athymic nude mice. Int J Cancer 1977;19:337-44.
342. Wigler M, Silverstein S, Lee LS, Pellicer A, Cheng Y, Axel R. Transfer of purified herpes virus thymidine kinase gene to cultured mouse cells. Cell 1977;11:223-32.
343. Caraux G, Pinloche S. PermutMatrix: a graphical environment to arrange gene expression profiles in optimal linear order. Bioinformatics 2005;21:1280-1.
344. Barth MJ, Hernandez-Ilizaliturri FJ, Mavis C, et al. Ofatumumab demonstrates activity against rituximab-sensitive and -resistant cell lines, lymphoma xenografts and primary tumour cells from patients with B-cell lymphoma. Br J Haematol 2012;156:490-8.
345. Nosari A. Infectious complications in chronic lymphocytic leukemia. Mediterr J Hematol Infect Dis 2012;4:e2012070.
346. Robak T, Dmoszynska A, Solal-Céligny P, et al. Rituximab plus fludarabine and cyclophosphamide prolongs progression-free survival compared with fludarabine and cyclophosphamide alone in previously treated chronic lymphocytic leukemia. J Clin Oncol 2010;28:1756-65.
347. Klepfish A, Gilles L, Ioannis K, Rachmilewitz EA, Schattner A. Enhancing the action of rituximab in chronic lymphocytic leukemia by adding fresh frozen plasma: complement/rituximab interactions & clinical results in refractory CLL. Ann N Y Acad Sci 2009;1173:865-73.
348. Klepfish A, Rachmilewitz EA, Kotsianidis I, Patchenko P, Schattner A. Adding fresh frozen plasma to rituximab for the treatment of patients with refractory advanced CLL. QJM 2008;101:737-40.
349. Badoux XC, Keating MJ, Wang X, et al. Fludarabine, cyclophosphamide, and rituximab chemoimmunotherapy is highly effective treatment for relapsed patients with CLL. Blood 2011;117:3016-24.
350. Smith MR. Rituximab (monoclonal anti-CD20 antibody): mechanisms of action and resistance. Oncogene 2003;22:7359-68.
351. Cheson BD. Ofatumumab, a novel anti-CD20 monoclonal antibody for the treatment of B-cell malignancies. J Clin Oncol 2010;28:3525-30.

352. D'Arena G, Musto P, Cascavilla N, Dell'Olio M, Di Renzo N, Carotenuto M. Quantitative flow cytometry for the differential diagnosis of leukemic B-cell chronic lymphoproliferative disorders. Am J Hematol 2000;64:275-81.
353. Alinari L, Lapalombella R, Andritsos L, Baiocchi RA, Lin TS, Byrd JC. Alemtuzumab (Campath-1H) in the treatment of chronic lymphocytic leukemia. Oncogene 2007;26:3644-53.
354. Cruz RI, Hernandez-Ilizaliturri FJ, Olejniczak S, et al. CD52 over-expression affects rituximab-associated complement-mediated cytotoxicity but not antibody-dependent cellular cytotoxicity: preclinical evidence that targeting CD52 with alemtuzumab may reverse acquired resistance to rituximab in non-Hodgkin lymphoma. Leuk Lymphoma 2007;48:2424-36.
355. Ginaldi L, De Martinis M, Matutes E, et al. Levels of expression of CD52 in normal and leukemic B and T cells: correlation with in vivo therapeutic responses to Campath-1H. Leuk Res 1998;22:185-91.
356. Pozzo F, Bittolo T, Bulian P, et al. *NOTCH1* Mutations Are Associated with Low CD20 Expression in Chronic Lymphocytic Leukemia: Evidences for a NOTCH1-Mediated Epigenetic Regulatory Mechanism.
357. Villamor N, Conde L, Martínez-Trillos A, et al. NOTCH1 mutations identify a genetic subgroup of chronic lymphocytic leukemia patients with high risk of transformation and poor outcome. Leukemia 2013;27:1100-6.
358. Geisler CH, van T' Veer MB, Jurlander J, et al. Frontline low-dose alemtuzumab with fludarabine and cyclophosphamide prolongs progression-free survival in high-risk CLL. Blood 2014;123:3255-62.
359. Yang XJ, Seto E. The Rpd3/Hda1 family of lysine deacetylases: from bacteria and yeast to mice and men. Nat Rev Mol Cell Biol 2008;9:206-18.
360. Gallinari P, Di Marco S, Jones P, Pallaoro M, Steinkühler C. HDACs, histone deacetylation and gene transcription: from molecular biology to cancer therapeutics. Cell Res 2007;17:195-211.
361. Shimizu R, Kikuchi J, Wada T, Ozawa K, Kano Y, Furukawa Y. HDAC inhibitors augment cytotoxic activity of rituximab by upregulating CD20 expression on lymphoma cells. Leukemia 2010;24:1760-8.
362. Di Gaetano N, Xiao Y, Erba E, et al. Synergism between fludarabine and rituximab revealed in a follicular lymphoma cell line resistant to the cytotoxic activity of either drug alone. Br J Haematol 2001;114:800-9.
363. Bologna L, Gotti E, Da Roit F, et al. Ofatumumab is more efficient than rituximab in lysing B chronic lymphocytic leukemia cells in whole blood and in combination with chemotherapy. J Immunol 2013;190:231-9.
364. Herter S, Herting F, Mundigl O, et al. Preclinical activity of the type II CD20 antibody GA101 (obinutuzumab) compared with rituximab and ofatumumab in vitro and in xenograft models. Mol Cancer Ther 2013;12:2031-42.
365. van Meerten T, van Rijn RS, Hol S, Hagenbeek A, Ebeling SB. Complement-induced cell death by rituximab depends on CD20 expression level and acts complementary to antibody-dependent cellular cytotoxicity. Clin Cancer Res 2006;12:4027-35.
366. Pleyer L, Egle A, Hartmann TN, Greil R. Molecular and cellular mechanisms of CLL: novel therapeutic approaches. Nat Rev Clin Oncol 2009;6:405-18.
367. Zenz T, Eichhorst B, Busch R, et al. TP53 mutation and survival in chronic lymphocytic leukemia. J Clin Oncol 2010;28:4473-9.
368. Seke Etet PF, Vecchio L, Nwabo Kamdje AH. Interactions between bone marrow stromal microenvironment and B-chronic lymphocytic leukemia cells: any role for Notch, Wnt and Hh signaling pathways? Cell Signal 2012;24:1433-43.
369. Cosimo E, McCaig AM, Carter-Brzezinski LJ, et al. Inhibition of NF-κB-mediated signaling by the cyclin-dependent kinase inhibitor CR8 overcomes prosurvival stimuli to induce apoptosis in chronic lymphocytic leukemia cells. Clin Cancer Res 2013;19:2393-405.
370. Osterborg A, Fassas AS, Anagnostopoulos A, Dyer MJ, Catovsky D, Mellstedt H. Humanized CD52 monoclonal antibody Campath-1H as first-line treatment in chronic lymphocytic leukaemia. Br J Haematol 1996;93:151-3.
371. Taylor RP, Lindorfer MA. Analyses of CD20 monoclonal antibody-mediated tumor cell killing mechanisms: rational design of dosing strategies. Mol Pharmacol 2014;86:485-91.

372. Bo MD, Del Principe MI, Pozzo F, et al. NOTCH1 mutations identify a chronic lymphocytic leukemia patient subset with worse prognosis in the setting of a rituximab-based induction and consolidation treatment. Ann Hematol 2014.
373. Zenz T, Vollmer D, Trbusek M, et al. TP53 mutation profile in chronic lymphocytic leukemia: evidence for a disease specific profile from a comprehensive analysis of 268 mutations. Leukemia 2010;24:2072-9.
374. Malcikova J, Smardova J, Rocnova L, et al. Monoallelic and biallelic inactivation of TP53 gene in chronic lymphocytic leukemia: selection, impact on survival, and response to DNA damage. Blood 2009;114:5307-14.
375. Clevers H, Alarcon B, Wileman T, Terhorst C. The T cell receptor/CD3 complex: a dynamic protein ensemble. Annu Rev Immunol 1988;6:629-62.
376. Buggins AG, Levi A, Gohil S, et al. Evidence for a macromolecular complex in poor prognosis CLL that contains CD38, CD49d, CD44 and MMP-9. Br J Haematol 2011;154:216-22.
377. Kamiguti AS, Lee ES, Till KJ, et al. The role of matrix metalloproteinase 9 in the pathogenesis of chronic lymphocytic leukaemia. Br J Haematol 2004;125:128-40.
378. Redondo-Muñoz J, Escobar-Díaz E, Samaniego R, Terol MJ, García-Marco JA, García-Pardo A. MMP-9 in B-cell chronic lymphocytic leukemia is up-regulated by alpha4beta1 integrin or CXCR4 engagement via distinct signaling pathways, localizes to podosomes, and is involved in cell invasion and migration. Blood 2006;108:3143-51.
379. Das J, Chen CH, Yang L, Cohn L, Ray P, Ray A. A critical role for NF-kappa B in GATA3 expression and TH2 differentiation in allergic airway inflammation. Nat Immunol 2001;2:45-50.
380. Larsson LG, Gray HE, Tötterman T, Pettersson U, Nilsson K. Drastically increased expression of MYC and FOS protooncogenes during in vitro differentiation of chronic lymphocytic leukemia cells. Proc Natl Acad Sci U S A 1987;84:223-7.
381. Caliceti C, Nigro P, Rizzo P, Ferrari R. ROS, Notch, and Wnt signaling pathways: crosstalk between three major regulators of cardiovascular biology. Biomed Res Int 2014;2014:318714.
382. Hasbold J, Lyons AB, Kehry MR, Hodgkin PD. Cell division number regulates IgG1 and IgE switching of B cells following stimulation by CD40 ligand and IL-4. Eur J Immunol 1998;28:1040-51.
383. Pascutti MF, Jak M, Tromp JM, et al. IL-21 and CD40L signals from autologous T cells can induce antigen-independent proliferation of CLL cells. Blood 2013;122:3010-9.
384. Rossi D, Gaidano G. ATM and chronic lymphocytic leukemia: mutations, and not only deletions, matter. Haematologica 2012;97:5-8.
385. Fang SH, Chen Y, Weigel RJ. GATA-3 as a marker of hormone response in breast cancer. J Surg Res 2009;157:290-5.
386. de Totero D, Reato G, Mauro F, et al. IL4 production and increased CD30 expression by a unique CD8+ T-cell subset in B-cell chronic lymphocytic leukaemia. Br J Haematol 1999;104:589-99.
387. Rudd CE. CD4, CD8 and the TCR-CD3 complex: a novel class of protein-tyrosine kinase receptor. Immunol Today 1990;11:400-6.
388. Talab F, Allen JC, Thompson V, Lin K, Slupsky JR. LCK is an important mediator of B-cell receptor signaling in chronic lymphocytic leukemia cells. Mol Cancer Res 2013;11:541-54.
389. Ronchini C, Capobianco AJ. Induction of cyclin D1 transcription and CDK2 activity by Notch(ic): implication for cell cycle disruption in transformation by Notch(ic). Mol Cell Biol 2001;21:5925-34.
390. Johnston LA, Edgar BA. Wingless and Notch regulate cell-cycle arrest in the developing Drosophila wing. Nature 1998;394:82-4.
391. Matsuno K, Diederich RJ, Go MJ, Blaumueller CM, Artavanis-Tsakonas S. Deltex acts as a positive regulator of Notch signaling through interactions with the Notch ankyrin repeats. Development 1995;121:2633-44.
392. Lai EC. Keeping a good pathway down: transcriptional repression of Notch pathway target genes by CSL proteins. EMBO Rep 2002;3:840-5.
393. Pursglove SE, Mackay JP. CSL: a notch above the rest. Int J Biochem Cell Biol 2005;37:2472-7.
394. Doetzlhofer A, Rotheneder H, Lagger G, et al. Histone deacetylase 1 can repress transcription by binding to Sp1. Mol Cell Biol 1999;19:5504-11.

395. Cunliffe VT. Eloquent silence: developmental functions of Class I histone deacetylases. Curr Opin Genet Dev 2008;18:404-10.
396. Obregon DF, Rezai-Zadeh K, Bai Y, et al. ADAM10 activation is required for green tea (-)-epigallocatechin-3-gallate-induced alpha-secretase cleavage of amyloid precursor protein. J Biol Chem 2006;281:16419-27.
397. Espinosa L, Inglés-Esteve J, Aguilera C, Bigas A. Phosphorylation by glycogen synthase kinase-3 beta down-regulates Notch activity, a link for Notch and Wnt pathways. J Biol Chem 2003;278:32227-35.
398. Hur EM, Zhou FQ. GSK3 signalling in neural development. Nat Rev Neurosci 2010;11:539-51.
399. De A. Wnt/Ca2+ signaling pathway: a brief overview. Acta Biochim Biophys Sin (Shanghai) 2011;43:745-56.
400. Oishi I, Suzuki H, Onishi N, et al. The receptor tyrosine kinase Ror2 is involved in non-canonical Wnt5a/JNK signalling pathway. Genes Cells 2003;8:645-54.
401. Ying J, Li H, Yu J, et al. WNT5A exhibits tumor-suppressive activity through antagonizing the Wnt/beta-catenin signaling, and is frequently methylated in colorectal cancer. Clin Cancer Res 2008;14:55-61.
402. Baskar S, Kwong KY, Hofer T, et al. Unique cell surface expression of receptor tyrosine kinase ROR1 in human B-cell chronic lymphocytic leukemia. Clin Cancer Res 2008;14:396-404.
403. Rosenwald A, Alizadeh AA, Widhopf G, et al. Relation of gene expression phenotype to immunoglobulin mutation genotype in B cell chronic lymphocytic leukemia. J Exp Med 2001;194:1639-47.
404. Granziero L, Ghia P, Circosta P, et al. Survivin is expressed on CD40 stimulation and interfaces proliferation and apoptosis in B-cell chronic lymphocytic leukemia. Blood 2001;97:2777-83.
405. Yamamura H, Yamamura A, Ko EA, et al. Activation of Notch signaling by short-term treatment with Jagged-1 enhances store-operated Ca(2+) entry in human pulmonary arterial smooth muscle cells. Am J Physiol Cell Physiol 2014;306:C871-8.
406. Chigurupati S, Venkataraman R, Barrera D, et al. Receptor channel TRPC6 is a key mediator of Notch-driven glioblastoma growth and invasiveness. Cancer Res 2010;70:418-27.
407. Rawstron AC, Hillmen P. Assessing minimal residual disease in chronic lymphocytic leukemia. Curr Hematol Malig Rep 2008;3:47-53.
408. Cortelezzi A, Sciumè M, Liberati AM, et al. Bendamustine in combination with ofatumumab in relapsed or refractory chronic lymphocytic leukemia: a GIMEMA Multicenter Phase II Trial. Leukemia 2014;28:642-8.
409. Byrd JC, Brown JR, O'Brien S, et al. Ibrutinib versus ofatumumab in previously treated chronic lymphoid leukemia. N Engl J Med 2014;371:213-23.
410. Coutre J, Leonard R, Furman I, Flinn S, De Vos K, Rai ea. Update on a phase 1 study of the selective PI3K-delta inhibitor, idelalisib (GS-1101) in combination with ofatumumab in patients with relapsed or refractory chronic lymphocytic leukemia. Haematologica (EHA Annual Meeting), 98 (s1) (2013) (abstract S1150); 2013.
411. Da Roit F, Engelberts PJ, Taylor RP, et al. Ibrutinib interferes with the cell-mediated anti-tumor activities of therapeutic CD20 antibodies: implications for combination therapy. Haematologica 2015;100:77-86.
412. Bojarczuk K, Siernicka M, Dwojak M, et al. B-cell receptor pathway inhibitors affect CD20 levels and impair antitumor activity of anti-CD20 monoclonal antibodies. Leukemia 2014;28:1163-7.
413. Cartron G, Dacheux L, Salles G, et al. Therapeutic activity of humanized anti-CD20 monoclonal antibody and polymorphism in IgG Fc receptor FcgammaRIIIa gene. Blood 2002;99:754-8.
414. Fiorcari S, Brown WS, McIntyre BW, et al. The PI3-kinase delta inhibitor idelalisib (GS-1101) targets integrin-mediated adhesion of chronic lymphocytic leukemia (CLL) cell to endothelial and marrow stromal cells. PLoS One 2013;8:e83830.
415. Ponader S, Chen SS, Buggy JJ, et al. The Bruton tyrosine kinase inhibitor PCI-32765 thwarts chronic lymphocytic leukemia cell survival and tissue homing in vitro and in vivo. Blood 2012;119:1182-9.

416. Riches JC, Davies JK, McClanahan F, et al. T cells from CLL patients exhibit features of T-cell exhaustion but retain capacity for cytokine production. Blood 2013;121:1612-21.
417. Sacco JJ, Botten J, Macbeth F, Bagust A, Clark P. The average body surface area of adult cancer patients in the UK: a multicentre retrospective study. PLoS One 2010;5:e8933.
418. Pandey S, Vyas GN. Adverse effects of plasma transfusion. Transfusion 2012;52 Suppl 1:65S-79S.
419. Baig NA, Taylor RP, Lindorfer MA, et al. Induced resistance to ofatumumab-mediated cell clearance mechanisms, including complement-dependent cytotoxicity, in chronic lymphocytic leukemia. J Immunol 2014;192:1620-9.
420. Zent CS, Taylor RP, Lindorfer MA, et al. Chemoimmunotherapy for relapsed/refractory and progressive 17p13-deleted chronic lymphocytic leukemia (CLL) combining pentostatin, alemtuzumab, and low-dose rituximab is effective and tolerable and limits loss of CD20 expression by circulating CLL cells. Am J Hematol 2014;89:757-65.
421. Williams ME, Densmore JJ, Pawluczkowycz AW, et al. Thrice-weekly low-dose rituximab decreases CD20 loss via shaving and promotes enhanced targeting in chronic lymphocytic leukemia. J Immunol 2006;177:7435-43.
422. Jitschin R, Braun M, Qorraj M, et al. Stromal cell-mediated glycolytic switch in CLL cells involves Notch-c-Myc signaling. Blood 2015;125:3432-6.
423. Shih IM, Wang TL. Notch signaling, gamma-secretase inhibitors, and cancer therapy. Cancer Res 2007;67:1879-82.
424. Bhat R, Watzl C. Serial killing of tumor cells by human natural killer cells--enhancement by therapeutic antibodies. PLoS One 2007;2:e326.